

The *Escherichia coli* haemolysin transporter

A paradigm for Type I secretion

Inaugural-Dissertation

zur

Erlangung des Doktorgrades der
Mathematisch-Naturwissenschaftlichen Fakultät
der Heinrich-Heine-Universität Düsseldorf

vorgelegt von

Stefan Jenewein

aus Heilbronn

September 2008

Aus dem Institut für Biochemie
der Heinrich-Heine Universität Düsseldorf

Gedruckt mit der Genehmigung der
Mathematisch-Naturwissenschaftlichen Fakultät der
Heinrich-Heine-Universität Düsseldorf

Referent: Prof. Dr. L. Schmitt
Koreferent: Prof. Dr. J. Jose

Tag der mündlichen Prüfung:

SUMMARY	IV
ZUSAMMENFASSUNG	VI
A. INTRODUCTION	1
1. Membrane transport	1
2. Bacterial Secretion Systems	2
3. Type I secretion	4
3.1 Architecture of Type I secretion systems	5
3.2 The outer membrane protein TolC	7
3.3 The membrane fusion protein HlyD	8
3.4 The ABC transporter HlyB	10
3.5 The toxin HlyA	11
4. ABC transporters	13
5. Mechanism of ABC transporters	16
6. Membrane protein overexpression	21
7. Aims and objectives	25
B. MATERIALS AND METHODS	26
1. Materials	26
2. Methods	40
2.1 Molecular biology	40
2.1.1 Cultivation and storage of <i>E. coli</i> and <i>L. lactis</i>	40
2.1.2 Blood haemolysis test on agar plates	40
2.1.3 Secretion tests with secretion competent <i>E. coli</i>	41
2.1.4 Transformation of competent <i>E. coli</i>	41
2.1.5 Transformation of competent <i>L. lactis</i>	42
2.1.6 DNA preparation, restriction and gel electrophoresis	43
2.1.7 Polymerase chain reaction (PCR)	44
2.1.8 Ligation	44
2.1.9 Introduction of point mutations	45
2.1.10 Ligation independent cloning (LIC)	47
2.2 Electrophoresis and protein detection	49

2.2.1	Protein determination	49
2.2.2	SDS-Polyacrylamide gel electrophoresis	50
2.2.3	Coomassie stain and silver stain	51
2.2.4	Immunodetection	51
2.3	Protein overexpression and purification	52
2.3.1	Protein overexpression	52
2.3.2	Membrane isolation	53
2.3.3	Membrane protein purification	53
2.3.4	Expression and purification of HlyB-NBD	54
2.3.5	Protein purification out of culture supernatant	55
2.3.6	Purification under denaturing conditions	56
2.3.7	Purification of maltose binding protein fusions	56
2.4	Protein analysis	57
2.4.1	ATPase activity determination	57
2.4.2	Trypsin protection studies	58
2.4.3	CD spectroscopy	59
2.4.4	Affinity measurements by intrinsic fluorescence quenching	60
2.4.5	Binding studies with TNP-nucleotides	61
2.4.6	Folding experiments	65
C.	RESULTS	68
1.	Nucleotide binding and hydrolysis of the haemolysin B NBD	68
1.1	Nucleotide binding to the NBD measured with tryptophan fluorescence	68
1.2	Nucleotide binding to the NBD measured by TNP fluorescence	72
1.3	The mode of TNP-ADP binding	77
1.4	How is ATP hydrolysed by HlyB-NBD?	83
1.4.1	HlyB-NBD undergoes a dimeric species during the ATP-hydrolysis cycle	83
1.4.2	Which mechanism follows the cleavage of the γ -phosphate?	87
1.5	ATPase activity of heterodimers composed of WT and H662A HlyB-NBD	90
2.	Cloning and expression of the inner membrane components of the haemolysin system	93
2.1	Cloning strategy and cloning of expression plasmids	93
2.2	Expression analysis in <i>E. coli</i>	97
2.3	Expression analysis in <i>L. lactis</i>	99
2.4	Analysis of the expressed proteins	101
2.4.1	Orientation in <i>L. lactis</i> membranes probes probed by trypsin protection	101
2.4.2	Detergent solubilisation	102
2.4.3	Purification of HlyB	103
2.4.4	CD spectroscopy of purified HlyB	104
2.4.5	ATPase activity of HlyB	105

3. Exploiting the Type I secretion system for heterologous expression	108
3.1 Generation of a vector pair suitable for expression of the secretion machinery and the fusion protein	108
3.2 Secretion of a C-terminal fragment of HlyA	110
3.3 Purification of the HlyA fragment from the culture supernatant	111
3.4 Cloning of fusion partners by LIC	114
3.5 Secretion tests with fusion proteins	116
3.6 Creating MalE-HlyA mutants for transport	121
3.7 Folding characteristics of the MalE mutants	125
3.8 Influence of SecB on the folding of the MalE fusions	132
 D. DISCUSSION	 135
1. The binding and hydrolysis mode of the nucleotide binding domain	135
1.1 Nucleotide binding to the HlyB-NBD	136
1.2 Characterisation of the TNP-ADP binding mode	140
1.3 The catalytic mode of the HlyB-NBD	142
 2. Cloning and expression of the inner membrane components of the haemolysin system	 147
2.1 Cloning and overexpression	147
2.2 Solubilisation and purification	149
2.3 ATPase induction by addition of HlyACterm	150
 3. Usage of fusions to an HlyA fragment for secretion	 151
3.1 Creating a system that allows screening of fusion proteins	151
3.2 Engineered fusion proteins which are able to secrete	153
3.3 A model for the “perfect” Type I substrate	157
 4. Outlook	 160
 REFERENCES	 161
 ABBREVIATIONS	 179
 APPENDIX	 181

Summary

The haemolysin export system of *Escherichia coli* is comprised of HlyB (an ATP-binding cassette (ABC) transporter), the membrane fusion protein HlyD, and the outer membrane channel TolC. It transports the 108 kDa toxin HlyA in a single step across the inner and outer membrane and constitutes the paradigm for Type I secretion.

Knowledge of the detailed mechanism of the ATPase reaction, which is the basis of transport in any particular ABC transporter is of main mechanistic interest. In this work the nucleotide binding domain (NBD) of HlyB was used to characterise the hydrolysis of the nucleotide. Nucleotide binding to the NBD was extensively characterized by fluorescence methods. An environmental sensitive mutant was generated to measure nucleotide binding. Quenching this amino acid allowed the determination of the affinity constants for nucleotides. Using Trinitrophenol(TNP)-derivatised nucleotides the data obtained for the mutant could be verified for the wildtype HlyB-NBD through competition experiments. Since TNP derivatised nucleotides exhibited a 50-100 fold higher affinity, the binding mode was characterized further by mutational and structural analysis showing that the increase of affinity is caused by flexible water-mediated interactions. To address the reaction mechanism of ATP hydrolysis recent structural work was supported in this work by extensive biochemical characterisation. As part of the presented work, it could be shown that cooperative ATP hydrolysis in the HlyB-NBD follows substrate assisted catalysis (SAC).

A broad screen including different plasmids, strains and growth conditions was performed to attempt the overexpression of the inner membrane components. While overexpression failed in the homologous host *E. coli*, expression was successful in *Lactococcus lactis*. The ATPase activity of full-length HlyB was strictly dependent on the substrate and showed an induction in the presence of the C-terminal secretion sequence of HlyA. In contrast to many other ABC transporters, this is one of the first examples where the ATPase activity of an ABC transporter is strictly coupled rather than just stimulated.

Exploiting the capability of secreting heterologous fusion proteins by the Type I machinery a vector pair was designed encoding on one hand for the inner membrane complex and one the other hand for any gene of interest fused to a C-terminal 23 kDa fragment of HlyA. Since

secretion failed for a number of fusion proteins, folding kinetics of the MalE-HlyA fusion was selectively changed. It could be clearly shown that mutations resulting in slower folding of the maltose binding protein MalE increased the secretion efficiency. This work is the first report in which a fusion protein was selectively converted into an appropriate substrate of a Type I machinery. The knowledge of how fusion proteins can be modified in order to be secreted will certainly help (i) choosing suitable targets for Type I secretion in biomedical and biotechnical applications and (ii) understanding the nature of Type I substrates and the secretion process itself.

Zusammenfassung

Das *Escherichia coli* Hämolyisin (Hly) System transportiert das aus 1023 Aminosäuren bestehende Toxin HlyA in einem einzigen Schritt über die innere und äußere Membran. Es ist das Musterbeispiel für die Typ I Sekretion und besteht aus dem ABC Transporter HlyB, dem Membranfusionsprotein HlyD und einem Protein der äusseren Membran, TolC.

Der Mechanismus wie die Hydrolyse von ATP stattfindet ist von außerordentlichem Interesse für ein detailliertes Verständnis von ABC Transportern. Um diesen Mechanismus aufzuklären, wurde in dieser Arbeit die isolierte Nukleotid bindende Domäne (NBD) von HlyB untersucht. Die Nukleotidbindung konnte über Fluoreszenzspektroskopie ausführlich untersucht werden. Mittels Mutation wurde ein umgebungssensitiver Aminosäurerest in die ATP Bindungstasche eingeführt. Durch die Veränderung der Fluoreszenzeigenschaften dieses Restes nach Nukleotidbindung konnte die Affinität bestimmt werden. Die erhaltenen Daten wurden durch die Verwendung von Trinitrophenol(TNP)-derivatisierten Nukleotiden bestätigt. Hierzu wurden die Derivate durch natürliche Nukleotide verdrängt. Die wesentlich höhere Affinität der TNP-derivate an die NBD wurde über biochemische und strukturelle Methoden untersucht. Hier zeigte sich, dass die erhöhte Affinität durch Wasser vermittelte Bindungen erklärt werden kann. Diese Arbeit unterstützte maßgeblich strukturelle Arbeiten zum Reaktionsmechanismus der ATP Hydrolyse. Biochemische Untersuchungen zeigten, dass die Hydrolyse im Fall der HlyB-NBD dem Mechanismus der Substrat assistierten Katalyse erfolgt.

Um den Proteinkomplex der inneren Membran erfolgreich zu exprimieren, wurden verschiedene Plasmide, Stämme und Wachstumsbedingungen verwendet. Im homologen Wirt *E. coli* konnte keine Überexpression etabliert werden. Währenddessen war im heterologen Wirt *Lactococcus lactis* die Überexpression erfolgreich. Die ATPase Aktivität des isolierten HlyB war eindeutig vom Substrat abhängig und zeigte eine Induktion der ATPase Aktivität nach Zugabe der C-terminalen Sekretionssequenz von HlyA. Im Gegensatz zu vielen anderen ABC Transportern ist die ATPase Aktivität von HlyB strikt an die Anwesenheit des Substrates gekoppelt.

Für biotechnologische und biomedizinische Fragestellungen ist das Type I System von Interesse, da es Proteine direkt in den Extrazellulärraum transportieren kann. In dieser Arbeit wurde ein Vektorpaar konstruiert, das zum einen den Proteinkomplex der inneren Membran kodiert und es zum anderen ermöglicht jedes beliebige Gen an das C-terminale 23 kDa HlyA Fragment zu fusionieren. Da verschiedene, getestete Fusionsproteine nicht erfolgreich sekretiert werden konnten, wurde das Fusionsprotein Maltosebindeprotein-HlyA gezielt modifiziert. Es konnte eindeutig gezeigt werden, dass Mutationen, die die Faltungsgeschwindigkeit herabsetzen, eine erhöhte Sekretion aufweisen. In dieser Arbeit ist zum ersten Mal dargestellt wie Proteine modifiziert werden können um ein für das Typ I Sekretionsystem geeignetes Substrat darzustellen.

A. Introduction

1. *Membrane transport*

Being a lipid bilayer with a hydrophobic core of around 40 Å, cellular membranes are impermeable for ions and only partially permeable for hydrophilic substances (Singer & Nicolson, 1972). The membrane is an essential component for example of bacteria, since it enables the differentiation into the cellular and extracellular space. It enables the bacteria to keep essential nutrients, ions and other small molecular compounds. Since the membrane is impermeable for nucleic acids and almost all proteins, these substances cannot diffuse freely across the membrane and remain in the cytosol. This border does not only define the cellular volume, but also keeps gradients of components, which are fundamental for a myriad of cellular processes such as the synthesis of ATP or the active uptake of extracellular substances. This barrier is also the major obstacle to overcome, if bacteria exchange compounds with the environment. Therefore, all cells have specialized proteins residing in the cellular membrane facilitating an in- or outward transport of all kinds of hydrophilic substances. The cells can thereby overcome the intrinsic impermeability of the lipid bilayer.

These membrane proteins ease the passive diffusion of ions across the membrane (*ion channels*; Hille, 1992) and facilitate the active export or import of low molecular weight compounds against a gradient either by coupling an existing gradient to this transport (*secondary transport*; Abramson et al, 2004) or by using the energy obtained either by hydrolysing energy rich molecules such as ATP or by other directly energizing processes such as light (*primary transporters*; Boyer, 1997; Lanyi, 2004). Not only transport proteins are integrated into the membrane; further vital proteins integrated into the bacterial membrane deal with the rather unspecific passing of molecules (Porins or MscL/S), signalling, locomotion or adhesion, just to mention a few.

2. Bacterial Secretion Systems

Protein synthesis is restricted to the cytoplasm. Proteins localized in the periplasm (in case of Gram-negative bacteria) or in the extracellular space need to be transported to their relevant localization. Additionally membrane proteins have to be integrated into the inner and for Gram-negative bacteria also into the outer membrane, respectively. Whereas ions or smaller compounds can easily be transported across the lipid bilayer by proteins described above (“channels” and “carriers”), the export of larger molecules like peptides, proteins acids requires more complex transport systems.

The general way for proteins to cross the bacterial inner membrane is the *sec*-dependent pathway (Driessen & Nouwen, 2008). This protein conducting channel is almost exclusively responsible for integration of membrane proteins into the inner membrane, although there are some exceptions (Kuhn, 1995) and accessory proteins are needed (Luirink et al, 2005). The core component of this secretion apparatus in *E. coli* is the heterotrimeric SecYEG complex that forms a channel through the cytoplasmic membrane (Robson & Collinson, 2006). Protein transport is energized by the hydrolysis of either GTP or ATP and the membrane potential (Wickner & Schekman, 2005).

In addition to the *sec* system the *tat* system facilitates transport of fully folded proteins across the cytoplasmatic membrane whereas the *sec* system only transports unfolded proteins (Lee et al, 2006). The *tat* system consists of three essential proteins (*E. coli tatABC*) and it is believed that the energy is supplied by the proton motive force. The *tat* system nicely complements the *sec* system since it transports folded proteins even with bound cofactors but it is far more energy consuming (Alder & Theg, 2003). Therefore it is not the standard route of how proteins cross the inner membrane and only ~ 5 % of the secreted proteins are shuttled by the *tat* system (Wicker and Schekman, 2005).

In Gram-positive bacteria both secretion systems would be sufficient to secrete proteins into the extracellular space, but in Gram-negative bacteria the outer membrane represents an additional barrier to overcome. Gram-negative bacteria have therefore evolved further mechanisms to cross the outer membrane.

Two strategies to overcome the inner and the outer membrane are pursued (Wickner & Schekman, 2005): i) Proteins are first transported across the inner membrane to the periplasm. If the protein is targeted to the extracellular space a further membrane protein complex,

residing in the outer membrane, transports the protein to the extracellular space. Examples for the described procedure are Type II secretion or the Type V secretion. ii) Type I, Type III, Type IV use transport machineries that recognize the protein directly after ribosomal synthesis and the protein is secreted over both bacterial membranes in one step to the extracellular space. In some cases the transport occurs even further across the host membrane into host cells.

Recently, a Type VI secretion system was identified (Pukatzki et al, 2006), but it is yet unclear how the secretion process is accomplished. An overview of how transport across bacterial membranes is accomplished is presented in Figure A1.

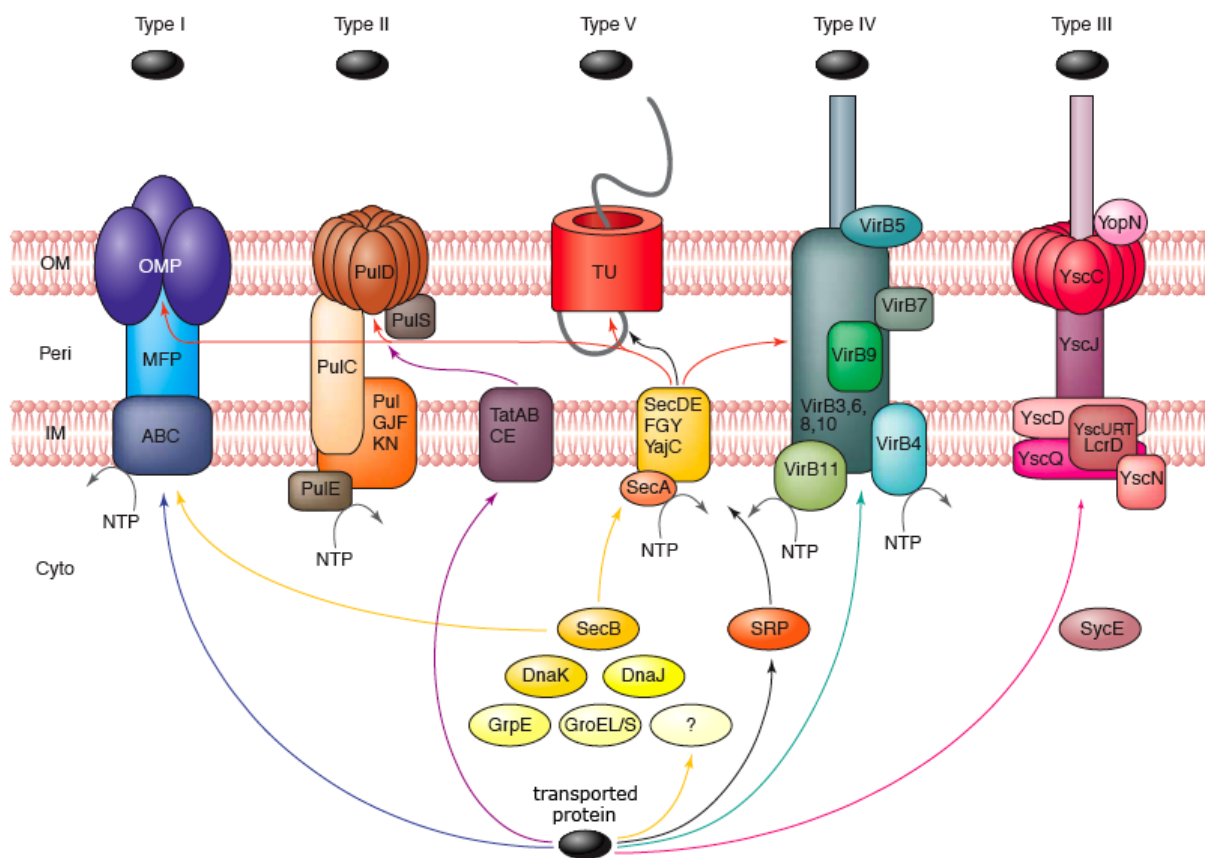


Figure A1: Schematic representation of the different protein secretion pathways in Gram-negative bacteria. The blue arrow represents proteins that are translocated through the inner and outer membranes by the Type I secretion apparatus. Purple arrows represent proteins that are targeted to the *tat* pathway. Yellow arrows represent proteins that are targeted to a secretion pathway via a molecular chaperone, such as SecB. Red arrows represent proteins that have been translocated through the inner membrane by the Sec apparatus after being targeted by a molecular chaperone, such as SecB. Proteins targeted to the Sec pathway via the SRP (signal recognition particle) are represented by black arrows, whereas those translocated through the inner and outer membranes by the Type IV secretion apparatus are represented by green arrows. Pink arrows show proteins translocated through the inner and outer membranes by the type III secretion apparatus. For simplicity the Type VI secretion system is not shown. Abbreviations: ABC, ATP-binding cassette exporter; Cyto, cytoplasm; IM, inner membrane; MFP, membrane fusion protein; OM, outer membrane; OMP, outer membrane protein TolC; Peri, periplasm; TU, translocation unit; NTP, nucleotide triphosphate. Adapted from Desvaux et al, 2004.

3. Type I secretion

In comparison to other transport machines, which are capable to transport their substrates across both membranes, the Type I secretion apparatus is a rather ‘simple’ molecular machine. It is composed of two inner membrane proteins; a so called membrane fusion protein (MFP), an ATP Binding Cassette (ABC) transporter and an outer membrane protein extending into the periplasm to complete the continuous tunnel to the exterior media. Since the energizing subunit in this system is an ABC transporter, Type I secretion is also called the ABC secretion pathway. In the model organism *E. coli* the paradigm for Type I secretion is the haemolysin system which was discovered in the early 1980s (Mackman & Holland, 1984; Welch et al, 1981; Welch et al, 1983) with the corresponding proteins being HlyB (ABC transporter), HlyD (MFP) and TolC in the outer membrane (Wandersman & Delepelaire, 1990). The best characterized substrate (also called allocrite in order to discriminate it from ATP, the hydrolysed substrate) for a Type I secretion machinery, is the 108 kDa haemolytic toxin, haemolysin A (HlyA), which is exported by the haemolysin system to the extracellular space. It is sometimes referred to as α -haemolysin in the literature, which is nevertheless quite distinct from the α -haemolysin secreted by *Staphylococcus aureus* (Bhakdi & Tranum-Jensen, 1991; Uhlen et al, 2000; Welch et al, 1981). It is a member of the repeats in toxins (RTX) family which contains glycine rich motifs able to bind calcium. Calcium binding to HlyA triggers refolding and subsequent toxicity. HlyA secretion is frequently associated with uropathogenic strains of *E. coli* in both animals and humans (Brooks et al, 1980), and it constitutes a significant clinical and veterinary problem.

Crosslinking studies and subsequent affinity purification have shown that all three transport components for HlyA secretion assemble during the transport process, forming a continuous channel-tunnel from the cytoplasm to the exterior (Balakrishnan et al, 2001; Thanabalu et al, 1998).

TolC is not only involved in Type I secretion, but also in the export of a wide range of antimicrobial compounds, including antibiotics, detergents, dyes and organic solvents. The corresponding inner membrane complex is a multidrug efflux pump working as a proton antiporter (e.g. AcrAB in *E. coli*; Ma et al, 1995). This might also be a reason why the *tolC* gene is not directly connected to the *hly* operon like the other inner membrane components.

In the *hly* operon all coding sequences specific for haemolysin secretion are found (Felmlee et al, 1985). The transcriptional order is *hlyC* \Rightarrow *hlyA* \Rightarrow *hlyB* \Rightarrow *hlyD*. HlyC could be later identified as an accessory protein required for the toxicity of HlyA and it catalyzes the acylation of HlyA at two distinct lysine residues (Stanley et al, 1994). Importantly, non-acylated HlyA is still secreted without any reduction in efficiency, but lacks the haemolytic properties.

The *hly* operon is transcribed from a promoter complex upstream of *hlyC* in which at least six different promoter sequences are organized in two distinct groups of promoter regions. Further upstream and separated by an insertion element IS2, an enhancer-like sequence termed *hlyR* was identified (Vogel et al, 1988).

The transcription of *hlyA* and other Type I secretion substrates is tightly regulated in order to ensure that secretion only occurs at a certain time in large amounts (Mourino et al, 1994). One might speculate that the precise conditions for the secretion of HlyA by *E. coli* only occurs in a host organism in which high aeration or body temperature might trigger the formation of the secretion apparatus in order to secrete HlyA during infection. This would also apply to the *Serratia marcescens* HasA system, another well characterized Type I secretion system, where iron uptake is only required during iron starvation (Letoffe et al, 1994). This kind of regulation is quite reasonable since inappropriate secretion would be a waste of energy. But still the detailed mechanisms of regulation are unclear.

3.1 Architecture of Type I secretion systems

As mentioned above Type I secretion systems are composed of an ABC transporter, a MFP and an outer membrane protein; HlyB, HlyD and TolC in the case of the *E.coli* haemolysin system.

HlyB contains an approximately 15 kDa N-terminal region resembling a C39 peptidase domain, followed by six predicted hydrophobic α -helical transmembrane segments and a C-terminal nucleotide binding domain (NBD) (Juranka et al, 1992; Welch et al, 1981). The second component is HlyD, which is anchored in the inner membrane by a single α -helical transmembrane segment, with a huge periplasmatic domain (Schulein et al, 1992; Wang et al, 1991). HlyB, like other ABC proteins, is thought to form a dimer, HlyD is thought to form a

trimer (Balakrishnan et al, 2001), although cross-linking studies have indicated higher oligomeric species of HlyD (Balakrishnan et al, 2001; I. B. Holland and J. Young, unpublished data). The outer membrane protein TolC, which binds to the inner membrane complex HlyB/HlyD upon interaction of the transport substrate HlyA, is a trimer (Koronakis et al, 1997).

HlyD and TolC provide the transenvelope channel-tunnel for the transport but are also crucial for folding of HlyA (Pimenta et al, 2005) whereas the ATPase activity of HlyB provides energy for certain essential steps involved in translocation (Koronakis et al, 1993).

Furthermore, HlyB is apparently involved in the recognition of the transport substrate HlyA (Benabdelhak et al, 2003) and may therefore initiate the transport cycle. HlyD, also involved in early interactions with HlyA (Balakrishnan et al, 2001), promotes together with HlyB the extrusion of HlyA across the inner membrane and ultimately to the extracellular space without any detectable periplasmic intermediate.

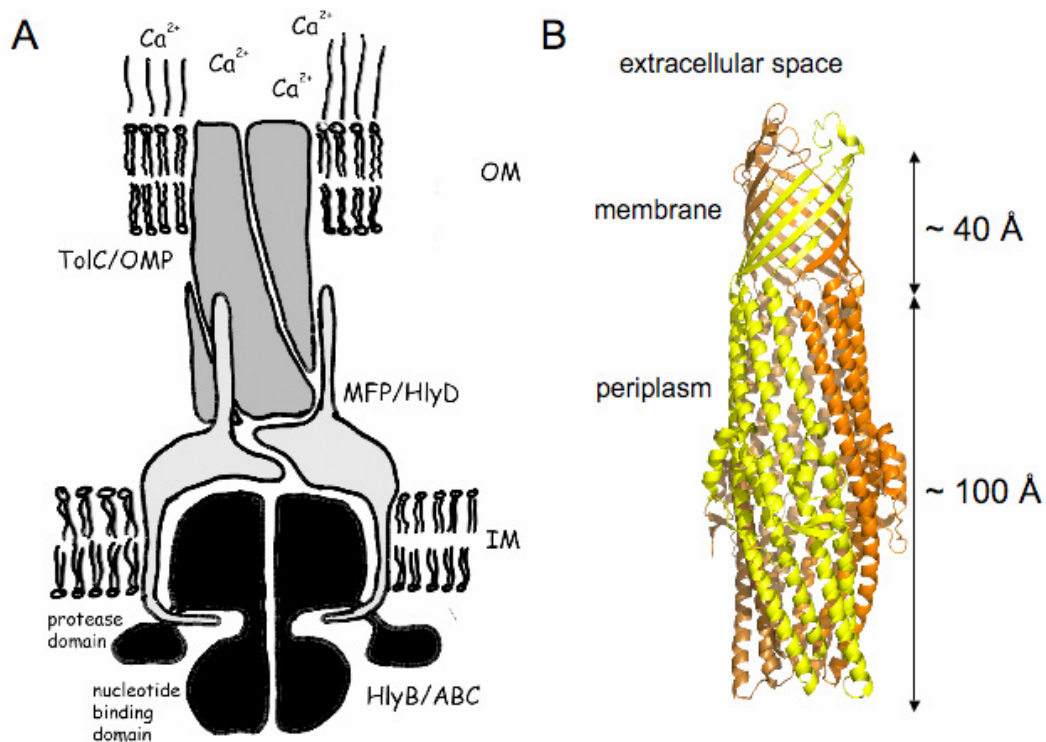


Figure A2: (A) Schematic representation of an assembled Type I secretion machinery of Gram-negative bacteria. The ABC transporter, HlyB is shown in black and the individual domains of the transporter are indicated. The MFP, HlyD is coloured in light grey. Both proteins reside in the inner membrane (IM). The outer membrane protein (OMP), TolC residing in the outer membrane is depicted in dark grey. Calcium ions are shown in the extracellular space underlining their importance for functional folding of most Type I secretion substrates.

(B) Crystal structure of the outer membrane component TolC with the upper membrane-spanning β -barrel domain and the α -helical bundles creating a continuous pore (Koronakis et al, 2000).

3.2 The outer membrane protein TolC

During the very early stages of studying haemolysin transport it was realized that during Type I secretion no periplasmic intermediate could be observed (Gray et al, 1986). Thus, either the inner and the outer membrane have to get into close contact or a long channel between them has to serve as a periplasmic “bypass” to the exterior. Reconstitution of TolC into a lipid bilayer allowed for the first time a structural investigation by electron microscopy (Koronakis et al, 1997). This analysis pointed out that TolC is a homotrimer with a single pore in the center and an additional domain extending into the periplasm. This became more evident when the beautiful high-resolution structure was published (Koronakis et al, 2000). The TolC homotrimer is a tapered hollow cylinder, 140 Å in length (Figure A2 B); it comprises a 40 Å long 12-stranded outer membrane β -barrel (the channel domain) that anchors a contiguous 100 Å long helical barrel projecting across the periplasmic space (the tunnel domain). A third domain, with a mixed α/β structure, forms a belt around the equator of the tunnel. Each of the three monomers contributes four antiparallel β -strands and four antiparallel α -helices (two continuous long helices and two pairs of shorter helices) forming the channel and the tunnel domains, respectively. The tunnel domain has a diameter of 20 Å which reduces to only 3.9 Å at the periplasmic end. Widening this opening is the key function of TolC in its associated export machines. The helices in TolC are densely packed and black lipid membrane measurements showed that opening cannot be induced by high voltage, low pH or even urea (Andersen et al, 2002). Based on these observations an allosteric mechanism most likely induced by contact with the MFP has been proposed for the opening of the TolC channel (Bavro et al, 2008). This is based on the observation that the three inner coiled coils of TolC differ from the outer coiled coils simply by small changes in superhelical twist. Therefore, it was envisaged that transition to the open state is achieved by the inner coil of each monomer realigning relatively to the outer coil thereby enlarging the aperture diameter. Interestingly, *in vitro*, when the inter- and intramolecular bonds that constrain the three inner coils in the closed conformation were disrupted by mutagenesis, a dramatic increase in current in black lipid membrane measurements was observed, indicating the opening of the entrance. On the other hand permanent closure of the channel, by introduction of disulphide bridges, abolished transport *in vivo*, although the transport substrate, HlyA, still triggered the recruitment of

TolC (Eswaran et al, 2003).

Recent crosslinking experiments showed that in the case of the drug transporter AcrA/MexA, the interaction with TolC/OprM, takes place in the distal region of the α -helical barrel domain of TolC (Lobedanz et al, 2007; Stegmeier et al, 2006). This region is predestined since it provides sufficient space for the unwinding of the coils with subsequent opening of the periplasmatic entrance of TolC.

It is important to mention here that TolC may also have a significant influence on the folding of Type I substrates (Vakharia et al, 2001) and may represent a folding cage together with HlyD.

3.3 The membrane fusion protein HlyD

The name membrane fusion protein, perhaps confusingly, is derived from the low degree of identity of bacterial MFPs with some viral membrane fusion proteins (Dinh et al, 1994). In bacteria, the MFP forms a long-distance contact between the inner and the outer membrane by interacting with both, the ABC transporter and the outer membrane component. The MFPs of Type I secretion systems like HlyD have a short cytoplasmic tail at the N-terminus followed by a stretch of hydrophobic residues. This forms a membrane spanning α -helix (Schulein et al, 1992; Wang et al, 1991). The largest part of the protein resides in the periplasm. Other MFPs, associated with drug efflux systems like AcrE from *E. coli*, are attached to the inner membrane via a lipid modification (Dinh et al, 1994).

Structural information on MFPs of Type I secretion systems is not yet available, although the crystal structures of related MFPs (e.g. MexA) involved in drug transport have been solved (Akama et al, 2004; Higgins et al, 2004). These structures may represent a useful guide to some aspects of HlyD and its homologues, although functionally important residues present in HlyD, e.g. the N-terminal domain (Balakrishnan et al, 2001) or the extreme C-terminus (Schulein et al, 1994) are absent in MexA. On the other hand, as predicted for HlyD, MexA has a large content of coiled coil elements in an overall elongated structure. A striking feature of the MexA structure, also predicted for HlyD, is a lipoyl domain containing a long α -helical hairpin as proposed earlier (Johnson & Church, 1999). The MexA structure was modelled to dock to the TolC structure (Higgins et al, 2004) with the hairpin domain forming the contact

surface. All structural constraints were satisfied when trimeric TolC was modelled with a nonamer of MexA. However, this is in contradiction to previous crosslinking studies for HlyD, supporting the idea of a trimer (Balakrishnan et al, 2001). Nevertheless the docking model predicts that the hairpin domain of AcrA forms the contact surface between ArcA and TolC. This was subsequently confirmed by biochemical studies employing crosslinking (Lobedanz et al, 2007; Stegmeier et al, 2006). Type I secretion membrane fusion proteins possess longer helical sequences than MexA, leading to the conclusion that, HlyD has either a very long hairpin domain or multiple helices are formed. The latter might be more likely since the ABC transporter HlyB has smaller periplasmic domains than MexB and the cognate periplasmic adaptor HlyD is larger than MexA. It might be the case that HlyD may take over some properties normally associated with the energizing module HlyB in forming the translocation pathway.

In addition to crosslinking studies, the close interplay between HlyD and HlyB is supported by suppressor mutant analysis (Schlor et al, 1997). These indicate that for example a *hlyD* mutant deficient in HlyA transport could be rescued by second site suppressor mutations in *hlyD* or *hlyB*.

The function of the MFP in the assembly of the Type I secretion machinery has been studied in three distinct systems: Has, Prt and Hly (Letoffe et al, 1996; Thanabalu et al, 1998). Overall, these studies gave similar results, with the transport substrate triggering the assembly of the Type I secretion system. However in these examples the role of the MFP was apparently different. Within HlyD, the 59 cytosolic residues located at the N-terminus appear to interact with the allocrite HlyA (Balakrishnan et al, 2001). Whereas in the Prt and Has systems, with less than 30 residues extending into the cytosol, there is no evidence for an interaction with the transport substrate (Letoffe et al, 1996). The deletion of the first 30 amino acids in HlyD (an amphipatic helix followed by a charged cluster) abolishes the interaction with HlyA and concomitantly the recruitment of TolC (Balakrishnan et al, 2001). The N-terminal part can only be seen in the Hly subfamily. This could indicate that a distinct region of the C-terminal secretion signal of HlyA is recognized by HlyD in contrast to the allocrite:MFP interaction in the Prt or Has family.

Another difference between the HlyA and the other families is the apparent absence of a preformed allocrite MFP/ABC-independent protein complex in the case of the Has and Prt systems. However, it is not known whether this reflects the real situation or just the difference

in the experimental procedures (co-purification versus crosslinking) in different laboratories. In either case, a stable inner membrane complex, e.g. between HlyB and HlyD, would be an important step towards the establishment of an *in vitro* transport assay. Equally important but less difficult would be a determination of the oligomerization state of HlyD. Is it a nonamer as predicted from the MexA structure or a trimer as predicted from crosslinking studies with HlyD? Both forms would create a symmetry mismatch with HlyB that is presumed to form a dimer.

3.4 The ABC transporter HlyB

Like other bacterial ABC transporters the *E. coli* HlyB has a nucleotide binding domain (NBD) and a transmembrane domain (TMD). The NBD and TMD are encoded on one gene and, therefore, HlyB represents a half-dimer (2 identical molecules of HlyB constitute the functional transporter unit).

HlyB, comparable to other Type I ABC proteins (e.g. CyaB and CvaB) has an additional N-terminal domain which belongs to the C39 peptidase family with a size of around 150 amino acids. In contrast, ABC exporters of the Prt family (HasD, PrtD or RsaD) lack this domain and the first transmembrane segment of the protein is close to the N-terminus. The function of this N-terminal domain in HlyB is obscure, since the transport substrates of Type I secretion systems are not cleaved prior to transport, nor do they contain a double glycine motif; a characteristic motif for substrates of this peptidase family. Finally, the sequence of the HlyB peptidase domain lacks key residues essential for protease activity (Wu & Tai, 2004). Topology studies of the TMD region of HlyB (Schulein et al, 1992; Wang et al, 1991) have shown that the C39-like region may be interrupted by two weakly predicted TM spanning regions. If they exist, they would completely alter any residual protease activity of this region.

HlyB is essential for HlyA secretion and this process depends on ATP hydrolysis (Koronakis et al, 1993). In addition, some mutations in HlyB are able to restore secretion defects caused by mutations in the C-terminal secretion signal of HlyA (Sheps et al, 1995; Sugamata & Shiba, 2005; Zhang et al, 1993). This indicated a direct interaction between HlyB and the transport substrate and was supported by results of surface plasmon resonance (SPR)

experiments, confirming that the NBD of HlyB directly interacts with the C-terminus of HlyA (Benabdelhak et al, 2003). Importantly, binding of HlyA decreased in the presence of ATP, suggesting that the allocrite HlyA is released from the NBD during the ATP hydrolysis cycle. This scenario fits with the idea that modulation of the *in vivo* ATPase activity by the allocrite is expected to avoid any waste of ATP. Indeed, such a modulation of ATPase activity has been reported in an earlier study. In this case the *in vitro* ATPase activity of PrtD was inhibited by the corresponding allocrite (Delepelaire, 1994).

Together with the SPR data from the HlyA studies this result indicates that binding of HlyA by the ABC transporter normally blocks ATP hydrolysis until further downstream transport processes are completed (Benabdelhak et al, 2003).

3.5 The toxin HlyA

HlyA belongs to the family of RTX toxins. The diagnostic structural feature of this family is the presence of a characteristic nonapeptide containing glycine rich repeats (GGXGXDXXX, where X can be any amino acid) that specifically binds calcium ions, giving rise to the name RTX toxins (Strathdee & Lo, 1989). The glycine rich repeats bind Ca^{2+} ions to form a parallel β -roll (Baumann et al, 1993) to induce a well-defined and stable fold of the toxin. It seems reasonable that this structure will be unstable in the absence of Ca^{2+} ions. This is actually the case in the cytosol of *E. coli* where the free Ca^{2+} concentration is around 300 nM (Jones et al, 1999). The presence of the unstructured toxin might either facilitate membrane transport or prevent lytic activity in the producing *E. coli* cell. Moreover, Ca^{2+} is crucial for the haemolytic activity of HlyA (Ludwig et al, 1988) and the activity of other members of the RTX family.

The mechanism of cell lysis is still unclear; some data suggests that HlyA binds unspecific (Valeva et al, 2005) whereas other data propose that HlyA dependent action is receptor-mediated (Lally et al, 1997; Morova et al, 2008).

Despite enormous variation in size, Type I secretion substrates share other features than RTX repeats (Delepelaire, 2004). They contain very few or no cysteines and have an acidic pI between 4 and 5. However, it is not yet clear if these properties are essential for efficient secretion. Furthermore, pore forming cytotoxins of the RTX family are subject to posttranslational modifications, i.e. acylation at specific lysine residues essential for activity of the toxin (Heveker et al, 1994; Stanley et al, 1994).

The remarkable feature of Type I secretion compared to other bacterial translocation processes like the *sec* or *tat* pathway is the C-terminal signal sequence. It is quite obvious that the C-terminal location of the Type I secretion signal implies that protein secretion can only occur after translation. Furthermore, Type I secretion signals are not removed after translocation and might be important for subsequent folding of the secreted protein (Kojima et al, 2003). In the case of HasA, an unusual cleavage of the C-terminus is observed but this occurs rather unspecifically at several sites (Letoffe et al, 1994).

Several studies, based on deletion analysis, localized the secretion signal of HlyA to the C-terminus (Mackman et al., 1987; Nicaud et al., 1986) and more specifically to the last 50 to 60 amino acids (Jarchau et al, 1994; Koronakis et al, 1989b; Mackman et al, 1987; Nicaud et al, 1986). These observations were confirmed by fusions of variable lengths of the HlyA C-terminus to otherwise non-secretable polypeptides (Kenny et al, 1991).

The secretion signal of the Type I transport substrates is not particularly hydrophobic in contrast to the N-terminal signal sequences of the *sec* or *tat* proteins. These sequences are not conserved at the level of their amino acid sequence, although in certain subgroups some conservation can be observed (Holland et al, 2003; Jenewein et al, 2008), namely the HlyA and the Prt subgroup. In these groups the secretion system recognizes and transports a unnatural substrate. The nodulation factor NodO from *Rhizobium leguminosarum* for example is transported by Hly type systems (Scheu et al, 1992) whereas proteases are not secreted (Delepelaire & Wandersman, 1990). In contrast, CvaB is exported by both families presenting the link between both groups (Fath et al, 1991).

All proteins of the HlyA family can be secreted by the *E. coli* HlyBD complex with a high efficiency, when expressed in *E. coli* despite some divergence in amino acid sequence pointing to a structural conserved motif. Certain studies highlight that there are “hot spots” required for secretion (Chervaux & Holland, 1996; Hui & Ling, 2002; Hui et al, 2000). Differences between these spots might assign the substrates to the different groups.

Degenerate protein recognition patterns, exemplified by Type I secretion, are not unique to this system and other ABC transporter systems also show a similar behaviour. For example, the transporter associated with antigen processing (TAP) in humans is also rather promiscuous with respect to the peptides bound and transported (Uebel et al, 1997).

The general model of ABC transporter function supports the idea that binding of the substrate to the transmembrane helices induces the binding and/or hydrolysis of ATP by the NBD. This results in a conformational change in the NBD, generating the power stroke that moves the

substrate across the bilayer (Higgins & Linton, 2004; van der Does & Tampe, 2004). This general model is confirmed by several studies of bacterial and mammalian ABC multidrug transporters, where drug molecules are ‘flipped’ from the inside to the outside of the cell due to ATP hydrolysis (Bolhuis et al, 1996). In addition, recent structural work supports a switch of the substrate binding site from the cytosolic to exterior side of the membrane during the ATP hydrolysis cycle (Dawson & Locher, 2007; Hollenstein et al, 2007b; Hvorup et al, 2007; Locher et al, 2002; Oldham et al, 2007).

The ABC transporter, driving polypeptide translocation by the Type I secretion mechanism, must work in a markedly different way from that envisaged for drug efflux. In this case a transport substrate such as HlyA most likely remains in the cytoplasm, in a complex with unidentified proteins or in a freely diffusing state, until the secretion signal initially docks to the ABC protein and/or the MFP.

Interestingly, in case of HlyA it was shown by *in vitro* measurements that ATP competes with HlyA for binding and can efficiently displace pre-bound HlyA from the NBD (Benabdelhak et al, 2003). Moreover, the HlyA/NBD interaction was abolished when the secretion signal region (the last 57 C-terminal amino acids) was deleted from the HlyA fragment. From these results it was proposed that an early stage in the translocation process involves binding of the secretion signal to the NBD. This induces a conformational change, promoting binding of ATP to the NBD. In turn it was proposed that this results in displacement of the HlyA molecule into the translocation pathway. However, at this stage of our understanding, it remains far from understanding whether this interaction of the HlyA molecule with the N-terminus of HlyD some time ago described (Thanabalu et al, 1998) precedes or follows these events.

4. ABC transporters

Apart from bacterial protein secretion ABC transporters perform a huge variety of transport processes. ABC transporters constitute one of the largest families of transmembrane proteins present in all known organisms (Holland et al, 2003). They use the energy derived from binding and hydrolysing ATP to drive the export or import of various molecules across cell membranes. In addition to secretion of proteins to the extracellular medium via the Type I secretion system, ABC transporters are responsible in *E. coli* for the import of essential

nutrients like maltose or histidine and the export of lipids or drugs (Holland et al, 2003). In eukaryotes only exporters can be found, whereas in bacteria and archaea importers and exporters are present. The most remarkable feature of ABC transporters is the wide substrate spectrum ranging from small ions in the case of the human ATP gated ion channel CFTR to large bacterial proteins exemplified by the *E. coli* haemolysin system or the *P. fluorescens* LapA secretion system, in which an adhesion factor of around 900 kDa is transported by its secretion machinery (Hinsa et al, 2003). Confined by those two extremes ABC transporters are capable of transporting metabolites like sugars or amino acids, peptides and hydrophobic substrates or conjugates thereof.

In humans 48+1 ABC transporter genes are found, comprising a huge variety of very specific functions. The absence or a genetic variation of ABC transporters can cause severe diseases like the all-too-common inherited disease of cystic fibrosis, which is caused by the absence of the ATP dependent chloride-ion channel CFTR (cystic fibrosis transmembrane conductance regulator; Gadsby et al, 2006; Riordan et al, 1989) in the plasma membrane. Also neurological diseases, retinal degeneration, cholesterol and bile transport defects, anaemia and drug response phenotypes are caused by abnormal ABC transporter function (Dean et al, 2001).

ABC transporters typically comprise a core domain of four domains, two TMDs and two cytosolic NBDs, encoded either by a single chain or separated polypeptides. An example of the domain architecture is shown in Figure A3, where structure of the Vitamin B₁₂ importer BtuCD is depicted (Locher et al, 2002).

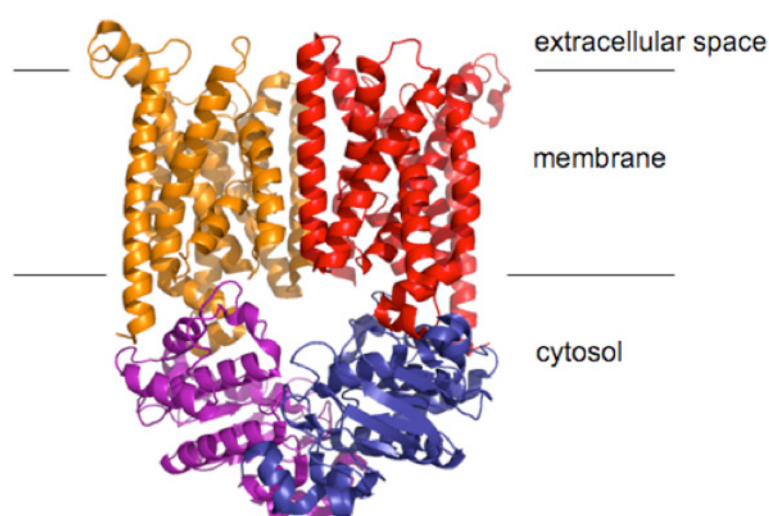


Figure A3: Modular structure of ABC transporters exemplified by the *E. coli* Vitamin B₁₂ importer BtuCD (Locher et al, 2002). Two NBDs (magenta and blue) residing in the cytosol are in close contact with the two TMDs (orange and red).

The NBDs display a high sequence similarity in all ABC transporters (Figure A4) despite their widely different allocrites. Contrarily, the TMDs display very little sequence homology. Additional domains and proteins like for example the MFP in case of the Type I secretion system, a substrate binding protein (SBP) in case of bacterial ABC importers or further transmembrane spanning α -helical segments like in the case of human Mrp1 (ABCC1) facilitate a higher substrate specificity and transport efficiency adjusted to special needs. All conserved motifs important for ATP binding and hydrolysis reside in the NBD (Higgins & Linton, 2004; van der Does & Tampe, 2004). Eight high-resolution structures of full-length ABC transporters and several NBDs have been solved (Dawson & Locher, 2006; Gerber et al, 2008; Hollenstein et al, 2007b; Hvorup et al, 2007; Kadaba et al, 2008; Locher et al, 2002; Oldham et al, 2007; Oswald et al, 2006; Schmitt et al, 2003; Smith et al, 2002b; Ward et al, 2007; Zaitseva et al, 2005a). From those structures and intensive biochemical data it has been concluded that ABC transporters need two NBD and two TMDs to form a functional unit (Fetsch & Davidson, 2002; Zaitseva et al, 2005a; Zaitseva et al, 2005b). However, the only structural information obtained so far for ABC transporters involved in Type I secretion are the crystal structures of the isolated NBD of HlyB in several states of the ATP hydrolysis cycle (Zaitseva et al, 2006). Like other ABC domains, this one is composed of two subdomains, the catalytic domain and the helical domain, the latter harbouring the ABC signature motif.



Figure A4: Sequence alignment of different NBDs. Conserved motifs are coloured. The Walker A and B motif is coloured in blue and red. The C-loop, or the signature motif, is shown in purple. The Q-loop and the P-loop are

depicted in orange and pink, respectively. The D-loop is black and the H-loop is brown. In red, marked with an A is the residue interacting with the adenine moiety of ATP via π - π -stacking.

Despite the high level of conservation, superimposition of several NBD structures revealed a small, so-called structurally diverse region (SDR) located in the helical domain, just in front of the C-loop. This region is presumed to play an important role in subunit interaction and/or intramolecular signalling (Schmitt et al, 2003).

5. Mechanism of ABC transporters

Despite of all the different substrates ABC transporters have a highly conserved energizing module, the NBD. Within the NBD the chemical energy stored in the terminal phosphoanhydridic bond of ATP is converted into mechanical energy leading to vectorial transport.

Common mechanistic features can be expected whereas in between the different subgroups (importers versus exporters) one might anticipate individual attributes. The common themes give rise to several essential questions remaining to be characterized for the different transporters and their corresponding allocrites:

- i) How many substrates are transported across the membrane per hydrolysis cycle or per hydrolysed ATP?

Conversion of the energy derived by the hydrolysis of ATP to the TMD movement is the driving force presumed to operate in all ABC transporters. The substrate translocation is strictly coupled to the ATP hydrolysis cycle (Chen et al, 2001). It has been shown for a SBP dependent import system that the stoichiometry of ATP hydrolysed per molecule of allocrite is two (Patzlaff et al, 2003). However, how this relatively simple model can be applied to transport substrates such as large proteins is not clear yet. However, it is hard to imagine that the transport of the 108 kDa large HlyA protein requires the hydrolysis of only two ATP molecules. It is estimated that the *sec* system consumes one ATP per around 20 amino acids

transported (Uchida et al, 1995). The *tat* system is thought to spend the equivalent of 10000 ATP/protein (Alder & Theg, 2003). It is beyond knowledge how energy consuming the Type I secretion is. Currently, evidence simply indicates that ATP hydrolysis is absolutely required to drive transport of HlyA to the exterior (Koronakis et al, 1993).

At this stage nobody understands degenerated ABC transporters, with one degenerated ATP hydrolysis pocket and thus unable to hydrolyse ATP (e.g. *Saccharomyces cerevisiae* PDR5 and Human TAP1/2). However, the transport process is still functional.

ii) How is ATP bound and hydrolysed?

It was realized that ATP hydrolysis is strictly coupled to transport of the cognate allocrites (Bishop et al, 1989; Chen et al, 2001). Studies of the mammalian multidrug resistance pump P-glycoprotein (P-gp) described the biochemistry of the ATPase cycle for the first time, showing that both sites are required for transport function and that ATP is bound and hydrolysed alternately (Senior et al, 1995). Similar models obtained for the bacterial maltose and histidine importer systems supported this model. If the two ATP-binding pockets hydrolyse ATP non-simultaneously, one can assume that both NBDs are coupled to distinct steps in the transport cycle; for example, ATP hydrolysis of the first ATP might fuel substrate translocation and the second might reset the transporter into the ground state.

Recent data challenged this model suggesting that every single ATP binding pocket undergoes a strict, concerted interaction with the opposite ATP binding pocket during the catalytic cycle. Excellently reviewed by Higgins and Linton (Higgins & Linton, 2004) the ATP switch model summerizes recent advances. In this model the transport cycle is initiated by the interaction of the substrate with the ABC transporter, thus enabling the binding of ATP as this has been shown for the Maltose permease (Mannering et al, 2001). Two ATP/Mg²⁺ molecules are sandwiched between two NBD monomers, as proven earlier by biochemical studies (Fetsch & Davidson, 2002) and structural work done for *M. jannaschii* MJ0796 (Smith et al, 2002). In this “head-to-tail” orientation of the NBDs the ATP binding pocket comes into close contact with the C-loop of the opposing dimer creating an ATPase active site (Figure A5).

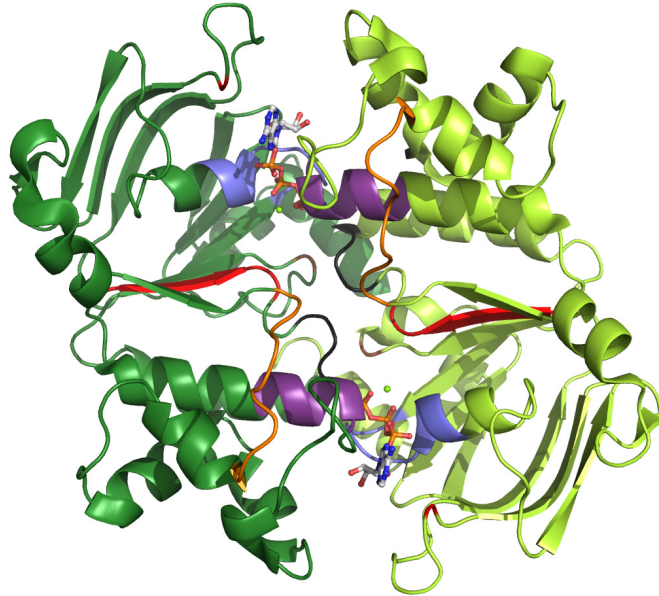


Figure A5: ATP/Mg²⁺-bound sandwich dimer of the HlyB-NBD mutant H662A. View from the membrane side. Conserved motifs are coloured. The Walker A and B motifs are coloured in blue and red, respectively. The C-loop is shown in purple. The Q-loop is depicted in orange and the D-loop is coloured black and the H-loop is brown. The residue interacting with the adenine moiety of ATP via π - π -stacking is coloured in red. Mg²⁺ is presented as green sphere. It can be readily seen that the C-loop complements the ATP binding pocket, thereby forming an hydrolysis competent state.

For transport the substrate binding site (with bound substrate) has to switch from a high affinity site accessible from one site of the membrane (“inside”) to a low affinity site accessible from the opposing site (“outside”), as it could be shown for multidrug transporters (Martin et al, 2001). This step is the major transport step in contrast to the alternating site model described previously where the ATP hydrolysis step and the transport step occurs simultaneously.

The substrate is consequently released at the other site of the membrane. This release triggers the cleavage of the β - γ phosphodiester bond of ATP (Higgins & Linton, 2004). The exact molecular mechanism how ATP hydrolysis is triggered is currently unknown. This model is established for multidrug transporters. It could not be fully adopted to SBP dependent importers, where an inhibition with substrate could not be observed since substrates cannot access the low affinity binding site residing inside the transporter. It seems also unlikely that the transport in Type I secretion systems can occur in one step, meaning the substrate is released before ATP hydrolysis. One might speculate that the trigger is non-functional and the ATP hydrolysis event is induced by substrate binding on a single site of the transporter (high affinity binding site). On the other hand it is still unclear what event is catalysed by ATP

hydrolysis in these ABC exporters. The translocation event itself could also be catalysed by for example the pH gradient.

A variation of this model, valid for all ABC systems, would be that ATP hydrolysis is a consequence of a closed ATP/Mg²⁺ dimer, in which a microenvironment is created where ATP can be hydrolysed (Hanekop et al, 2006). This idea is supported by the fact that a stable nucleotide bound NBD dimer could only be obtained after mutating key essential amino acids for ATP hydrolysis (Smith et al, 2002b; Zaitseva et al, 2005a; Zaitseva et al, 2005b).

Looking at other systems it seems likely this scenario takes place: The GTPase activating protein (GAP) of the *ras* signal transduction pathway inserts the side chain of a conserved arginine into the active site of the Ras protein. The positive charge of this “arginine finger” compensates the negative charges of the oxygen atoms of the γ -phosphate in the transition state, thereby accelerating the GTPase hydrolysis by orders of magnitude (Ahmadian et al, 1997). Another prominent example is displayed the F₁F₀-ATPase where an arginine of the α -subunit completes a catalytic ensemble of residues located in the β -subunit (Nadanaciva et al, 1999).

ATP is hydrolysed in a stepwise and highly cooperative manner. The communication between the *cis* ATP binding pocket and the *trans* binding pocket is most likely arranged by the D-loop (Zaitseva et al, 2006). Finally, after ATP is hydrolysed, P_i is released either according to the phosphate tunnel hypothesis (Zaitseva et al, 2006) or after the dimer is torn apart according to the electrostatic repulsion hypothesis (Smith et al, 2002b). ADP destabilises the dimer and is finally released and consequently the ABC transporter is reset to its basal state.

It appears that two ATP molecules are commonly bound and hydrolysed during a transport cycle in a cooperative fashion. However, for some ABC transporters, where important catalytic residues are degenerated, only a single hydrolytic event may destabilise the “closed NBD dimer” and restore the transporter to its basal state. The other ATP pocket with functional binding but deficient in hydrolysis might have a more regulatory role like it was shown for Mrp1 and other ABC proteins (Gao et al, 2000).

It is not possible yet to be unequivocal about the mechanism of catalysis, particularly given that with the current dataset one cannot assess e.g. asymmetric ABC transporters.

iii) How is the energy derived by the ATPase reaction transmitted to the TMD?

As outlined the key step during transport is the dimerisation of the NBDs. This dimerisation is transmitted to the TMD via non-covalent interactions at the “transmission interface”, presenting the NBD-TMD contact surface.

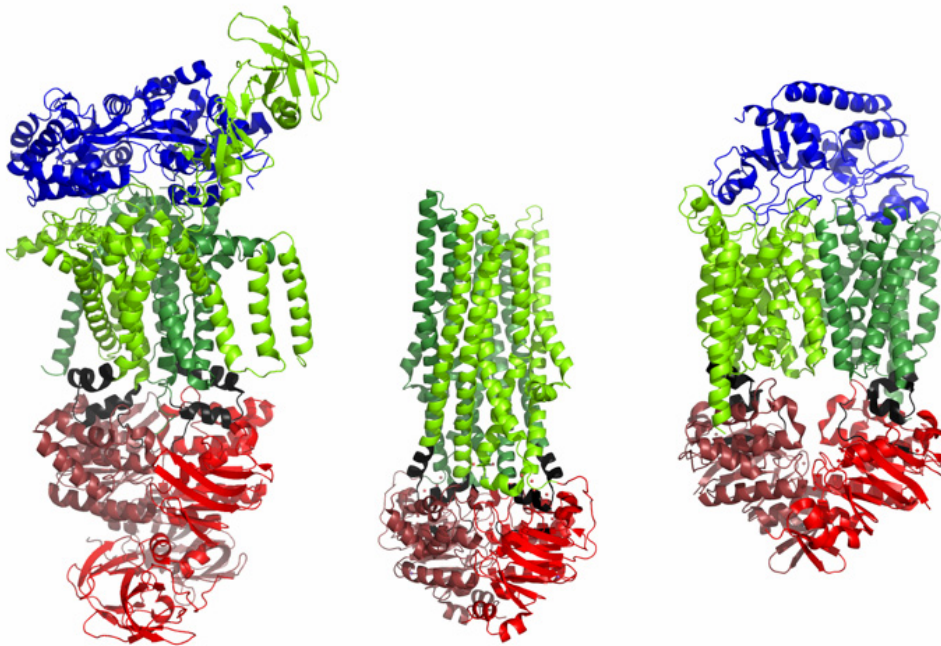


Figure A6: Crosstalk in ABC transporters. In the figure the structures of the maltose permease MalFGK₂E (left, Oldham et al, 2007), The putative MDR ABC transporter SAV1866 (middle, Dawson & Locher, 2006) and the vitamin B₁₂ importer BtuCDF (right, Hvorup et al, 2007) are shown. Coupling helices of the TMD and motifs residing in the NBD contributing to the interaction surface are coloured in black. In the TMD two short helical segments are structural well conserved in importers and exporters. The central theme on side of the NBD, contributing to the interface, are residues around the Q-loop up to the X-loop, which is part of the SDR, are also coloured in black. Whereas the interactions in case of the maltose permease and the vitamin B₁₂ importer occur between NBD A and TMD A and NBD B and TMD A, respectively, in case of SAV1866 the TMD A interacts with NBD B and A and *verse visa*.

The NBDs contribute structurally to this interface with amino acids in between the Q-loop and the signature motif (called X-loop in agreement with the SDR proposed in earlier work; Dawson & Locher, 2006; Schmitt et al, 2003), while the TMDs of the structural well characterized transporters all show similar α -helical segments accomplishing the contacts to the NBDs pointing to the fact that not only the NBD is highly conserved but also the energy transmission to the TMD. Despite the high similarity of the coupling helices, these helices are domain swapped in case of the exporter Sav1866, meaning the coupling helices of TMD B interact with the X-loop of NBD A, where in case of the known importers the helices of TMD A interact with the X-loop of NBD A (Figure A6).

Future work has to focus on structural work of different, individual stages occurring during transport in a single ABC transporter.

6. Membrane protein overexpression

In both, prokaryotes and eukaryotes, 20–30% of all genes encode membrane proteins (Wallin & von Heijne, 1998). These proteins residing in the interface of the interior and exterior of cells or cellular organelles perform vital transport functions, signal transduction and other crucial cellular processes. The natural abundance of membrane proteins is usually too low to isolate sufficient material for functional and structural studies. Membrane protein overexpression with subsequent successful purification is challenging not only because of the poor protein yield, but also because of the need to choose a proper detergent, shielding the hydrophobic transmembrane segments. In the last years a lot of knowledge has arisen which is illustrated by the steadily growing number of high-resolution structures obtained by overexpression of membrane proteins (Wagner et al, 2006), but still less than 0.5 % of structures deposited in the pdb represent membrane proteins (for a comprehensive and up-to-date list see http://blanco.biomol.uci.edu/Membrane_Proteins_xtal.html).

The key questions in the overexpression of membrane proteins are i) what are the bottlenecks limiting the overexpression of membrane proteins and ii) which experimental setup is most likely the solution to overcome this problem.

i) Compared to soluble proteins membrane protein expression is a more challenging task. After being released by the ribosome the polypeptide has to be targeted to the membrane. This targeting and insertion of heterologously overexpressed membrane proteins has been extensively studied in *E. coli*. *In vitro* translation crosslinking approaches have shown that heterologously expressed membrane proteins make contact with the signal recognition particle (SRP), the Sec translocon and YidC (Raine et al, 2003).

Nevertheless, this does not necessarily mean that the *E. coli* components are optimal for assistance in the targeting, insertion and folding of heterologously expressed membrane proteins into the membrane. Some of the charged residues in the yeast Sec61 translocon that are proposed to be important for proper functioning are not conserved in the prokaryotic Sec translocon (Rapoport, 2007). Thus, it is very well possible that subtle differences in the insertion process could contribute to the difficulties experienced in the heterologous

overexpression of membrane proteins. After release of the translocon into the lipid environment the lipid composition can interfere with folding and correct function. Also folding of soluble domains of membrane proteins might require the presence of certain chaperones not present or not in a sufficient amount in the chosen host (Baneyx & Mujacic, 2004).

It is known that for certain proteins a proper posttranslational modification like glycosylation is required not only for the function but also for the folding. This might be absent if an eukaryotic membrane protein is heterologously overexpressed in a prokaryotic host (Baneyx & Mujacic, 2004).

Furthermore if the desired protein is dominantly overexpressed the translocon can be overloaded and the lack of essential host proteins attenuates the growth. The accumulation of non-native or foreign structures in a membrane can induce stress responses with following induction of proteolytic systems underlining the need of an orchestrated expression of the desired protein together with host proteins. In addition recently it has been shown that overexpression of membrane proteins in the cytoplasmic membrane severely hampers also protein homeostasis in the cytoplasm. This is likely to be another major reason for the toxicity of membrane protein overexpression (Wagner et al, 2007).

ii) Certain expression hosts have a clear advantage compared to other regarding posttranslational modification, yield and easiness, see for example (Midgett & Madden, 2007). Here, I will restrict on the usage of prokaryotic hosts, which are the most favourite choice.

It has been shown in a comprehensive analysis of a large-scale overexpression screen of *E. coli* membrane proteins that levels of membrane-integrated proteins do not correlate with easily characterized (and manipulated) sequence characteristics such as codon usage, protein size, hydrophobicity and number of transmembrane helices (Daley et al, 2005). So even in its natural host only a sketchy picture is drawn which factors benefit expression of membrane proteins. What approach can be done in order to push this expression to higher yields?

Choice of the right host or strain: More than a decade ago derivatives of the commonly used overexpression *E. coli* strain BL21(DE3) with improved characteristics for membrane protein overexpression were isolated (Miroux & Walker, 1996). The isolation was based on the ability of the cells to cope with toxic effects of the overexpression of a particular membrane protein. The resulting *E. coli* strains C41(DE3) and C43(DE3) are the best known examples of strains isolated from this screen. The toxicity of the target protein is reduced and plasmid

stability is improved, particularly in C43(DE3) (Dumon-Seignovert et al, 2004). For reasons Growth is hardly affected on induction of membrane protein overexpression. Furthermore yields are increased due to membranes accumulating in the cytosol (Arechaga et al, 2000). The C41(DE3) and C43(DE3) strains are now widely and very successfully used to overexpress membrane proteins in *E. coli*. A more dramatic effect can be seen if one switches from the Gram-negative overexpression host *E. coli* to the Gram-positive bacteria *Lactococcus lactis* due a slight change in codon usage, membrane protein integration mechanism, membrane composition and further factors influencing protein expression. *L. lactis* has been successfully used in overexpression of several prokaryotic and eukaryotic membrane proteins (Kunji et al, 2005; Kunji et al, 2003). It has been shown that some proteins expressing only with a poor yield or non-functional in *E.coli*, *L. lactis* serves a successful host for these proteins (Monne et al, 2005). Since *L. lactis* is easy to cultivate and manipulate it is worth considering this organism before using eukaryotic overexpression hosts is considered.

Choice of expression conditions: As mentioned above high translation rates can hamper host survival or the expression of the protein. It has been beneficial to decrease the translation rate by lowering the culture temperature, changing the inducer concentration or by choosing another promoter (Lewinson et al, 2008; Surade et al, 2006). If any cofactors like metals or ligands are known one might supplement the media with such factors. But also cofactors like chaperones or bound proteins coexpressed with the target have been proven to be beneficial for some cases although this has to be tested empirically (Sorensen & Mortensen, 2005).

Engineering the protein: In addition to the optimization of expression conditions or the choice of the host one can also engineer the protein itself; either by optimization of the codon usage or by taking for example a close homologue of the chosen protein in order to improve not only yield but also other downstream factors like stability (Baneyx & Mujacic, 2004). Also a selective change of certain amino acids might trigger the right insertion into the membrane (Rapp et al, 2006).

Well-known for membrane proteins as well as for soluble proteins is the fact that N-terminal or C-terminal fusions to the protein have a significant impact on yield (Lewinson et al, 2008; Mohanty & Wiener, 2004). A N-terminal fusion of certain sequences might also help membrane targeting and integration. Mistic, a *Bacillus subtilis* protein, has been reported to improve the expression of several eukaryotic membrane proteins, by targeting them to the

membrane and might therefore represent a “membrane integration chaperone” (Roosild et al, 2005). Further experiments are needed in order to approve its general ability.

Fusions might not only helping folding or integration but also detection are widely used in larger proteomic projects (Daley et al, 2005; Drew et al, 2006) and they might help to solve for example topology issues. In a recent report an additional possibility was applied successfully: an internal fusion was used to overcome the presence of highly flexible loops hampering stabilisation and crystallization (Rosenbaum et al, 2007).

In a nutshell there is a way to rationalize membrane protein overexpression: In order to maximize the number of targets being expressed, several highly homologues genes should be chosen and tested for overexpression in distinct vectors with different types of promoters, using N- or C-terminal tags. The choice of the host depends crucial on the target chosen.

7. Aims and objectives

The HlyB-NBD is the energizing module of the Hly system. Characterisation of this isolated domain will deepen the knowledge of the mechanism of ATP hydrolysis valid also for other ABC transport systems. Along with structural insights into nucleotide binding domains biochemical work was essential to proof concepts how the chemical energy derived by ATP hydrolysis is obtained. Solving the problem how ABC transporters ensure that ATP hydrolysis only occurs well ordered with the mechanisms needed for substrate translocation is a major challenge in the field of ABC transporters.

Enormous progress had been made in understanding the molecular assembly of the Type I secretion machinery. Certainly highlighted by the structure of TolC solved in 2000 (Koronakis et al, 2000), but also other reports provided important insights into the knowledge of the overall architecture (Letoffe et al, 1996; Thanabalu et al, 1998). However, how the single components work, how they interplay with each other is not yet clear. In-depth biochemical studies were largely hampered by the very low expression.

The main focus of this thesis was to create tools to study the inner membrane components to set the basis for a detailed characterisation by biochemical and biophysical methods. An important problem to be solved was certainly the very low expression of the inner membrane components of the Hly system hampering *in vitro* studies for almost 20 years now. Successful overexpression would enable extensive biochemical studies.

Reminiscent of the *sec* machinery, proteins immediately displaying their successful transport by an activity or change in size are needed. HlyA itself is rather inconvenient to work with, therefore new proteins hitch-hiking with the HlyA secretion signal through the transporter were needed as reporter. However, since the requirements for Type I secretion substrates were not clear, these requirements needed to be determined.

B. Materials and Methods

1. Materials

Media

Agar-Agar	Serva
Ampicillin	Roth
Arabinose	Roth
Ascorbate	AppliChem
Glycine	Roth
β -Glycerol phosphate	Sigma-Aldrich
Chloramphenicol	Roth
Columbia Blood Agar plates	bioMerieux
Glucose	Caesar & Loretz
Isopropylthiogalaktoside (IPTG)	AppliChem
Kanamycin	Roth
Magnesium sulfate	Fluka
Peptone from beef	Roth
Peptone from caseine	Roth
Peptone from soj	Roth
Sucrose	AppliChem
Tetracycline	Roth
Tryptone/Peptone	Difco
Yeast extract	Difco

Buffers, salts and additives

DTT (1,4-Dithiotreitol)	AppliChem
Calcium chloride (CaCl_2)	Grüssing
Acidic acid	Normapur
EDTA (Ethylendiamine-tetra-acidic acid)	AppliChem
Glycine	Roth
Glycerol 98%	Caesar & Loretz
HEPES (4-(2-hydroxyethyl)-1-piperazineethanesulfonic acid)	AppliChem
L-Histidine	Fluka
Hydrochloric acid, 37% (HCl)	Riedel-de Haën
Imidazole	Fluka
Maltose	J.T. Baker
Magnesium chloride (MgCl_2)	Fluka
MES (2-(N-Morpholino)-ethansulfonic acid)	Fluka

Sodium phosphate (Na_2HPO_4)	Normapur
Sodium phosphate (NaH_2PO_4)	Roth
Sodium malonate	Sigma
PMSF (Phenylmethylsulphonyl fluoride)	Roth
Potassium chloride (KCl)	Sigma
Protease inhibitors cocktail (Roche Complete [®] tablets)	Roche
Sulfuric acid, 96% (H_2SO_4)	Fisher
SDS (Sodium dodecylsulphate)	Fluka
Sodium azide (NaN_3)	Fluka
Sodium chloride (NaCl)	J.T. Baker
TCA (Trichloroacetic acid)	Fluka
TRIS (Trizma, Tris(hydroxymethyl)-aminomethan)	Sigma
Tween 20	Fluka
Urea	Riedel-de Haën

Solvents

Aceton	Riedel-de Haën
Formaldehyde 37 %	Roth
Chloroform	Roth
DMSO (Dimethylsulfoxide)	Roth
Ethanol	Roth
ddH ₂ O Milli-Q ⁵⁰ Plus	Millipore
Isobutanol	Roth
Isopropanol	Roth
Methanol	Roth

Detergents

Asolectin (Soj bean)	Fluka
Big Chaps	Anatrace
C ₁₂ E ₈	Anatrace
DM (Decyl-β-D-maltopyranosid)	Glycon
DDM (Dodecyl-β-D-maltopyranosid)	Glycon
FC-14 (FOS-CHOLINE-14)	Anatrace
NDM (Nonyl-β-D-maltopyranosid)	Glycon
OG (Octyl-β-glucopyranosid)	Glycon
SDS (Sodiumdodecylsulfate)	Serva
Triton X-100	Roth
Tween-20	Roth

Markers

Molecular weight marker kit for gelfiltration
Native Marker
PageRuler 1000bp Ladder
PageRuler 100bp Ladder
Prestained Protein Molecular Weight Marker

Sigma
Invitrogen
MBI Fermentas
MBI Fermentas
MBI Fermentas

Nucleotides

AMP (Adenosine-5'-monophosphate)
ADP (Adenosine-5'-diphosphate)
ATP (Adenosine-5'-triphosphate)
Beryllium chloride (BeCl_2)
Sodium fluoride (NaF)
Sodium azide (NaN_3)
TNP-ADP (2'(or 3')-O-(2, 4, 6-trinitrophenyl)-adenosine-5'-diphosphate)
TNP-AMP
TNP-ATP (2'(or 3')-O-(2, 4, 6-trinitrophenyl)-adenosine-5'-monophosphate)

Fluka
Fluka
Fluka
Sigma-Aldrich
Sigma-Aldrich
Fluka

Molecular Probes
Molecular Probes

Molecular Probes

Columns column material

Superdex 3.2/30 PC gel filtration
HR 26/60 Superdex 200 gel filtration
NTA agarose beads / NTA sepharose beads
Q-Sepharose FF HiTrap
Strep-Tactin Sepharose
Tricorn GL10/300 Superdex 200 gel filtration
 Zn^{2+} /IDA 1ml HiTrap
 Zn^{2+} /IDA 5ml HiTrap
Amylose-Sepharose

GE Healthcare
GE Healthcare
Qiagen
GE Healthcare
IBA GmbH, Göttingen
GE Healthcare
GE Healthcare
GE Healthcare
New England Biolabs

Other chemicals

β -Mercaptoethanol
Acrylamid/Bisacrylamid solution (37.5:1; 30%)
Agarose GTQ
Ammoniummolybdate Tetrahydrate
APS (Ammoniumperoxodisulphate)
Bromphenol blue

Roth
Roth
Roth
Fluka
Roth
Sigma-Aldrich

Coomassie Brilliant Blue R-250	Roth
Coomassie Plus Bradford solution	PIERCE
DSP (Dithiobis(succinimidylpropionate))	PIERCE
ECL <i>advance</i> solution 1 + 2	GE Healthcare
Ethidium bromide solution (10 mg/ml)	Roth
Malachite green	Sigma-Aldrich
NBT/BCIP tablets	Sigma-Aldrich
Phenol/chloroform/isoamyl alcohol mixture (25:24:1)	Roth
Sodium carbonate (Na ₂ CO ₃)	Roth
Silver nitrate (Ag ₂ NO ₃)	Fluka
TEMED (Tetramethylethylenediamine)	Merck
Xylencyanole	Roth
HellmaEx	Hellma

Enzymes and proteinous additives

AmpLigase	Epicentre
BSA) (Bovine serum albumin)	Roth
Calf intestine phosphatase	Fermentas
Deoxyribonuclease I (DNase I)	Sigma
Factor Xa	NEB
Lysozyme	Fluka
<i>Pfu</i> DNA Polymerase	Fermentas
<i>Phusion</i> DNA Polymerase	Finnzymes
Restriction enzymes (NcoI, BspHI, ClaI, SmaI, XmaI, BamHI, EcoRI, SacI, NdeI, XbaI, SwaI, KpnI, DpnI)	Fermentas & NEB
T4 DNA Ligase	NEB
T4 DNA Polymerase	Roche
T4 Polynukleotidkinase (PNK)	Fermentas
<i>Taq</i> DNA Polymerase	NEB
SecB	Gift of J. de Keyzer, Groningen

Antibodies

anti-HlyA from rabbit	provided by Prof. K. Kuchler, Vienna
anti-HlyB from rabbit	provided by Prof. K. Kuchler, Vienna
anti-HlyD from rabbit	provided by Prof. B. Holland, Paris
anti-His (pentaHis antibody)	Quiagen
Streptactin-AP	Chemicon
anti-rabbit antibody coupled to horse radish peroxidase (HRP) from goat	Sigma-Aldrich
anti-mouse antibody coupled to HRP from goat	Dianova

DNA kits

QIAquick Gel Extraction Kit
NucleoBond PC 100 Plasmid Midi Kit
NucleoSpin Plasmid Mini Kit

Quiagen
Macherey-Nagel
Macherey-Nagel

Consumables

Amicon Ultra 15 (MWCO 10 kDa)
Amicon Ultra 15 (MWCO 30 kDa)
Amicon Ultra 15 (MWCO 50 kDa)
Amicon Ultra 4 (MWCO 30 kDa)
Amicon Ultra 4 (MWCO 50 kDa)
Microtiterplates
PVDF blotting membrane
Reaction tubes 1.5 ml and 2.0 ml
Reaction tubes 15 ml and 50 ml
Reaction tubes for PCR (singles or stripes)
Dialysis tube (cut-off 6-8 kDa / 10-12 kDa)
Empty plastic columns (1 ml, 10 ml)
Pipette tips

Millipore
Millipore
Millipore
Millipore
Millipore
Greiner Bio-One
Pall corporation
Eppendorf
Sarstedt
Greiner
Spectrapor
Biorad
Sarstedt

Strains

Escherichia coli strains:

XL1 blue	endA1 gyrA96(nal ^R) thi-1 recA1 relA1 lac glnV44 F'[:Tn10 proAB ⁺ lacI ^q Δ(lacZ)M15] hsdR17(r _K ⁻ m _K ⁺). A Stratagene strain (www.stratagene.com).
MC1061	hsdR2 hsdM+ hsdS+ araD139 Δ(ara-leu)7697 Δ(lac)X74 galE galK galU+ rpsL (StrR) mcrA mcrB1. Parent strain of TOP10/DH10B provided by E. Geertsma (University of Groningen) (Casadaban & Cohen, 1980) genotype update in 2008 (Durfee et al, 2008).
BL21 (DE3)	F ⁻ ompT gal dcm lon hsdS _B (r _B ⁻ m _B ⁻) λ(DE3 [lacI lacUV5-T7 gene 1 ind1 sam7 nin5]), (Studier & Moffatt, 1986; Wood, 1966) courtesy of Prof. R. Tampé, University of Frankfurt.
BL21 (DE3) C41	as BL21 (DE3) modified in (Miroux & Walker, 1996) courtesy of Prof. R. Tampé, University of Frankfurt.
BL21 (DE3) C43	as BL21 (DE3) modified in (Miroux & Walker, 1996) courtesy of Prof. R. Tampé, University of Frankfurt.

Top10	F- mcrA Δ(mrr-hsdRMS-mcrBC) φ80lacZΔM15 ΔlacX74 nupG recA1 araD139 Δ(ara-leu)7697 galE15 galK16 rpsL(StrR) endA1 λ- genotype update in 2008 (Durfee et al, 2008). Supplied by Invitrogen.
SE5000	araD139Δ(argF-lac)U169 rpsL150 relA1 flb-3501 deoC1 ptsF25 rbsR recA56 received from M. Blight (Gherardini et al, 1990).
S541	araΔ(lac-pro) rpsL thi supD+ fimE::IS1 Δbgl-AC11 ΔlacZ-Y217 courtesy of Prof. Karin Schnetz, University of Cologne.
S2303	araΔ(lac-pro) rpsL thi supD+ fimE::IS1 Δbgl-AC11 ΔlacZ-Y217 hns::kan courtesy of Prof. Karin Schnetz, University of Cologne.
S614	araΔ(lac-pro) rpsL thi supD+ fimE::IS1 Δbgl-AC11 ΔlacZ-Y217 hns::amp courtesy of Prof. Karin Schnetz, University of Cologne.
WM2429	also BW25113, <i>lacIq rrnBT14 LacZWJ16 hsdR514 araBADAH33 rhaBADLD78</i> , <i>E. coli</i> Genetic Stock Center, Yale University.

Lactococcus lactis strains:

NZ9000	MG1363 derivate with pepN::nisRK (Kuipers et al, 1997). MG1363 is a plasmid-free derivative of <i>L. lactis</i> ssp. <i>cremoris</i> NCDO712 (see also www.MG1363.net); provided by NIZO.
NZ9700	Nisin producing transconjugant of MG1363 containing the nisin-sucrose transposon Tn5276 (Kuipers et al, 1993); provided by NIZO.

Plasmids

pCRTopo	<i>E.coli</i> ; cloning vector; amp ^R , kan ^R	Invitrogen
pET401	<i>E.coli</i> ; cloning vector; amp ^R	K. van Wely, Groningen, unpublished
pBADHisB	<i>E.coli</i> ; expression vector; amp ^R	Invitrogen
pBADnLIC	<i>E.coli</i> ; expression vector; amp ^R	(Geertsma & Poolman, 2007)
pET324	<i>E.coli</i> ; expression vector; amp ^R	C. Does, Groningen (van der Does et al, 1996)
pK184	<i>E.coli</i> ; expression vector, kan ^R	(Jobling & Holmes, 1990)
pET28b	<i>E.coli</i> ; expression vector; kan ^R	Novagen
pNZ8048	<i>L.lactis</i> ; expression vector; cm ^R	NIZO

pBAD18amp	<i>E.coli</i> ; expression vector; amp ^R	IB Holland, Paris (Guzman et al, 1995)
pLG813	<i>E.coli</i> ; expresses HlyCA; cm ^R	IB Holland, Paris (Kenny et al, 1992)
pLG814	<i>E.coli</i> ; expresses HlyBD; kan ^R	IB Holland, Paris (Kenny et al, 1992)
pLG815	<i>E.coli</i> ; like pLG814, Insert with other orientation	IB Holland, Paris
pPSG122	<i>E.coli</i> ; pBAD18amp, HlyB-NBD (aa 467-707)	IB Holland, Paris (Benabdelhak et al, 2005)
pPSG131	<i>E.coli</i> ; pBAD18amp, HlyA-Cterm (aa 807-1023)	IB Holland, Paris (Benabdelhak et al, 2003)

Oligonucleotides

The sequences for the used oligonucleotides is provided in Table B1. Oligonucleotides were supplied by MWG-Biotech in the lyophilized state. Before usage the sample were dissolved to a concentration of 100 pmol/μl according to the manufacturers data with a TRIS/EDTA buffer (10 mM TRIS, 0.1 mM EDTA).

Table B1: Used oligonucleotides in this work.

Hly1_for	GCTATCCATGGCGAATTCTGATTCTTGTGCATAAAATTGATTATGGG	C
Hly2_rev	GGTTATTTCGGGGATTATCGATTGGTCAGTTAATTGC	C
Hly3_for	GCAATTAAC TGACCAATCGATAAATCCCCGGAATAACC	C
Hly4_rev	CGTGTCTAGATTACAGGATCCCGTCTGACTGTAAGTATATAAGTAACTG	C
Hly4woBam_rev	CGGTTCTAGATTGTTAGTCTGACTGTAAGTATATAAGTAACTG	C
Hly5_for	GCTATCCATGGCGAATTCTAAACATGGTTAATGGGGTTCAGCGAG	C
Hly6_for	CGTTATGAAAATGTATCCCGGGTTGAAAAAAGCC	C
Hly7_rev	GGCTTTTTTCAACCCGGGATACATTTTCATAACG	C
Hly8_rev	CGTGTCTAGATTACAGGATCCACGCTCATGTAACTTTCTGTTACAGACTC	C
Hly8woBam_rev	CGTTGTCTAGATTCTTAACGCTCATGTAACTTTCTGTTACAGACTC	C
CHisBam_for	GATCTCAATCGAAGGGCGCCATCACCATCACCATCACCATCACCATCATTAAAG	O
ChisBam_rev	GATCCTTAATGATGGTGATGGTGATGGTGATGGTGATGGCGCCCTTCGATTGA	O
NHisEco_for	AATTCTCATCACCATCACCATCACCATCACCATCATAGCATCGAAGGGCGC	O
NHisEco_rev	AATTGCGCCCTTCGATGCTATGATGGTGATGGTGATGGTGATGGTGATGAG	O
HlyA 395_rev	CTGGTGTGATTACCCTGCCGTCTT	S
HlyBSeq1589_for	GACATGATCTTGCGTTGGCCGATCC	S
HlyBSeq389_for	CTGTTGCCGGGAAACTGGCGAAATTGAC	S
HlyBSeq400_rev	CGGCAACAGAAAGAACGGGAA	S
HlyDSeq2580_for	CACTGTTACAGACCAGGCTGGAACAAACTC	S
pBAD_for	ATGCCATAGCATTTTTATCC	S
HlyB_D551A_for	GGTTGTGTTGCAGGCCAATGTGCTGCTTAATCG	M
HlyB_D551N_for	GGTTGTGTTGCAGCGCAATGTGCTGCTTAATCG	M
HlyB_D551Q_for	GGTTGTGTTGCAGGAGAATGTGCTGCTTAATCG	M
HlyB_N611A_for	GGCAGGATTATCCGGAGGTCAAGCTCAACGCATCG	M

HlyB_N611D_for	GGCAGGATTATCCGGAGGTCAAGATCAACGCATCG	M
HlyB_N611K_for	GGCAGGATTATCCGGAGGTCAAAAGCAACGCATCG	M
HlyB_S504A_for	TATTGGTATTGTCGGACGTGCTGGTTCAGG	M
HlyB_S504A_rev	TGTGCTTTTCTGAACCAGCACGTCCGAC	M
HlyALIC_for	CATGCATCACCATCACCATCATGGTGAGAATTTATATTTAAATCCCACCCTTC CAGCATCGAAGGCCG	O
HlyALIC_rev	CATGCGGCCTTCGATGCTGGAAGGGTGGGATTTAAATATAAATTCTCACCAT GATGGTGATGGTGATG	O
Ifnar1-SD12LIC_for	ATGGTGAGAATTTATATTTTCAAGGTAAAAATCTAAAATCTCCTC	C
Ifnar1-SD12LIC_rev	TGGAAGGGTGGGATTTACCATTTTCTGGTGGAGGTAG	C
Ifnar1-SD34LIC_for	ATGGTGAGAATTTATATTTTCAAGGTGAAATGAACTACCTCCACC	C
Ifnar1-SD34LIC_rev	TGGAAGGGTGGGATTTACCTTTAGAGGTATTTCTGGTTTTG	C
Ifnar2LIC_for	ATGGTGAGAATTTATATTTTCAAGGTAGTTATGATTTCGCTGATTAC	C
Ifnar2LIC_rev	TGGAAGGGTGGGATTTACCTGAAAATTCTGATTCCTGGC	C
IFN α 2LIC_rev	TGGAAGGGTGGGATTTACCTTCCTTACTTCTTAAACTTTCTTG	C
IFN α LIC_for	ATGGTGAGAATTTATATTTTCAAGGTTGTGATCTGCCGCAGACTC	C
IFN β LIC_for	ATGGTGAGAATTTATATTTTCAAGGTAGCTACAACCTTGCTTGG	C
IFN β LIC_rev	TGGAAGGGTGGGATTTACCGTTTCGGAGGTAACCTG	C
LICcalB_for	ATGGTGAGAATTTATATTTTCAAGGTATGCTACCTTCCGGTTCGGAC	C
LICcalB_rev	TGGAAGGGTGGGATTTACCGGGGTGACGTGC	C
LICFtbzip_for	ATGGTGGAGAATTTATATTTTCAAGGTATGCAAGATCCAAACCCTAAC	C
LICFtbzip_rev	TGGAAGGGTGGGATTTACCGAACGTACTGCTGCTTTC	C
LICSecpos_for	ATGGTGGAGAATTTATATTTTCAAGGTATGGGCTCCGG	C
LICSecpos_rev	TGGAAGGGTGGGATTTACCGGAGCCCATACCTTG	C
MBPLIC_for	ATGGTGAGAATTTATATTTTCAAGGTATGAAATCGAAGAAGGTAAAC	C
MBPLIC_rev	TGGAAGGGTGGGATTTACCGGAGCTCGAATTAGTCTGCGCGTC	C
MalE_A276G_for	CCGAACAAAGAGCTGGGGAAAGAGTTCCTC	M
MalE_A276G_rev	TTCGAGGAACTCTTCCCCAGCTCTTTGTTC	M
MalE_V8G_for	CGAAGAAGGTAAACTGGGCATCTGGATTAAC	M
MalE_V8G_rev	GCCGTTAATCCAGATGCCAGTTTACCTTC	M
MalE_Y283D_for	AAGAGTTCCTCGAAAACGATCTGCTGACTG	M
MalE_Y283D_rev	CATCAGTCAGCAGATCGTTTTCGAGGAACTC	M

C=cloning primer, S=sequencing primer, M=mutagenesis primer, O=oligonucleotide for sequence insertion

Media

If not otherwise stated media components were solubilised in deionized water. Media was sterilised with sterile 0.22 μ m filters or by autoclaving (wet cycle, 20 min, 121 °C). Media was stored at a dark and cold place prior to usage. Recipes are stated in components required per litre media.

LB media

Tryptone/Peptone	10 g
Yeast extract	5 g
NaCl	5 g

2xYT media

Tryptone/Peptone	16 g
Yeast extract	10 g
NaCl	5 g

SOC media

Yeast extract	5 g
Tryptone/Peptone	20 g
NaCl	0.5 g
KCl	2.5 mM
MgCl ₂	10 mM
MgSO ₄	10 mM
Glucose	0.5 %
Add sterile Glucose after autoclaving	

M17 media (GM17 with glucose)

β-Glycerophosphate	19 g
Peptone from Casein	5 g
Peptone from soy	5 g
Peptone from beef	5 g
Yeast extract	2.5 g
Ascorbate	0.5 g
MgSO ₄	1 mM
Glucose	0.5 %
Add sterile Glucose after autoclaving	

ZYM-5052

Tryptone/Peptone	10 g
Yeast extract	5 g
Na ₂ HPO ₄	25 mM
KH ₂ PO ₄	25 mM
NH ₄ Cl	50 mM
Na ₂ SO ₄	5 mM
MgSO ₄	2 mM
0.2x trace metal mixture	
Glycerol	0.5 %
Glucose	0.05 %
α-Lactose	0.2 %
L-Arabinose	2 mM
Metals, glycerol, glucose, lactose and arabinose are sterile filtrated and added before usage.	

1000x trace metals mixture

FeCl ₃	50 μM
MnCl ₂ ·4H ₂ O	10 μM
ZnSO ₄ ·7H ₂ O	10 μM
CoCl ₂ ·6H ₂ O	2 μM
CuCl ₂ ·2H ₂ O	2 μM
NiCl ₂ ·6H ₂ O	2 μM
Na ₂ MoO ₄ ·2H ₂ O	2 μM
Na ₂ MoO ₄ ·5H ₂ O	2 μM
H ₃ BO ₃	2 μM
CaCl ₂	20 μM
dissolved in 10 mM HCl and sterile filtrated	

LB Agar

LB media supplemented with 1.5 % Agar-Agar

GM17 Agar

GM17 media supplemented with 1.2 % Agar-Agar

SGM17-Agar

M17 media supplemented with 1.2 % Agar-Agar and 0.5 M sucrose

Media additives

Antibiotics:

	Stock solution	final concentration
Ampicillin (in H ₂ O)	100 mg/ml	100 µg/ml
Tetracycline (in 50 % Ethanol)	25 mg/ml	25 µg/ml
Kanamycin (in H ₂ O)	30 mg/ml	30 µg/ml
Chloramphenicol (in 70 % EtOH)	30 mg/ml	30 µg/ml (<i>E. coli</i>) 6 µg/ml (<i>L. lactis</i>)

Sugars and inductor solutions

Glucose	40 % (v/v)	
Sucrose	2.5 M	
IPTG	1 M	sterilised by filtration
L-Arabinose	1 M	sterilised by filtration

Buffers for PAGE and Western Blot

4x Stacking Gel buffer

TRIS/HCl pH 8.85	1.5 M
SDS	0.4 % (w/v)

4x Resolving gel buffer

TRIS/HCl pH 6.8	0.5 M
SDS	0.4 % (w/v)

SDS running buffer

TRIS	50 mM
Glycine	190 mM
SDS	0.1 % (v/v)

No pH adjustment needed, pH 8.3 is set

Transfer buffer

1x Running buffer with MeOH	20 % (v/v)
--------------------------------	------------

TBS

TRIS pH 8.0	20 mM
NaCl	250 mM

TBS-T

TBS with Tween [®] 20	0,1 % (v/v)
-----------------------------------	-------------

Blocking solution

TBS-T with 3 % milk powder and 0.05% Na-azide
3 % BSA was used for Strep-/His-Tag detection

Coomassie stain

Acidic acid	10 % (v/v)
Methanol	40 % (v/v)
Coomassie R-250	0.25 % (v/v)

Coomassie destain

Acidic acid	10 % (v/v)
Methanol	40 % (v/v)

Fixation solution for silver stain

Ethanol	30 % (v/v)
Acidic acid	10 % (v/v)

Thiosulphate buffer

Na-acetate pH 6.0	100 mM
Ethanol	30 % (v/v)

Silver nitrate solution

Silver nitrate	0.5 % (w/v)
Formaldehyde (37%)	25 µl/100ml

Developer (fresh before usage)

Na-carbonate	0.25 % (w/v)
Formaldehyde (37%)	50 µl/100ml

5x SDS-Sample buffer (membrane proteins)

Urea	6 M
Stacking gel buffer	0.8x
SDS	3.2 % (w/v)
Bromphenol blue	0.02 % (w/v)
Glycerol	40 %

SDS-5x Sample buffer (soluble proteins)

Stacking gel buffer	0.8x
SDS	3.2 % (w/v)
Bromphenol blue	0.02 % (w/v)
Glycerol	40 %

Sample buffer was typically supplemented with reducing agents. (20 mM DTT or 286 mM β-Mercaptoethanol).

Buffers for DNA gels

TAE buffer

TRIS	40 mM
Acetic acid	20 mM
EDTA	1 mM
Prepared as 50x buffer pH 8.0	

TBE buffer

TRIS	90 mM
Boric acid	90 mM
EDTA	1 mM
prepared as 10x buffer pH 8.0	

10x DNA loading buffer

10x TAE buffer	
Bromphenol blue	0.25 %
Xylene cyanol	0.25 %
Glycerol	50 %

Protein buffers

Resuspension buffer

HEPES pH 7.4	50 mM
NaCl	150 mM

Membrane buffer

HEPES pH 7.4	50 mM
NaCl	150 mM
Glycerol	10 % (v/v)

Low imidazole HlyB-NBD (A-NBD1)

Na P _i pH 8	25 mM
KCl	100 mM
Glycerol	20 %
Imidazole	10 mM

High imidazole HlyB-NBD (A-NBD2)

Na P _i pH 8	25 mM
KCl	100 mM
Glycerol	20 %
Imidazole	300 mM

Gel filtration buffer NBD (B-NBD)

CAPS-NaOH pH 10.4	10 mM
Glycerol	20 %

Low histidine HlyB/D (A1)

TRIS pH 7.8	50 mM
NaCl	150 mM
Glycerol	10 % (v/v)
Histidine	1 mM
Detergent	5x CMC

High histidine HlyB/D (A2)

TRIS pH 7.8	50 mM
NaCl	150 mM
Glycerol	10 % (v/v)
Histidine	75 mM
Detergent	5x CMC

Gel filtration buffer (B)

HEPES pH 7.4	50 mM
NaCl	150 mM
Glycerol	10 %
Detergent	5x CMC

Instruments

Purification systems

FPLC system (P-500 pump/LCC-500 plus unit)	GE Healthcare
Äkta Basic	GE Healthcare
Smart system	GE Healthcare

Optical instruments

ELISA plate reader Polarstar	BMG Lab technology
CHEM GENIUS ²	Syngene
CO8000 cell density meter	WPA biowave
Cary 50 Scan absorption instrument	Varian Instruments
FluoroLog-3	Horiba Jobin-Ivon
J-810 spectropolarimeter	Jasco
Nanodrop ND-1000	Peqlab
UV/VIS or fluorescence cuvettes (0.12 ml, 0.3 ml, 1.4 ml, 3 ml all with d = 1cm)	Hellma
CD cuvette (d = 0.2 cm)	Hellma

Centrifuges

Sorvall Evolution RC	Thermo
Eppendorf 5417R	Eppendorf
Eppendorf 5415D	Eppendorf
Sorvall Discovery M120 SE	Thermo
Sorvall Discovery 90 SE	Thermo

Electrophoretic instruments

Power supply PowerPac HC	BioRad
SDS vertical electrophoresis unit	Chem. Werkstätten Universität Düsseldorf
DNA horizontal electrophoresis unit (22 cm)	Chem. Werkstätten Universität Düsseldorf
XCell SureLock Mini cell (Novex gels)	Invitrogen
Trans-Blot Semi-Dry system	Biorad

Incubators

Incubator
Shaking incubator Multitron

Heraeus
Infors

Others

Basic Z cell disruptor
French Press
Balances
Milli-Q⁵⁰ Plus
SDS-PAGE casting unit
Multiporator electrotransformation device
Thermocycler T-personal
Thermoblock, Thermomixer compact
Branson Sonifier
pH meter
Vortex-Genie 2
Gilson pipettes; P-2, -10, -20, -200, -1000
Pipettboy

Constant systems
Thermo Scientific
Kern
Millipore
Chem. Werkstätten Universität Düsseldorf
Eppendorf
Whatman Biometra GmbH
Eppendorf
Heinemann Labortechnik
WTW
Scientific Industries
Gilson
Ben & Dickenson

2. Methods

2.1 Molecular biology

2.1.1 Cultivation and storage of *E. coli* and *L. lactis*

In this study single colonies were used for inoculation of media. Single colonies were obtained by streaking *E. coli*/*L. lactis* cells onto LB/M17 Agar supplemented if necessary with the appropriate antibiotics. After overnight incubation at 37°C/30°C single colonies were picked and inoculated in appropriate liquid media supplemented with then appropriate antibiotics. For *E. coli*, flasks large enough to ensure sufficient aeration were used (5 l flasks for 1 l cultures, 3 l for 0.5 l cultures etc.). For *L. lactis* flasks with twice the culture volume were used. *E. coli* cultures were incubated 12-16 h in a shaking incubator at 220 rpm and 37°C. *L. lactis* cultures were incubated 16-20 h in an incubator at 30°C.

For short term storage (12 h) liquid cultures were stored at 4°C, while cells were stored on appropriate agar plates (2 weeks) or as cryostock (saturated cultures supplemented with 20 % sterile glycerol, flash frozen in liquid nitrogen and stored at -80°C, practical storage life > 5 years) for long term storage.

2.1.2 Blood haemolysis test on agar plates

The bacterial secretion of activated HlyA could be monitored by growth of secreting *E. coli* cells onto Columbia blood agar plates. The plates were supplemented with 5 mM CaCl₂, appropriate antibiotics and inducers and dried for 15 min in a flow hut. Single colonies were diluted by streaking the cells onto plates. After growth for 16 h a visible white halo around the colonies can be observed in case of the secretion of active HlyA.

2.1.3 Secretion tests with secretion competent *E. coli*

If the translocator unit HlyBD/TolC is present in *E. coli*, the secretion signal is recognized by the inner membrane components and consequently exported. Using this approach not only full length HlyA can be transported, but also fragments thereof, containing the secretion signal.

As well protein fusions to the C-terminal secretion signal can be transported.

The genes for the inner membrane complex were plasmid-encoded by pK184-HlyBD, an lactose/IPTG-inducible, kanamycin resistance mediating low copy vector, with low background expression of HlyBD. This vector can be complemented with a ColE1 or pMB1 plasmid encoded for HlyA or fusions of HlyA. In this work pLG813, encoding HlyA and HlyC, was used for the secretion of active HlyA. Here, no induction was necessary due to the constitutive or leaky promoters in both plasmids.

Alternatively pSOI-fusions were used, encoding the C-terminus of HlyA with an N-terminal fusion under the control of an arabinose promoter. To study secretion in liquid media autoinducible media ZYM-5052 with added arabinose was inoculated with single colonies and incubated at 30 °C / 37°C overnight. For screening procedures cells were harvested at this point, whereas for larger volumes the arabinose in the overnight culture was omitted and fresh autoinducer without glucose was inoculated with 2% of the overnight culture. At OD₆₀₀ = 0.4 1 mM IPTG was added to boost the expression of HlyBD and 30 min later (OD₆₀₀ = 0.6) arabinose was added to induce the secreted protein. Chemical defined autoinducer media was also test to avoid interference of media components

After a certain time, cells were harvested by centrifugation at 6.000xg and the supernatant was analyzed by SDS-PAGE. All secretion tests were performed at 37 °C. Secretion test with MalE fusions were performed at 30 °C in line with the fluorescence measurements..

2.1.4 Transformation of competent *E. coli*

Competent *E. coli* cells are able to take up DNA. In this work the RbCl₂ method according to Hanahan was used to prepare transformation competent *E. coli* cells (Hanahan, 1983). In brief, a single colony of a certain *E. coli* strain was used to inoculate a 5 ml culture of LB media. The next day the overnight culture was transferred to a 3 l flask containing 500 ml

2xYT. The culture was incubated at 37°C and 220 rpm until OD₆₀₀ of ~ 0.5. The bacterial suspension was transferred to sterile centrifuge bottles and centrifuged for 10 min at 4000 g. Subsequent procedures were done at 0°C on wet ice in the cold room. The supernatant was completely removed and the sediment was resuspended in 165 ml buffer RF1 (100 mM RbCl₂, 50 mM MnCl₂, 30 mM KAc, 10 mM CaCl₂, 15 % (w/v) Glycerol, pH 5.8; sterilised by filtration). After incubation on ice for one hour the suspension was centrifuged for 10 min at 4000 g. The pellet was resuspended in 40 ml buffer RF2 (10 mM MOPS, 10 mM RbCl₂, 75 mM CaCl₂, 15 % (w/v) glycerol, pH 6.5; sterilised by filtration) and incubated on ice for 15 min. The suspension was dispensed into sterile 1.5 ml tubes, flash frozen in liquid nitrogen and stored for subsequent usage at -80 °C.

Cell aliquots were thawed on ice for 10 min. DNA was added (2 ng for circular plasmids and up to 500 ng for ligation reactions or PCR products; maximal volume of 10% (v/v) of the transformation mix) and incubated for 15 min on ice. The cells were transferred for 60 sec to a 42°C heat block and again for 60 sec on ice. For regeneration, 10x suspension volume SOC media was added and the bacteria were gently shaken at 37°C for 1 hour. The bacteria were centrifuged for 5 min at 6.000 g and the pellet was resuspended in the reflux. The bacteria were spread onto prewarmed and dry LB Agar plates with appropriate selection marker.

2.1.5 Transformation of competent *L. lactis*

Competent *L. lactis* were obtained according to Wells *et al.* (Wells et al, 1993). In brief, high concentrations of glycine weaken the cell wall, while sucrose is needed as an osmotic stabiliser. A single colony of *L. lactis* NZ9000 was used to inoculate a 5 ml culture GM17. After incubation at 30°C for 10 h the culture was used to inoculate 50 ml SGM_G1 (GM17, 0.5 M sucrose, 1 % glycine). After overnight incubation, the culture was used to inoculate 400 ml SGM_G2 (GM17, 0.5 M sucrose, 2 % glycine). After incubation at 30°C and occasional gently shaking, the culture was grown until OD₆₀₀ of 0.5 is reached. Subsequent procedures were done on ice in the cold room with sterile pipettes and tubes. The culture was pelleted at 5000 g for 15 min at 4°C. The pellet was resuspended with 250 ml icecold WB⁺ (0.5 M sucrose, 10% glycerol, 50 mM EDTA, pH 7.5). The suspension was incubated on ice for 15 min and subsequently centrifuged for 15 min at 5000 g. The pellet was resuspended in 125 ml icecold WB (0.5 M sucrose, 10% glycerol) and again centrifuged for 15 min at 5000 g. The

pellet was resuspended in 5 ml WB (0.5 M sucrose, 10 % glycerol) and flash frozen aliquots are stored until usage at -80°C.

For transformation, the cells were thawed on ice for 10 min and DNA was added to the cells. To avoid sparking, the DNA needed to be desalted by dialyses or precipitation. The cells were transferred into a pre-chilled electroporation cuvet (0.1 cm) and the electroporation was performed at 1.7 kV (expected half time of the pulse 5 ms). Icecold SGM17MC was immediately added (M17, 0.5 M sucrose, 20 mM MgCl₂, 2 mM CaCl₂) and incubated for 10 min on ice. For regeneration the suspension was incubated at 30 °C for 2 h. The cells were spread onto prewarmed and dry SGM-Cm Agar plates (GM Agar with 0.5 M sucrose and 5 µg/ml chloramphenicol) and incubated at 30°C for 1-2 days.

2.1.6 DNA preparation, restriction and gel electrophoresis

For plasmid preparation commercial available kits were used considering all optional washing steps (Mini up to 20 µg plasmid DNA, Midi up to 500 µg plasmid DNA). DNA was eluted or resuspended in TlowE (10 mM TRIS, 0.1 mM EDTA pH 8.5).

DNA fragments obtained by PCR were analyzed by agarose gel electrophoresis. If unspecific fragments were present, the PCR product was gel extracted. Otherwise DpnI was added to the extension mix to digest the template and the DNA fragment was recovered by PCR purification.

Restriction digests were performed with buffers provided by the supplier and according to the manufacturers' protocol. Analytical digests were performed as 10 fold over-digest, whereas preparative digests were performed as 50 fold over-digest.

Prior agarose gel electrophoresis DNA loading buffer was added and electrophoresis was performed using a field strength of 600 V/m. The agarose content of the gel was chosen according to the size of the DNA fragment, but for DNA ranging from 0.4 kb up to 10 kb 1 % agarose was chosen as standard. For analytical purposes a TBE buffered system was selected while for preparative purposes a TAE buffered system was chosen. For size estimation a DNA marker was always used. To visualize the DNA after separation the gel was incubated for 10 min in an ethidium bromide solution (1 µg/ml in TAE buffer). If necessary, DNA

fragments could be retrieved by excising the desired DNA band with subsequent extraction using a gel extraction kit according to the manufacturers' protocol.

The concentration of DNA was either roughly estimated by comparison with corresponding fragments of the marker or more accurately measured by absorption at 260 nm with a Nanodrop UV/Vis spectrophotometer. Pure DNA had a $Abs_{280}/Abs_{260} = 1.8 - 2.0$, while $Abs_{230}/Abs_{260} < 1$.

2.1.7 Polymerase chain reaction (PCR)

PCR was used to amplify DNA fragments, to introduce point mutations and flanking regions. For the different purposes different polymerases were chosen. For detection of certain DNA sequences present in a bacterial colony, the *Taq* Polymerase was chosen. For amplification with further downstream processing the proof reading *Phusion* polymerase was used. The buffer composition was according to the manufacturers note. In case of amplifications with the *Taq* polymerase 35 cycles with an extension time of 1 kb/min were performed, while in case of the *Phusion* polymerase only 30 cycles and an extension time of 2 kb/min were performed. The annealing temperature was in both cases 3°C lower than the melting temperature of the primer.

To add a 3' desoxyadenosine-overhang after amplification by *Phusion* Polymerase dATP and *Taq* Polymerase was added to the reaction mix and incubated for 30 min at 72°C. The resulting modified DNA could be used in subsequent Topo reactions.

2.1.8 Ligation

In ligation reactions the T4 DNA ligase catalyzes the formation of a phosphodiester bond juxtaposed 5' phosphate and 3' hydroxyltermini in DNA powered by the hydrolysis of ATP. Prepared vector and insert (restricted, purified and analyzed for concentration) with compatible ends for ligation were mixed with the ratio vector:insert = 1:3 with a total amount of 100 - 400 ng DNA. Fresh T4 DNA ligase buffer and 5 Weiss Units T4 DNA ligase were added and the reaction mix was incubated overnight at 16 °C. The T4 DNA ligase was heat

inactivated for 10 min at 65 °C and DNA was transformed. *L. lactis* constructs were precipitated before transformation whereas *E. coli* constructs were directly transformed in RbCl₂ competent cells. Resulting colonies were pre-screened by colony PCR using a complement vector and insert primer pair or directly inoculated in 5 ml cultures with subsequent plasmid preparation and restriction analysis. Proper plasmids were further verified by sequencing applying the Sanger dideoxy method for correct insert sequence (BMFZ, Düsseldorf).

Certain properties, like affinity tags could be added by insertion of double stranded oligonucleotides into linearized vector DNA. The vector was therefore linearized by restriction, treated with calf intestine phosphatase to prevent religation and purified by gel extraction. As insert two complement oligonucleotides were annealed creating double stranded DNA fragments with overhangs suited for the linearized vector DNA.

Oligonucleotides were melted and hybridized by heating an equimolar ratio at 95°C for 1 min with a linear gradient to 50 °C for 5 min. The resulting insert was phosphorylated at the 5' position using ATP and the T4 Polynucleotide Kinase. After heat inactivation and dilution the vector and insert was mixed and ligated with the T4 DNA ligase. Upon transformation the resulting colonies were checked for desired insert presence and orientation by using an oligo and a compatible vector bound primer as primer pair in a colony PCR. Proper plasmids were further verified by sequencing applying the Sanger dideoxy method for correct insert sequence (BMFZ, Düsseldorf).

2.1.9 Introduction of point mutations

For a site-specific change in a certain DNA sequence a PCR derived method was used. A schematic overview of the procedure is shown in Figure B1.

In brief, primers encoding the desired sequence were designed with each having a short shift to the 5' prime site of the template. Hence, primers resulted in a higher melting temperature to the template compared to the complementary primer.

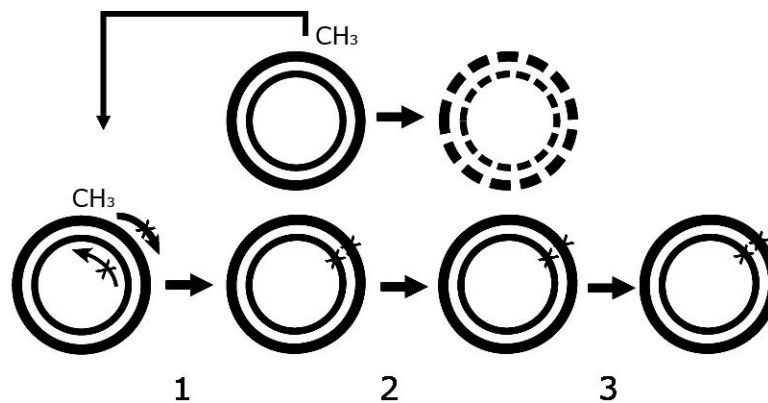


Figure B1: Introduction of point mutations: (1) PCR cycle (2) DpnI digest (3) obtained plasmid. X marks the position of the initial base pair mismatch, the site of the base exchange.

The PCR was performed with the *Phusion* Polymerase with only 18 cycles (Step 1, Figure B1). To avoid the successful transformation of the template, the vector was methylated, parental template was digested directly in the extension mix with DpnI cutting methylated or semimethylated DNA (Step 2, Figure B1). The PCR product, containing the desired sequence, could be transformed into high-competent *E. coli* cells yielding colonies carrying the plasmid with the designated mutation. The correct sequence was verified by sequencing with the Sanger dideoxy method (BMFZ, Düsseldorf).

A maximum of 8 base exchanges were successfully performed. Depending on the size of the template plasmid, mutations in plasmids up to 8.5 kb were introduced without any difficulty.

If several point mutations were introduced a variation of this protocol was used. Up to three primers were used with similar annealing temperatures annealing on either the sense or antisense strand of the template. In addition to the components needed for PCR the heat stable ligase *AmpLigase* and its co-factor NAD^+ were added to the reaction mix. The PCR was performed as above with the exception that the extension temperature was adjusted to 68°C to enable the ligation reaction. After the reaction, the template was digested with DpnI and the circular ssDNA was transformed into high-competent *E. coli* cells yielding colonies carrying the plasmid with the designated mutations. The correct sequence was verified by sequencing applying the Sanger dideoxy method (BMFZ, Düsseldorf). Due to the fact that this method was slightly less efficient, the first mutagenesis method was favoured for routine introduction of point mutations.

2.1.10 Ligation independent cloning (LIC)

LIC in theory

The cloning of a large number of inserts in a certain vector is often hampered by the presence of needed restriction sites in the inserts sequence. To overcome the problem of adjusting the cloning procedure for every single insert the technique of ligation independent cloning (LIC) was used (Aslanidis & de Jong, 1990).

LIC is based upon the binding of a large, single-stranded overhang present in the vector to a large, single-stranded overhang with the corresponding anti-sense sequence in the insert. This non-covalent binding is stable enough to be successfully transformed into *E. coli*. *In vivo* the breakage of the DNA is repaired by the host enzymes.

Before generating the ssDNA overhangs the vector backbone was linearized by the blunt end cutting restriction enzyme *SwaI*. Using the 3'⇒5' exonuclease activity of the T4 DNA polymerase, these 15-18 bases long defined 5' overhangs were generated. To avoid an overdigest desoxynucleotides were added to the reaction mix (GTP was added to the reaction mix to block the digest at the G in the sequence). The procedure is illustrated in Figure B2.

Vector treatment:

SwaI digest

Met His His His His His His His His His His His Gly Glu Asn Leu Tyr
5' ATG CAT CAT CAC CAT CAT CAC CAT CAC CAT CAT GGT GAG AAT TTA TAT TT ↓ AAATCCCACCTCCAG
3' TAC GTA GTA GTG GTA GTA GTG GTA GTG GTA GTA CCA CTC TTA AAT ATA AA TTTAGGGTGGGAGGGTC

Treatment with T4 DNA Polymerase in presence of dCTP

Met His His His His His His His His His His His Gly Glu Asn Leu Tyr
5' ATG CAT CAT CAC CAT CAT CAC CAT CAC CAT C
AAATCCCACCTCCAG
3' TAC GTA GTA GTG GTA GTA GTG GTA GTG GTA GTA CCA CTC TTA AAT ATA AA C

Insert treatment:

PCR

N is Gly Glu Asn Leu Tyr Phe Gln Gly Met X
5' AT GGT GAG AAT TTA TAT TTT CAA GGT ATG gene TGA AAA TCC CAC CCT CCC A
3' TA CCA CTC TTA AAT ATA AAA GTT CCA TAC gene ACT TTT AGG GTG GGA GGG T

Treatment with T4 DNA polymerase in presence of dGTP

N is Gly Glu Asn Leu Tyr Phe Gln Gly Met X
 5' AT GGT GAG AAT TTA TAT TTT CAA GGT ATG **gene** TG
 3' GTT CCA TAC **gene** ACT TTT AGG GTG GGA GGG T

Annealing of prepared insert an vector:

N-terminus:

Met His His His His His His His His His His Gly Glu Asn Leu Tyr Phe Gln Gly Met
 5' ATG CAT CAT CAC CAT CAT CAC CAT CAC CAT CAT CAT GGT GAG AAT TTA TAT TTT CAA GGT ATG **gene**
 3' TAC GTA GTA GTG GTA GTA GTG GTA GTG GTA GTA CCA CTC TTA AAT ATA AA. GTT CCA TAC **gene**

C-terminus:

X
 5' **gene** TG. AAA TCC CAC CCT CCC AG
 3' **gene** ACT TTT AGG GTG GGA GGG TC

Figure B2: Schematic overview of the LIC procedure. X denotes the Stop codon.

For fusions with the HlyA secretion signal the sequences were modified to enable a read-through to the HlyA gene (the stop codon was omitted in case of pSOI).

LIC in practice

The insert was amplified by PCR using primers with suitable overhangs for the LIC cassette. Template, primers and remaining dNTP were removed by DpnI digest followed by PCR purification. If unspecific products were present DpnI could be omitted and the desired product was directly purified by gel extraction (elution buffer TlowE; 10 mM TRIS, 0.1 mM EDTA, pH8.5). Using the Nanodrop device the DNA concentration was determined by measuring the absorption at 260 nm.

The vector was phenol/chloroform extracted to further purify the vector since DNA preparations of Midi or Mini preparations were not sufficiently pure (elution buffer TlowE; 10 mM TRIS, 0.1 mM EDTA, pH8.5). The vector was blunt end cut overnight at 25 °C with SmaI by adding 40 U to 6 – 8 µg vector DNA. The restriction was gel purified and the DNA concentration was determined by measuring the absorption at 260 nm.

200 ng (240 ng for pSOI) of the prepared vector DNA was adjusted with water to a volume of 10 µl, 3 µl of 5x T4 DNA polymerase buffer, 1.5 µl dCTP (25 mM) and 0.5 µl T4 DNA polymerase were added and incubated for 30 min at room temperature. In addition, an amount

of insert was taken, corresponding to the same amount of vector molecules present ($\text{ng insert} = 0.05 \text{ ng/bp} \cdot \text{insert size}$). The insert DNA was also adjusted with water to a volume of 10 μl , 3 μl of 5x T4 DNA polymerase buffer, 1.5 μl dGTP (25 mM) and 0.5 μl T4 DNA polymerase were added and incubated for 30 min at room temperature. The T4 DNA polymerase was heat inactivated at 75 °C for 20 min.

The resulting DNA was mixed with a vector to insert ratio of 1:3 (2 μl vector and 6 μl insert). Only vector DNA was always taken as negative control. The DNA was incubated 5 min at room temperature and then transformed in competent *E. coli* cells.

2.2 Electrophoresis and protein detection

2.2.1 Protein determination

To determine the protein concentration the Bradford method was used as modified by the Coomassie Plus Assay in microtiter plate format (Bradford, 1976). For calibration given concentrations of bovine serum albumin (BSA) were used to obtain a standard curve. After adding the Coomassie Plus reagent and 10 min incubation the absorption at 584 nm was measured using a 96 well plate reader.

For soluble proteins the absorption at 280 nm was used to measure concentration. The extinction coefficient was calculated with ProtParam (www.expasy.ch/tools/protparam.html). To exclude any perturbation derived by the solvent components the solvent was used as reference. For higher concentrations above 1 mg/ml, largely depending on the protein characteristics, the Nanodrop device was used (with 1 mm, 0.1 mm pathlength) whereas for smaller concentrations the standard UV/Vis spectrophotometer was used with a 10 mm pathlength.

2.2.2 SDS-Polyacrylamide gel electrophoresis

The separation of proteins according to their molecular weight was performed with discontinuous SDS-polyacrylamide gel electrophoresis (SDS-PAGE). By addition of SDS proteins are unfolded and homogenously charged according to their length of the polypeptide chain. The homogenous charged proteins can be separated in a polyacrylamide matrix according to their size. Certain proteins like membrane proteins differ from the usual amount of bound SDS (1.4 g SDS/ 1 g protein) and therefore have a slight different running behaviour (binding more SDS, running at an apparent smaller molecular weight). After separation proteins were either directly visualized by staining or electrotransferred to a PVDF membrane for immunoblotting.

The stacking gel contains always the same density of polyacrylamide, whereas the density of the polyacrylamide matrix in the resolving gel determines which mass range is resolved best (Table B2).

Table B2: Content of stacking gel/resolving gel and useful mass range.

	Stacking gel	Resolving gel		
	4.5%	7%	10%	15%
(Bis-)Acrylamide sol. 30%	5.25 ml	17.5 ml	25 ml	37.5 ml
Stacking gel buffer	5 ml	-	-	-
Resolving gel buffer	-	18.75 ml	18.75 ml	18.75 ml
ddH ₂ O	21 ml	37.5 ml	31.25 ml	18.75 ml
APS (10 % (w/v) in water)	210 µl	300 µl	300 µl	300 µl
TEMED	70 µl	70 µl	70 µl	70 µl
Mass range		50-200 kDa	30-150 kDa	12-80 kDa

In brief, the components of the resolving gel were mixed and APS and TEMED were added to start polymerization. The mixture was quickly poured into the gel chamber and the gels were covered with isopropanol. After an hour polymerization the isopropanol was discarded and APS and TEMED were added to the stacking gel. The resolving gel was covered with the stacking gel and teflon spacers were pushed into the stacking gel.

Prior electrophoresis protein samples were supplemented with 5x sample buffer. Soluble proteins and whole cell extracts were heated for 10 minutes at 65°C. For membrane protein

samples 5x membrane protein sample was used and the SDS-PAGE samples were heated 10 minutes at 37 °C.

Electrophoresis was performed at 160 V until bromphenol blue had been migrated through the resolving gel.

2.2.3 Coomassie stain and silver stain

Routinely the separated proteins were stained with Coomassie R-250 by panning the SDS-PAGE gel for 1 hour in staining solution and removing the excess dye by panning the gel in several cycles of destain solution until no background was visible.

The detection limit of the Coomassie Dye is around 0.1 µg protein/per band depending on the protein. If a more sensitive detection was desired, the SDS-PAGE gel was silver stained. This detection method is 10-100 fold more sensitive than Coomassie staining. In brief the SDS-PAGE gel was fixed with fixation solution for 15 min. Subsequently, thiosulphate buffer was added for 15 min and washed 4 times with distilled water. Subsequently silver nitrate solution was added to the gel for 25 min. For detection the gel was washed once with water, once with developer solution and then incubated with developer solution until the protein bands were visible. The reaction was stopped by adding 2 ml glacial acidic acid.

2.2.4 Immunodetection

Immunodetection by Western blotting is a widely used technique for the sensitive detection of proteins. This technique takes advantage of specific recognition towards a sequence in a target protein.

Proteins were separated by SDS-PAGE. The gel was panned with transfer buffer as well as 6 sheets of filter paper and a methanol activated PVDF membrane. The gel was piled onto the PVDF membrane with 3 filter papers on bottom and on top of the sandwich. Air bubbles in the pile were avoided and the cathode was carefully applied.

By applying a current of 100 mA per gel for 90 min proteins were transferred towards the anode being immobilised on the hydrophobic PVDF membrane.

To saturate unspecific binding the membrane was blocked for 30 min with Blocking buffer containing milk powder or BSA as blocking reagent (milk powder was used for polyclonal antisera, whereas BSA was used for detection of Strep-/His-tags). The membrane was subsequently incubated for 2 hours with the first antibody or binding partner. The streptavidin-AP conjugate could be immediately detected by NBT/BCIP.

For the antibody-based detection mechanisms, the secondary HRP-coupled-antibody was added for 30 min after washing the membrane three times for 5 min with TBS-T. Prior detection, unspecific bound secondary antibodies were removed by washing the membrane twice with TBS. For detection the ECL *advance* kit was used.

Table B3: Used antibodies or conjugates for immunodetection with corresponding target, source, organism and dilution. BB1 denotes TBS-T with 3% milk powder and BB2 denotes TBS-T with 3% BSA.

<i>Antibody/conjugate</i>	<i>Target</i>	<i>Organism</i>	<i>dilution</i>	<i>source</i>
α -HlyA	C-terminus HlyA	Rabbit	1:4000 in BB1	K. Kuchler, Vienna
α -HlyB	NBD HlyB	Rabbit	1:4000 in BB1	K. Kuchler, Vienna
α -HlyD	Soluble HlyD part	Rabbit	1:4000 in BB1	B. Holland, Paris
α -His	pentaHis	Mouse	1:1000 in BB2	Qiagen
Streptavidin-AP	Biotin/StepTagII	-	1:4000 in TBS-T	Chemicon
Anti-rabbit-HRP	F _c -fragment Rabbit Ab	Goat	1:20000 in TBS-T	Sigma-Aldrich
Anti-mouse-HRP	F _c -fragment Mouse Ab	Goat	1:20000 in TBS-T	Dianova

2.3 Protein overexpression and purification

2.3.1 Protein overexpression

To overexpress proteins heterologously the plasmid encoding the desired gene under the control of an inducible promotor was transformed into an expression strain (*L. lactis* NZ9000/*E. coli* K12 and derivatives). Single colonies were picked from an agar plate containing a selection marker to inoculate the pre-cultures. The dense pre-cultures were used

to inoculate a larger culture volume up to 24 litres with a starting OD₆₀₀ of 0.05 (dilution of 1 to 50). The overexpression was started for initial trials by adding the suited inducer in the late logarithmic phase of cell growth (OD₆₀₀=0.6-1.0). Arabinose was used for pBAD plasmids, IPTG for *lac*-promotor dependent plasmids and the Nisin A containing culture supernatant of *L. lactis* NZ9700 was added to induce overexpression in *L. lactis*. Usually after 3 hours cells were pelleted at 6000g and the resulting sediment was resuspended in buffer RB (50 mM HEPES pH 7.4, 150 mM NaCl). The suspension was again sedimented and the resulting pellet was frozen at -20°C.

Before induction a culture aliquot was taken if a test-expression was performed and also after distinct intervals after the induction. Aliquots were pelleted and resuspended in sample buffer to an optical density of OD₆₀₀ = 5. The samples were analyzed with SDS-PAGE either by coomassie G-250 staining or by immunodetection for the presence of the desired protein.

2.3.2 Membrane isolation

As first purification step for membrane protein isolation of the cellular membrane was performed. The cell pellets were thawed on ice and resuspended with buffer RB (50 mM HEPES pH 7.4, 150 mM NaCl). To this solution DNaseI (0.5 mg DNaseI per ml suspension) was added and if required protease inhibitors were added at this step. Suspensions containing *L. lactis* were incubated with 10 mg/ml lysozyme at 30°C prior to lysis. Cells were lysed using 3 passages in a cell disruptor at 2.5 kbar with a 0.18 mm jet. *E. coli* lysates were directly centrifuged with a high-speed step (125.000 g, 90 min) whereas *L. lactis* lysates were centrifuged with two low-speed steps (13.500 g, 30 min; 25.000 g, 45 min) before the high-speed step (125.000 g, 90 min).

The resulting membrane pellets were homogenized in RBmemb (50 mM HEPES pH 7.4, 150 mM NaCl, 10 % glycerol), directly used or flash frozen in liquid nitrogen and stored at -80°C.

2.3.3 Membrane protein purification

Membrane proteins had to be solubilised prior further purification steps. The initial screen for

the best detergent (Table B4) included several detergents with the isolated membrane adjusted to the concentration of 10 mg/ml protein.

Table B4: Used detergents in this work with some of their characteristics.

	Class	Abbreviation	CMC % (w/v)	% (w/v) for solubilisation	% (w/v) for purification
Big Chap	Cholesterol derivate	Big Chap	0.25	1	0.5
Octyl-β-D-glucopyranoside	Non-ionic	OG	0.53	3	0.75
Dodecyl-β-D-maltoside	Non-ionic	DDM	0.0087	1	0.02
Tetradecylphosphocholine	Zwitterionic	FC-14	0.0046	1	0.02
Sodium-dodecyl-sulfate	Ionic	SDS	0.075	1	0.2
TRITON[®] X-100	Non-ionic	TX-100	0.015	1	0.1
Lauryldimethylamine-N-oxide	Zwitterionic	LDAO	0.023	1	0.1

The proteins were solubilised for 1 h at 4°C. To separate unsolubilised proteins and aggregates the solubilise was centrifuged for 45 min at 180.000 g. The supernatant, containing the solubilised membrane proteins, was loaded on a 1 ml Ni²⁺-IMAC sepharose column, equilibrated with buffer A1. After washing the column with 30 CV buffer A1 the protein was eluted using a linear gradient from buffer A1 to buffer A2 over 30 CV. Fractions were analyzed with SDS-PAGE.

For further purification and separation of insoluble proteins the protein containing fractions were combined and concentrated using an ultrafiltration unit (MWCO 30 kDa). 500 µl of the concentrated protein was applied onto Superdex200 10/300 GL for further purification, whereas only 100 µl of protein solution was applied for analytical purposes. In both cases the gel filtration column was preequilibrated with 2 CV of buffer B. The resulting elution was analyzed by SDS-PAGE or BN-PAGE.

2.3.4 Expression and purification of HlyB-NBD

The expression and purification of the HlyB-NBD followed the procedure described in (Zaitseva et al, 2004). In brief, pPSG122 was used to overexpress HlyB-NBD under the

control of an arabinose inducible promotor in *E. coli* DH5 α strains. After induction with 0.02 % L-arabinose at an OD₆₀₀ of 1.0, cells were grown at 20°C for 3 h. The culture was harvested by centrifugation and resuspended in buffer A1-NBD. The suspension was stored at -20 °C and thawed on ice for purification. Lysis was performed with three passages in a cell disrupter system at 2.6 kBar using a 0.18 mm jet. Unbroken cells, inclusion bodies and membranes were separated by centrifugation at 125.000x g for 90min at 4 °C. The supernatant was loaded onto a precharged 5 ml Zn²⁺-IDA column equilibrated with buffer A1-NBD. After washing the column with 20 CV buffer A1-NBD the protein was eluted with a linear gradient to buffer A2-NBD over 30 CV. Fractions were analyzed by SDS-PAGE and fractions containing HlyB-NBD were combined and concentrated in an ultrafiltration unit (MWCO 10 kDa) to 2 ml. Separation of aggregates and buffer exchange was performed with a Superdex 200 pg 16/60 column equilibrated with 2 CV buffer B-NBD. Peak fractions containing soluble HlyB-NBD were combined and the protein solution was adjusted to 100 mM CAPS pH 10.4 by adding appropriate volume CAPS stock solution (500 mM, pH 10.4). To prevent dimerization caused by a single cysteine 5 mM TCEP was added. The protein was further concentrated to a concentration of 10 - 30 mg/ml and could be stored on ice for several weeks. The protein was analyzed via SDS-PAGE and UV/VIS prior storage for purity and concentration (theoretical extinction coefficient: $\epsilon_{280} = 15400 \text{ M}^{-1} \text{ cm}^{-1}$).

2.3.5 Protein purification out of culture supernatant

Protein secreted into the supernatant of *E. coli* could be purified by affinity chromatography (media ZYM-5052 or LB; chemical defined media was also successfully tested). The supernatant was therefore diluted with one volume 50 mM TRIS pH 8, 150 mM NaCl and loaded on a precharged and preequilibrated Zn²⁺-IDA column. After washing with buffer GA weakly bound protein were eluted with 10 % buffer GB for 10 CV. Protein was eluted at 100 % buffer GB.

2.3.6 Purification under denaturing conditions

For certain applications the purification under denaturing conditions is suitable. For example inclusion bodies can be recovered. Inclusions body purification was performed but will not be further outlined since no purification is presented in this work starting with inclusion bodies. But to avoid any degradation this method was also suitable.

Cell pellets were resuspended in 20 mM HEPES, 6 M Urea pH 7.6 (supplemented with 1 Roche Complete[®] protein inhibitor tablet per 50 ml). Cells were broken by sonifying (3 cycles, 30 sec) and proteins were fully denatured by rotating the suspension for 2 hours at 4 °C. Unbroken cells were removed by centrifugation for 20 min at 6000x g. The supernatant was transferred into a fresh tube and Ni²⁺-NTA resin was added to the solution and incubated for 30 min at 4 °C. The suspension was poured into an empty column. After washing with buffer GA (supplemented with 6 M urea) weakly bound protein were eluted with 10 % buffer GB (supplemented with 6 M urea) for 10 CV. Protein was eluted at 100 % buffer GB (supplemented with 6 M urea). It is important to stress that if working with purification systems special care has to be taken. Any precipitation of urea in these systems is detrimental and to prevent this buffer temperature had to be properly adjusted to the environmental conditions.

2.3.7 Purification of maltose binding protein fusions

Proteins containing the maltose binding protein (MalE) could be further purified by affinity purification using an amylose-sepharose column. Amylose resin was added to the protein solution and incubated for 30 min at 4 °C. The suspension was poured into an empty column. Unbound protein was removed by washing with 20 CV 50 mM TRIS pH 8, 150 mM NaCl. MalE was selectively eluted by the elution buffer with maltose (50 mM TRIS pH 8, 150 mM NaCl, 10 mM maltose).

If MalE fusions were purified out of whole cell extracts, the initial purification step prior amylose sepharose was affinity purification by metal-chelate chromatography to avoid purification of intrinsic MalE. Therefore the same scheme with buffers devoid of urea as described above for purification under denaturing conditions was used.

2.4 Protein analysis

2.4.1 ATPase activity determination

ATPase activity was determined by measuring the released P_i content with a colorimetric assay (Baykov et al, 1988).

The reaction was performed at 22°C in a microtiter plate with a reaction volume of 25 μ l, consisting of 20 μ l protein solution (with additives and puffer), which was preincubated in the plate and 5 μ l Mg^{2+} /ATP which was added to start the reaction. At a desired time point the reaction was stopped by adding 175 μ l of 20 mM sulphuric acid. 50 μ l of the malachite green solution was added, thoroughly mixed and incubated for 15 min. After the incubation the absorption was measured at 620 nm. For calibration, a phosphate standard ranging from 0-5 nM P_i was measured. Wells containing the reaction mix with 10 mM EDTA or only buffer were also measured to determine the zero absorption value derived by ATP autohydrolysis or P_i contamination in the protein buffers.

Malachite green stock solution	Malachite green	0.122 % (w/v)
	Sulphuric acid	20 % (v/v)
Ammonium molybdate solution	Ammonium molybdate 4 H ₂ O	7.5 % (w/v)
Tween solution	Tween 20	11 % (v/v)
Malachite Green solution (always fresh)	Malachite green stock	4 ml
	Ammonium molybdate solution	1 ml
	Tween solution	80 μ l
	<i>thoroughly vortexed after mixing</i>	
Starter solution	0-4 mM ATP/5 mM MgCl ₂	

The ATPase activity was evaluated in the dependence to the ATP concentration according to the Michaelis-Menten equation.

$$v = \frac{v_{\max} \cdot c_{ATP}}{K_M + c_{ATP}} \quad \text{or} \quad k = \frac{k_{cat} \cdot c_{ATP}}{K_M + c_{ATP}} \quad \text{Equation I}$$

In Equation I v stands for specific ATPase activity at a certain ATP concentration and is given in $\text{nmol}_{ATP} \cdot (\text{min} \cdot \text{mg}_{\text{Protein}})^{-1}$ as unit. K_m and v_{\max} denote the Michaelis-Menten constant (given in μM) and the maximal specific ATPase activity at infinite substrate concentration (given in $\text{nmol}_{ATP} \cdot (\text{min} \cdot \text{mg}_{\text{Protein}})^{-1}$). k and k_{cat} describe the turnover number at a certain ATP concentration or the overall maximal turnover at infinite substrate concentration (given both in min^{-1} as unit).

All ATP measurements were also analyzed with the Hill equation (Equation II) and compared to the standard Michaelis-Menten equation.

$$v = \frac{v_{\max} \cdot c_{ATP}^h}{K_M^h + c_{ATP}^h} \quad \text{or} \quad k = \frac{k_{cat} \cdot c_{ATP}^h}{K_M^h + c_{ATP}^h} \quad \text{Equation II}$$

In this equation h denotes the Hill coefficient representing the extend of cooperativity.

2.4.2 Trypsin protection studies

Trypsin protection studies can be used to study the orientation of a membrane protein. If a large domain is accessible to trypsin it will be degraded whereas a domain residing inside the vesicle is shielded and will only be degraded if the vesicle is solubilised. If bacteria are broken (by French press) the resulting vesicles are inverted, meaning that the inner leaflet is now at the outside (Futai, 1974; Hertzberg & Hinkle, 1974).

Therefore membranes were isolated as outlined above and diluted to a concentration of 0.5 mg/ml in 20 mM HEPES, pH 7.4. A fresh trypsin stock solution was prepared in 1 mM HCl

with a concentration of 10 mg/ml. A serial dilution with ddH₂O resulted in trypsin solution with a concentration of 5 mg/ml, 1 mg/ml, 0.5 mg/ml, 0.1 mg/ml, 0.05 mg/ml.

For trypsin digest 45 µl of protein was supplemented with 5 µl of the above prepared dilutions. 5 µl ddH₂O was added as negative control whereas 1 % (w/v) Triton X-100 (final concentration) was added as positive control. Digests were performed on ice for 15 min. The reaction was stopped by adding 150 µl 10 % (w/v) TCA. After 30 min incubation on ice precipitated proteins were pelleted for 10 min at 20000x g at 4 °C. The sediment was washed with 1 ml ice-cold acetone and the dried pellet was resuspended in 24 µl 2.5x SDS sample buffer. 10 µl sample were loaded on a SDS-PAGE and analyzed by coomassie staining and Western blotting.

2.4.3 CD spectroscopy

CD spectroscopy can be used to judge the relative content of the different secondary structures. It is preferable used for secondary structure determination over IR since it is easy to perform and predicts the helical content of the protein with appropriate accuracy (Bloemendal & Johnson, 1995).

Measurements were performed with a Jasco J-810 spectropolarimeter with a 0.2 cm cuvette. The instrument enabled a wavelength scan as well as a temperature scan. During the wavelength scan the increment was 0.5 nm using a measurement speed of 20 nm·min⁻¹. For accuracy 10 single spectra were accumulated. The molar ellipticity (Θ_{mol} in deg·cm²·dmol⁻¹) was calculated as given in Equation III:

$$[\Theta]_{mol} = \frac{\Theta \cdot M}{10 \cdot c \cdot d} \quad \text{Equation III}$$

The data was evaluated using K2D2 (<http://www.ogic.ca/projects/k2d2/>), a neural network program using the secondary structure information of known structures (Perez-Iratxeta & Andrade-Navarro, 2008).

2.4.4 Affinity measurements by intrinsic fluorescence quenching

The intrinsic fluorescence depends mostly on the surrounding of the tryptophans present in the protein. If this environment is disturbed either a shift of the emission peak or a decrease in the emission maximum is observed. Thus, tryptophans can be used to measure rearrangements in proteins or binding to proteins (Lakowicz, 1999).

Among other interactions HlyB binds nucleotides mediated by an π - π interaction of a tyrosine residue towards the base moiety of the nucleotide. Mutating this tyrosine to tryptophan, binding can be easily assessed because π - π stacking has a tremendous effect on the fluorescence behaviour of tryptophans. If this tryptophan is completely quenched one would expect that the fluorescence decreases by roughly 50 %, since another tryptophan is present (W540) in wild type HlyB-NBD.

The purified Y477W protein was diluted from storage buffer into 100 mM HEPES, 20 % glycerol pH 7.0 to a concentration of 3 μ M (5 mM MgCl₂ is optionally added). The intrinsic tryptophan fluorescence was excited at 295 nm and a continuous spectrum was recorded from 320 nm to 380 nm (25 °C, slit d = 2 nm, 2 nm steps, integration time t = 2 s, Horiba FluoroLog-3). This spectrum represented the unquenched spectrum of the protein.

Nucleotides were added from different stock solutions with continuous stirring of the cuvette (stock solutions 7 mM / 35 mM / 70 mM). After addition and incubation for 20 s, a spectrum was recorded. With increased nucleotide concentrations a decrease of fluorescence was observed. The resulting fluorescence was corrected for dilution effects. For evaluation $\Delta F/F_0$ were plotted versus the nucleotide concentration. The resulting curve was composed out of two components, a linear component corresponding to collisional quenching and a component due to specific binding of the nucleotide. Out of the latter component a binding constant could be fitted (Equation IV). In Equation IV, ΔF denotes the difference in between measured fluorescence and starting fluorescence F_0 . K_D is the equilibrium binding constant.

$$\Delta F / F_0 = \frac{\Delta F / F_{0,\max} \cdot [Nucleotide]}{K_D + [Nucleotide]} \quad \text{Equation IV}$$

2.4.5 Binding studies with TNP-nucleotides

An alternative approach to study the affinity of nucleotides is to use a fluorescence sensor attached to the nucleotide. This procedure avoids point mutants in the protein since they might influence, although marginal, the binding properties.

In this case, the bound fluorescence nucleotide analogue changes its fluorescence properties upon binding to the protein. This can be monitored e.g. by fluorescence polarization or resonance energy transfer in case of ethenoadenosine nucleotides or N-methylanthraniloyl (MANT) nucleotides or more straight forward by measuring a direct change in fluorescence intensity or emission maximum in case of MANT nucleotides or trinitrophenyl (TNP) nucleotides (TNP-AXP, where X denotes T, D or M). Here TNP nucleotides were used. The TNP nucleotides frequently exhibit a spectral shift and fluorescence enhancement upon protein binding and actually bind with higher affinity than ATP to several proteins. These properties can be easily used to quantify the binding of nucleotides to the protein.

Since the fluorescence nucleotides have a different binding affinity to most proteins, the equilibrium constant reflects the natural nucleotide can be determined by competitions experiments according to Faller (Faller, 1989).

All measurements were done at room temperature with a Horiba Fluorolog-3 fluorescence photometer using a stirring unit for continuous stirring in a 1.4 ml cuvet. The TNP moiety was excited at 408 nm and the emission was measured between 538 and 542 nm in 2 nm steps. Slits width were set to 2 nm and to avoid outliers an integration time of 6 s was used. The buffer (100 mM HEPES pH 7, 20 % glycerol +/- 4 mM MgCl₂) was filtered and degassed. Appropriate stock solutions were used to keep dilution below 4 % of the total volume. Dilution effects were later included in the calculations.

Data calculation

In equilibrium binding experiments of the protein, here HlyB-NBD, with TNP-AXP, the mixture of HlyB-NBD (P_0) and TNP-AXP (L_0) is composed of unbound species (P_{free} and L_{free}) and HlyB-NBD/TNP-ATP complexes (PL_N). The ligand number (N) represents the

stoichiometry of HlyB-NBD/TNP-nucleotide complexes (i.e. how much flourophor bound per protein molecule; see Equation V and Equation VI).

$$L_0 = L_{free} + N \cdot PL_N \quad \text{Equation V}$$

$$P_0 = P_{free} + PL_N \quad \text{Equation VI}$$

The total fluorecence of TNP-AXP (F_{total}) is accordingly composed of fluorecence of unbound TNP-AXP ($F_{L,free}$) and HlyB-NBD/TNP-AXP complexes (F_{PLN}) according to Equation VII.

$$F_{total} = F_{PLN} + F_{L,free} \quad \text{Equation VII}$$

To account for concentration-dependent inner filter effects of TNP-AXP at concentrations (L_0) higher than 6 μM , the fluorescent constants Q_1 and Q_2 are introduced (Equation VIII). These constants have to be calculated with and without Mg^{2+} in the absence of the protein and are required later for evaluation.

$$F_{L,free} = L_{free} \cdot Q_1 + L_{free}^2 \cdot Q_2 \quad \text{Equation VIII}$$

The fluorecence of HlyB-NBD/TNP-AXP complexes (F_{PLN}) is enhanced several fold compared to unbound TNP-AXP and can be described with Equation IX. Assuming that $[\text{HlyB}] \ll [\text{TNP-AXP}]$.

$$F = F_{L,free} + F_{PL,complex} \quad \text{Equation IX}$$

$F_{PL,complex}$ can be written with an enhancement factor γ .

$$F_{PL,complex} = N \cdot PL_N \cdot Q_1 \cdot \gamma$$

Equation VII, Equation VIII and Equation IX are combined to give Equation X

$$F_{total} = L_0 \cdot Q_1 + L_0^2 \cdot Q_2 + N \cdot PL_N \cdot (Q_1 \cdot (\gamma - 1) - 2 \cdot L_0 \cdot Q_2) \quad \text{Equation X}$$

The concentration of HlyB NBD/TNP-AXP complexes (PL_N) can be calculated with the dissociation constant (K_{DL}) according to the law of mass. This assumes non-cooperative binding and binding sites with equal affinity for the TNP-AXP (see Equation XI further converted with Equation V and Equation VI) or Equation XII (derives from Equation XI)

$$K_{DL} = \frac{L_{free} \cdot P_{free}}{PL_N} = \frac{(L_0 - N \cdot PL_N) \cdot (P_0 - PL_N)}{PL_N} \quad \text{Equation XI}$$

$$N \cdot PL_N = \frac{1}{2} \left[(K_{DL} + L_0 + N \cdot P_0) - \sqrt{(K_{DL} + L_0 + N \cdot P_0)^2 - 4 \cdot N \cdot P_0 \cdot L_0} \right] \quad \text{Equation XII}$$

with $(K_{DL} + L_0 + N \cdot P_0) = A$

Combining Equation XII and Equation X gives Equation XIII that is used to analyze equilibrium binding fluorescence data.

$$F_{total} = L_0 \cdot Q_1 + L_0^2 \cdot Q_2 + \left[(0.5 \cdot Q_1 \cdot (\gamma - 1) - L_0 \cdot Q_2) \left[A - \sqrt{A^2 - 4 \cdot N \cdot P_0 \cdot L_0} \right] \right]$$

Equation XIII

The term in front of the bracket can be abbreviated, since it is responsible for maximal fluorescence:

$$F_{\max} = 0.5 \cdot Q_1 \cdot (\gamma - 1) - L_0 \cdot Q_2$$

$$F_{total} = L_0 \cdot Q_1 + L_0^2 \cdot Q_2 + F_{\max} \left[A - \sqrt{A^2 - 4 \cdot N \cdot P_0 \cdot L_0} \right] \quad \text{Equation XIV}$$

Thus, the K_D of TNP-AXP can be fitted with Equation XVI after determination of the constants Q_1 and Q_2 and measuring F_{total} by titration of TNP-AXP to HlyB-NBD. Competitive binding studies for HlyB-NBD/TNP-ADP complexes with AXP were analyzed taking two independent equilibria into account (see Equation XVII and Equation XIX).

$$K_{D_L} = \frac{(L_0 - N \cdot PL_N) \cdot (P_0 - PL_N)}{PL_N}, \text{ with } [AXP] = 0 \quad \text{Equation XV}$$

$$K_{D_L} = \frac{(L_0 - N \cdot PL_N) \cdot (P_0 - PL_N - P_{AXP})}{PL_N}, \text{ with } [AXP] \neq 0 \quad \text{Equation XVI}$$

$$K_{D_{AXP}} = \frac{AXP_0 \cdot (P_0 - PL_N - P_{AXP})}{P_{AXP}}, [AXP] \neq 0, \text{ since } [AXP]_0 \gg P_0 \quad \text{Equation XVII}$$

Equation XI, Equation XVI and Equation XVII were combined to give Equation XIX.

Equation XIX was used with the assumption of Equation XVIII to analyze normalized fluorescence of competitive binding experiments.

$$\frac{F_{PL_N, AXP \neq 0}}{F_{PL_N, AXP = 0}} \approx \frac{F_{tot, AXP \neq 0} - F_{buffer, AXP \neq 0}}{F_{tot, AXP = 0} - F_{buffer, AXP = 0}} \quad \text{Equation XVIII}$$

$$\frac{F_{PL_N, AXP \neq 0}}{F_{PL_N, AXP = 0}} = \frac{A + AXP_0 \cdot \frac{K_{D,L}}{K_{D,AXP}} - \sqrt{(A + AXP_0 \cdot \frac{K_{D,L}}{K_{D,AXP}})^2 - 4 \cdot N \cdot P_0 \cdot L_0}}{A - \sqrt{A^2 - 4 \cdot N \cdot P_0 \cdot L_0}} \quad \text{Equation XIX}$$

2.4.6 Folding experiments

A straightforward method to assess the folding of a protein is the use of intrinsic fluorescence, where the environment of tryptophans can be measured (Lakowicz, 1999). During folding this environment is changed, thus the change can be determined either in equilibrium where a certain concentration of a denaturing agent is added and after a certain time (i.e. equilibrium), the fluorescence is determined or it can be measured kinetically where upon change in the concentration of the denaturing agent the fluorescence is measured with time. The advantage of tryptophan measurements over other techniques such as circular dichroism is that not only the rapid formation of secondary structure elements can be measured but also the formation of the tertiary structure can be visualized in a very sensitive manner (Royer, 2006).

Fluorescence intensity was measured using a Horiba Fluorolog-3 fluorescence spectrophotometer with an excitation wavelength of 295 nm (slit width of $d=2$ nm), an emission wavelength of 350 nm (slit width of $d=5$ nm) and an integration time of 0.5 s. To avoid photobleaching in long kinetic experiments, the excitation shutter was closed in between single points (experiment time $t > 1000$ sec). All fluorescence measurements were performed at 30 °C identical to the *in vivo* secretion experiments.

For equilibrium studies of folding, native proteins (60 nM, out of a concentrated stock solution of approximately 2 mg/ml) were added to varying concentrations of urea in 150 μ l of 10 mM HEPES (pH 7.6 adjusted with KOH), and the fluorescence intensity of each sample was measured after equilibration for 10 h at 30 °C in a 150 μ l fluorescence cuvette. If SecB was added a 4 molar ratio of SecB to the refolding protein was used.

For kinetic studies of unfolding the reactions were initiated by adding approximately 10 ng of native protein to a solution of 2 M to 5 M urea in 10 mM HEPES (pH 7.6, final volume 3 ml) held in a stirred cuvette in the chamber of the spectrophotometer.

For the series of refolding studies, protein was unfolded by incubation for over night in 5 M urea in 10 mM HEPES (pH 7.6). Folding was initiated by addition of the denatured protein (approximately 10 ng) to a predetermined volume of a solution of buffered urea such that the final urea concentration was used as indicated for each experiment. The addition of protein was performed manually. The time that elapsed between addition of the sample and the first recording of fluorescence intensity was approximately 3 s. The relaxation time to achieve the new equilibrium was extracted from a plot of the change in fluorescence versus time following a mono-exponential behaviour.

For all measurements the dilution of the urea concentration was taken into account. For equilibrium unfolding transitions the data was calculated according to Pace (Pace, 1986) using a two state model by fitting the data using GraphPad Prism 5. The two state-model assumes that two major forms are present, the native and the unfolded form (Equation XX); where N is the native form, U the unfolded form and K_{app} the equilibrium constant described by $K_{app}=[U]/[N]$:



It can be shown by $K_{app}=[U]/[N]$ and $F_{app} = [U]/([U]+[N])$ that F_{app} , the apparent fraction of the unfolded form, is as follows:

$$F_{U,app} = \frac{K_{app}}{1 + K_{app}} \quad \text{Equation XXI}$$

The equation $K_{app} = e^{-(\Delta G_{H_2O} + m[\text{urea}])/RT}$ (Pace, 1986) was substituted into the above equations to calculate $\Delta G_{H_2O}^0$ and m values, where $\Delta G_{H_2O}^0$ is the free energy difference in the absence of denaturant, and m is a parameter that describes the cooperativity of the unfolding transition. The latter equation assumes that there is a linear dependence of $\Delta G_D^{H_2O}$ observed in the transition region continues to zero concentration. The observed changes in fluorescence signals were converted to an apparent fraction of unfolded protein, $F_{U,app}$,

$$F_{U,app} = \frac{Y_{obs} - Y_N}{Y_U - Y_N} \quad \text{Equation XXII}$$

where Y_{obs} refers to the observed fluorescence intensity observed at a particular urea concentration and Y_N and Y_U refer to the calculated values for the native or unfolded form, respectively at the same denaturant concentration. A linear dependence of Y_{obs} on the urea concentration was observed in the pre- and posttransition base-line regions with slope differing from zero due to solvent effects. Linear extrapolations from these base lines yielded the concentration independent values for $Y_{N,0}$ and $Y_{U,0}$. Concentration dependent values for Y_N and Y_U can be calculated from the following equations,

$$Y_N = Y_N^0 + m_N \cdot [Urea] \quad \text{Equation XXIII}$$

$$Y_U = Y_U^0 + m_U \cdot [Urea]$$

Equation XXIV

where m_N and m_U are the slopes of the pre- or post-transition regions (native and unfolded forms, respectively). The above equations were combined to obtain a single equation for the dependence of the fluorescence intensity on the denaturant concentration, which can finally be fitted as follows:

$$Y_{obs} = (Y_N^0 + m_N \cdot [Urea]) + \frac{e^{-(\Delta G^{0,H_2O} - m \cdot [Urea])/RT}}{1 + e^{-(\Delta G^{0,H_2O} - m \cdot [Urea])/RT}} \cdot [(Y_U^0 + m_U \cdot [Urea]) - (Y_N^0 + m_N \cdot [Urea])]$$

Equation XXV

In addition, the $\Delta G^{0,Urea}$ values were calculated for the single points around the transition state and plotted versus urea concentration. A linear behaviour was expected, whereas the y-axis intercept denotes the $\Delta G^{0,H_2O}$.

Time dependent folding and unfolding data was determined by fitting the data to a monoexponential function (k rate constant; F_0 fluorescence measured at $t=0$; F_∞ fluorescence at infinite time).

$$F_{obs} = F_o + (F_\infty - F_o) \cdot (1 - e^{-k_f \cdot t}) \text{ or } F_{obs} = F_\infty + (F_o - F_\infty) \cdot e^{-k_u \cdot t}$$

Equation XXVI

Depending on the experimental setup a decrease (unfolding, $k_{u,app}$) or an increase (folding, $k_{f,app}$) of fluorescence is observed. The rate constants were transformed into the relaxation time τ ($\tau=1/k$) and plotted logarithmically versus the urea concentration. The y-axis intercept of the linear portion of this plot denotes the rate for folding and unfolding at zero denaturant.

C. Results

1. *Nucleotide binding and hydrolysis of the haemolysin B NBD*

Nucleotide binding with subsequent hydrolysis contributes to a manifold of cellular processes. It is not only closely connected to processes, which directly use the energy derived from the hydrolysis of the triphosphate moiety. The binding and hydrolysis of nucleotides is also important for versatile regulation processes such as G-Proteins (Schweins & Wittinghofer, 1994) or cytoskeleton regulation (Carlier, 1991). In these processes the NTP bound state differs considerably from the NDP bound state, enabling the protein to switch between different modes, e.g. monomer/dimer or bound/non-bound.

In ABC transporters the binding and hydrolysis of ATP drives the vectorial transport of molecules across cellular membranes (Davidson et al, 2008). ATP binding and hydrolysis is crucial to alternate between the monomeric and dimeric species of the NBD (Zaitseva et al, 2006). This behaviour is directly coupled to the membrane domain. The binding of nucleotides to the NBD is well-characterized for some systems and resembles the binding of a myriad of other nucleotide binding proteins (Walker et al, 1982); however the exact mechanism how hydrolysis takes place and which residues are responsible for which step during the hydrolysis cycle was still unclear at the beginning of this work.

1.1 Nucleotide binding to the NBD measured with tryptophan fluorescence

An alignment of different ABC-NBDs is shown in Figure C1. The Walker A (or P-loop, Walker et al, 1982) is highly homologous and can serve as alignment constrain for the otherwise minor homologous parts of the sequence. Around 25 residues upstream of the Walker A motif in between the first and second β -strand an aromatic residue is highly conserved among most ABC domains. An alignment of over 18000 ABC domains revealed a

88% likelihood that an aromatic residue is present. The exchange to other aromatic residues only slightly influences the function (Kim et al, 2006). The role of this aromatic residues has been well-known, e.g. (Zaitseva et al, 2005b) but only recently this residue was named A-loop (Aromatic residue interacting with the adenine ring of ATP; Ambudkar et al, 2006).

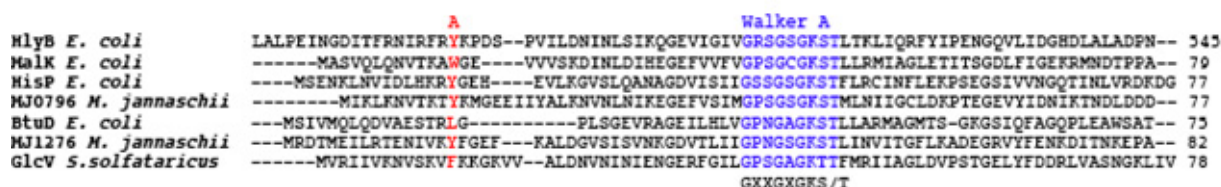


Figure C1: Sequence alignment of the initial 75 amino acids of several nucleotide binding domains. In red the A-loop, containing the aromatic residue responsible for π - π stacking is shown; in blue the Walker A motif wrapping around the phosphates of the bound nucleotide is displayed.

In case of HlyB the tyrosine at position 477 is responsible for this π - π interaction supported not only by the alignment but also by the nucleotide bound structure (Figure C8). A tryptophan at this position would be preferred due to its improved fluorescence properties. To generate the Y477W mutant of HlyB-NBD, plasmid pPSG122 was used as template and the mutation was introduced using the ligase chain reaction (LCR) with the degenerated primer Y477Wfor.

The Y477W mutant was overexpressed and purified as outlined in Materials and Methods.

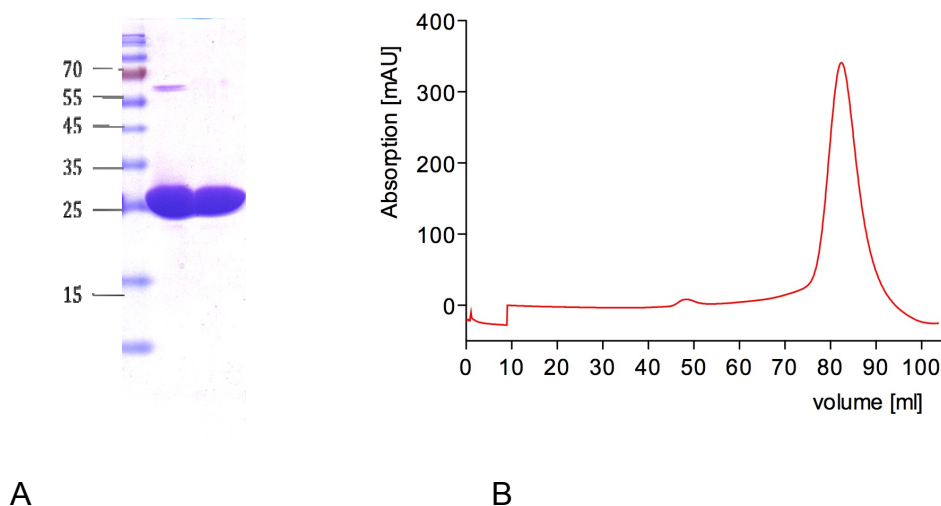


Figure C2: Purification of HlyB-NBD Y477W. (A) Coomassie stained SDS-PAGE of HlyB-NBD Y477W after purification. Shown is the marker, a protein sample without and with the addition of 5 mM DTT. (B) Gelfiltration of HlyB-NBD Y477W using a Superdex200 16/60 pg column. Shown is the absorbance at 280 nm.

After the final gel filtration step the yield was around 5 mg of pure protein/litre culture as judged by SDS-PAGE (Figure C2, left panel) and UV/Vis spectroscopy. This is around 50 % of the yield for the WT NBD. The protein preparation was homogenous as judged by gel filtration and SDS-PAGE (Figure C2, right panel).

The exchange of this aromatic residue to another aromatic residue does only marginally harm the substrate transport or the ATP hydrolysis, as it could be shown for P-glycoprotein (transport and hydrolysis, Kim et al, 2006) and OpuAA (hydrolysis, Horn et al, 2008). A decrease of the ATPase activity was observed for the HlyB-NBD Y477W mutant (Table C1).

Table C1: Kinetic Parameters of HlyB-NBD WT and HlyB-NBD Y477W at a 0.2 mg/ml enzyme concentration in 100 mM HEPES pH 7.0, 20% glycerol, 10 mM MgCl₂ (protein concentration 0.072 mg/ml, reaction time 12 min). $K_{0.5}$ is the concentration at the halfmaximal turnover and resembles the Michaelis-Menten constant in Michaelis-Menten kinetics, k_{cat} is the turnover and h denotes the hill coefficient.

	$K_{0.5}$ [mM]	k_{cat} [min ⁻¹]	h
HlyB-NBD wt	0.36 ± 0.05	5.6 ± 0.7	1.31 ± 0.13
HlyB-NBD Y477W	0.63 ± 0.36	1.3 ± 0.2	1.42 ± 0.34

To determine the steady state affinity of different nucleotides 3 μ M of HlyB-NBD Y477W were incubated with increasing amount of nucleotides as outlined in materials and methods. In Figure C3 the titration of the Y477W mutant with ATP or ADP in the absence of Mg²⁺ (ADP: blue line, closed triangles; ATP: red line, open squares) is shown as an example.

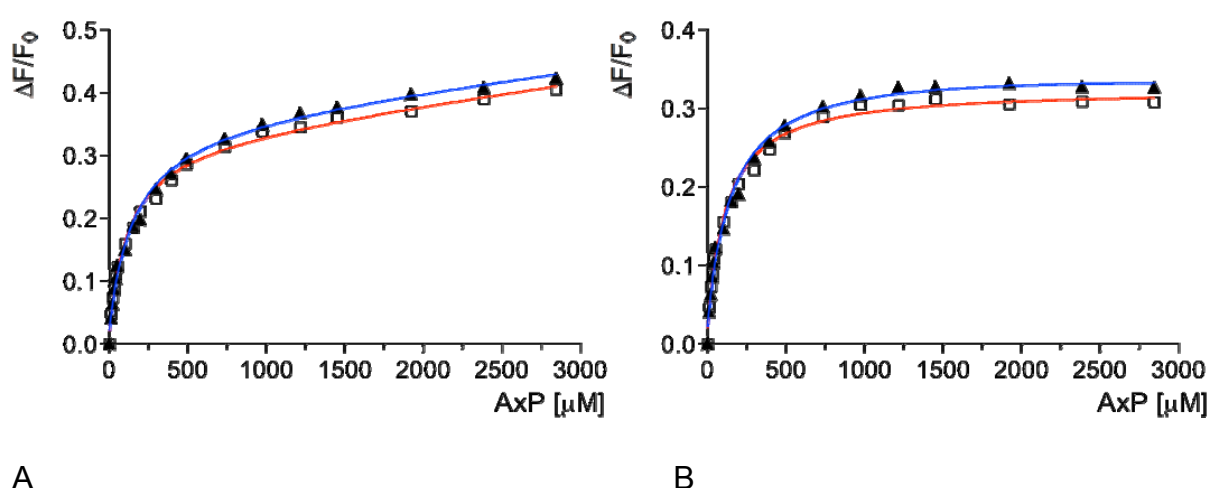


Figure C3: Inverse fluorescence quenching of the HlyB-NBD mutant Y477W depending on the nucleotide concentration. ΔF is the difference between the initial fluorescence F_0 and the measured fluorescence at a certain nucleotide concentration. (A) Dilution corrected data of fluorescence quenching. ADP: open squares; ATP: blue triangles. (B) Data including the correction for unspecific, collisional quenching.

As shown in Figure C3 B the maximal quenching was only 30 % explained by the presence of another tryptophan in the NBD. Furthermore the maximal quenching strongly depended on the buffer system used. The fluorescence in buffers with malonate or MES was decreased up to an amount of only 10 % quenching (data not shown). Absorption measurements of an increasing concentration of nucleotides in buffer solution showed a linear behaviour, therefore inner filter effects could be excluded (data not shown).

With this method in hand the equilibrium binding constants for several nucleotides in absence or presence of Mg^{2+} could be determined (Table C2).

Table C2: Dissociation constants of the HlyB-NBD Y477W/ATP, AMPPNP, or ADP complexes in the presence or absence of Mg^{2+} in 100 mM HEPES, pH 7, and 100 mM NaCl at $22\text{ }^{\circ}\text{C} \pm 1\text{ }^{\circ}\text{C}$.

Nucleotide	Dissociation constant K_D [μM]
ATP	98.3 ± 11.5
ATP/ Mg^{2+}	87.8 ± 11.2
AMPPNP	68.6 ± 5.8
AMPPNP/ Mg^{2+}	138.0 ± 18.4
ADP	89.7 ± 8.8
ADP/ Mg^{2+}	77.1 ± 13.2
AMP	$> 10\text{ mM}$

For all nucleotides the binding constants were in a similar range and the binding was independent of the salt concentration (not shown) in contrast to the situation of OpuAA, a NBD of an ABC transporter involved in osmoprotection, where binding in high salt was more affine in high salt (not published and Horn et al, 2003).

It is remarkable that ADP binds to the NBD within the experimental error with a similar affinity than ATP, but considering the physiological situation, in which ATP is in access to ADP, ADP cannot influence transport by inhibition of hydrolysis.

1.2 Nucleotide binding to the NBD measured by TNP fluorescence

The exchange of the Y477 alters the kinetics parameters slightly as it could be shown in Table C2 (Zaitseva et al, 2005b). Does the affinity measured above resemble the WT situation? Therefore it was reasonable to verify the data measured with the Y477W mutant by an alternative method. Using TNP modified nucleotides one could measure the affinity of nucleotides to the wildtype NBD. The quantum yield of TNP as a fluorescence probe is significantly sensitive to the environment and binding to proteins effects its fluorescence properties (Hiratsuka, 2003). Several control experiments had to be done beforehand. First, the fluorescence signal of TNP-AXP (where X is M, D or T) was titrated into buffer to account for the inner filter effects and background absorption has to be determined. Second, the affinity of the modified nucleotide could be measured by titrating this nucleotide to the protein. At last, by competing out the modified nucleotide with unmodified nucleotide the affinity of ATP or ADP was measured.

In Figure C4 the titration of TNP-ADP and TNP-ADP/Mg²⁺ into buffer is shown (100 mM HEPES pH 7, 20% glycerol).

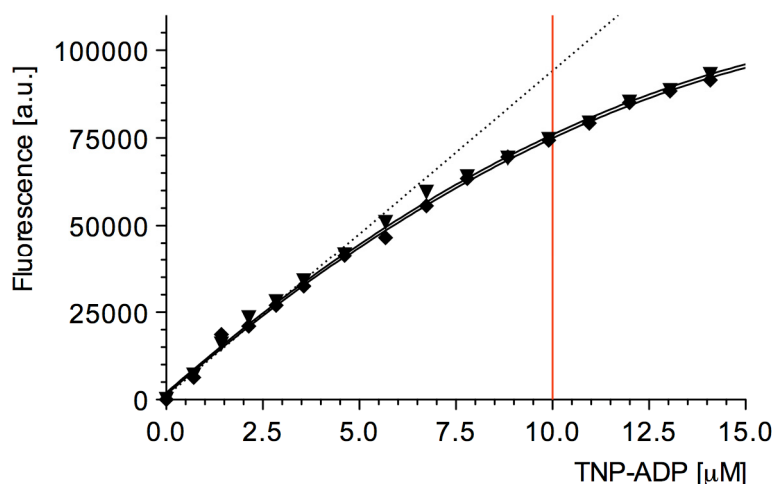


Figure C4: Fluorescence of TNP-ADP in buffer with (closed diamonds) and without (closed triangles) Mg²⁺. Shown are the values of two independent measurements. The data was evaluated according Equation VIII yielding the constants Q_1 and Q_2 . The dotted line represents the fluorescence intensity if inner filter effects would be neglected. The red line at 10 μ M represents the TNP-ADP concentration used for competition experiments.

At low concentrations the fluorescence of non-bound TNP-AXP exhibited a linear behaviour if the concentration is increased. At higher concentrations inner filter effects caused a significant deviation of this behaviour. This behaviour could be sufficiently described with Equation VIII (Lakowicz, 1999). Q_1 and Q_2 are listed in Table C3.

Table C3: Constants Q_1 and Q_2 for titrations with TNP-AXP \pm Mg^{2+} accounting for the inner filter effects.

	Q_1 [a.u. μM^{-1}]	Q_2 [a.u. μM^{-2}]
TNP-ATP	-212.8 ± 18.8	10427 ± 362
TNP-ATP (Mg^{2+})	-234.5 ± 13.2	10632 ± 258
TNP-ADP	-225.8 ± 9.8	9657 ± 191
TNP-ADP (Mg^{2+})	-221.8 ± 9.4	9564 ± 184

The constants Q_1 and Q_2 describing the inner filter effects were independent of the divalent ion, but some variation could be seen if TNP-ATP is used instead of TNP-ADP (Table C3). In a second step, the affinity of the wild type HlyB-NBD to TNP-AXP \pm Mg^{2+} was measured. Therefore 6 μM of HlyB-NBD in 100 mM HEPES pH 7, 20% glycerol were titrated with increasing amounts of TNP-AXP in the presence or absence of 4 mM $MgCl_2$.

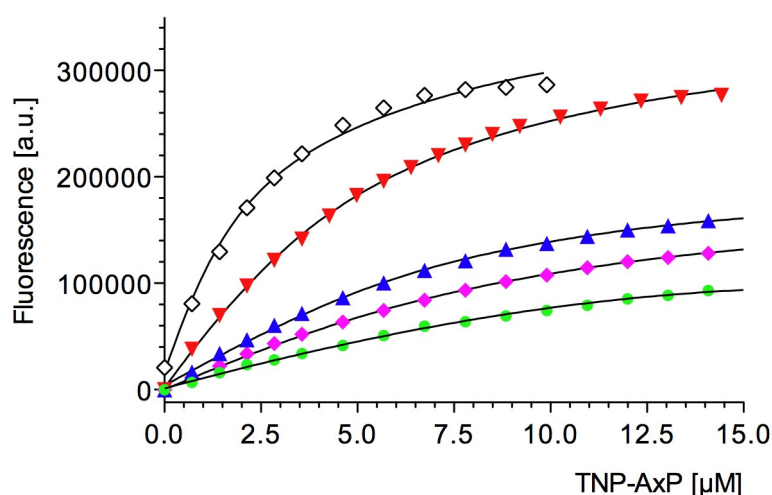


Figure C5: Fluorescence of TNP-AXP added to HlyB-NBD. For a clearer arrangement the titration of TNP-ADP into buffer is also shown (green circles). TNP-ADP/ Mg^{2+} : purple diamonds; TNP-ATP/ Mg^{2+} : blue triangles; TNP-ADP: red triangles; TNP-ATP: open diamonds. The data was evaluated according Equation XIV yielding to the different binding constants.

The fluorescence of the TNP nucleotides increased upon binding to the protein as it can be seen in Figure C5. An enhancement factor described this phenomenon and could be either calculated out of the data shown in Figure C5 or measured more accurate as slope if protein is titrated to a certain concentration of TNP-AXP (Equation IX, data not shown). It ranges from an 80 % increase upon binding in case of TNP-ADP/Mg²⁺ to a 900 % increase due to binding of the TNP-moiety of TNP-ATP to the protein (not shown). In the presence of Mg²⁺ the enhancement factor was decreased resulting in a poor signal to noise ratio. The affinity constants are calculated with Equation XIV and are shown in Table C4.

Table C4: Affinity constants of nucleotide analogues to the wildtype HlyB-NBD; TNP-AMP exhibited no enhancement, therefore it was concluded that it did not bind.

	K _D [μM]
TNP-ATP	0.75 ± 0.15
TNP-ATP (Mg ²⁺)	0.44 ± 0.13
TNP-ADP	1.20 ± 0.09
TNP-ADP (Mg ²⁺)	0.78 ± 0.12

The affinities for the TNP nucleotides were around 100 fold higher then those derived from the Y477W mutant with AXP. This increase in binding affinity is equivalent to binding energy difference of ~ 3 kcal·mol⁻¹ leading to the conclusion that an additional non-covalent bond is formed upon TNP-AXP binding.

To measure the affinity of the wildtype HlyB-NBD to ATP or ADP and to underline the fact that the tighter binding is not due to the wildtype situation and rather due to the TNP-moiety, pre-bound TNP-ADP was competed out by ATP or ADP. By adding ATP or ADP the fluorescence was decreased since the TNP moiety is not bound any longer to the protein Figure C6.

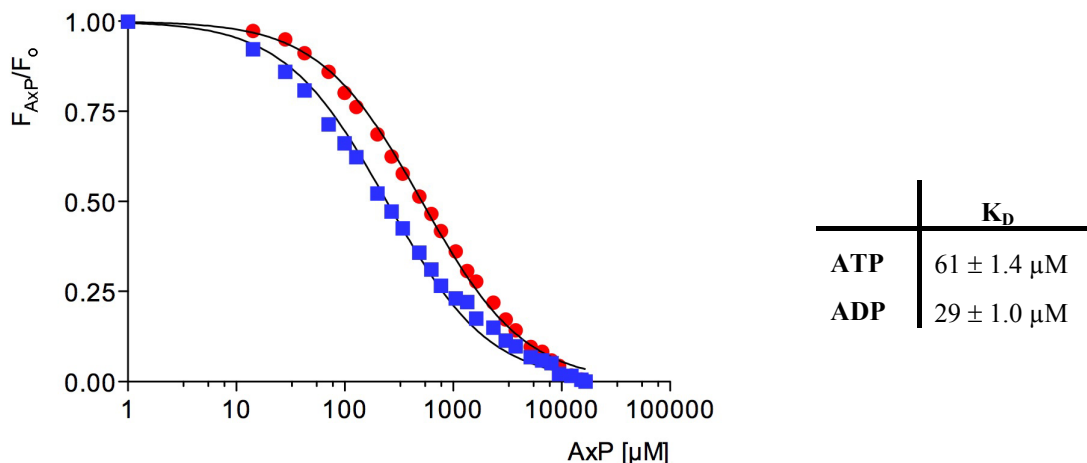
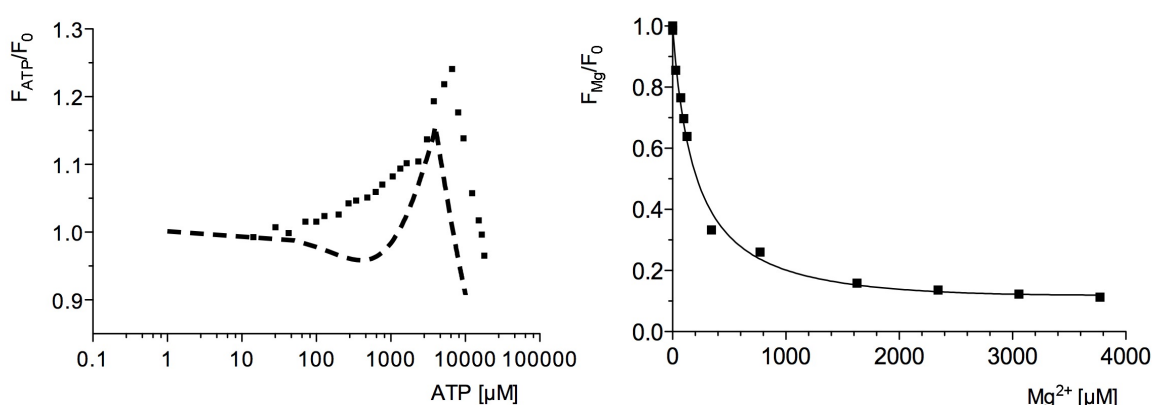


Figure C6: Competition of ATP/ADP with TNP-ADP. F_{AXP} denotes the fluorescence at a certain ADP or ATP concentration, while F_0 is the initial fluorescence. 10 μM TNP-ADP was preincubated with 4 μM HlyB-NBD in 100 mM HEPES pH 7 and 20 % glycerol and (out of stock solutions) of 10 mM 20 mM, 50 mM, 100 mM, 200 mM, 500 mM, ADP (circles) or ATP (squares) was added up to the final concentration of 16 mM. Data were fitted according to Equation XIX. If AMP was added no decrease attributed to competition was detectable (data not shown).

The affinity of ATP to the NBD was $61 \pm 1.4 \mu\text{M}$ and for ADP $29 \pm 1.0 \mu\text{M}$. These values reflected the wildtype situation, whereas the values obtained with intrinsic tryptophan quenching are higher, but were still in a similar range. Thus, the TNP moiety increased the affinity of the nucleotide as it was proposed. The competition experiments were also done in the presence of 4 mM Mg^{2+} to determine the affinity in presence of the metal co-factor (Figure C7, left panel, squares).



A

B

Figure C7: Influence of Mg^{2+} on TNP-ADP complexes. (A) Competition of bound TNP-ADP with ATP in the presence of 4 mM Mg^{2+} . Squares are measured values and the dashed line represents the simulated curve in which the affinity of $\text{ATP}/\text{Mg}^{2+}$ was assumed to be 100 μM (see text for details). Mg^{2+} depletion effects are included. (B) Titration of Mg^{2+} onto preformed TNP-ATP/NBD complexes. The data were fitted with a 1:1 binding behaviour resulting in an Mg^{2+} affinity of $205 \pm 30 \mu\text{M}$.

In sharp contrast to the expectation shown in Figure C6, the fluorescence remained initially unchanged then increased and suddenly dropped upon addition of ATP (Figure C7). This behaviour could be explained by depletion of Mg^{2+} by binding to the added ATP (up to a ATP concentration of 7 mM, Figure C7). The total fluorescence can be expressed as the sum of the fluorescence of TNP-ADP bound to the HlyB-NBD and of the fluorescence of bound TNP-ADP/ Mg^{2+} . This could be calculated with the equation $F_{\text{total}} = a \cdot F_{\text{TNPADPMg}^{2+}} + b \cdot F_{\text{TNPADP}}$ with a and b representing a fraction correlated by $a + b = 1$. Since the enhancement factor γ for TNP-ADP/ Mg^{2+} was 1.8 and 6 for TNP-ADP an increase of F_{TNPADP} caused by a decrease of the Mg^{2+} concentration corresponding to an initial increase of fluorescence. At higher ATP concentrations TNP-ADP was competed out, as measured by the decrease of the total fluorescence. Taking these effects into account, one could simulate a theoretical curve as shown in Figure C7, left panel. The dashed line corresponds to the sum of the theoretical curve for the TNP-ADP/ Mg^{2+} experiment (multiplied with factor a) and the theoretical curve for the TNP-ADP experiment (multiplied with factor b). The simulation shown in Figure C7 A was performed with an assumed binding affinity of ATP or ATP/ Mg^{2+} of 100 μM .

Titration of Mg^{2+} into the preformed TNP-ATP/NBD complex enabled to measure the binding constant of Mg^{2+} to TNP-ATP. The affinity is $205 \pm 30 \mu\text{M}$, which was in agreement with published literature (105 μM ; (Wilson & Chin, 1991), where ITC was used to study interactions of ATP with divalent ions. The affinity of Mg^{2+} is only a rough estimation of the affinity since different protonation states and the second Mg^{2+} binding site was neglected¹.

The addition of higher concentrations of Mg^{2+} (e.g. 50 mM Mg^{2+}) would prevent such depletion effects, but the enhancement factor γ was only 1.05 at this concentration (data not shown) hampering the possibility of a meaningful competition experiment.

To summarize, nucleotide analogues are a powerful tool to measure for example binding affinity of nucleotides. Divalent ions drastically influence fluorescence behaviour limiting the conclusions that can be drawn in presence of the co-factor for the HlyB system.

¹ at the given pH most ATP molecules are deprotonated and the second binding site has a affinity of roughly 20 mM, therefore the estimation is justified (Storer and Cornish-Bowden, 1976).

1.3 The mode of TNP-ADP binding

In the previous section it was shown that TNP nucleotides exhibit a 50 - 100 fold higher affinity than unmodified nucleotides. This higher affinity can only be accomplished by an additional contact of the protein to the nucleotide adding $\sim 3 \text{ kcal}\cdot\text{mol}^{-1}$ to the binding energy required for the increase of affinity. In order to understand the binding at a molecular level a crystal structure with bound co-factor is essential. Based on the crystallization conditions of HlyB-NBD with bound ADP, TNP-ADP bound HlyB-NBD crystals could be obtained by soaking. Therefore crystals of HlyB-NBD with bound ADP were soaked into a 1:1 solution of 70 mM CAPS pH10.4, 30 % glycerol and 10 μM TNP-ADP in 100 mM TRIS-Cl pH 8.0, 10 % PEG 6000 and 5 % MPD (Oswald et al, 2008a; Zaitseva et al, 2005a).

With intense yellow coloured crystals, it was possible to obtain the TNP-ADP bound structure at the resolution of 1.6 Å (Figure C8). Data statistics are shown in (Oswald et al, 2008a).

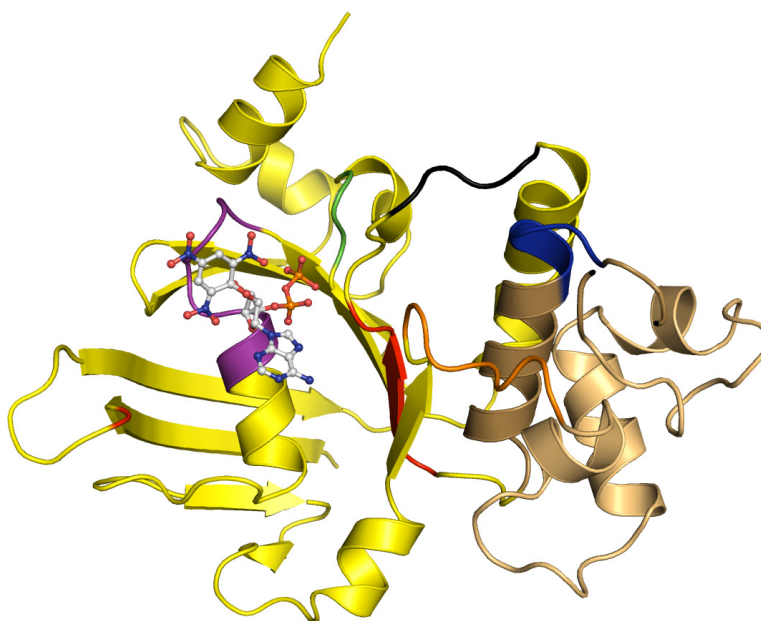


Figure C8: Overall structure of HlyB-NBD with bound TNP-ADP at 1.6 Å (Oswald et al, 2008). The catalytic and helical domains are coloured in yellow and sand, respectively. Conserved motifs are coloured. The Walker A and B motif is coloured in purple and red (residues 502-510 and residues 625-630). The C-loop is shown in blue (residues 606-610). The Q-loop (residues 550-556) is depicted in orange and the D-loop (residues 634-637) is coloured black and the H-loop is green (residues 661-663). The residue interacting with the adenine moiety of ATP via π - π -stacking is coloured in red (Y477). The ADP of TNP-ADP resembles the binding mode of the ADP bound structure.

As shown in Figure C8 the HlyB-NBD adopted a two-domain architecture. The catalytic domain (in yellow) was composed of a six-stranded, anti-parallel, β -sheet flanked by four

helices. This domain contains all residues necessary for the nucleotide binding, or in this case TNP-ADP. In addition, the ABC specific α -helical subdomain with the ABC specific C-loop is present (coloured in sand). A detailed view of the TNP-ADP binding site is shown in Figure C9.

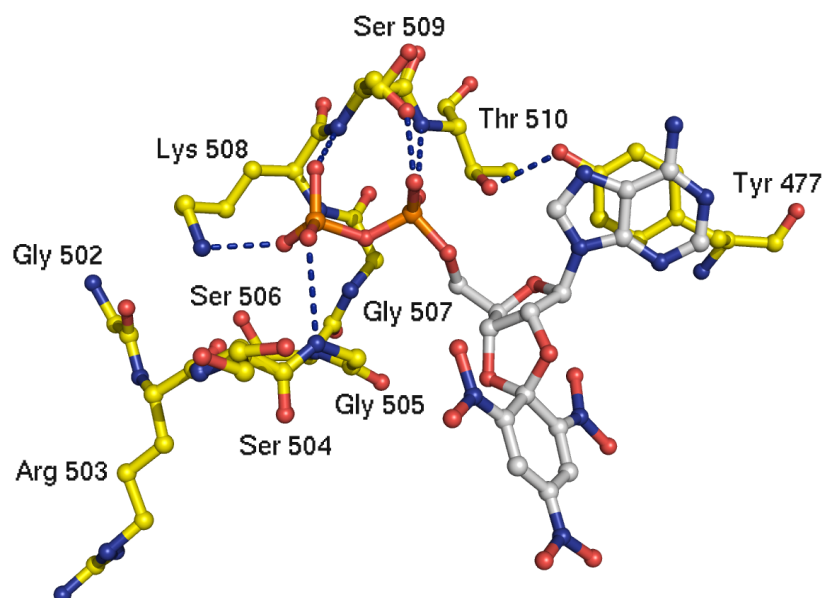


Figure C9: The nucleotide binding site of the TNP-ADP HlyB complex. Shown are residues of the Walker A motif (amino acids 502 -510) and the aromatic residue Y477, engaging the adenine moiety via a π - π interaction. Blue dashed lines highlight the interactions between the HlyB-NBD and the TNP-ADP.

As expected from the ADP bound structure of the HlyB-NBD, residues of the Walker A interacted with the α and β phosphate of TNP-ADP via interaction of the side chains (Lys508, Ser509 and Thr510) and via interactions with the protein backbone (Gly505, Gly507, Ser509 and Thr510). Furthermore the hydroxyl side chain of Thr510 aligned the aromatic Tyr477 forming a platform for π - π stacking. For the Walker A motif the side chains of the two serine residues (Ser504 and Ser 509) exhibited dual conformations. During initial calculation a remarkable and unexpected feature of the ligand TNP-ADP was observed: The overall B-factor of the protein and the ADP moiety of TNP-ADP was around 15-25 \AA^2 whereas the TNP moiety had a increased B-factor of 42-55 \AA^2 . Since TNP is bonded to the 2' and 3' position of the ribose a rotational motion was hard to imagine. Thus, a mixed occupancy was concluded. This was reasonable especially in the light that the crystals were obtained by soaking the fluorophor into the ADP bound NBD crystal. Including ADP and TNP-ADP into the model resulted into two almost equal occurring conformations: One conformation with bound ADP and the canonical conformation of both serines and the other conformation with

bound TNP-ADP and the rotated serine side. This is indicated in Figure C9 and highlighted in black ball-and-stick representation in Figure C10.

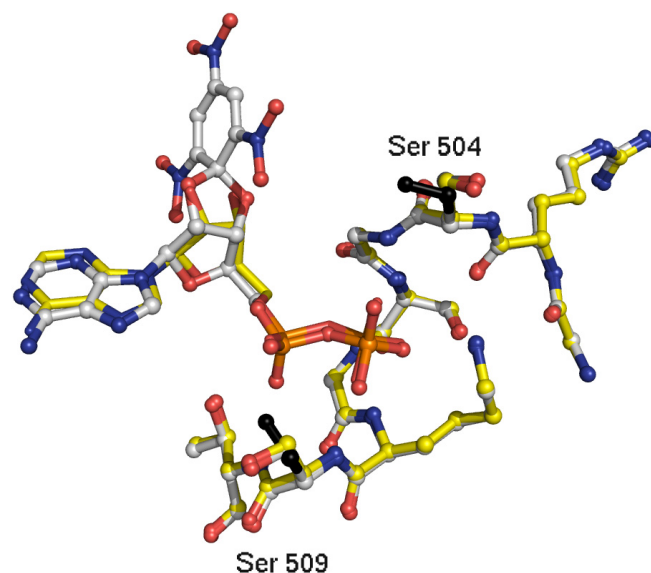


Figure C10: Nucleotide binding site of TNP-ADP. Superimposition of the wildtype HlyB-NBD in complex with TNP-ADP and in complex with ADP (yellow, pdb file 2FF7 Zaitseva et al, 2006). The Walker A motif is shown from residue 502-510. TNP-ADP specific positions of Ser504 and Ser509 side chains are highlighted in black.

In Figure C10 a superimposition of the wildtype HlyB-NBD in complex with TNP-ADP and in complex with ADP is shown. It revealed an almost perfect overlay with an rmsd of 0.32 Å for the 243 C α atoms and 0.08 Å for the Walker A motif. Although the rotated serine side chains were due to the binding of the TNP moiety, no well-defined interactions of the TNP moiety with the protein could be observed. However the quality of the data allowed introduction of the water molecules present in the binding pocket. Figure C11 shows the TNP-binding pocket including the water molecules mediating TNP-protein interactions.

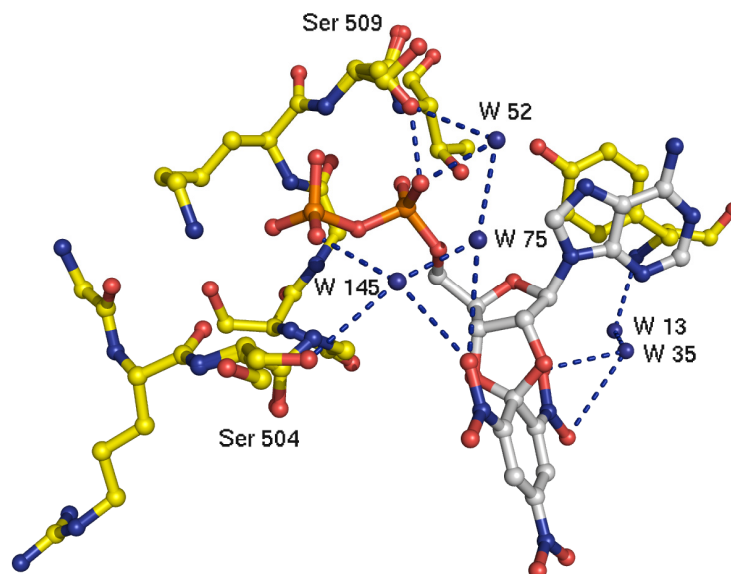


Figure C11: Nucleotide binding site of TNP-ADP with added water molecules. The Walker A motif is shown from residue 502-510. TNP-ADP specific positions of Ser504 and Ser509 side chains are highlighted in black. TNP specific water molecules and their interactions are shown as blue spheres and dashed blue lines.

The shown water molecules were already present in the ADP bound structure (Zaitseva et al, 2006) but in here they enabled the additional contacts of the TNP-nucleotide. The ortho-nitro group of the TNP moiety interacted via hydrogen bonds with water 35. Water 35 then interacted with water 13 that finally forms a hydrogen bond with the amide backbone of Tyr477. The other ortho-nitro group of TNP interacted with waters 145 and 75, while water 145 connected the side chain of Ser504 with the β -phosphate moiety. However, this latter interaction occurred only with the TNP-specific conformation of Ser504. As also observed in the ADP/HlyB-NBD complex, water 75 interacts with the α -phosphate moiety and water 52. Water 52 interacted with the α -phosphate moiety in both structures, but in the presence of TNP-ADP, specifically locked the side chain of Ser509 in the new conformation. This in turn induced a new hydrogen bond between Ser509 and the α -phosphate that is absent in the ADP-structure of the HlyB-NBD. In summary, these water-mediated interactions of the TNP-moiety generated two novel protein-ADP interactions (involving water 145 and 52/75), producing conformational changes in the two serine side chains, that could explain structurally the increased affinity of the fluorophore-modified nucleotide for the ABC ATPase, or more in general for P-loop ATPase, most of all having these two conserved residues, or other residues enabling hydrogen bonding.

Nevertheless, the question remained whether these novel conformations of Ser504 and Ser509 are a prerequisite for binding or whether these are a consequence of water molecules

specifically recruited into the binding site due to the presence of the TNP moiety. To tackle this question, the mutant S504A using the primers S504Afor and S504Arev and the plasmid encoding for the wild type HlyB-NBD as a template was generated. To further discriminate in between a general influence on the nucleotide binding, the double mutant Y477W/S504A was also generated enabling measuring the nucleotide affinity by tryptophan quenching. Hereby primers S504Afor and S504Arev were used with the plasmid encoding for the Y477W as a template.

If the novel TNP-specific conformation of Ser504 would be a prerequisite for binding and consequently results in the higher affinity, mutation of this residue should clearly affect TNP-nucleotide affinity.

Both mutants could be successfully overexpressed and purified. Not surprisingly, both mutants exhibited no ATPase activity, as the mutated amino acid was in the highly conserved Walker A motif ($< 1\%$ of the wildtype activity, data not shown). The Y477W/S504A was used to measure the affinity of ADP, while the S504A mutants was used to determine the affinity for TNP-ADP (both are shown in Figure C12).

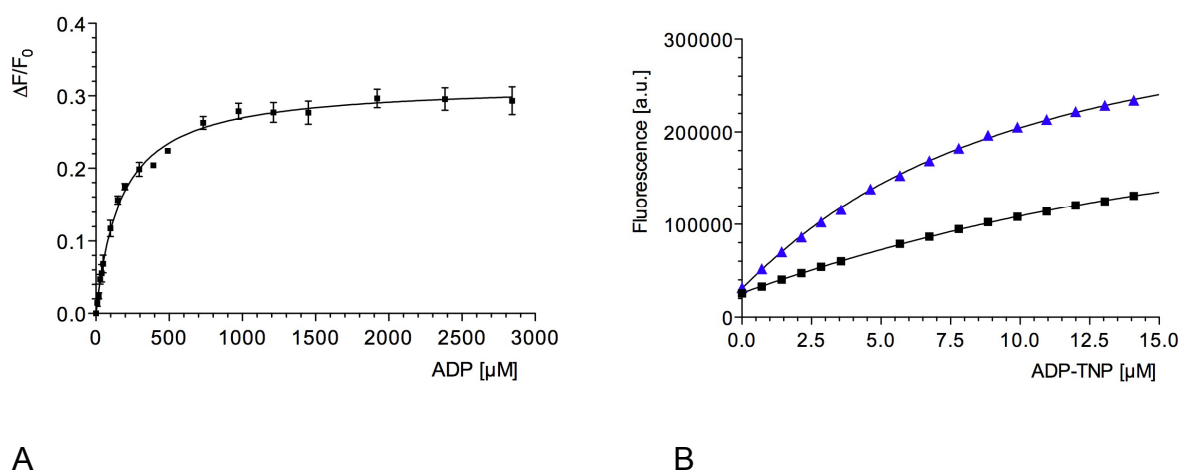


Figure C12: Affinity measurements for the HlyB-NBD mutants Y477W/S504A and S504A (A) Fluorescence quenching of the HlyB-NBD mutant Y477W/S504A with ADP. The affinity of ADP was $174 \pm 11 \mu\text{M}$ compared to $89.7 \pm 8.8 \mu\text{M}$ measured for the Y477W mutant. (B) Affinity measurement of TNP-ADP for the S504A mutant. The affinity was $2.2 \pm 0.24 \mu\text{M}$ compared to $1.20 \pm 0.088 \mu\text{M}$ as measured for the wildtype NBD.

The affinity for ADP of the Y477W/S504A was about 2-fold lower than for the Y477W mutant ($174 \pm 11 \mu\text{M}$ compared to $89.7 \pm 8.8 \mu\text{M}$). Also the affinity for TNP-ADP decreased by around the factor of two ($2.2 \pm 0.2 \mu\text{M}$ compared to $1.20 \pm 0.09 \mu\text{M}$). This indicated that

the serine to alanine mutant does slightly influence the nucleotide binding by the factor of two, but unexpectedly no effect on TNP-ADP binding was observed.

To reveal the differences of the bound TNP-ADP in the S504A HlyB-NBD mutant and the wild type protein the crystal structure of the S504A with bound TNP-ADP was solved. As for the wildtype protein, first ADP bound crystals were generated. But instead of soaking in the TNP-ADP, streak seeding was used to obtain crystals (Oswald et al, 2008b). By adding microcrystals to a TNP-ADP and S504A containing crystallisation solution TNP-ADP bound crystals were generated.

It was possible to determine the molecular structure at 2.0 Å. Data statistics are shown in (Oswald et al, 2008a). With the technique of streak seeding a uniform incorporation of TNP-ADP could be achieved.

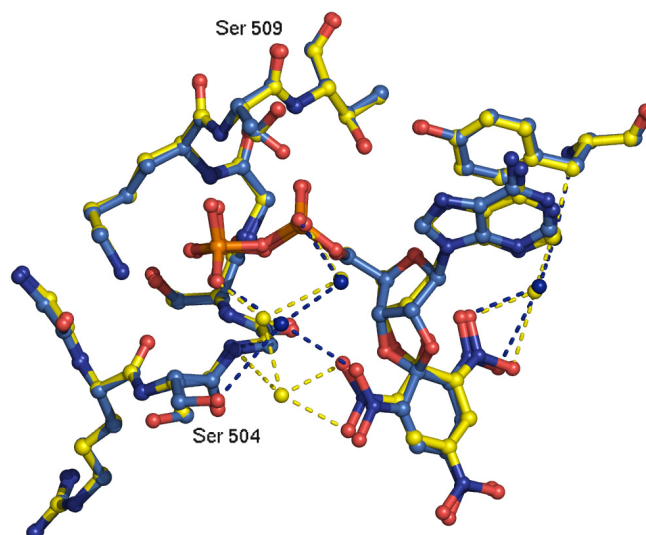


Figure C13: Overlay of the TNP-binding pocket of the S504A mutant with the wildtype. The S504A mutant is shown in cyan, also the corresponding TNP-ADP and the water molecules. Strikingly, the loss of the serine side chain is compensated by an additional water molecule next to the ortho-nitro group of TNP.

As shown in Figure C13, again no direct interactions of the TNP moiety could be observed. Furthermore, no dual conformation was observed. Why is the affinity of nucleotides for the mutant similar as for the wild type, since one would expect the loss of the S504 mediated bond? The comparison in Figure C13 revealed the presence of an additional water molecule in the S504A mutant. This unique water molecule connected the ortho-nitro group of TNP via a second water molecule to the β -phosphate and is directly linked to the backbone of A504. The

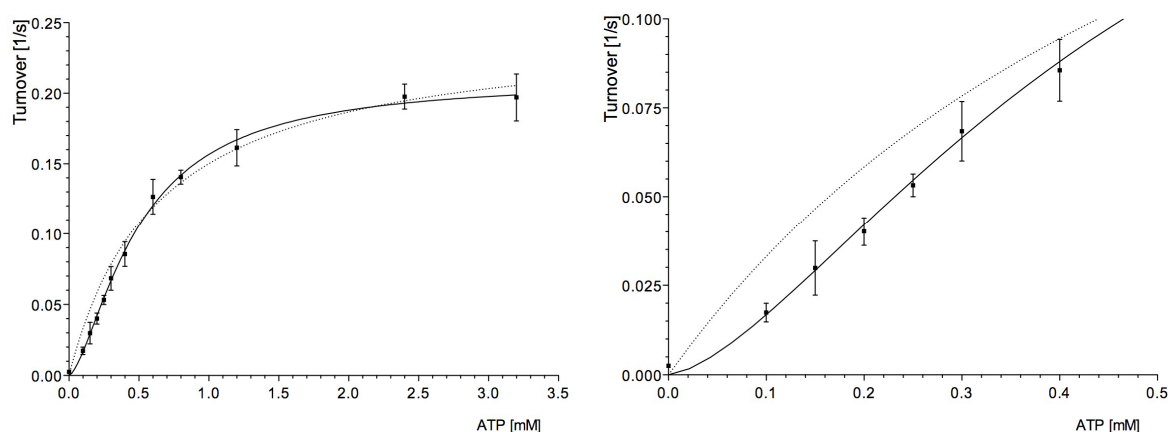
other ortho-nitro group revealed a similar binding as it could be shown for the wild type. The remodelling of the water network seemed to compensate the loss of the serine side chain.

1.4 How is ATP hydrolysed by HlyB-NBD?

Although recent successes in solving the crystal structures of ABC transporters have laid the foundation for a new era of studies using structure-guided mutagenesis, many issues relating to the mechanism of action of ABC transporters are still obscure. An important issue is the catalytic mechanism of ATP hydrolysis by the NBDs, which can be further subdivided into two major components. The first pertains to the actual cleavage of the terminal phosphate and the second to NBD–NBD communication. In the following results, a model how the hydrolysis takes place will be presented, which is verified by experimental data.

1.4.1 HlyB-NBD undergoes a dimeric species during the ATP-hydrolysis cycle

In standard Michaelis-Menten kinetics, no influence of the communication between the single active sites in enzymes is included. Every active site is treated separately. Cooperativity in terms of an increased activity upon increasing either substrate or protein concentration points to several conclusions: The active species exhibits mandatory more than one active site and furthermore those active sites interact with each other during the catalytic cycle (here: during the hydrolysis of ATP). This behaviour can be described by the additional factor h to the Michaelis-Menten equation (Equation II). h is the Hill coefficient describing the degree of cooperativity. Figure C14 shows an ATPase of the HlyB-NBD with increasing ATP concentrations whereas in Table C5 the results are shown ($c_{\text{HlyB-NBD}}=0.2$ mg/ml in 100 mM HEPES pH 7, 20 % glycerol, 10 mM MgCl_2 , reaction time 3 min).



A

B

Figure C14: ATPase activity as a function of ATP concentration at a 0.2 mg/ml enzyme concentration in 100 mM HEPES pH 7.0, 20% glycerol, 10 mM MgCl_2 and varying ATP concentrations. ATPase activity was determined from the average of at least two independent experiments with deviations of data points from the mean given as error bars. (A) represents the full concentration range and (B) is a zoom on smaller substrate concentrations highlighting the cooperative behaviour. Data were fitted with a fixed Hill coefficient of 1 (=Michaelis-Menten behaviour; dotted line) or with a variable Hill coefficient (solid line).

Table C5: Kinetic parameters as function of ATP concentration. Note that compared to Table C1 k_{cat} is largely increased due to the higher protein concentration.

	$K_{0.5}$ [mM]	k_{cat} [min^{-1}]	h
HlyB-NBD wt	0.34 ± 0.08	12.6 ± 0.7	1.52 ± 0.16

In Figure C14 B a close-up to lower ATP concentrations is shown. The measured values clearly deviated from the Michaelis-Menten behaviour (Figure C14, dotted lines), but could be accurately fitted by the Hill equation. The Hill coefficient was 1.52 ± 0.16 indicating a cooperative ATPase activity. If cooperative behaviour is seen between active sites on spatial divided proteins one would also expect a dependence of the turnover number if the protein concentration is increased, since lower protein concentrations would disadvantage oligomer formation. In case of a non-cooperative enzyme function one would expect a constant turnover number independent of the protein concentration.

ATPase measurements with increasing protein concentration underlined the hypothesis that an oligomeric species is part of the ATP hydrolysis cycle (Figure C15). Here an apparent K_D in the presence of ATP/Mg^{2+} can be calculated corresponding to the half maximal turnover in Figure C15 (0.033 mg/ml or 1.2 μM HlyB-NBD)

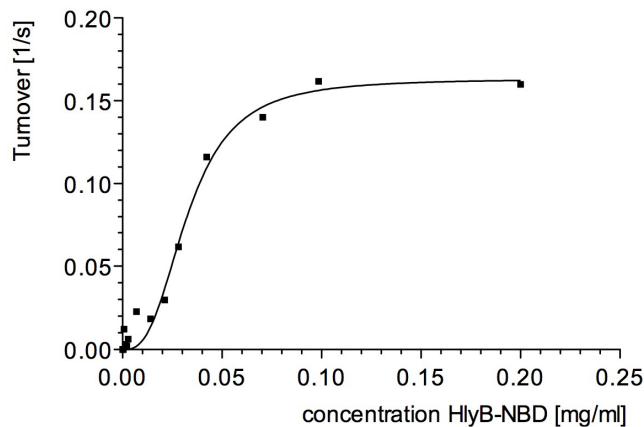


Figure C15: ATPase activity as a function of HlyB-NBD concentration at a ATP concentration of 1 mM in 100 mM HEPES pH 7, 20% glycerol, 10 mM MgCl_2 . ATPase activity was determined from 3 min to 30 min whereas ATPase activity was constant up to 45 min in this buffer.

Looking at the monomeric structure of HlyB-NBD revealed that a dimer or oligomer would make perfect sense to explain the presence of the C-loop. The C-loop resides in the helical domain with a distance of around 30 Å to the ATP binding site (see Figure C9, here TNP-ADP is shown as nucleotide). It was shown on other systems that mutations in the C-loop abolished the ATPase activity (Schmees et al, 1999), so that one might speculate that the C-loop transmits a signal to the ATP binding pocket. Since it is hard to believe that this signal can be passed within a monomer an elegant solution would be that an opposing (trans) NBD supplies the C-loop to the cis ATP binding pocket.

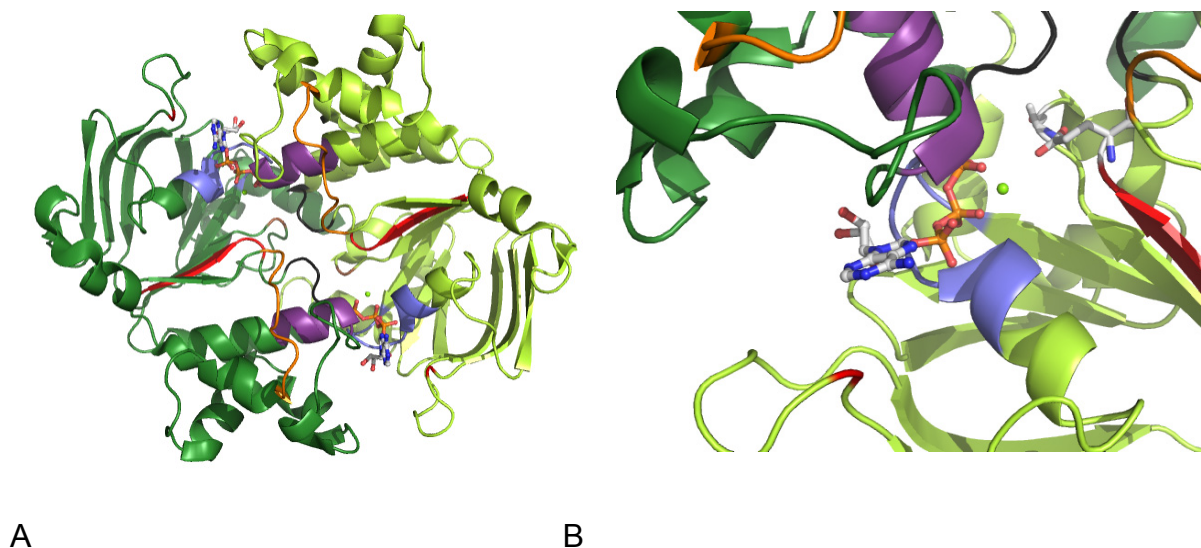
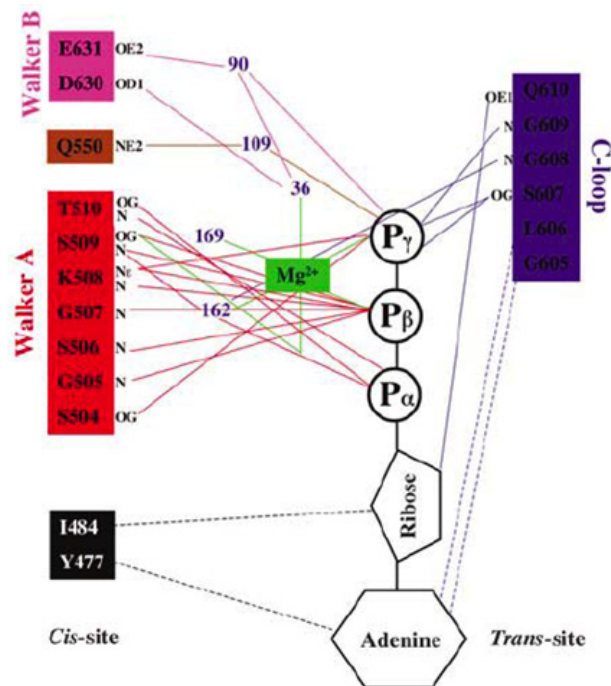


Figure C16: ATP/ Mg^{2+} -bound sandwich dimer of the HlyB-NBD mutant H662A. (A) View from the membrane side. Conserved motifs are coloured as follows: Walker A and B motifs in blue and red, the C-loop in purple, the



1.4.2 Which mechanism follows the cleavage of the γ -phosphate?

From the above outlined results, it could be concluded that the catalytic cycle of an NBD is composed of nucleotide association, NBD dimerization, ATP hydrolysis, and dissociation of the NBDs and nucleotides (NBD association and dissociation could also be just a slight opening to release the nucleotides). Any of these steps regardless representing chemical or diffusion-controlled reactions might be the rate-limiting step under steady-state conditions. To investigate the relative contribution of these steps, the reaction velocity of the ATPase activity of wild-type HlyB-NBD in solutions of different viscosity was analyzed (Zaitseva et al, 2005a). Since molecular diffusion coefficients depend inversely on the viscosity of the solution, diffusion-controlled reactions are slowed down in the presence of increasing concentrations of a viscogenic reagent such as sucrose (Martin & Hergenrother, 1999). The turnover number of ATPase activity was not significantly affected by changes in viscosity. It is noteworthy to mention that the ATPases in sucrose were performed at protein concentrations higher than 0.1 mg/ml favouring NBD dimerization (Figure C14). Therefore, diffusion-controlled reactions such as nucleotide association or dissociation or NBD dimerization seem unlikely to be rate-limiting factors (Cole et al, 1994). Rather, a chemical reaction such as proton abstraction or ATP hydrolysis itself governs the reaction velocity under steady-state conditions. Since a chemical reaction such as ATP hydrolysis seems to be rate limiting, one can assume two different and extreme scenarios: ‘general base catalysis’ (Fersht, 1999) or substrate assisted catalysis (SAC, Dall'Acqua & Carter, 2000). If ATP hydrolysis depends on the action of a general base, for example the previously proposed glutamate (Smith et al, 2002), E631 in HlyB, proton abstraction or water polarization would represent the rate-limiting step of hydrolysis. If SAC applies, no proton abstraction would be involved in the rate-limiting step. Given that the chemical reaction is rate-limiting as shown above, one possibility to distinguish both extreme cases is the use of solvent isotope effects (Schowen & Schowen, 1982). Therefore steady-state measurements in the presence of D₂O were performed. To account for the deuterium-induced pH shift, buffer in 100% D₂O (100mM HEPES, 20% glycerol) was adjusted prior mixing to pH 7.4.

As shown in Figure C18, the ATPase activity remained essentially the same over the range 0–60% D₂O with respect to v_{\max} . Similarly, no decrease in the k_{cat} values or in the catalytic efficiency ($k_{\text{eff}}=k_{\text{cat}}/K_{0.5}$) was observed (Figure C17 B).

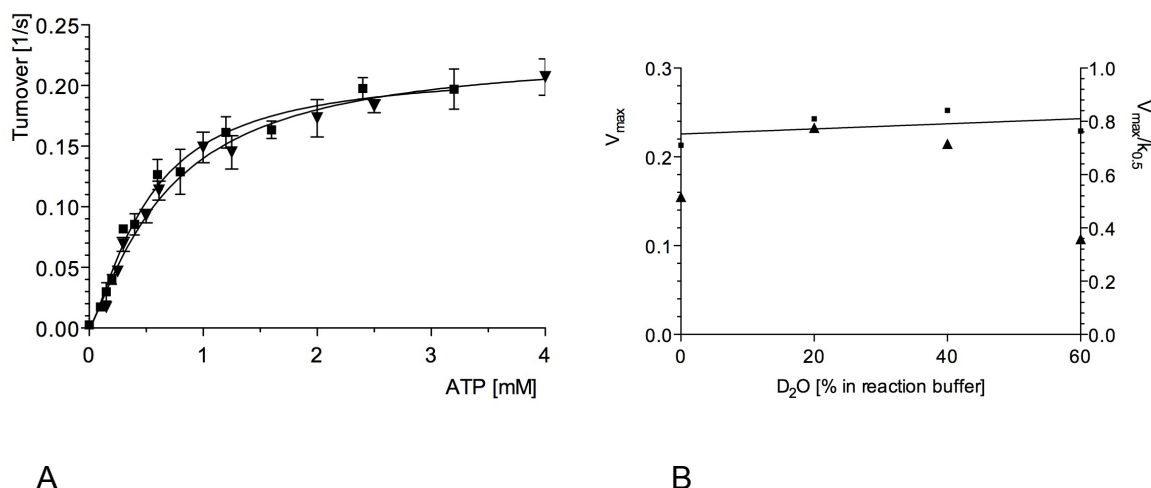


Figure C18: ATPase activity as a function of ATP concentration at a 0.2 mg/ml enzyme concentration in 100 mM HEPES pH 7.0, 20% glycerol, 10 mM MgCl₂ and varying D₂O concentrations. ATPase activity was determined from the average of at least two independent experiments with deviations of data points from the mean given as error bars. (A) Steady state kinetics for 0% D₂O (squares) and 60% D₂O (inverted triangles). (B) v_{\max} values for 0%, 20%, 40% and 60% D₂O (squares); catalytic efficiency is drawn as triangles. To account for the deuterium-induced pH shift, buffer in 100% D₂O (100mM HEPES, 20% glycerol) was adjusted to pH 7.4.

Extrapolation of the k_{cat} values to 100% D₂O resulted in a $k_{\text{cat};\text{H}_2\text{O}}/k_{\text{cat};\text{D}_2\text{O}}$ of 0.79 for HlyB-NBD, similar to the value of 0.71 reported for p21ras (Schweins & Warshel, 1996). The experiment in D₂O implied that proton abstraction might not be the rate-limiting step in this system.

Unfortunately however, this result left open the possibility of a base-dependent catalytic step that is not rate-limiting. It could well be that the P_i diffusion out of the dimer is rate-limiting. We chose therefore to assess further the relative roles of the H662 and E631 residues and analyzed the pH dependence of ATPase activity for the wild type and the E631Q mutant. If E631 would be directly involved in catalysis, a change in pH dependence would be expected in the E631Q mutant since Gln is a poorer base than Glu. The pH dependence of the wild type and that of the E631Q mutant (retaining around 10% residual activity) are virtually identical, providing further evidence that E631 does not participate directly in catalysis (here not shown, (Zaitseva et al, 2005b)). Again this result does not exclude the possibility that a base mechanism may still operate upstream of the rate-limiting step in the catalytic cycle. Nevertheless, all these results, combined with the evidence that H662 plays a crucial role in catalysis, verified by fact that ATP/Mg²⁺ containing dimers could be obtained, compelled us to consider alternative mechanisms. Thus, SAC might apply, where the substrate participating

in catalysis might be either ATP itself, as it has been suggested for some GTPases (Schweins et al, 1995), or conceivably the cofactor, Mg^{2+} .

Further support for SAC derived from the fact that ATPase activity was modulated by divalent metal ions (Table C6). Here the kinetic parameters k_{cat} and $K_{0.5}$ were determined in the presence of different divalent ions. Turnover numbers for the HlyB-NBD ATPase activity decreased with $Mg^{2+} > Mn^{2+} > Co^{2+}$, as well as the catalytic efficiency ($k_{eff}=k_{cat}/K_{0.5}$). k_{cat} and k_{eff} correlated with the pK_a values of the metal ion-aqua complexes and their strength to act as a Lewis acid but not with their atomic radius.

Table C6: Modulation of the kinetic parameters $K_{0.5}$ and k_{cat} using different divalent ions.

<i>Cation</i>	Mg^{2+}	Mn^{2+}	Co^{2+}
$K_{0.5}$ [mM]	0.33 ± 0.04	0.37 ± 0.03	0.30 ± 0.04
k_{cat} [s^{-1}]	0.199 ± 0.004	0.177 ± 0.003	0.056 ± 0.002
pK_a^a	11.4	10.6	8.9
Ion radius [\AA]^a	0.78	0.91	0.82

^a taken from (Basolo & Pearson, 1967)

This modulation of activity indicated that the proton abstraction step is influenced by the presence of different metal ions. To exclude that the different divalent ions had any effect on dimerization, a protein dependent ATPase was also performed in the presence of the corresponding divalent ion. The apparent K_D remained unchanged (Table C7). Moreover, analysis of the dissociation constants of TNP-ATP and TNP-ADP revealed that the metal ions also did not influence nucleotide affinities to the NBD (Table C7). This is consistent with the idea that the rate-limiting step of the catalytic cycle of the HlyB-NBD is ATP-hydrolysis, a chemical reaction.

Table C7: Divalent ions neither change nucleotide affinity nor dimerization of the NBDs.

<i>Cation</i>	Mg^{2+}	Mn^{2+}	Co^{2+}
K_D TNP-ATP/ Me^{2+} [μM]	7.23 ± 1.09	6.50 ± 1.07	6.77 ± 0.62
K_D TNP-ADP/ Me^{2+} [μM]	2.34 ± 0.31	1.85 ± 0.41	2.62 ± 0.79
$K_{D,app,dimerization}$ [μM]	1.2 ± 0.2	1.3 ± 0.3	1.4 ± 0.3

The TNP-derivates were used since tryptophan quenching using the Y477W mutant of HlyB-NBD was not possible using divalent ions most likely due to quenching effects (data not shown). Measuring the affinity of the natural nucleotide was also not possible due to the fact that the divalent ions are depleted during competition experiment as elaborated in the first part

of this section. However, since the only concern was the relative difference in affinity due to the presence of different divalent metal ions, TNP-derivatized nucleotides were justifiably used as a valuable reporter.

1.5 ATPase activity of heterodimers composed of WT and H662A HlyB-NBD

The dimer formed by the HlyB-NBD during the catalytic cycle is composed out of two identical proteins. This is a common feature of most prokaryotic ABC systems. Looking at eukaryotic systems several well characterized systems exhibit an asymmetric behaviour. In those cases the C-loop of NBD2 is degenerated whereas the Walker A, Walker B with the following carboxylate and a functional H-loop is present. In contrast NBD1 exhibits a non-canonical C-loop with an amino acid exchange at position of the highly conserved histidine exemplified by CFTR or by the TAP1/2 transporter (Aleksandrov et al, 2002; Ernst et al, 2006).

To extend the functional analysis of HlyB-NBD as model system for all ABC systems and to simulate asymmetric behaviour, mixing experiments similar to the ones performed for HisP were designed (Nikaido & Ames, 1999). Assuming that the NBD dimer with two ATP-binding sites is a catalytically active species, various molar ratios of the ATPase deficient H662A mutant and the wild-type HlyB-NBD were combined, and the steady-state ATPase activity of the dimers was measured. As shown in Figure C19 A, at a constant protein concentration and different molar ratios (3:1, 1:1, and 1:3), a linear relationship of activity versus amount of the wild-type protein was observed. Thus, at a 1:1 molar ratio, the steady-state ATPase activity was 50% of the wild-type level. This was consistent with formation of 25% H662A/H662A dimers, 50% H662A/WT, and 25 % WT/WT dimers, were H662A/H662A homodimers are inactive, WT/WT homodimers are fully active, while H662A/WT heterodimers showed half of the WT/WT activity.

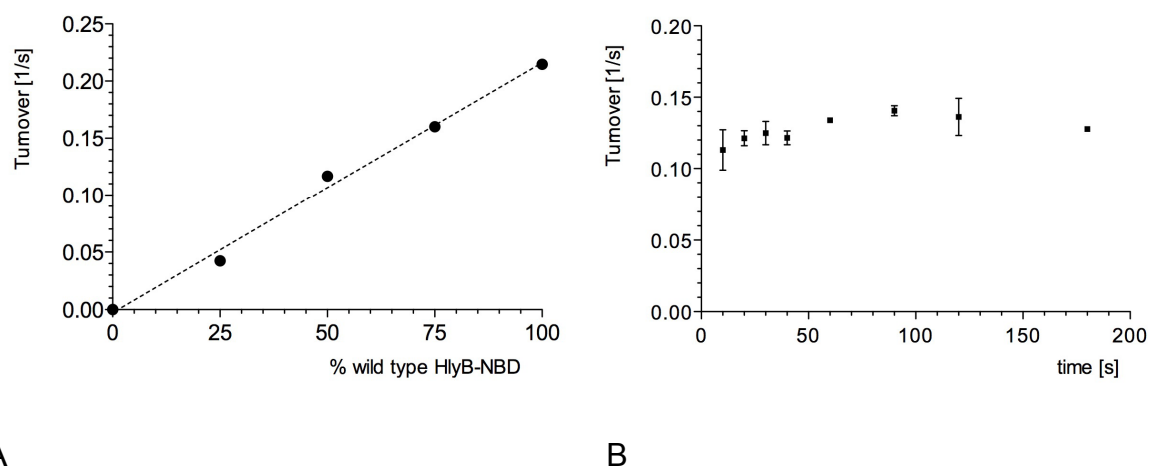


Figure C19: ATPase mixing experiments at a 0.1 mg/ml enzyme concentration in 100 mM HEPES pH 7.0, 20% glycerol, 10 mM MgCl_2 (A) k_{cat} values of different mixing ratios. k_{cat} was determined by a steady-state ATPase like shown in Figure C14A. (B) Time-dependent mixing experiments. In this experiment the HlyB-NBD concentration for 10 to 40 sec was 0.2 mg/ml whereas it was reduced to 0.1 mg/ml for the values measured for 60 to 180 sec.

This result indicated that ATP hydrolysis occurs in one ATP-binding site independent of the other site of the NBD heterodimer. Such a scenario is reminiscent of the model of ATPase activity proposed for Mdl1p-NBD (Janas et al, 2003), which states that the hydrolysis of each ATP molecule in Mdl1p-NBD occurs in a sequential fashion. This conclusion is based on the assumption that an unrestricted random association of monomers upon mixing is happening. One can argue that subunits can be associated in a preferential manner, resulting in a favourable formation of the homodimers in the ATP-supplemented solution. In that case, only WT/WT homodimers would be responsible for the detected ATPase activity. However, this scenario seemed unlikely in view of a nonlinear dependence of ATPase activity on protein concentration observed in the protein range of 0 - 0.2 mg/ml for the wt HlyB-NBD (Figure C15). Thus, at a 1:1 molar protein ratio of WT and mutant tested at 0.1 mg/ml total protein concentration, the final level of ATP hydrolysis should then be less than 50%, assuming the existence of only homodimers in the solution. The same logic applied to the experiments performed at 25% or 75% of wt proteins in a mixture with H662A mutant. Importantly, the initial ATPase activity of a 1:1 mixture did not change over time (Figure C19 B). The initial ATPase activity remained constant during the first 180 s following substrate addition. The first data point was acquired after the first ATPase cycle (k_{cat} is 0.1 ATP s^{-1} under the conditions of the assay). If heterodimers have no ATPase activity, the detected activity would be 25% of that with WT homodimers only. After the second ATPase cycle (20 s), an activity of 33.5% would be observed, and so on. However, since no such change in ATPase activity

was detectable (Figure C19 B), one has to conclude that the H662A/WT heterodimers must possess 50% of the ATPase activity of the WT/WT homodimer. Thus, the linear relationship between activity and increasing the concentration of the mutant NBD (Figure C19 A) indicates that both WT/H662A heterodimers and WT/WT homodimers contributed to the detected ATPase activity.

2. Cloning and expression of the inner membrane components of the haemolysin system

The successful overexpression and purification of integral membrane proteins in sufficient amounts for biophysical and biochemical studies present a major challenge in the field of membrane protein biochemistry. It has been known that HlyB and HlyD are difficult to overexpress in sufficient amounts in *E. coli* (J. Young and I.B. Holland, personal communication) and also in other organisms like *S. cerevisiae* (Kolling & Hollenberg, 1996). To overcome obstacles in the overexpression, we used recent insights into membrane protein expression to pave the way towards higher protein yields. A diverse ensemble of modified constructs with different promoters, different tag positions and different vectors promised an improvement.

2.1 Cloning strategy and cloning of expression plasmids

In *E. coli* the inner membrane components of the haemolysin system *hlyB* (2124 bps) and *hlyD* (1437 bps) are encoded on a single operon together with *hlyA* and *hlyC*. In between *hlyB* and *hlyD* an intergenic 16 bp long sequence is present containing a ribosome-binding site for *hlyD*. For overexpression, these fragments were separately cloned: *hlyB* (primers Hly1 and Hly4), *hlyD* (primers Hly5 and Hly8) and *hlyB*, *hlyD* on a single DNA fragment divided only by the natural intergenic DNA sequence (primers Hly1 and Hly8). Furthermore the single genes were splitted into halves to enable cassette-wise cloning and easy introduction of additional features later on (primer Hly2, Hly3, Hly6 and Hly7; Figure C20).

Therefore a silent mutation was introduced in *hlyB* to create a ClaI restriction site (primer Hly2 and Hly3 annealing at position 1226 of *hlyB*) and also in *hlyD* (SmaI restriction site with primer Hly6 und Hly7 annealing at position 690 of *hlyD*).

Introduction of the affinity tags with a protease cleavage site (factor Xa) was done post-cloning by addition of an oligonucleotide pair either at the 5' end (N-terminus; oligonucleotides NHisEco_for/ NHisEco_rev) or at the 3' end (C-terminus, oligonucleotides

CHisBam_for/CHisBam_rev). The resulting constructs are shown in Figure C20 B.

Additional restriction sites were added at the end and at the beginning of the genes to enable introduction of these oligonucleotides (EcoRI at the 5' end and BamHI at the 3' end), resulting in additional amino acids added to each end (AKS at the N-terminus GIL at the C-terminus, the changed N-terminus was carefully checked for proper codon usage and agreement to the N-end rule; Tobias et al, 1991).

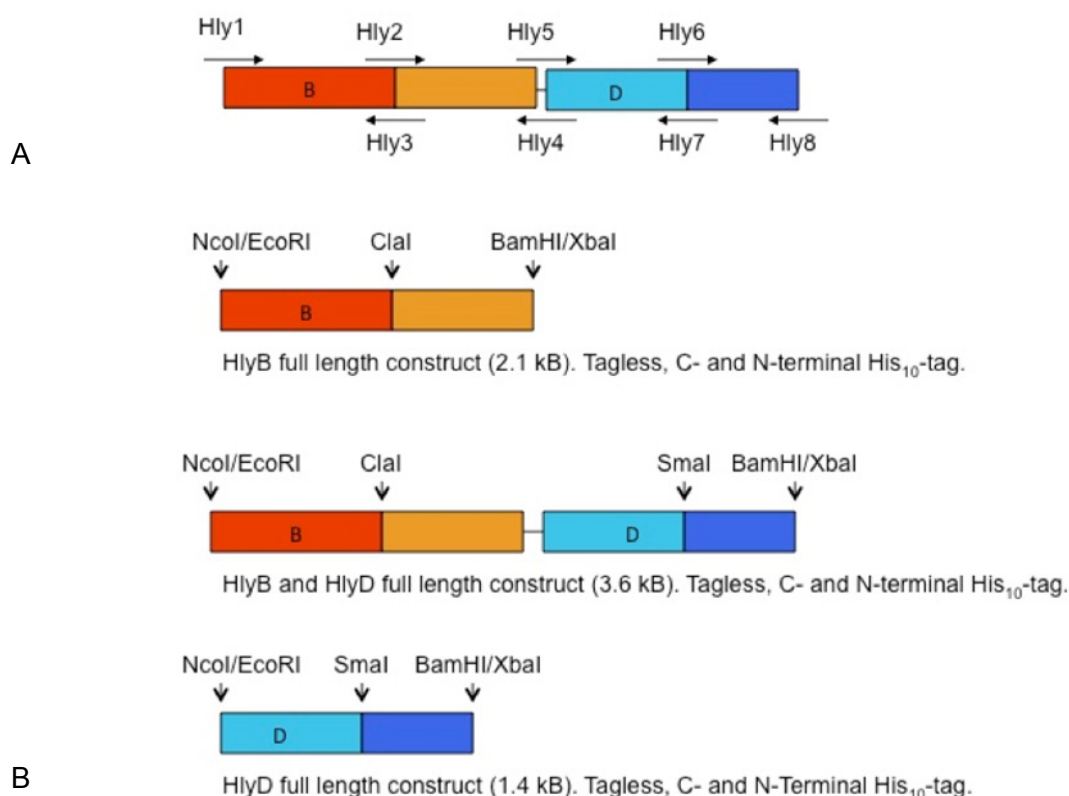


Figure C20: Illustration of the different constructs for the inner membrane components. Red and orange bars depict HlyB constructs and blue and light blue bars depict HlyD constructs. (A) Schematic view of the primers used for cloning. (B) Schematic overview of the different constructs used for cloning into different expression plasmids.

As cloning vector the pBluescript derivate pET401 was used, since it contained all required restrictions sites in its multiple cloning site and added additional restriction sites downstream of the genes (NcoI, ClaI, SmaI, XbaI, SacI and NotI). Cloning was further eased by using blue and white screening. The constructs shown in Figure C20 B were successfully cloned into pET401. If cloning was not feasible and not accomplished after a second cloning procedure the construct was further cloned in a Topo vector using the pCR-Topo vector (Invitrogen) according to the manual of the manufacturer and then subcloned into pET401. The affinity tag was introduced by opening the vector with the suitable restriction enzyme and the oligo was

added (for example pSJ003 was opened to generate pSJ004 or pSJ005). In case of pSJ011 and pSJ015 the vector was only partially digested since *hlyD* itself contained an EcoRI restriction site. The partially digested plasmid was used to introduce the affinity tag.

Table C 8: Initial constructs in the cloning vector pET401

Name	Vector	Insert	Restriction sites	Note
pSJ001	pET401	5'-HlyB	NcoI/ClaI	No tag
pSJ002	pET401	3'-C-HlyB	ClaI/XbaI	No tag
pSJ003	pET401	HlyB	NcoI/XbaI	No tag
pSJ004	pET401	HlyB	NcoI/XbaI	C-Term His10Xa
pSJ005	pET401	HlyB	NcoI/XbaI	N-Term His10Xa
pSJ006	pET401	3'-HlyB/5'-HlyD	ClaI/SmaI	
pSJ007	pET401	5'-HlyD	SmaI/XbaI	
pSJ008	pET401	HlyB/3'-HlyD	NcoI/SmaI	
pSJ009	pET401	HlyB/HlyD	NcoI/XbaI	
pSJ010	pET401	HlyB/HlyD	NcoI/XbaI	C-Term His10Xa
pSJ011	pET401	HlyB/HlyD	NcoI/XbaI	N-Term His10Xa
pSJ012	pET401	5'-HlyD	NcoI/SmaI	
pSJ013	pET401	HlyD	NcoI/XbaI	
pSJ014	pET401	HlyD	NcoI/XbaI	C-Term His10Xa
pSJ015	pET401	HlyD	NcoI/XbaI	N-Term His10Xa

After construction of the plasmids shown in Table C 8, the inserts pSJ003, pSJ004, pSJ005, pSJ009, pSJ010, pSJ011, pSJ012, pSJ013, pSJ014 and pSJ015 were subcloned into following expression vectors (four *E. coli* vectors and one *L. lactis* vector):

- pET28b(+): strong T7 promotor (IPTG inducible), confers kanamycin resistance, needs chromosomal encoded T7 RNA-polymerase (for example *E. coli* BL21(DE3)).
- pBADHisB: arabinose inducible promotor, dose dependent expression, medium copy vector, confers ampicilin resistance, strain with defect in arabinose metabolism preferred.
- pET324: Trc promotor (IPTG inducible), medium copy vector, confers ampicilin resistance, regulated expression (lacIq).
- pK184: lac promotor (IPTG inducible), low copy vector, confers kanamycin resistance, due to different origin (p15a) complementation possible.

- pNZ8048: pNisA promotor (induced by Nisin A), medium copy, confers chloramphenicol resistance.

Table C9: Cloned constructs for expression trials. Constructs with yellow shading were successfully cloned. White shadings indicated constructs that were planned but not not done.

	Parent Vector	Insert	Restriction site ¹⁾	Tag
pSJ016	pET28b(+)	HlyB	NcoI/BamHI	C-Term His ₁₀ Xa
pSJ017	pET28b(+)	HlyB/HlyD	NcoI/BamHI	C-Term His ₁₀ Xa
pSJ018	pET28b(+)	HlyD	NcoI/BamHI	C-Term His ₁₀ Xa
pSJ019	pET28b(+)	HlyB	NcoI/SacI	
pSJ020	pET28b(+)	HlyB	NcoI/SacI	N-Term His ₁₀ Xa
pSJ021	pET28b(+)	HlyB/HlyD	NcoI/SacI	
pSJ022	pET28b(+)	HlyB/HlyD	NcoI/SacI	N-Term His ₁₀ Xa
pSJ023	pET28b(+)	HlyD	NcoI/SacI	
pSJ024	pET28b(+)	HlyD	NcoI/SacI	N-Term His ₁₀ Xa
pSJ025	pBADHisB	HlyB	NcoI/SacI	
pSJ026	pBADHisB	HlyB	NcoI/SacI	C-Term His ₁₀ Xa
pSJ027	pBADHisB	HlyB	NcoI/SacI	N-Term His ₁₀ Xa
pSJ028	pBADHisB	HlyB/HlyD	NcoI/SacI	
pSJ029	pBADHisB	HlyB/HlyD	NcoI/SacI	C-Term His ₁₀ Xa
pSJ030	pBADHisB	HlyB/HlyD	NcoI/SacI	N-Term His ₁₀ Xa
pSJ031	pBADHisB	HlyD	NcoI/SacI	
pSJ032	pBADHisB	HlyD	NcoI/SacI	C-Term His ₁₀ Xa
pSJ033	pBADHisB	HlyD	NcoI/SacI	N-Term His ₁₀ Xa
pSJ034	pK184	HlyB	NcoI/SacI	
pSJ035	pK184	HlyB	NcoI/SacI	C-Term His ₁₀ Xa
pSJ036	pK184	HlyB	NcoI/SacI	N-Term His ₁₀ Xa
pSJ037	pK184	HlyB/HlyD	NcoI/SacI	
pSJ038	pK184	HlyB/HlyD	NcoI/SacI	C-Term His ₁₀ Xa
pSJ039	pK184	HlyB/HlyD	NcoI/SacI	N-Term His ₁₀ Xa
pSJ040	pK184	HlyD	NcoI/SacI	
pSJ041	pK184	HlyD	NcoI/SacI	C-Term His ₁₀ Xa
pSJ042	pK184	HlyD	NcoI/SacI	N-Term His ₁₀ Xa
pSJ043	pET324	HlyB	NcoI/XbaI	
pSJ044	pET324	HlyB	NcoI/XbaI	C-Term His ₁₀
pSJ045	pET324	HlyB	NcoI/XbaI	N-Term His ₁₀
pSJ046	pET324	HlyB/HlyD	NcoI/XbaI	
pSJ047	pET324	HlyB/HlyD	NcoI/XbaI	C-Term His ₁₀ Xa
pSJ048	pET324	HlyB/HlyD	NcoI/XbaI	N-Term His ₁₀ Xa
pSJ049	pET324	HlyD	NcoI/XbaI	
pSJ050	pET324	HlyD	NcoI/XbaI	C-Term His ₁₀ Xa
pSJ051	pET324	HlyD	NcoI/XbaI	N-Term His ₁₀ Xa
pSJ052	pNZ8048	HlyB	NcoI/XbaI	
pSJ053	pNZ8048	HlyB	NcoI/XbaI	C-Term His ₁₀ Xa
pSJ054	pNZ8048	HlyB	NcoI/XbaI	N-Term His ₁₀ Xa
pSJ055	pNZ8048	HlyB/HlyD	NcoI/XbaI	
pSJ056	pNZ8048	HlyB/HlyD	NcoI/XbaI	C-Term His ₁₀ Xa
pSJ057	pNZ8048	HlyB/HlyD	NcoI/XbaI	N-Term His ₁₀ Xa
pSJ058	pNZ8048	HlyD	NcoI/XbaI	
pSJ059	pNZ8048	HlyD	NcoI/XbaI	C-Term His ₁₀ Xa
pSJ060	pNZ8048	HlyD	NcoI/XbaI	N-Term His ₁₀ Xa

¹⁾ the restriction site used here denotes always the restriction of the insert. The vector was cut with same enzyme with the exception of pK184, which was cutted BspHI/SacI, due to an internal NcoI site. BspHI creates compatible ends to NcoI allowing ligation but no recutting.

In Table C9 cloned constructs are shown (yellow shadings). During cloning constructs containing *hlyB* were preferred due to the in-depth experience with the NBD of this ABC transporter.

2.2 Expression analysis in *E. coli*

Expression is not only influenced by the choice of the plasmid, but also by the chosen strain, temperature and induction time and length. To exemplify how expression analysis was performed the expression of His₁₀Xa-HlyB-HlyD out of pSJ030 is shown in detail (Figure C21). Similar analysis was done with pSJ016, pSJ020, pSJ039 and pSJ044. Here the inducer was IPTG instead of arabinose.

In brief the vector was transformed into two *E. coli* strains: Top10 and the Walker strain Bl21 C43; the first one was chosen because it lacks a functional arabinose metabolism and the second one because it is protease deficient and it is supposed to improve membrane protein expression (Miroux & Walker, 1996). For expression tests with pET28b(+) *E. coli* Bl21 instead of Top10 was used due to the absence of the T7 polymerase in the Top10 strain.

Single colonies were used to inoculate an overnight culture, which was used in the morning to inoculate fresh LB media. These cultures were grown at 20°C and 30°C respectively and induction was started at an OD₆₀₀=0.5 by adding two different inductor concentrations (final concentration in case of arabinose 0.002% (w/v) and 0.02% (w/v) and in case of IPTG 0.1 mM and 1 mM). Before induction a "blank" sample was taken, where no induction should be visible. After induction at certain time points (30 min, 60 min and 180 min post induction) the OD₆₀₀ was determined and 5 ml aliquots were taken and pelleted.

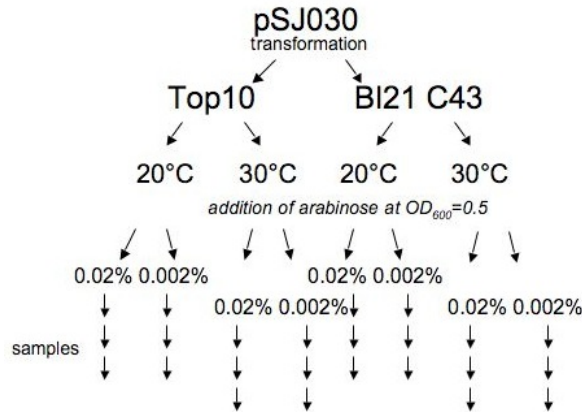


Figure C21: Expression analysis in *E. coli* exemplified by pSJ030. See text for details.

The harvested cells were resuspended in 500 µl resuspension buffer broken by lysozyme treatment and sonifying. After a low spin step the membranes were sedimented. The membranes were resuspended in 2.5 x SDS sample buffer (membrane) as follows:

$\text{Volume}_{\text{Samplebuffer}} = 25 \cdot \text{Volume}_{\text{Sample(5ml)}} \cdot \text{OD}_{600}$. 10 µl of this sample were loaded on a SDS-

PAGE gel. Gels were done in duplicate, while one was coomassie-stained as loading control, the other one was blotted for immunodetection with a HlyB specific antibody. In Figure 22 A such an immunoblot is shown (*E. coli* Top10 with pSJ030).

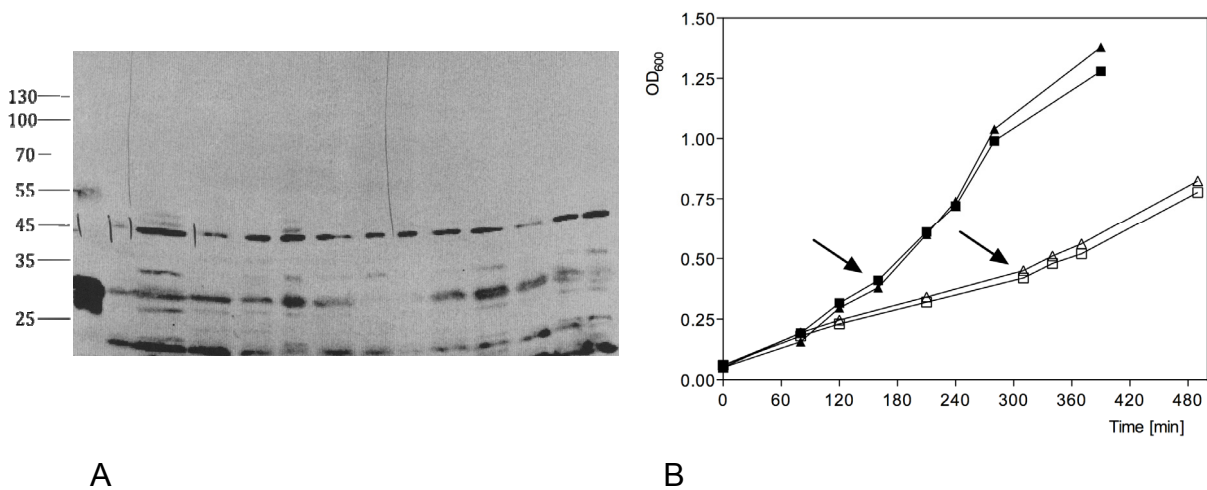


Figure C22: Expression analysis of the HlyB/HlyD encoding construct pSJ030 (pBADHisB-His₁₀Xa-HlyB-HlyD). (A) Western blot probed with HlyB specific antibody. Lanes after the marker are HlyB-NBD as positive control, cells before induction, then 6 samples of 20°C expression test and 6 sample of 30°C expression test. It is important to stress here that in contrast to Figure C39 a homemade ECL solution was used, which was approximately 50 fold less sensitive. (B) Corresponding growth curve of the expression test. Arrows mark the time of induction. Closed symbols represent the expression at 30 °C, open symbols represent the expression at 20 °C respectively. Squares denote the induction with 0.02% arabinose, triangles denote the induction with 0.002% arabinose.

Surprisingly, the samples expressed neither full-length HlyB nor HlyD (a Western blot directed against HlyD is not shown) and since the bands visible in the immunoblot are also visible in the control sample before induction, these bands correspond most likely to cross reactions of the HlyB antibody. In Figure C22 B the growth behaviour of the *E. coli* cultures is shown. The cell growth is not disturbed by addition of the inducer.

As shown here, all other plasmids were tested with either HlyB alone or HlyB and HlyD encoded. The results resembled the results shown in Figure C22. None of the tested constructs showed any detectable expression. To exclude any influence of occasional observed rare codons, the helper plasmid pRARE (Novagen) was introduced to compensate for rare tRNA species. However, this approach was also not successful (data not shown). Also the usage of strains with deleted histone like proteins, previously shown to be involved in regulation of the haemolysin system (Mueller et al, 2006), did not improve the expression.

2.3 Expression analysis in *L. lactis*

Since expression in *E. coli* did not generate the desired results we changed the expression host. Encouraged by several promising reports the Gram-positive host *L. lactis* was used (Kunji et al, 2005; Kunji et al, 2003). In contrast to *E. coli* the expression is not induced by a low molecular metabolite but rather by a small protein, Nisin A. It docks to the outer membrane protein NisK, induces a two-component system, which and thereby activates the *nisA* promoter upstream of the gene to be expressed. Therefore several constructs were cloned downstream of a *nisA* promoter present in the plasmid pNZ8048 (Table C9). For induction different amounts of Nisin A (0.1% (v/v) and 1% (v/v)) was added at certain optical densities (OD₆₆₀ of 0.5, 0.8 and 1.2). Nisin A was obtained from the supernatant of *L. lactis* strain NZ9700. This strain secretes nisin A and after pelleting the cells the supernatant was directly used for induction. The result of this expression test is shown in Figure C23.

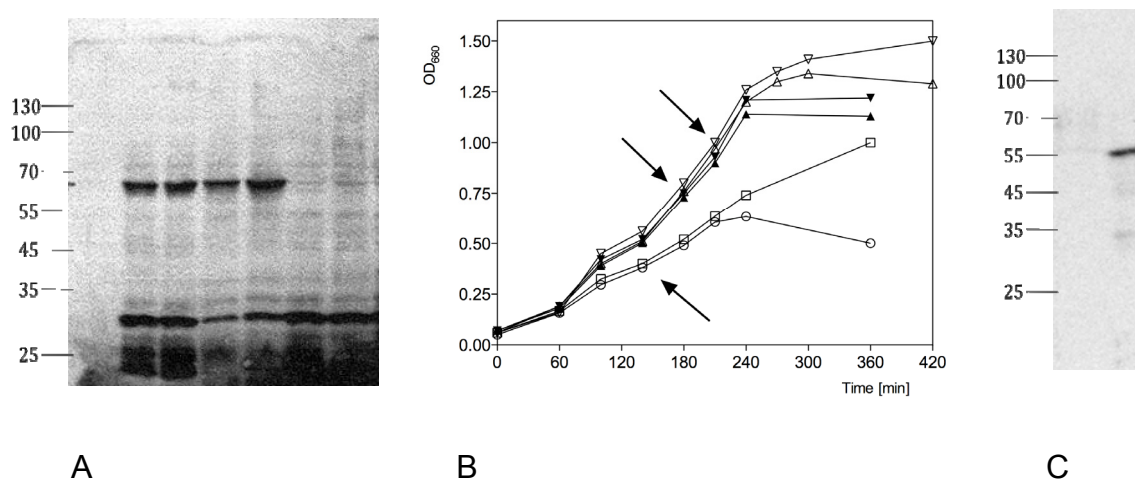


Figure C23: Expression analysis of the HlyB and HlyD encoding constructs pSJ054 and pSJ057 (pNZ8048-His₁₀Xa-HlyB and pNZ8048-His₁₀Xa-HlyD) in *L. lactis*. (A) Western blot probed with a HlyB specific antibody. Lanes after the marker are the induction with 0.1% and 1 % Nisin containing supernatant at OD₆₆₀ of 0.5, induction with 0.1% and 1 % Nisin containing supernatant at OD₆₆₀ of 0.8, induction with 0.1 % and 1 % Nisin containing supernatant at OD₆₆₀ of 1.2. The samples shown are taken after 3 hours of induction. It is important to stress here that in contrast to Figure C39 a homemade ECL solution was used, which was approximately 50fold less sensitive. (B) The corresponding growth curve of the expression test. Arrows mark the time of induction. Open circle and open square represent the induction at an OD₆₆₀ of 0.5. Closed triangles represent the induction at an OD₆₆₀ of 0.8 and open triangles induction at an OD₆₆₀ of 1.2. (C) Expression of HlyD in *L. lactis* probed with an HlyD specific antibody. Shown here are the lanes before induction at an OD₆₆₀ of 0.8 and after three hours growth.

As clearly visible in Figure C23 A expression was successful as HlyB can be probed with a specific antibody. Addition of Nisin A at a higher optical density abolished expression, but inducing expression in the mid-logarithmic phase resulted in overexpression. Since Nisin A itself also influences the cell growth of *L. lactis*, the resulting growth inhibition (as it can be seen in Figure C23 B) also decreases the yield of the cell mass. The expression was therefore induced as late a possible (OD₆₆₀ of 0.8-0.9) by adding 0.2 % (v/v) Nisin A containing supernatant. Using the construct encoding for HlyB and HlyD (pSJ057) it was possible to express HlyB and HlyD (Figure C23 A and C).

HlyB migrated around the apparent molecular weight of 70 kDa, in line with the observation that membrane proteins are shifted to lower molecular weight. MALDI-TOF analysis revealed a molecular weight of 81.5 kDa for His₁₀-HlyB (data not shown).

2.4 Analysis of the expressed proteins

2.4.1 Orientation in *L. lactis* membranes probes probed by trypsin protection

A major challenge in the expression of two membrane systems like the Type I secretion system is that the biological activity cannot be measured readily *in vitro* since the set up of an *in vitro* activity is experimentally very demanding and has not yet been done for such systems. Furthermore, overexpression takes place in *L. lactis* so that an *in vivo* activity test seems not very promising due to the lack of the outer membrane with the essential protein TolC. To assess membrane integration trypsin protection analysis was performed. If both proteins are properly integrated into the membrane they should have the same orientation as in *E. coli*, i.e. the large periplasmatic domain of HlyD is located outside and the NBD of HlyB inside. If the cells are broken by French press or a similar technique inside-out vesicles are generated (Futai, 1974; Hertzberg & Hinkle, 1974) resulting in the inversion of protein orientation. In this case the large domain of HlyD should reside in the vesicle and the NBD of HlyB should be accessible from the outside. Membrane preparation of *L. lactis* and subsequent trypsin digest was performed as outlined in Materials and Methods. Samples were analyzed by Western blotting (Figure C24).

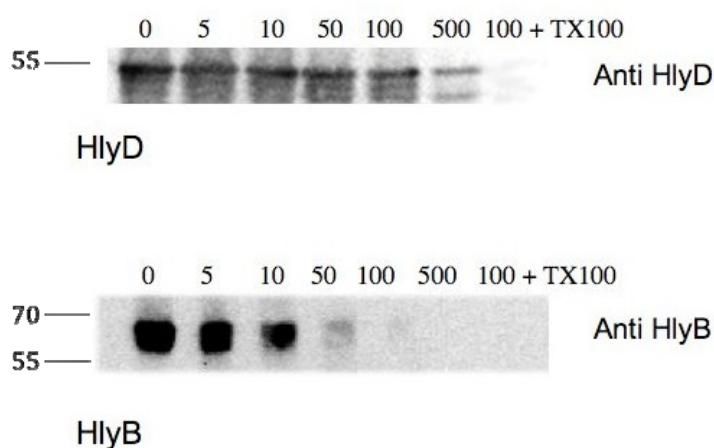


Figure C24: Trypsin protection assay for inside-out vesicles containing HlyB and HlyD. In the upper panel the samples are probed for HlyD with a HlyD specific antibody, whereas in the lower panel the samples were probed for HlyB with a HlyB specific antibody.

HlyB was highly susceptible to trypsin whereas HlyD is largely protected and could only fully degraded in the presence of detergent, lysing the vesicles. In case of the membrane vesicles of *L. lactis* the large periplasmatic domain of HlyD is inside (therefore in the exterior in case of intact cells) and the NBD of HlyB is on the outside of the vesicle (therefore in the interior in case of intact cells). This resembles the *E. coli* situation. Therefore the overexpression of HlyB/HlyD does not lead to a misintegration or unspecific aggregation on the cell membrane.

2.4.2 Detergent solubilisation

Membrane proteins need to be solubilised with a suitable detergent prior purification. This step is of enormous importance for the ability to purify and to stabilise the protein, since membrane proteins can be extremely stable in lipid bilayer but often become unstable and rapidly loose activity after detergent extraction (Bowie, 2001; Prive, 2007). Experiments focussed on HlyB and the co-solubilisation of HlyB and HlyD. Six detergents out of different classes were used as an initial detergent screen (Big Chap, OG, DDM, FC-14, TX-100, LDAO details see in Materials and Methods). The detergent was added out of a stock solution to membranes (10 mg/ml) in membrane buffer. The mixture was incubated at 4 °C with gently shaking for 1 hour. After incubation the unsolubilised material was removed by ultracentrifugation from the detergent-protein complexes (200000 g, 4 °C, 1h), while the pellet was resuspended with SDS sample buffer. To check the possibility of purification Ni²⁺-NTA agarose was added to the supernatant, after washing the column material with membrane buffer the protein was eluted by adding membrane buffer supplemented with 200 mM imidazole. The obtained fractions were analyzed by Western blotting (Figure C25).



Figure C25: Solubilisation screen for HlyB with several detergents as probed by Western blot with an HlyB specific antibody. + denotes the membrane prior solubilisation. The detergent used the shown samples is shown above the box. Lanes are according the order next to the positive control: solubilised material, not solubilised material, wash Ni²⁺-NTA material, eluate Ni²⁺-NTA material.

Judging the efficiency in solubilisation following behaviour results with increasing solubilisation ability: FC-14 > LDAO > DDM > TX-100 > Big Chap = OG. A more comprehensive detergent screen performed later by a colleague confirmed these results with a very strong preference towards the FosCholine group of detergents (Oswald, 2008). All detergents solubilising HlyB can also be used for purification indicated by the fact that HlyB can be successfully eluted with imidazole (DDM, FC-14, LDAO, TX-100). The best detergent was FC-14 and was consequently used for further purifications.

2.4.3 Purification of HlyB

The objective of any purification is pure, stable and active protein. The solubilisation of HlyB with FC-14 and a subsequent purification by metal-ion-chelate chromatography yielded pure and stable protein with a yield of 0.5 mg/liter culture. After concentrating the sample to 10 mg/ml the sample was analysed by analytical gel filtration yielding a symmetric peak, pointing to a homogenous protein fraction (Figure C26 A).

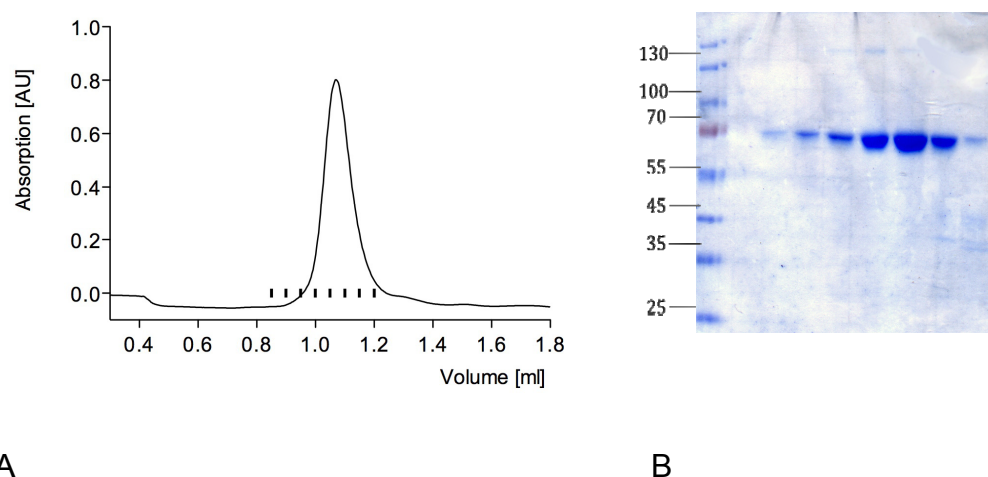


Figure C26: Purification of HlyB. (A) Analytical gel filtration of concentrated IMAC eluate on a SMART system Superdex200 PC 3.2/30 as column. Dashes denote the fractions analyzed by SDS-PAGE (B) Corresponding SDS-PAGE of the gel filtration.

Comparison with standard proteins resulted in an apparent molecular weight of 250 kDa corresponding to a potentially dimeric species of HlyB in detergent micelles (2 x 81.5 kDa +

bound detergent). If HlyB and HlyD containing membranes were solubilised with any detergent useful for the solubilisation of HlyB, no co-fractionation of HlyB and HlyD was seen as it was expected (Thanabalu et al, 1998). The membrane complex present might be only marginally stable and is disrupted upon solubilisation. A stable complex was also not reported for the HasA system (Letoffe et al, 1996). Testing the presence of the membrane complex by crosslinking failed in *L. lactis* in contrast to results of Koronakis and coworkers (Thanabalu et al, 1998) who established a crosslink procedure in *E. coli*. Any systematic error in cross-linking procedure cannot be ruled out, therefore no reasonable conclusion concerning the functional formation of the HlyB/D complex can be conducted.

2.4.4 CD spectroscopy of purified HlyB

Harsh detergents are able to keep proteins nicely in solution but tend to partially unfold proteins. Since the biological activity is not preserved such a detergent would be useless. HlyB alone is not expected to function as a protein transporter, underlined by the fact that inside-out vesicles containing HlyB do not import the highly secreted HlyACterm, if a modification of the straight-forward method elaborated for protein conducting channel SecYEG was performed (van der Does et al, 2003; data not shown). To reduce the buffer background the protein solution was extensively dialysed against 20 mM P_i pH 7.4, 100 mM NaCl, 5 % glycerol and 0.01 % FC-14. Measurements were performed and analyzed as described in material and methods. The spectrum is shown in (Figure C27).

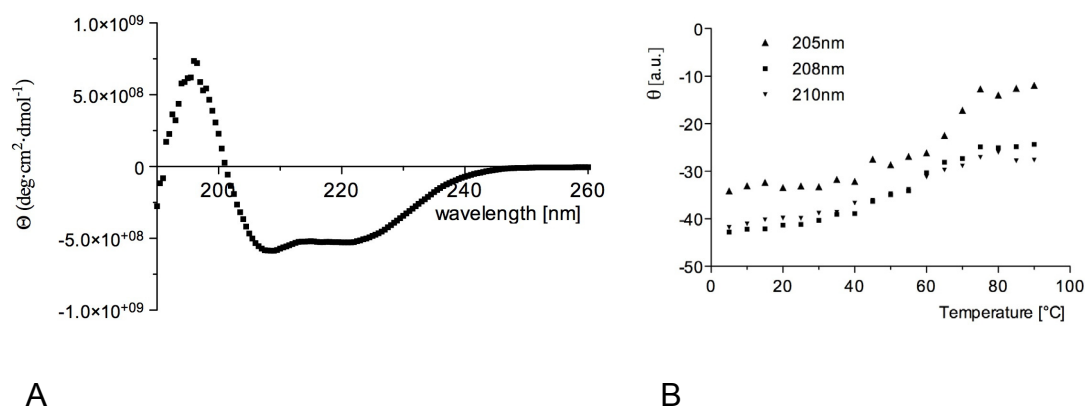


Figure C27: CD spectra of purified HlyB. (A) The spectrum from 190 nm to 240 nm is shown. (B) The temperature dependence of chosen points of the characteristic α -helical portion is shown.

The CD spectrum shows a largely α -helical protein (two minima around 208 nm and 220 nm). An estimation of the secondary structure content can be done for example with K2D2, which tolerates data down to only 190 nm. The secondary structure is predicted to have 84 % α -helical segments, only 2 % β -sheets and 14 % is random coil. This prediction is unsatisfactory because seen immediately from the structure of the NBD the content of β -sheets is certainly more than 2 % (see for example Figure C8). However secondary structure predictions are not a clear-cut reflection of the reality especially if data below 200 nm important for β -sheets is not reliable measured for example due to buffer components (Perez-Iratxeta & Andrade-Navarro, 2008).

2.4.5 ATPase activity of HlyB

The activity of ABC transporters is not only defined by the vectorial transport of the substrate, but also by the ATPase activity. To test if the purified HlyB is active in terms of ATPase activity the peak fractions of the gel filtration (in 10 mM HEPES pH 7.4, 150 mM, 10 % glycerol, 0.02 % FC-14) were used for ATPase assay. With knowledge of the results of the NBD, fractions containing the H662A mutant of HlyB exhibited unexpectedly also an ATPase activity. This observation could be due to residual protein contaminations. By adding NaN_3 these minor contaminations, leading to residual ATPase activity, were successfully blocked (Figure C28 A).

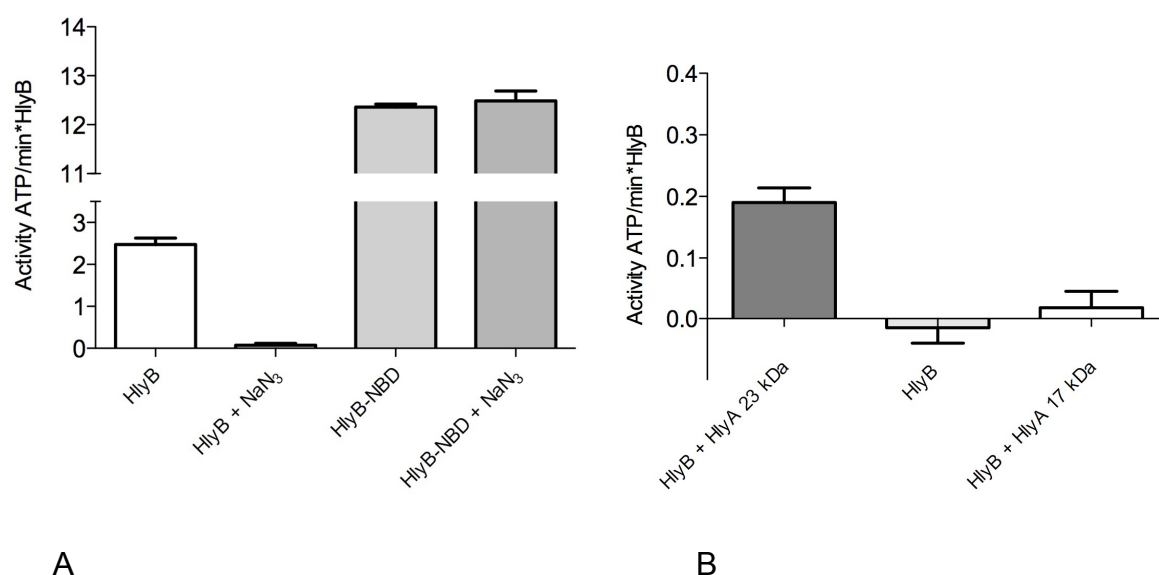


Figure C28: Influence of addition of azide and HlyA on the ATPase of HlyB. (A) Azide inhibits selectively minor contaminations present in the gel filtration fractions of HlyB. The NBD is not affected by the addition of

azide. (B) Adding the HlyACterm can induce the ATPase. As further control the 17 kDa HlyA lacking the extreme C-terminus.

Azide is known to inhibit the F_1 part of the F_1F_0 ATPase (Bowler et al, 2006), but any inhibition by azide of ABC transporters has not reported so far. This is supported by the fact that the NBD is not affected by the addition of azide.

Here, HlyB was not active in detergent in the presence of azide, which inhibited impurities. Addition of HlyD, also purified out of *L. lactis* with FC-14 did not lead to any ATPase activity in line with results that addition of HlyD does not reconstitute the complex (data not shown). However, ATPase activity is clearly seen upon addition of the substrate. If 10 μ M HlyACterm was added to the detergent solubilised HlyB an increase of ATPase could be observed to an ATPase activity of 0.2 ATP/min after background correction (Figure C28 B). To avoid any disturbing buffer effects HlyACterm was present in the same buffer like HlyB. Specificity was also demonstrated by addition of a degradation product of the HlyACterm fragment which lacks the C-terminal 57 amino acids (17 kDa HlyA, Benabdelhak et al, 2003) Here no ATPase induction was observed (Figure C28 B). The ATPase induction is therefore clearly derived by the C-terminus, which is detrimental for protein secretion.

Using the induced activity one can determine the binding constant of HlyACterm to HlyB by increasing the amount of added HlyACterm (Figure C29 A).

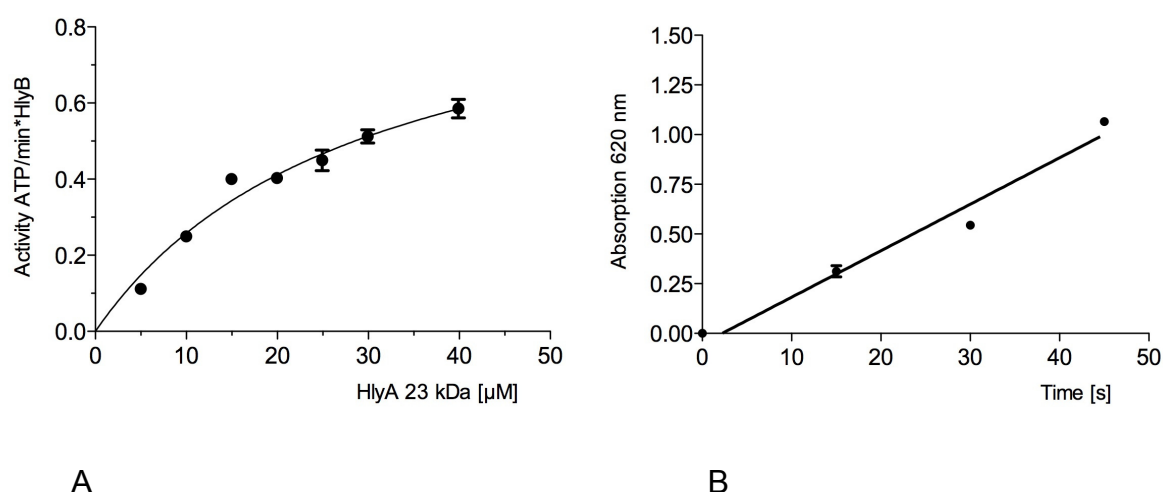


Figure C29: Induction of the ATPase of HlyB by adding HlyACterm (A) Induced ATPase activity of HlyB as function of added HlyA. (B) Time dependence of the ATPase activity upon addition of HlyACterm to HlyB.

The fully stimulated HlyB exhibits a maximal turnover of 1.0 ATP/min and the measured K_D is $28 \pm 6.4 \mu$ M. This is in line with the measured interaction by SPR where a K_D of $4 \pm 2 \mu$ M

was determined for HlyACterm to the HlyB-NBD (Benabdelhak et al, 2003). To reliably detect such a low ATPase activity the measurements were performed for 45 min at room temperature. HlyB was active during this time (Figure C29 B).

3. Exploiting the Type I secretion system for heterologous expression

Targeting synthesized proteins for secretion into the culture medium presents significant advantages: Inclusion body formation as well as protein degradation can be avoided and purification is eased. By this, secretion for heterologous protein expression is a very useful technique, but secretion can be used not only for purification processes also for *in vivo* vaccination (Gentschev et al, 2000). Unfortunately, *E. coli* normally secretes only a few proteins into the extracellular media. In case of the Hly system the fusion of the 50-60 C-terminal amino acids would allow, in principle, the fusion protein to be recognized and transported by the Hly transport machinery. The major advantage of the Hly system is the bypass of the periplasm during secretion and that the *sec* machinery is not overloaded. Thus, no crowding of the desired protein in the periplasm occurs.

The aim of the following part was to elucidate a straightforward scheme to fuse any sequence to the HlyA C-terminus and to find a suitable complementation plasmid encoding for the transport machinery. Further limitations affecting the transport process should be recognized and overcome.

3.1 Generation of a vector pair suitable for expression of the secretion machinery and the fusion protein

Several features are important if a vector is designed to fuse any protein to the C-terminal sequence of HlyA: i) The vector must be compatible to the vector present in the cell encoding for HlyBD to allow efficient growth. ii) The vector must contain the C-terminal sequence of HlyA in frame to the fusion protein. Therefore an efficient cloning site must be present. The fusion protein should be inducible independently of the HlyBD protein complex. The vector encoding for the secretion machinery is preferably a low copy vector thereby just facilitating the transport without influencing cell growth or physiology. The induction of the secretion machinery is either constitutively or mediated by a weak promoter.

Looking at the previous section a perfect vector pair was therefore the combination of pK184-HlyBD with a modified pBADHisB vector (both vectors are shown as plasmid maps in the appendix).

Since the plasmid pK184-HlyBD was already present (see the previous section), only the pBADHisB vector had to be modified. To ensure that a maximal number of genes can be integrated into the vector, either a flexible restriction enzyme based system or an alternative system needed to be designed. The integration of a flexible restriction site like *Sfi*I was considered but a ligation independent cloning site was preferred.

Which size should the C-terminal fragment of HlyA have? At the time the Type I secretion signal was discovered it was recognized that the C-terminal part of the secreted substrate of around 50-60 amino acids was essential for secretion (Gray et al, 1986). However, the secretion was much more efficient if a larger C-terminal fragment of around 23 kDa was used for secretion (amino acids 807-1023, Kenny et al, 1991; Nicaud et al, 1986). Therefore, this 23 kDa fragment, namely HlyACterm, was chosen as fusion partner for the design of HlyA fusions.

To construct such a plasmid the following steps were performed: the gene encoding HlyACterm was amplified by PCR using Hly23kDa_for and Hly23kDa_rev as primers and pLG813 as template. The insert was ligated in the vector using the NcoI and HindIII restriction sites. After verification of the sequence, a LIC cassette was integrated into the NcoI site. This vector, named pSOI, was suitable for cloning any sequence upstream of C-terminal fragment of HlyA in frame.

The features are shown in Figure C30 A. Downstream of the LIC site a factor Xa site and the sequence of the C-terminal fragment of HlyA was present, whereas upstream of this cassette the arabinose promoter was encoded.

The addition of 5' AT GGT GAG AAT TTA TAT TTT CAA GGT ATG *gene specific without start codon* 3' to the forward primer and of 5' T GGA AGG GTG GGA TTT ACC *gene specific without stop codon* 3' to the reverse primer enabled LIC into the SmaI site (Figure C30 B).

A

B

3.2 Secretion of a C-terminal fragment of HlyA

110

hours induction. (B) Secretion tested with different arabinose concentrations. Lanes after the marker: Cells induced with 1 mM arabinose, cells induced with 10 mM arabinose, supernatant of cells induced with 1 mM arabinose and with 10 mM arabinose.

Systematic screening of different culture conditions pointed to that fact that secretion was largely independent of the chosen growth conditions. However some slight variations are shown in Table C10. Autoinducer media represents a convenient way of inducing multiple cultures at similar conditions (Busso et al, 2008; Studier, 2005) and was therefore preferred.

Table C10: Effects of variations on the secretion of HlyACterm.

Variation	Effect
- strain SE5000, WM2429	<i>Strains do secrete in similar amounts</i>
- media 32Y (complex rich autoinducer media), MDA-5052 (enriched, chemical defined autoinducer media), ZYM-5052 (complex autoinducer media), 2xYT, LB	<i>Secretion observed in every media tested. Autoinducer media was tested successfully. Chemical defined media showed clear secretion, but poorer growth.</i>
- inductor lactose, IPTG, arabinose	<i>pK184-HlyBD contains a leaky lac promotor, therefore traces of lactose in the media enables the secretion. 1 mM IPTG was routinely used for LB and 2xYT media, whereas 0.2 % lactose was used in autoinducing media. Any change of concentration had no effect. For induction of the HlyA fragment using LB and 2xYT media the arabinose concentration less critical, using autoinducer media higher concentration of arabinose yielded into a far higher HlyA concentration in the supernatant (see Figure 31). Earlier induction (LB, 2xYT) of the secretion apparatus yielded in a higher secretion level, due to prolonged secretion, but even at induction in the late logarithmic phase at OD₆₀₀ of 2.4 with IPTG followed by an induction with arabinose at OD₆₀₀ of 4 secretion was observed</i>
- duration of secretion	<i>Longer secretion results in higher secretion levels. The longer the secretion the higher the OmpT degradation (see below). Therefore autoinducer media increased degradation.</i>

3.3 Purification of the HlyA fragment from the culture supernatant

Secretion of proteins into the media can be exploited for expression and purification processes. Therefore the proteins need to be purified with a suitable method. pSOI encodes for a Hexahistidintag for purification. To test the feasibility of purification, the HlyA fragment was expressed, using pSOI with a two amino acids spacer (GS) integrated into the the LIC cassette of pSOI (otherwise the startcodon would not be in frame with the gene).

The resulting HlyA fragment did not only possess the C-terminus of HlyA, but also all other features shown in Figure C30 were present. Therefore the protein mass increased to 27.6 kDa. The protein was expressed using ZYM-5052. For purification two different methods were used: either purification via ion exchange chromatography using a Q-sepharose HiTrap FF column (calculated pI of the HlyA fragment 5.5) or via affinity chromatography using a HiTrap Chelating column with Zn^{2+} -IDA as functional group.

In case of ion exchange chromatography the protein eluted at a salt concentration of around 200 mM NaCl whereas employing affinity chromatography the protein eluted at an imidazole concentration of around 90 mM. In Figure C32 A and B a SDS-PAGE of both purification procedures is shown.

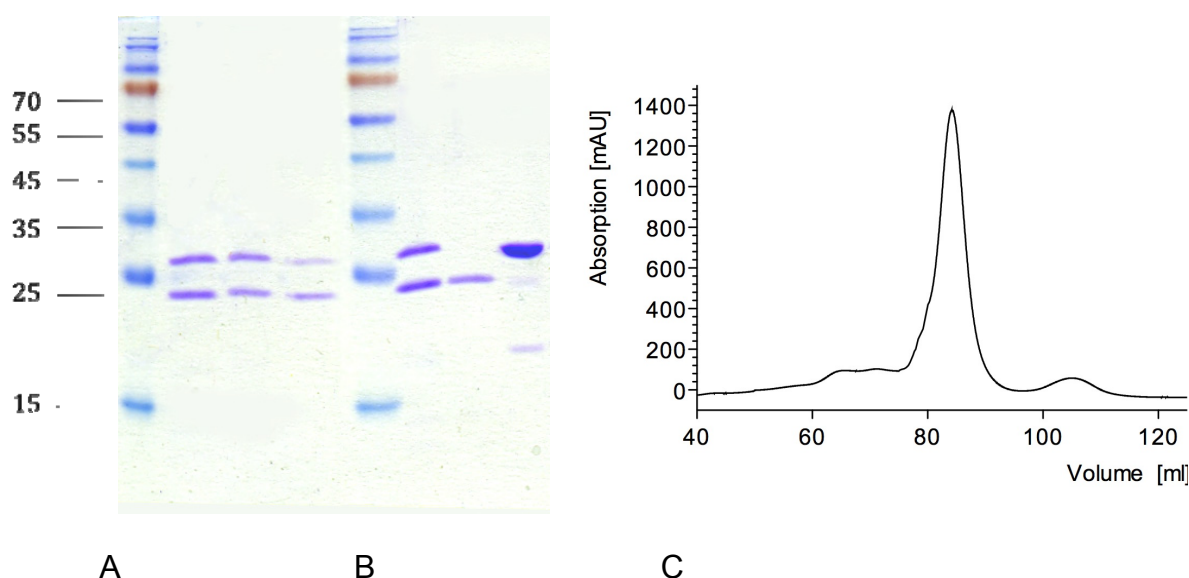


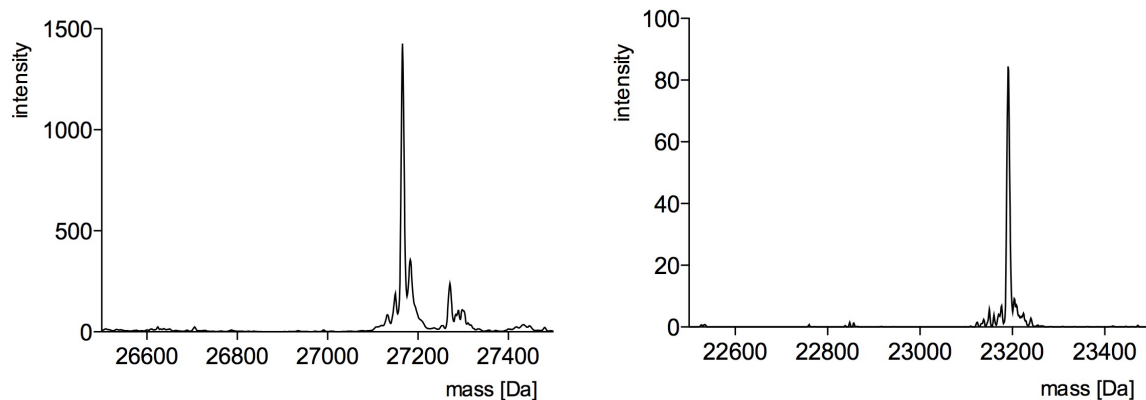
Figure C32: Purification of the HlyACterm from the supernatant of *E. coli* WM2429. (A) 15% SDS-PAGE of the purification by ion exchange chromatography. Shown are lanes for marker, applied sample, flow through and eluate. (B) 15% SDS-PAGE of the purification by affinity chromatography. Shown are lanes for marker, applied sample, flow through and eluate. Clearly visible is a degradation product of the HlyA fragment. (C) Size exclusion experiment of the affinity purified HlyA fragment (Superdex 200 16/60 pg).

In Figure C32 A and B the different purification fractions are shown. Also shown in Figure C32 C a size exclusion experiment demonstrating the solubility of the HlyA fragment.

As seen in Figure C32 two different isoforms of the HlyACterm were present in the supernatant. Performing an immunoblot with an HlyA specific antibody or an anti-penta-His-antibody for this fraction revealed, that this smaller fragment was an N-terminal degradation product of HlyA, because it was detected with the anti-HlyA-antibody, but not with the anti-

penta-His-antibody, whereas the large fragment was detected with both antibodies (data not shown).

This unspecific protease cleavage occurred at the very N-terminal end of the HlyA fragment and was, after careful inspection faintly visible in earlier tests with pPSG131 (see for example Figure C31 B). The cleavage, if taking place after the transport process, would even be a very convenient way to remove almost the complete HlyACterm fragment. This was already systematically done for HlyA fusions (Hanke et al, 1992). OmpT, the major outer membrane protease, was suspected also here to be the reason for this proteolytic cleavage. However, HlyA does not encode a clearcut dibasic motif typical for OmpT substrates (McCarter et al, 2004). In order to systematically choose the right strain or, alternatively knocking down the protease site, the cleavage site was identified by mass spectrometry. For ESI-TOF analysis, both constructs were thoroughly dialysed against 2 mM TRIS pH 8. The construct was purified by metal-ion-chelate affinity chromatography and corresponds to a size of 27166 Da \pm 2 Da according to ESI-TOF (Figure C33 A). This corresponds to the HlyA fragment in pSOI with cleavage sites and spacer (calculated mass: 27167 Da).



MHHHHHHGENLYFQGMGSGKSHPPSSIEGR**M**GNSLAK NVLSGGKGNDKLYGS...

C

Figure C33: Identification of the secreted fragments by ESI-TOF analysis. (A) The fragment as encoded by pSOI (with GS as amino acid spacer, underlined) purified by metal chelate chromatography. (B) The degraded fragment thereof. (C) Cleavage site in HlyACterm (indicated by the red arrow). The bold methionine denotes the original start of HlyACterm without Hexahistidintag, Tev protease site and factor Xa cleavage site.

The degraded product lacked an affinity tag and was therefore purified by metal-ion-chelate affinity chromatography (removal of the larger fragment; only the flow through was taken), ion exchange chromatography (Q-sepharose) and gel filtration yielding a pure degraded product with a size of 23191 Da +/- 4 Da according to ESI-TOF (Figure C33 B). The cleavage site was immediately at the beginning of HlyACterm as shown in Figure C33 C and could be assigned to be a well tolerated OmpT cleavage site (AKNV, Dekker et al, 2001).

The purification of the secreted and tagged protein was straightforward when affinity chromatography was chosen and yielded pure protein. Out of 25 ml culture supernatant 2 mg of the HlyA fragment could be purified, pointing to a possible yield of almost 100 mg per litre culture. Purification of the HlyA fragment secreted into chemical defined media was also successful circumventing the problem of possible interfering effects by media components.

3.4 Cloning of fusion partners by LIC

Secretion into the extracellular media prevented HlyACterm from aggregation in the cell. If the secretion apparatus is not present, HlyA and HlyACterm forms inclusion bodies. Avoidance of inclusions bodies is a major challenge in protein expression and secretion would be an elegant solution to that problem.

If choosing genes for HlyA fusions a detailed knowledge of the common features of the Type I secretion substrates is helpful. Obvious features of Type I secretion substrates are the acidic pI and the lack or unusual low amount of cysteines (Delepelaire, 2004). In the majority of substrates glycine rich repeats are found, however *S. marcescens* HasA lacks these repeats (Delepelaire, 2004). Due to the degenerated C-terminal signal probable substrates are identified by these glycine repeats. Therefore, many other substrates might still be unknown.

To challenge the transport machinery, proteins with a higher pI and a normal “amount” of cysteines were chosen in addition to proteins with similar physicochemical properties like the Type I substrates. To rescue proteins and to avoid inclusion body formation, several proteins forming inclusion bodies were also chosen. Since the proteolytic digest of HlyA does not influence the amount of protein secreted the identified OmpT cleavage site remained unchanged. Also the Hexahistidintag for purification resides at the N-terminus and purification of the desired proteins would not be changed. In addition cleavage by factor Xa

occurs almost at this site, so an OmpT activity would not only be a convenient diagnostic motif but also a possibility to remove the HlyA fragment (Hanke et al, 1992).

An overview of the chosen fusions partners with some of their physicochemical parameters is presented in Table C11.

Table C11: Proteins chosen for N-terminal fusion to the HlyA C-terminus.

Protein	Function	IB ¹⁾ in <i>E. coli</i>	Size [kDa] (Protein/ Fusion)	Nr. of Cysteins	pI	Ref.
<i>E. coli</i> MalE ²⁾	Maltose binding	No	40.7/67.9	0	5.1	(Riggs, 2001)
Human Interferon α 2	Signalling	Yes	19.2/46.4	4	6.0	(Piehler & Schreiber, 1999)
Human Interferon β	Signalling	Yes	19.9/47.1	3	8.9	(Derynck et al, 1980)
Human Ifnar2 EC ³⁾	Signalling	Yes	24.3/51.5	6	4.9	(Lamken et al, 2004)
Human Ifnar1 EC 1,2 ³⁾⁴⁾	Signalling	Yes	23.7/50.9	4	6.5	(Lamken et al, 2005)
Human Ifnar1 EC 3,4 ³⁾⁴⁾	Signalling	Yes	24.4/51.6	4	7.1	(Lamken et al, 2005)
<i>C. antarctica</i> CalB ²⁾	Lipase	Yes	33.2/60.4	6	5.8	(Blank et al, 2006)
<i>P. aeruginosa</i> Lip3 ²⁾	Lipase	Yes	33.9/61.9	1	6.3	(Ogino et al, 2004)
<i>E. coli</i> HlyACterm	Toxin fragment	Yes	23.8/27.2	0	5.4	(Benabdelhak et al, 2003)

¹⁾ IB = Inclusion bodies at 37 °C ²⁾ without own secretion sequence ³⁾ EC = extracellular, soluble part ⁴⁾ 1, 2 denotes the first two immunoglobulin domains, where 3, 4 denote the last two immunoglobulin domains.

The chosen fusion partners did not contain any intrinsic glycine rich repeats, but since the HlyA fragment in pSO1 contains 3 repeats with the consensus sequence GGXGXD (X = every amino acid) all fusion proteins are classified as RTX proteins.

The sequences encoding the proteins were cloned into pSOI via LIC. MalE, CalB and Lip3 are secreted via the sec dependent pathway and contained a suitable secretion signal. To avoid any competitive effect this secretion sequence at the N-terminus was removed. In case of the interferon receptors Ifnar1 and Ifnar2 only extracellular, soluble domains were chosen.

3.5 Secretion tests with fusion proteins

For secretion tests pK184-HlyBD containing *E. coli* WM2429 were transformed with pSO1-X (X denotes the fusion protein). Single colonies were taken to inoculate ZYM-5052 autoinducer media. After 14 h at 37 °C cells were harvested and the supernatant was analyzed for the secreted protein whereas the pellet was either directly analyzed by SDS-PAGE or further fractionated.

The requirement for successful secretion is the expression of the fusion protein. Therefore different arabinose concentrations were tested (0.1 mM, 1 mM and 10 mM). The results are exemplified by samples expressing Ifnar1EC1,2-HlyA and Ifnar2EC-HlyA as shown in Figure C34.

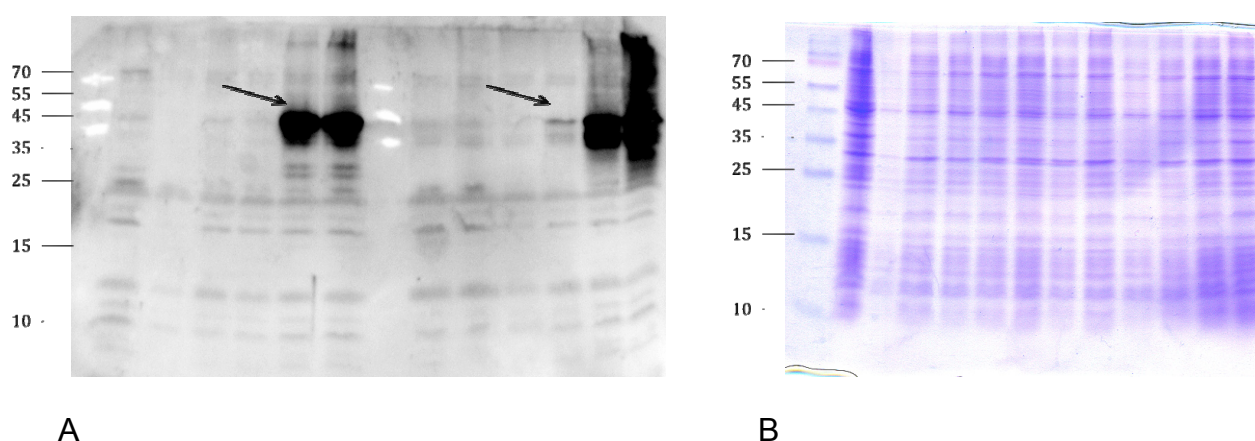


Figure C34: Expression of the fusion proteins Ifnar1EC1,2-HlyA and Ifnar2-HlyA in autoinducer media with different arabinose concentrations. (A) Western blot with anti HlyA antibody detecting the fusion protein Ifnar1EC1,2 (left of the blot) and the fusion protein Ifnar2EC-HlyA (right of the blot). 0.1 mM, 1 mM and 10 mM arabinose in pairs. (B) Corresponding 15 % SDS-PAGE with Coomassie brilliant blue staining demonstrating equal loading. Lanes in B resemble the same protein fractions as in A. An arrow indicates the fusion protein.

As shown in Figure C34 A higher arabinose concentrations caused higher expression of the Ifnar fusion proteins. This pattern was observed for all other fusion proteins.

As a result the secretion tests with all fusion proteins were performed with ZYM-5052 autoinducer media supplemented with 10 mM arabinose prior inoculation.

The supernatant of the secretion tests for all fusion proteins are shown in Figure C35. In brief, a single colony was used to inoculate a 25 ml culture of autoinducer media ZYM-5052 supplemented with 10 mM arabinose. After 14 h growth at 37 °C the cultures were harvested

and the supernatant was analyzed for the secreted protein by SDS-PAGE (Figure C35 A and B).

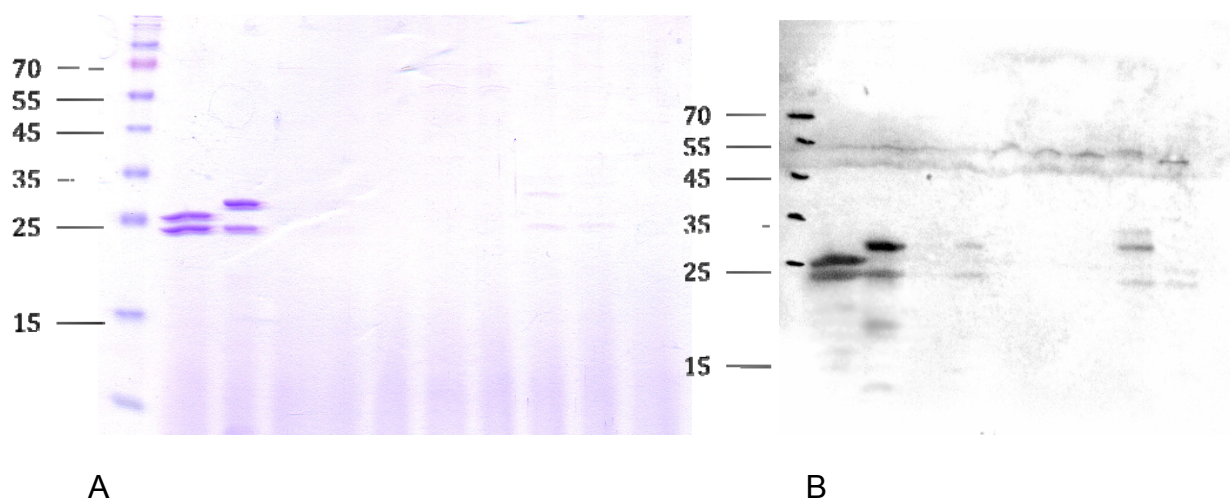


Figure C35: Secretion of the fusion proteins in autoinducer media. Samples on SDS-PAGE and Western blot with expected molecular mass in brackets: Marker, HlyACterm (pPSG131/24.6 kDa), HlyACterm (pSO1/27.2 kDa), MalE-HlyA (67.9 kDa), Interferon α 2-HlyA (46.4 kDa), Interferon β -HlyA (47.1 kDa), Ifnar2EC-HlyA (51.1 kDa), Ifnar1EC1,2-HlyA (50.9 kDa), Ifnar1EC3,4-HlyA (51.6 kDa), CalB-HlyA (60.4 kDa), Lip3-HlyA (61.9 kDa). (A) 15 % SDS-PAGE with Coomassie brilliant blue staining. (B) Corresponding Western blot with anti HlyA antibody detecting the HlyA part of the fusion protein.

As it can be seen in Figure C35 successful secretion was only observed in case of the HlyA fragments which are only fused to a N-terminal Hexahistidintag and the protease recognition sites in case of the pSO1 derivatives. All other fusion constructs did not secrete in a comparable manner. Faint bands are detected by an HlyA specific antibody in case of Interferon α 2-HlyA, Ifnar1EC3,4 and CalB, leaving the possibility that in those cases secretion occurred albeit in a very inefficient manner. In those cases the size of the detected band did not correspond to the expectation, but since a band of the size of the OmpT degradation product of HlyA of around 23.5 kDa was present, a cleavage of those proteins after successful secretion could not be ruled out.

To rule out that the expression failed the cell pellet was analyzed for the presence of the desired proteins (Figure C36).

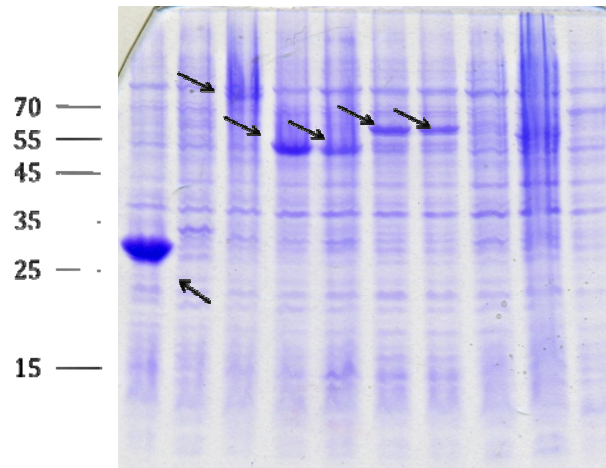


Figure C36: Cell lysates of cells expressing the fusion proteins: 15 % SDS-PAGE with Coomassie brilliant blue staining. Marker, HlyACterm (pPSG131/24.6 kDa), HlyACterm (pSO1/27.2 kDa), MalE-HlyA (67.9 kDa), Interferon α 2-HlyA (46.4 kDa), Interferon β -HlyA (47.1 kDa), Ifnar2EC-HlyA (51.1 kDa), Ifnar1EC1,2-HlyA (50.9 kDa), Ifnar1EC3,4-HlyA (51.6 kDa), CalB-HlyA (60.4 kDa), Lip3-HlyA (61.9 kDa). Proteins with visible overexpression marked as arrows.

In the whole cell lysates shown in Figure C36 it is clearly seen that at least in the case of HlyACterm (out of pPSG131), MalE-HlyA, Interferon α 2-HlyA, Interferon β -HlyA, Ifnar2EC-HlyA, Ifnar1EC1,2-HlyA the expression was visible and therefore successful (arrows in Figure C36).

HlyACterm secreted as soluble protein whereas inclusion bodies are the intracellular fate of this protein. In order to characterize the fate of the fusion proteins the cells were further fractionized. The cells were broken analytically by a French Press mini cell and inclusion bodies were prepared. The supernatant was, in case of HlyACterm (pPSG131), HlyACterm (pSO1), MalE-HlyA, Interferon α 2-HlyA, again centrifuged at low speed in order to clear the supernatant quantitatively from the aggregated protein. The membranes were isolated using a high-speed step. In Figure C37 the inclusion bodies containing fraction is shown.

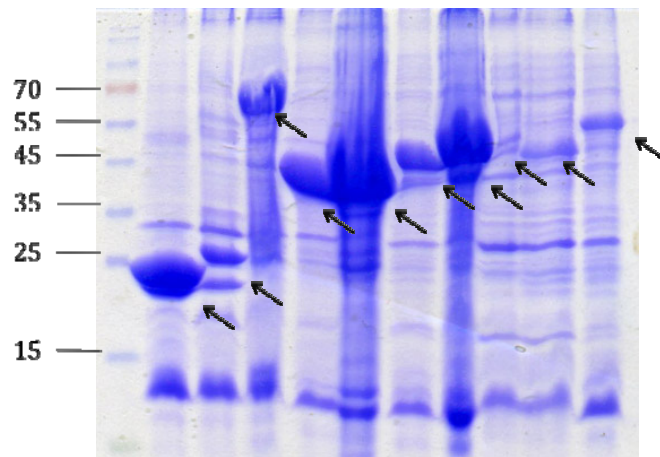


Figure C37: Crude inclusion bodies of the different fusion proteins. 15 % SDS-PAGE with Coomassie brilliant blue staining. Marker, HlyACterm (pPSG131/24.6 kDa), HlyACterm (pSO1/27.2 kDa), MalE-HlyA (67.9 kDa), Interferon α 2-HlyA (46.4 kDa), Interferon β -HlyA (47.1 kDa), Ifnar2EC-HlyA (51.1 kDa), Ifnar1EC1,2-HlyA (50.9 kDa), Ifnar1EC3,4-HlyA (51.6 kDa), CalB-HlyA (60.4 kDa), Lip3-HlyA (61.9 kDa). Proteins are indicated with an arrow.

All of the fusion proteins exhibited inclusion body formation at 37 °C. Visual estimation of the inclusion body formation indicated that Ifnar1EC3,4-HlyA, CalB-HlyA and Lip3-HlyA produced less inclusion bodies compared to all other proteins which had a strong tendency to form inclusion bodies. Very remarkable was the difference between HlyACterm fragments. Both were expressed under the same promoter and contain almost the same sequence, but it seemed that the two protease recognition sites lead to a fivefold reduction in the amount of inclusion body formation. It must be noted that the secretion levels are similar leading to the conclusion that the secretion apparatus might be the limiting component for at least these fragments (Figure C34).

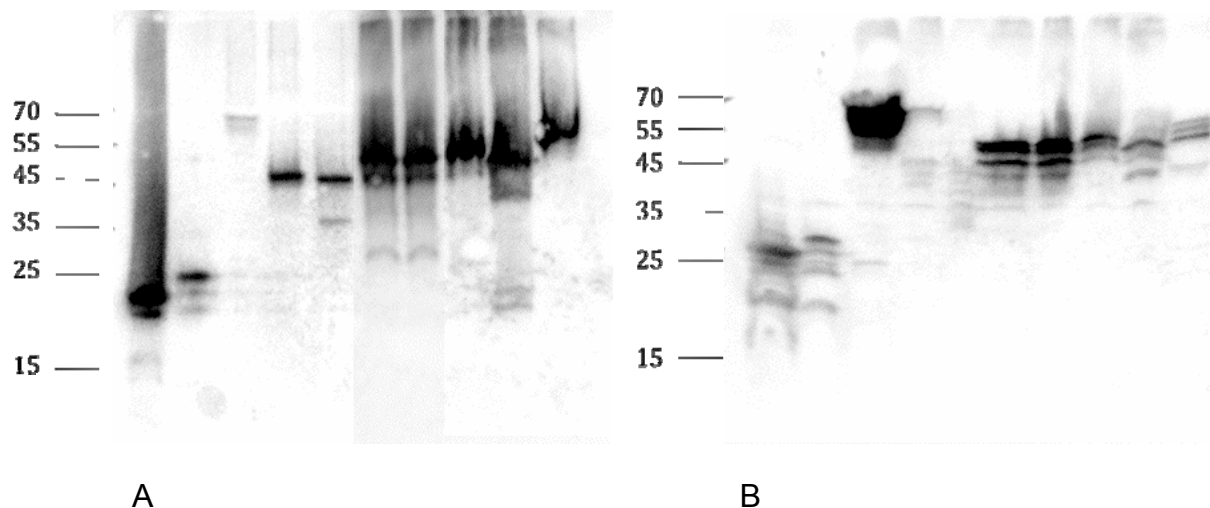


Figure C38: Comparison of the presence of the different fusion proteins in the soluble or insoluble cytosolic fraction probed with an HlyA specific antibody. (A) Inclusion bodies and (B) soluble cytosolic fraction. Shown are marker, HlyACterm (pPSG131/24.6 kDa), HlyACterm (pSO1/27.2 kDa), MalE-HlyA (67.9 kDa), Interferon α 2-HlyA (46.4 kDa), Interferon β -HlyA (47.1 kDa), Ifnar2EC-HlyA (51.1 kDa), Ifnar1EC1,2-HlyA (50.9 kDa), Ifnar1EC3,4-HlyA (51.6 kDa), CalB-HlyA (60.4 kDa), Lip3-HlyA (61.9 kDa).

Comparison of the soluble and the non-soluble cytosolic fractions revealed that most proteins exhibited a strong inclusion body formation (Table C12), whereas others are expressed as soluble proteins (MalE-HlyA, Ifnar2EC-HlyA, Ifnar1EC1,2-HlyA). Another very interesting observation was that the faint bands observed in the Western blot of the supernatant (Figure C38 B) were not observed here. This also pointed to the possibility that the fusions of Interferon α 2-HlyA, Ifnar1EC3,4 and CalB to HlyA are secreted although at a very low efficiency.

Table C12: The abundance of the different fusion proteins in either the soluble fraction or the insoluble fraction.

Protein	Inclusion bodies	Soluble
MalE-HlyA	+/-	+++
Interferon α 2-HlyA	+	-
Interferon β -HlyA	+	--
Ifnar2 EC-HlyA	++	+
Ifnar1 EC 1,2-HlyA	++	+
Ifnar1 EC 3,4-HlyA	++	+/-
CalB-HlyA	++	+/-
Lip3-HlyA	++	+/-
HlyACterm (pPSG131)	++	-
HlyACterm (pSO1)	+	-

The rating ranges from very no expression (---) to very dominant expression (+++).

The addition of the C-terminus of HlyA was not only unable to mediate efficient secretion but is also unable to prevent inclusion body formation. Only the MalE fusion was still soluble as it was previously shown for fusions of different proteins to MalE (Riggs, 2001).

A rather unlikely scenario was that the lack of secretion was caused by the absence of the HlyB and HlyD proteins. To exclude this the membrane fraction was probed for HlyB and HlyD by the specific antibodies (Figure C39).

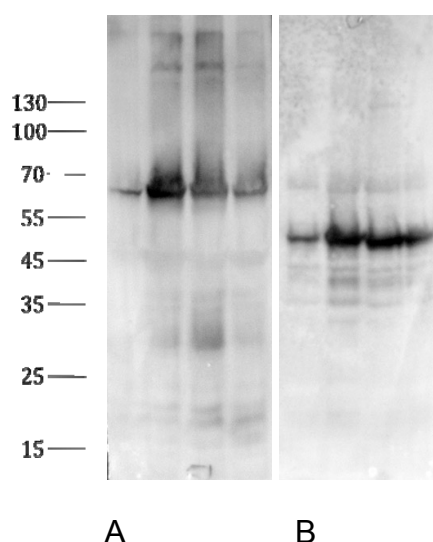


Figure C39: Membrane fractions of the cells used in secretion test probed for the secretion apparatus. (A) Detection of HlyB by an HlyB specific antibody. (B) Detection of HlyD by an HlyD specific antibody. From left to right following systems were analyzed: HlyACterm (pPSG131), HlyACterm (pSO1), MalE-HlyA (67.9 kDa), Interferon $\alpha 2$ -HlyA (46.4 kDa).

The secretion apparatus was present in all tested membrane fractions (Figure C39).

Astonishingly, in case of the secretion of HlyACterm out of pPSG131 very little HlyB and HlyD were detected pointing to a very imbalanced protein expression due to the highly expressed, inclusion bodies forming HlyA fragment.

3.6 Creating MalE-HlyA mutants for transport

Inclusion bodies are usually formed upon accumulation of large amounts of protein in a non-native state. In the absence of the secretion system, RTX proteins have a high propensity to form inclusion bodies (personal observation and IB Holland, personal communication). In the cytosol, at low Ca^{2+} concentrations the transport substrates were only loosely folded and not

in their native, biological conformation. Since the ribosomal elongation rate is around 10-20 amino acids per second (Liang et al, 2000; Young & Bremer, 1976; dependent on the environment and the strain) it would take at least 10 sec (100 sec) in case of HlyACterm (wild type HlyA, 108 kDa) before the essential C-terminal sequence is synthesized, labelling the fusion protein as Type I substrate. Any folding during that timescale would require an unfoldase or would prevent transport. In case of HlyA no chaperones are required, in line with the presence of an unfolded state (Blight & Holland, 1994). Also the full length HlyA shows no change in fluorescence upon transfer from high urea to an aqueous buffer in absence of Ca^{2+} , whereas in presence of Ca^{2+} in the refolding buffer the fluorescence increases by a factor of 2. This is in line with almost no structural change in absence of Ca^{2+} , whereas a tremendous structural rearrangement has to occur in the presence of Ca^{2+} (Thorsten Jumpertz personal communication and own observations, not shown).

Consequently, the inability of the Hly system to transport the fusion of MalE-HlyA might be caused by the completely folded MalE impeding with the export process.

In order to challenge that hypothesis several mutants of MalE were constructed being slow folding mutants of MalE (Val8Gly, Ala276Gly and Tyr283Asp* Chun et al, 1993). Using pSO1-MalE as template these mutants were generated by using the primers V8Gfor/V8Grev, A276Gfor/A276Grev and Y283Dfor/Y283Drev.

The MalE-HlyA fusions were transformed into WM2429 containing pK184-HlyBD After 14 h at 37 °C, cells were harvested and the pellet was directly analyzed by SDS-PAGE, while the supernatant was precipitated by adding TCA (10 % (w/v) final concentration) and resolved in 2.5x SDS sample buffer to obtain a fivefold concentration of the supernatant. Resulting SDS-PAGE gels are shown in Figure C40 A, B and C.

* note to nomenclature: residue Val8 is the residue valine 8 in the mature, processed protein

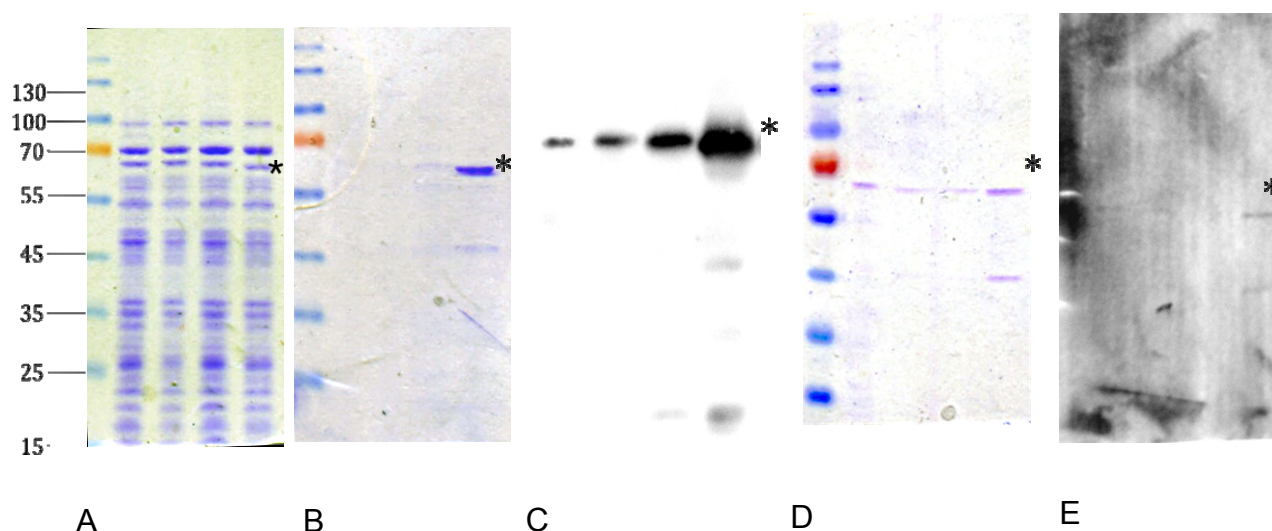


Figure C40: Secretion test with different MalE mutants fused to HlyA. Lanes in A, B and C: marker, MalE-WT-HlyA, MalE-V8G-HlyA, MalE-A276G-HlyA and MalE-Y283D-HlyA. The asterisks denote the expressed fusion construct. (A) Whole cell lysates of cells expressing the different constructs. (B) Fivefold concentrated supernatants of A. (C) Western blot B using an specific HlyA antibody (D) Purification of the MalE-Y283D-HlyA construct. Lane 1 is the supernatant used for purification, lane 2 the eluate of the NTA-Agarose, lane 3 the fivefold concentrated flow-through of the amylose column and lane 4 the eluate of the amylose column. (E) Western blot with penta-His specific antibody with same application as in D.

In Figure C40 A the cells show equal expression of the fusion protein, which is also supported by immunoblotting (data not shown). In Figure C40 B, it is clearly seen that almost exclusively the mutant MalE-Y283D-HlyA was secreted, whereas weak secretion was also observed for MalE-A276G-HlyA (see also Figure C40 C). The Western blot in Figure C40 C shows that MalE-WT-HlyA and MalE-V8G-HlyA might also secrete at low efficiency, but detection of lysed cells might also be possible. However, the amount of the secreted protein in case of the MalE-Y283D-HlyA mutant was 10 % compared to HlyA_{Cterm} as judged by densitometric SDS-PAGE analysis (10 mg/per litre culture).

Was the MalE mutant still proper folded and able to bind its substrate? Therefore the secreted mutant MalE-Y283D-HlyA was first affinity purified by NTA-agarose out of the supernatant and then probed for binding to an amylose sepharose. Results of this purification are shown in Figure C40 D and E. After two affinity chromatography steps with extensive washing a specific elution was visible, although the binding to the amylose column was not tight enough to ensure a complete retention. Nevertheless the mutation of the MalE-Y283D confers maltose import *in vivo* as it was already reported (Collier et al, 1988). For MalE-Y283D-HlyA a similar degradation product as for HlyA itself was observed, as proven by the presence of the corresponding MalE fragment (Figure C40 D) and by the presence of the

hexahistidintagged MalE product of around 68 kDa and 42 kDa (Figure C40 D and E). Successful binding to an amylose sepharose was also seen for the cytosolic fractions of MalE-WT-HlyA, MalE-V8G-HlyA and MalE-A276G-HlyA underlining that the maltose binding protein is functionally folded in all constructs (data not shown).

It has been shown previously that that in case of the mutants the unfolding remains unchanged (Park et al, 1988; Chun et al, 1993). Therefore the folding rate of the MalE-Y283D mutant would be decelerated by a factor of 250 compared to the wildtype and the relaxation time τ^2 would be at least 175 s for the MalE-Y283D instead of 0.7 s for the wildtype (Park et al, 1988). For the inefficiently secreted mutant MalE-A276G τ would be 9 s. Strikingly the HlyA secretion signal will be earliest translated after 10 s as outlined above pointing to a kinetic partitioning meaning slow folders will still be in a transport competent state, whereas the fast folders fold quickly and are not available for transport.

In order to characterize the folding behaviour of the mutant fusion proteins compared to the wildtype fusion protein, these proteins were purified out of the bacterial cytosol. Single colonies containing pK184-HlyBD and pSOI-MalE (and mutants thereof) were used to inoculate LB media supplemented with antibiotics. This stationary culture was used to inoculate 2xYT media. At an $OD_{600} = 0.5$ expression was induced by adding 10 mM arabinose. Cells were harvested after 5 hours. HlyA expressed in a soluble state is intrinsically instable and heavily degraded in the cytosol. To keep the degradation minimal, cell pellets were resuspended in 20 mM TRIS, pH 8 and 6 M Urea with subsequent metal chelate chromatography. The eluate dialysed against 20 mM HEPES, pH 7.6, 6 M Urea is shown Figure C41 A.

These fractions were used for refolding experiments. To obtain soluble, native protein the protein dissolved in urea was refolded by dialysis against 20 mM HEPES-KOH, pH 7.6. Since purification with a Hexahistidintag did not yield highly pure protein, proteases were still present. The HlyA fragment is highly susceptible to those proteases and a partial degradation could not be avoided (Figure C41 B). Therefore the fusion protein was cleaved by the site-specific protease factor Xa. The MalE protein was selectively purified using amylose sepharose. The eluate was thoroughly dialyzed to remove maltose used for elution. The resulting fractions were used for kinetic and equilibrium folding studies (Figure C41 C).

² the relaxation time τ is used instead of the k_f for better understanding with $\tau^{-1} = k_u + k_f$ and at low concentration of denaturant k_u is neglectible over k_f . Therefore with $\tau^{-1} \approx k_f$.

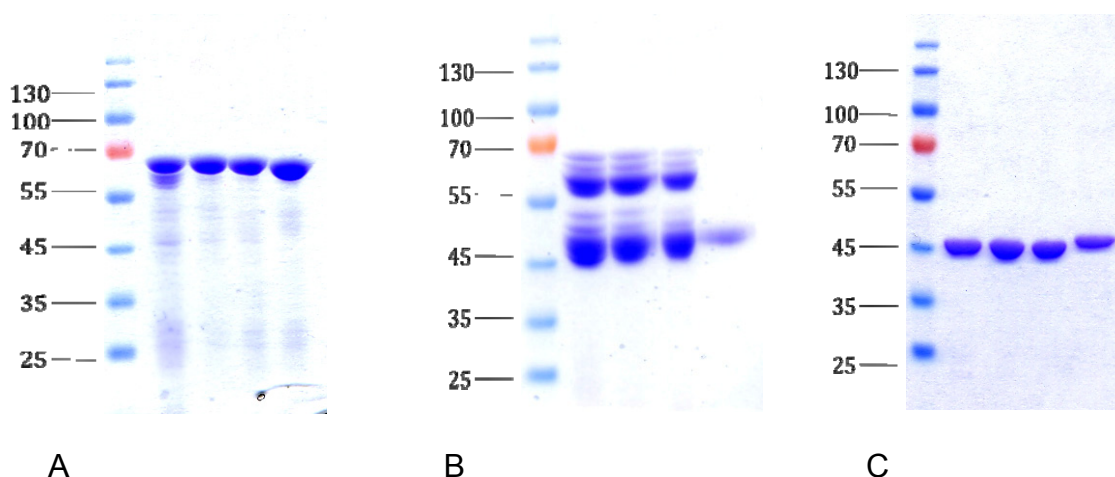


Figure C41: Purification of the fusion proteins out of the cytosol. (A) Results of the denaturing metal chelate chromatography. Shown are MalE-WT-HlyA, MalE-V8G-HlyA, MalE-A276G-HlyA and MalE-Y283D-HlyA. (B) Refolded fractions of the elutions shown in A. (C) Refolded fractions after factor Xa treatment with subsequent amylose sepharose affinity chromatography. Note the uncommon running behaviour of the MalE-Y283D-HlyA already noted here (Tomkiewicz et al, 2008).

3.7 Folding characteristics of the MalE mutants

To characterize the early events after the nascent polypeptide chain is released from the ribosome the full-length fusion construct MalE-HlyA was refolded into 20 mM HEPES-KOH, pH7.6 containing no or less urea than required for denaturation. At first the emission spectra of the completely unfolded protein MalE-WT-HlyA in urea was measured and compared to the spectra with the same amount of protein in buffer without urea. The peak height at 354 nm of the folded MalE-WT-HlyA was around two-fold of the unfolded protein constituting the range of the measurements.

In Figure C42 the increase with time upon folding exemplified for 0.5 M urea is shown.

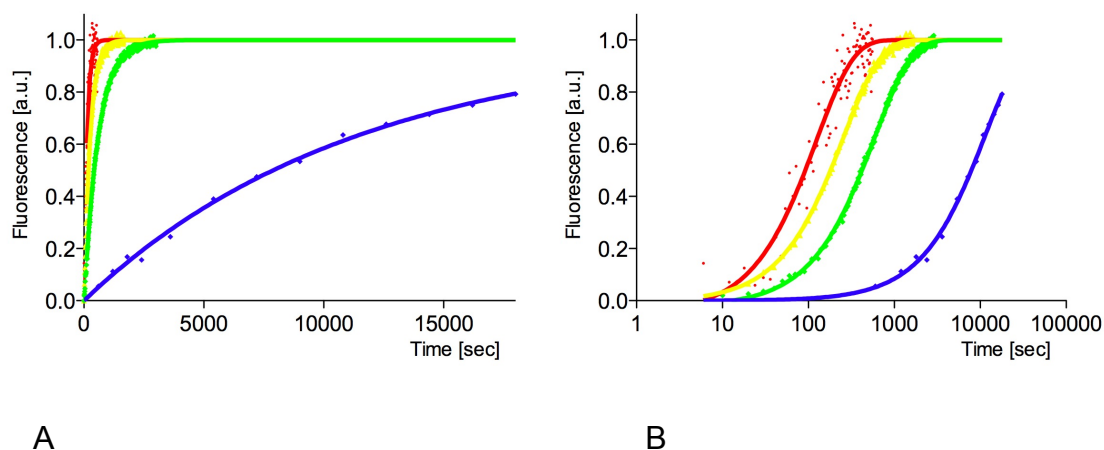


Figure C42: Refolding of MalE-HlyA fusions into 0.5 M urea as measured by fluorescence. (A) Linear plot (B) logarithmic plot. Colouring is as follows: red: MalE-WT-HlyA; yellow: MalE-V8G-HlyA, green: MalE-A276G-HlyA; blue: MalE-Y283D-HlyA.

The wildtype fusion folded fast compared to the mutant fusions especially compared to MalE-Y283D-HlyA fusion (by the factor of 100 at the urea concentration shown in Figure C42). A comprehensive picture of the folding behaviour could be drawn from the plot of all folding rates (here relaxation time) versus urea concentration (Figure C43). This plot corresponded to the left arm of a chevron plot (Fersht, 1999). At low concentrations of urea a typical chevron roll-over was observed, meaning that the folding rate deviated from the anticipated two-state model (dashed lines). This behaviour is usually a diagnostic motif for the occurrence of a folding intermediate. It can be caused for example by kinetics traps in which cis-trans isomerization reactions of a non-prolyl cis peptide bond become rate limiting (Fersht, 1999). Also, the possibility exists that proline isomerization reactions becomes rate limiting (with $\tau = 10\text{-}100$ s at 25 °C, (Cook et al, 1979; van Nuland et al, 1998). However the overall tendency of the observed rate for the proteins did not change if a classic two state behaviour was assumed as it was already done for MalE (Chun et al, 1993; Park et al, 1988).

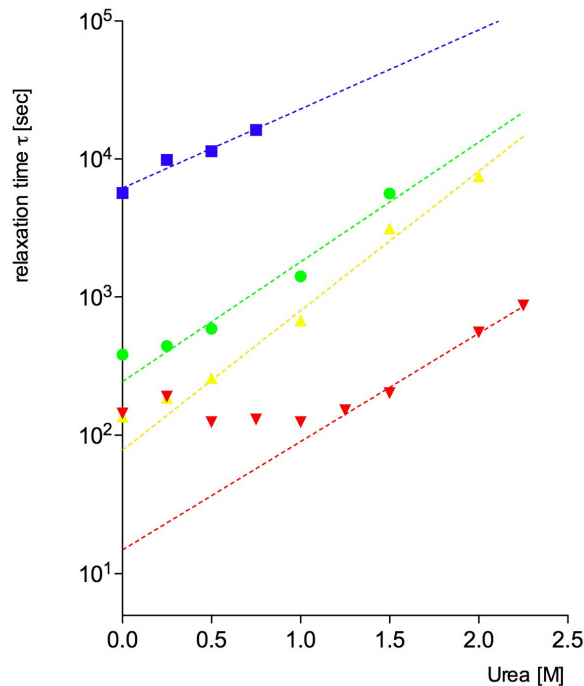


Figure C43: Refolding of MalE-HlyA fusions into urea measured with fluorescence. Dashed lines denote the extrapolation towards zero urea, equivalent to the relaxation time without any denaturant. Colouring as follows: red: MalE-WT-HlyA; yellow: MalE-V8G-HlyA, green: MalE-A276G-HlyA; blue: MalE-Y283D-HlyA.

Following the change in fluorescence allowed the determination of the folding rate by extrapolation of the linear portion to the y-axis. The extrapolated value corresponds to the value in the absence of any disturbing urea. The relaxation time τ for folding of the different variants into aqueous puffer was 14.8 ± 1.1 s for the MalE-WT-HlyA fusion, 78 ± 4.3 s for MalE-V8G-HlyA, 240 ± 15.5 s for MalE-A276G-HlyA and 6150 ± 70 s for MalE-Y283D-HlyA respectively. The measured relaxation time for the processed form of MalE was an order of magnitude faster ($\tau = 0.7$ s), whereas the unprocessed form of MalE protein was slower ($\tau = 28$ s, (Park et al, 1988)). It is important to stress that the fusion protein does not only contain a C-terminal extension in form of the 23 kDa fragment of HlyA, but also the N-terminal Hexahistidintag and a Tev cleavage site at the N-terminus. This extension close to domain I of MalE could very likely influence the folding behaviour like the secretion signal does. Intriguingly was the tendency of the folding speed: MalE-WT-HlyA > MalE-V8G-HlyA > MalE-A276G-HlyA > MalE-Y283D-HlyA which resembled the secretion behaviour.

For a complete picture not only the folding rate was necessary but also the behaviour in equilibrium. Therefore protein in the native state was transferred into 20 mM HEPES, pH 7.6 containing a defined amount of urea from 0 to 5 M. For these measurements only the MalE core protein was used, since the refolded fusion protein was very susceptible to proteases and

degraded to some extent during refolding procedure (Figure C41 B). Within the above measurements shown in Figure C43, no degradation was observed as tested by SDS-PAGE analysis. Refolding by dialysis with consecutively performed amylose sepharose affinity chromatography yielded active and pure MalE protein (Figure C41 C). Maltose was removed by dialysis. Results of the equilibrium transition are presented in Figure C44.

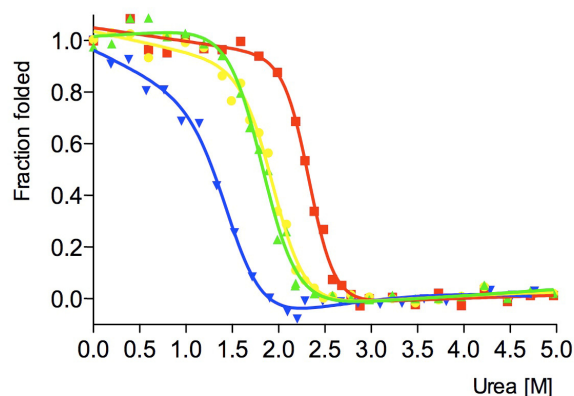


Figure C44: The equilibrium transition curve for unfolding of different MalE proteins. Colouring as follows: red: MalE-WT-HlyA; yellow: MalE-V8G-HlyA, green: MalE-A276G-HlyA; blue: MalE-Y283D-HlyA.

As shown in Figure C44 the equilibrium transition from the folded to the unfolded form followed the characteristics seen in the kinetics measurements with the midpoint of the urea induced unfolding shifted to higher urea concentrations with MalE-WT-HlyA > MalE-V8G-HlyA > MalE-A276G-HlyA > MalE-Y283D-HlyA. To derive $\Delta G_D^{H_2O}$ the values around the transition point can be fitted in a linear fashion (Figure C45). A more accurate determination was done by fitting the transition curve with Equation XXV since more data points were included in the analysis (curve shown in Figure C44).

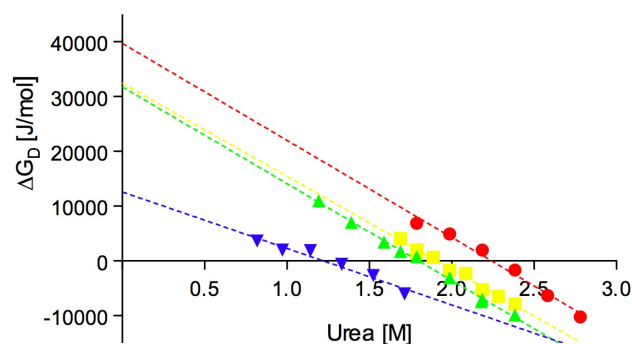


Figure C45: ΔG_D as a function of urea concentration. The interception of the linear curve presents the $\Delta G_D^{\text{H}_2\text{O}}$ value. Colouring as follows: Red: MalE-WT-HlyA; yellow: MalE-V8G-HlyA, green: MalE-A276G-HlyA; blue: MalE-Y283D-HlyA.

In Table C13 the values for $\Delta G_D^{\text{H}_2\text{O}}$ calculated either by the linear fit or by fitting the full data are shown in Figure C44.

Table C13: Values for $\Delta G_D^{\text{H}_2\text{O}}$ for the MalE proteins derived by two different fitting methods.

$\Delta G_D^{\text{H}_2\text{O}}$ [kJ/mol]	Linear fit	Fitted acc. Equation XXV	$\Delta\Delta G_D^{\text{H}_2\text{O}}$ to wildtype (Chun et al 1993)
MalE-WT	39.7 ± 2.7	42.7 ± 5.2	-
MalE-V8G	32.4 ± 1.4	28.1 ± 2.5	4.6
MalE-A276G	31.8 ± 0.7	24.5 ± 3.1	6.3
MalE-Y283D	12.6 ± 1.5	16.7 ± 2.7	13.4

Since the kinetic data was derived from the fusion proteins and the equilibrium data was obtained with the MalE core proteins, a comparison of the data can only be done if also for the MalE core proteins kinetic data was obtained. This is indispensable because the measured data differs from the data in the literature (Table C13 and Chun et al, 1993), most likely due to the additional amino acids at the N- and C-terminus of the protein.

To measure the unfolding the native MalE proteins, proteins was diluted into a defined concentration of urea and the fluorescence decrease was followed over time. The rates for unfolding are shown in Figure C46.

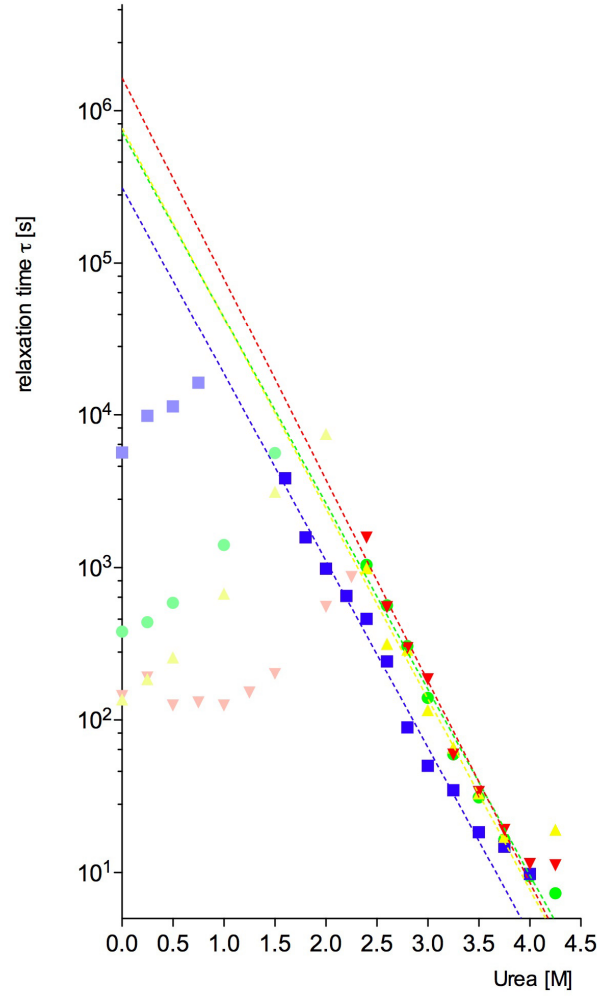


Figure C46: Unfolding and refolding of MalE proteins in urea measured with fluorescence. Dashed lines denote the extrapolation towards zero urea, equivalent to the relaxation time without any denaturant. Intensive colours denote the unfolding of the MalE core proteins. Red: MalE-WT-HlyA; yellow: MalE-V8G-HlyA, green: MalE-A276G-HlyA; blue: MalE-Y283D-HlyA. Same colour coding, but in light colours are the values for the refolding of the fusion proteins taken from Figure C43.

The relaxation times for the unfolding of the different variants into aqueous puffer derived from Figure C46 is $16.5 \pm 0.62 \cdot 10^5$ s for the MalE-WT, $7.7 \pm 0.31 \cdot 10^5$ s for the MalE-V8G mutant, $7.2 \pm 0.24 \cdot 10^5$ s for the MalE-A276G mutant and $3.1 \pm 0.11 \cdot 10^5$ s for the MalE-Y283D mutant respectively. Comparing these values, which are all in the same range, to the values of $\Delta G_D^{\text{H}_2\text{O}}$ obtained by the equilibrium transition curve, indicated that the difference in folding rate dictated $\Delta G_D^{\text{H}_2\text{O}}$. To verify this with experimental data, the folding data for the MalE core proteins were measured (Figure C47 A-D).

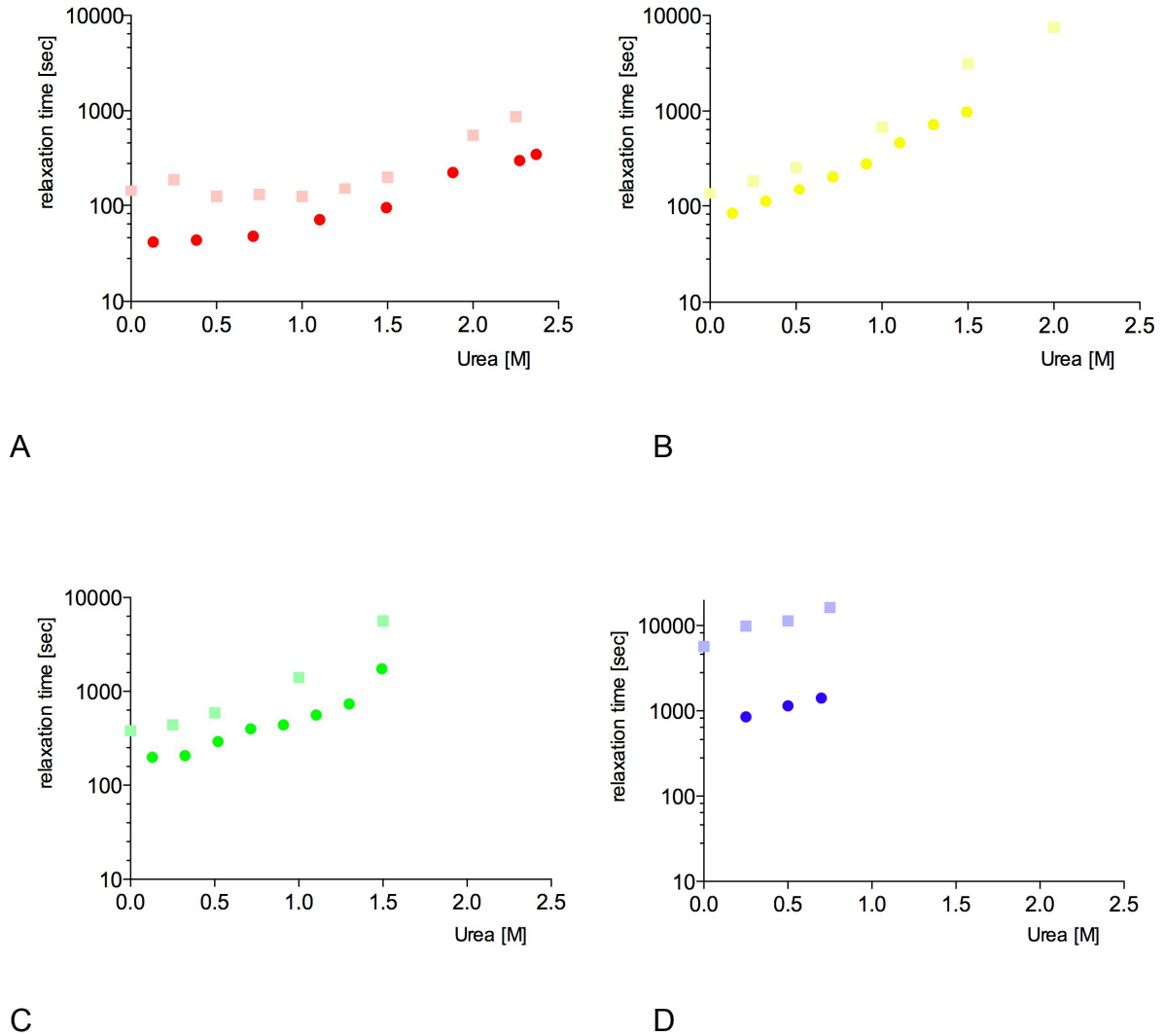


Figure C47: Refolding of MalE core proteins into urea containing buffer measured with fluorescence. Dark coloured circles denote the MalE core proteins whereas the fusion proteins are depicted in lighter coloured squares. Shown as follows: (A) red MalE-WT; (B) yellow MalE-V8G; (C) green MalE-A276G; (D) blue MalE-Y283D.

Shown in Figure C47 A-D is the folding kinetics of the core MalE proteins. In all cases folding was accelerated due to the absence of the HlyA fragment. This additional domain interfered with the folding pathway thereby slowing down the overall kinetics.

Using the extrapolation as done above for the fusion protein gave the following results (in brackets the relaxation times for the fusion protein): MalE-WT 15.8 ± 1.5 s (14.8 ± 1.1 s), MalE-V8G 60.0 ± 0.9 s, (78 ± 4.3 s), MalE-A276G 149.0 ± 2.3 s (240 ± 15.5 s) and for MalE-Y283D 641.2 ± 2.5 s (6150 ± 70 s). Most strikingly, the slower the folding rate, the higher the amount of secreted protein.

To test the reliability of the data measured for the MalE core proteins the unfolding and folding rates could be used to calculate the free energy for unfolding. In principle this should be similar to the values measured by equilibrium. In Table C14 the values are listed.

Table C14: Values for $\Delta G_D^{H_2O}$ for the MalE proteins derived by either equilibrium or kinetic methods

$\Delta G_D^{H_2O}$ [kJ/mol]	Fitted according Equation XXV	Calculated from kinetics
MalE-WT	42.7	29.2
MalE-V8G	28.1	23.8
MalE-A276G	24.5	21.3
MalE-Y283D	16.7	15.5

Equilibrium parameters derived were higher than those from kinetics likely due to the effects of proline isomerisation. However, *in vivo* the rate might be accelerated by peptidyl-prolyl isomerases (PPI), if the prolines are accessible to the enzyme. Therefore the measured kinetic folding rate might be faster *in vivo* and consequently $\Delta G_D^{H_2O}$ measured by kinetics here might not reflect the *in vivo* situation.

3.8 Influence of SecB on the folding of the MalE fusions

In *E. coli* SecB bridges the place of translation, the ribosome, to the place of translocation, the SecA/SecYEG complex, by keeping the preproteins in an unfolded, transport-competent state (Driessen, 2001). MalE secretion is adversely affected by the absence in *secB* (Collier et al, 1988; Collier & Bassford, 1989). SecB has a dual function for the secretion of MalE: It retards the folding of MalE (Weiss et al, 1988) and it improves the delivery of MalE to the membrane (Hartl et al, 1990). If the folding data for the MalE-HlyA obtained *in vitro* is transferred to the *in vivo* situation SecB has to taken into account as published for other systems (Hardy & Randall, 1991; Wolff et al, 2003). To address the influence of SecB, refolding of all MalE-HlyA species was performed in the presence of SecB. Therefore SecB (a gift of J. de Keyzer, Groningen) was prediluted in 20 mM HEPES, pH 7.6 to a final concentration of 1.5 μ M, whereas the MalE-HlyA fusion was then added to refold at a concentration of 0.36 μ M. SecB was added consequently in a ratio of around 4:1. Refolding

was performed as outlined above in the absence of SecB. In Figure C48 the kinetics are shown.

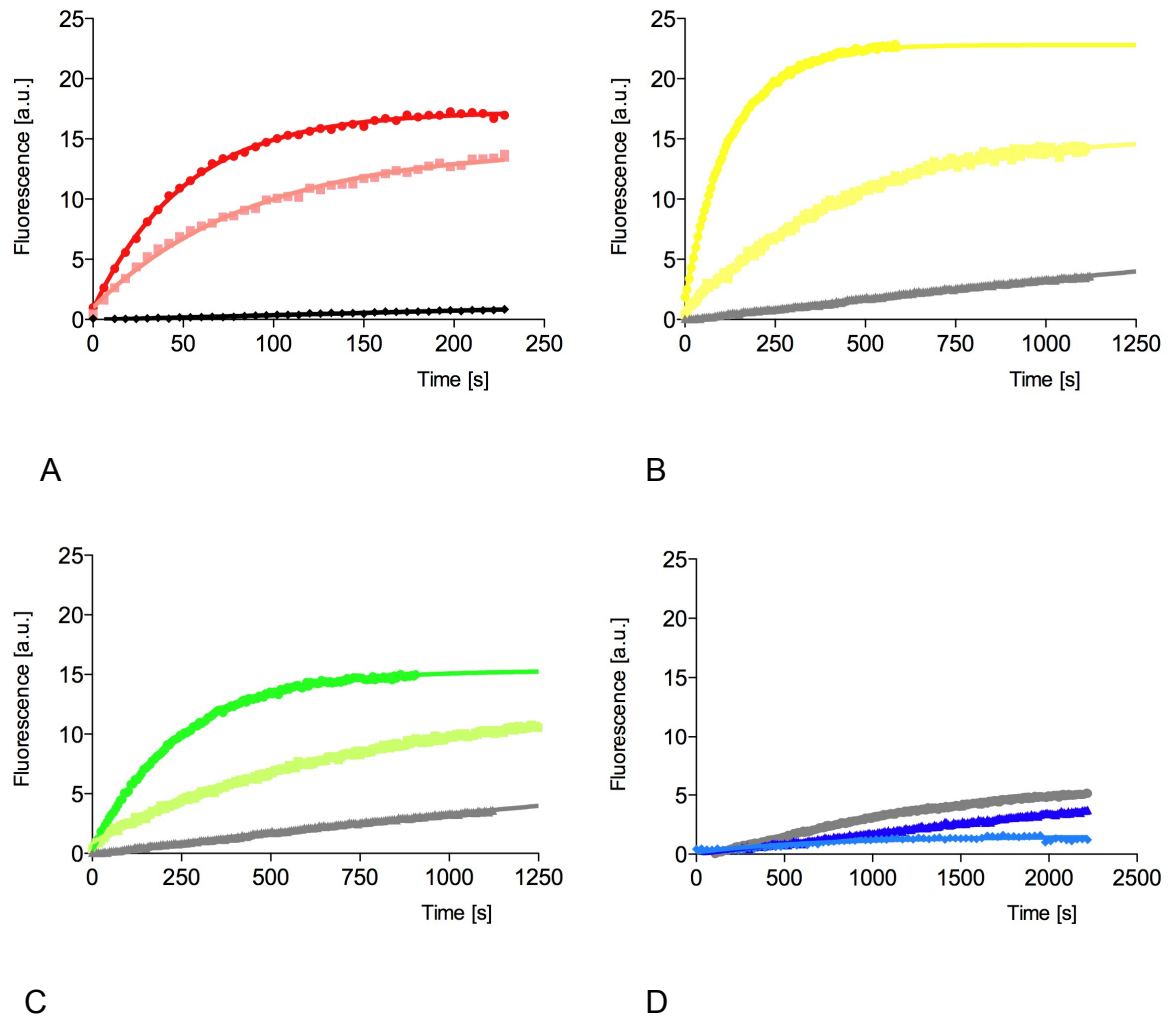


Figure C48: Retardation of refolding of MalE-HlyA fusion upon addition of 4fold excess of SecB as shown by normed fluorescence traces. (A) MalE-WT-HlyA without SecB (dark red) and in the presence of 4-fold excess SecB (light red). Also shown is only SecB (black). (B) MalE-V8G-HlyA without SecB (dark yellow) and in the presence of 4-fold excess SecB (light yellow). Also shown is only SecB (grey). (C) MalE-A276G-HlyA without SecB (green) and in the presence of 4-fold excess SecB (lime). Also shown is only SecB (grey). (D) MalE-Y283D-HlyA without SecB (dark blue) and in the presence of 4-fold excess SecB (light blue). Also shown is only SecB (grey).

The refolding in the absence of SecB followed similar kinetics than shown in Figure C42. SecB, if added to the solution alone, changed the fluorescence, what can be explained by a dynamic tetramer/dimer equilibrium of SecB (Topping et al, 2001). The fluorescence trace was not subtracted reasoning that the tetramer/dimer equilibrium is severely influence by addition of substrate. The addition of the fusions to the refolding buffer containing SecB retarded the folding by a factor of 1.7 (MalE-WT-HlyA), 3.3 (MalE-V8G-HlyA) and 3 for

MalE-A276G-HlyA. These numbers might be slightly higher due to the interference of SecB fluorescence. However, these numbers clearly show slower folding and more important a direct interaction of the fusion proteins with SecB.

In case of MalE-Y283D-HlyA (Figure C48 D), the fluorescence was even decreased in the presence of SecB compared to the sum of the traces of SecB and MalE-Y283D-HlyA. This can be explained by a blockage of folding by a difference in fluorescence behaviour.

However, it cannot be ruled out that the folding of MalE-Y283D-HlyA is only greatly reduced or even blocked; nevertheless, within the measuring time the folding was blocked for this protein.

As summary, the above results clearly show that for the first time a fusion to the HlyA secretion signal can be engineered by introducing selective amino acids mutations. The most successful secretion was observed with a very slow folding mutant (MalE-Y283D-HlyA), whereas the MalE-A276G-HlyA was far less secreted. Recent data show that upon generation of double mutants the mutants secrete with following order: MalE-WT-HlyA < MalE-V8G-HlyA < MalE-A276G-HlyA < MalE-V8G/A276G-HlyA < MalE-Y283D-HlyA < MalE-V8G/Y283D-HlyA < MalE-A276G/Y283D-HlyA; being in line with the presumed results. However, the double mutants need still to be characterized for their activity and their *in vitro* refolding behaviour.

D. Discussion

1. The binding and hydrolysis mode of the nucleotide binding domain

ABC transporter constitute one of the largest membrane protein families. Common to all ABC systems is a highly conserved nucleotide-binding domain (NBD), capable of hydrolyzing ATP. The NBD is unequivocally characterized by several short sequence motifs including the Walker A and Walker B motifs and, unique to ABC proteins, the C-loop also called signature motif, located in front of the Walker B motif (Davidson et al, 2008).

ABC systems couple the energy of ATP hydrolysis to a large variety of biological processes. Best-known is the subclass of ABC transporters coupling the hydrolysis of ATP to vectorial transport over biological membranes. Largely unknown, but also of considerable biological relevance, are non-transport-related ABC systems involved in translation, elongation, DNA repair or ribosome maturation (Kispal et al, 2005; Lammens et al, 2004).

The subclass of ABC transporters can be divided further into

- i) Importers, only found in prokaryotes and archaea, which mediate the uptake of nutrients, metals, vitamins or compatible solutes.
- ii) Exporters, which are involved in the extrusion of peptides, lipids, drugs or whole proteins.

Common to all ABC systems is the highly homologous NBD, therefore it is thought that fuelling the ABC system with the energy of ATP hydrolysis is always following a similar scheme. Knowing the single steps of the catalytic cycle of ATP hydrolysis of some ABC systems would help to understand how ABC systems in general are able to transfer the chemical energy of ATP hydrolysis into a mechanical motion for example needed to perform transport process.

To approach the catalytic cycle of an ABC system, the isolated NBD of an ABC transporter can serve as easy and straightforward model system.

1.1 Nucleotide binding to the HlyB-NBD

At present, more than 300 000 thousand proteins are annotated to selectively bind nucleotides in order to fulfil a biological process (<http://www.ebi.ac.uk/ego/GTerm?id=GO:0000166>). Only 10 % of these proteins are linked to transport processes. In addition nucleotide binding is involved in a myriad of cellular functions such as protein modulation, kinase activity, ligase activity, translation or ATP synthesis. This raises the question how these multiple functions are accomplished. How do the proteins bind the nucleotides, how strong is the binding and if present, how do these proteins accomplish a selective binding of e.g. ATP or GTP?

Among the nucleotide binding proteins several subgroups are known. ABC proteins belong to the subgroup of purine binding proteins and can be further classified as P-loop containing nucleoside triphosphate hydrolases (P-loop is also called Walker A). Other groups of purine binding proteins are P-type ATPases but also NAD binding proteins with their typical Rossman fold. Well-known members of the P-loop ATPases are the ATP synthase, myosin, helicases, AAA-ATPases, small GTPases and ABC transporters. The P-loop is described by a highly conserved phosphate binding motif. In addition to this motif additional motifs and domains ensure in P-loop NTPases that the NTP hydrolysis is coupled to a specific function.

The first structure of a P-loop NTPase was the structure of the RecA-ADP complex (Story & Steitz, 1992). Solving further 3D structures of ATPases revealed a similar fold indicating that RecA is the paradigm for all proteins sharing both canonical Walker A- and B-motifs. In ABC transporters the catalytic domain also resembles the core domain of RecA and is therefore also called RecA-like domain (Schmitt & Tampe, 2002). A structural alignment of the ATP binding pocket of HlyB with the ATP binding pocket of RecA is shown in Figure D1.

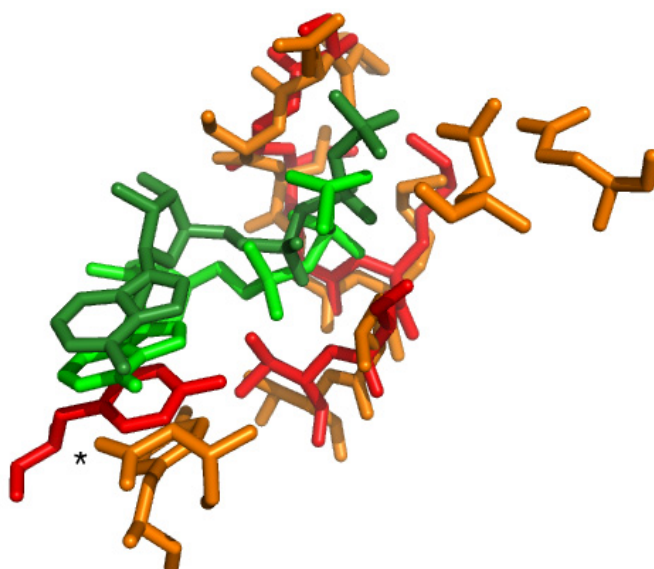


Figure D1: Overlay of the ATP binding pocket of HlyB with the ATP binding pocket of RecA. Residues of HlyB are depicted in red with ATP bound by HlyB depicted in dark green. Residues of RecA are depicted in orange with ATP bound by RecA in green. The P-loop wraps around the phosphates. The asterisk denotes the position of the aromatic residue involved in π - π stacking. The aspartate residue close to the aromatic residue in RecA provides the selectivity for ATP over GTP. Structure of HlyB-NBD H662A with bound ATP (pdb-entry: 2FGJ) and structure of RecA with bound ATP/Mg²⁺ (pdb-entry: 1MO5) were aligned in Coot.

On a molecular level the P-loop has an extensive hydrogen bonding network with the α - and β -phosphates of the bound nucleotide. As it was realized early, some P-loop mutants do not bind any nucleotides because any disturbance of this network abolishes nucleotide binding and therefore rendering the NTPase inactive (Shyamala et al, 1991). The P-loop represents a basic platform for nucleotide binding. In Table D1 affinity constants of several P-loop NTPases are summarized.

Table D1: Equilibrium binding constants of different nucleotides to P-loop NTPases

	ATP	ADP	GTP	Ref.
<i>E. coli</i> RecA	18 μ M	19 μ M	> 750 μ M	(Watanabe et al, 1994)
<i>E. coli</i> F1 β -subunit	71 μ M	120 μ M	1200 μ M	(al-Shawi et al, 1990)
Human p21 ^{ras 3)}	50 μ M	50 μ M	10 pM	(Goody et al, 1991; Rensland et al, 1995)
Rabbit Myosin S1 fragment	32 pM	10 μ M	~ 1 pM	(Goody et al, 1977; White et al, 1993)
<i>E. coli</i> HlyB-NBD wt	61 μ M	29 μ M	ND	This work

³ without guanine nucleotide exchange factor

It is remarkable that nucleotides are generally bound with an affinity of around 10-100 μM . These affinities imply that nucleotides are mostly bound *in vivo*, since the intracellular nucleotide concentrations (NTP) range in between 0.5 and 5 mM. The triphosphates are preferably bound due to the ATP/ADP ratio higher than one (with a desired ratio of 10 in *E. coli*; Koebmann et al, 2002). Therefore the similar affinity of the hydrolysis end product NDP does not interfere with the function. Also remarkable is that certain NTPases display much tighter nucleotide binding down to the impressing high affinity of 10 pM in case of the GTPase p21^{ras}. These proteins exhibit further contacts to i) the base such as in case of p21^{ras}, in which the additional guanine binding motif (N/TKXD) is present, therefore favouring GTP binding or ii) to the γ -phosphate like in the heavy chain of myosin, discriminates ATP and ADP. In these cases these high affinities are desired, since for example in case of myosin, a high association kinetics with a slow dissociation kinetics is required for ATP, in contrast to the slower association rate and faster dissociation rate of ADP.

Since ATP binding and ADP release are not rate limiting in case of ABC transporters, an affinity sufficient to saturate the NBDs is most suitable. But one has to keep in mind that nucleotide binding to ABC transporters alone does not allow hydrolysis, further steps are needed to trigger ATP-hydrolysis.

Most ABC transporters are also fuelled by GTP or even exhibit a preference for GTP in case of CvaB (Morbach et al, 1993; Zhong & Tai, 1998) but one has to question if this feature is of any functional relevance, since the nucleotide pools with the cell are usually coupled to the ATP concentration and the ATP/ADP ratio. Only additional amino acids increase the affinity for several magnitudes underlining the fact that the general nucleotide binding of P-loop NTPase is formed by a single central motif (P-loop) binding to the phosphates. The sugar moiety can be widely modified (Rensland et al, 1995) and finally the base is bound by a rather unspecific π - π or cation- π interactions (Mao et al, 2003).

Intrinsic protein fluorescence originates from the aromatic amino acids tryptophan, tyrosine and phenylalanine. The indol groups of tryptophans are the dominant source of absorbance and emission in proteins. In contrast to tyrosine and phenylalanine the emission maximum of tryptophan is around 70 nm shifted compared to the excitation maximum. This feature and the fact that the emission maximum as well as the emission wavelength is highly sensitive to the local environment allows the measurement of e.g. binding of substrates but also of rearrangements in the protein like folding. In case of the MalK the nucleotide binding domain of the maltose permease, it was recognized that nucleotide binding greatly reduces the

intrinsic fluorescence (Schneider et al, 1994) but only several years later this method was used to determine the nucleotide affinity (Smith et al, 2002), although in this report only qualitatively binding to an ATPase inactive mutant could be shown. In the latter report the authors already exploited the structural knowledge derived from NBD structures (Hung et al, 1998; Karpowich et al, 2001; Yuan et al, 2001) and used a mutant comparable to the Y477W mutant of HlyB-NBD used in this work where the aromatic residue involved in π - π -stacking with the base moiety was exchanged to the far better fluorescence probe tryptophan (Figure D1). Instead of modifying the ATP binding pocket it is also possible to use either radioactive nucleotides or, easier and safer, fluorescent analogues like TNP-ADP. Here TNP-ADP/TNP-ATP was successfully used. TNP analogues have to be competed out to determine the affinity for the natural nucleotides ATP/ADP. Limited by quenching due to the divalent cofactor Mg^{2+} this method could only be readily applied without this cofactor, although this is no general feature of ABC-NBDs (Ernst et al, 2006; Horn et al, 2003).

The dissociation constants for ADP and ATP are in the same range as it could be shown in two independent methods (tryptophan quenching and TNP-ADP competition). The affinities for both ATP and ADP reported for the isolated N-terminal NBD of MRP-1 (Ramaen et al, 2003) are in a reasonably close agreement with the results of our studies but in contrast to data for P-gp, where dissociation constants for ATP and ADP differ by one order of a magnitude (Sauna et al, 2001). In the case of the HlyB-NBD, the presence or absence of the cofactor Mg^{2+} in the nucleotide/HlyB-NBD complexes had no effect on the K_D values. This implies that cofactor binding does not induce large conformational changes within the nucleotide-binding site that could influence overall affinity, although the cofactor might be involved in the communication in between both binding sites (Zaitseva et al, 2006).

Nevertheless, one has to be cautious, since the affinity of a NBD toward nucleotides might be further modulated by the presence of TMDs. One could imagine that the presence of the TMD stabilises the Walker A in a 3_{10} helical conformation reported previously for HlyB-NBD (Schmitt et al, 2003) or in the unusual conformation reported for the nucleotide-free state of GlcV (Verdon et al, 2003a) drastically affecting the nucleotide binding ability.

The nucleotide affinity in case of HlyB-NBD was largely independent of ionic strength in contrast to OpuAA, where a significant influence of the salt concentration is present (Horn et al, 2003). In case of OpuAA, involved in osmoprotection, this could be of functional relevance whereas for other ABC transporters this modulation might not be present.

1.2 Characterisation of the TNP-ADP binding mode

TNP modification of nucleotides is known to increase the affinity towards ABC proteins compared to unmodified nucleotides by the factor 10 to 100. Since TNP is environmentally sensitive, binding to proteins increases its quantum yield, consequently bound nucleotide analogues exhibit a fluorescence increase by the factor 2 to 10 (Hiratsuka, 2003). This feature allows discrimination between bound and non-bound fluorophores and thereby studying the affinity, binding kinetics and FRET measurements. One might also think of using TNP as a starting point to create a (non-)fluorescence probe with even further increased affinity. This modified nucleotide could be used to enrich ATP binding proteins for proteomic purposes or one could even imagine a sequence specific probe enabling labelling and inhibiting certain ATP binding proteins like it was earlier suggested (Bilwes et al, 2001).

Only two structures with bound TNP derivatives have been solved so far. A catalytic domain of an adenylate cyclase was solved with TNP-ATP (Mou et al, 2006) and also CheA, a bacterial histidine kinase, was solved with TNP-ATP (Bilwes et al, 2001). In the latter case the TNP moiety renders the protein unable to hydrolyse TNP-ATP because specific interactions with the protein direct the phosphates in a hydrolysis deficient position. In case of HlyB-NBD the position of nucleotide moiety of TNP-ADP is almost identical with the position of ADP (Figure A5 and Figure D2). Although not tested it seems almost certain that the ATPase activity is also abolished due to severe steric clashes in the dimeric form with the opposing C-loop (Figure D2). Any disturbance in the positioning of the highly conserved C-loop prevents successful ATP-hydrolysis.

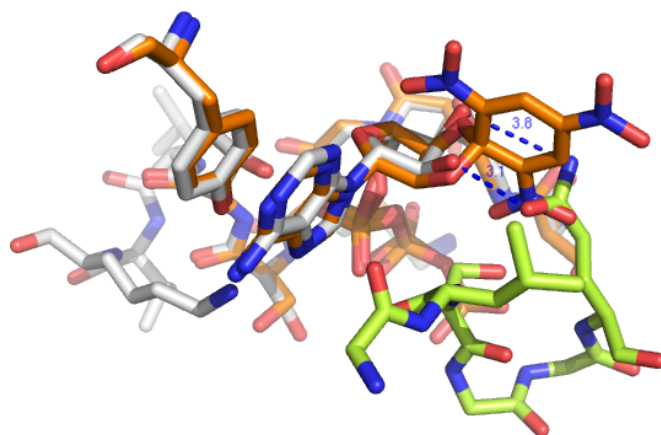


Figure D2: Overlay of the HlyB-NBD with bound TNP-ADP (orange carbons) with the dimeric structure of the HlyB-NBD mutant H662A with bound ATP (white carbons; lime green carbons denote the C-loop of the opposing monomer in the dimeric structure). An ortho-nitro group of the TNP moiety would encounter a steric clash with the glutamine of the opposing C-loop if the dimer would be formed. In the dimeric structure the glutamine connects the 2' OH of the ribose via hydrogen bonding. Distances to the glutamine are shown in broken blue lines. Structure of HlyB-NBD H662A with bound ATP (pdb-entry: 2FGJ) and structure of HlyB-NBD with bound TNP-ADP (pdb-entry: 2PMK) were aligned in Pymol.

As mentioned in the Results section the TNP moiety binds only through water molecules to the protein and thereby the increase of the affinity can be explained. This water network is highly flexible as it could be shown by introduction of a mutant (HlyB S504A). This mutant abolished an existing water mediated contact. Thus, no change in affinity of the TNP nucleotide was detected. But structural work could show that this missing water contact is replaced by a new contact. Therefore TNP nucleotides might be an unsuitable starting point for the development of novel 'affinity-tailored' fluorescence-modified nucleotides binding to monomeric ABC NBDs.

Is it promising at all to work with ribose modified nucleotides? Variations in the base are usually accepted even though the affinity can vary for individual ABC transporters. Therefore base modification might be possible but the results are difficult to generalise. On the other hand slight modifications at the ribose moiety (dATP) only slightly influence the turnover (Mao et al, 1999; Urbatsch et al, 1994). Looking at the physiological active species an analogue, though not a fluorescent one, might be possible tightly interacting with the Gln of the C-loop (Gln610 in HlyB) and thereby being a tool to lock the dimeric species, providing a wonderful tool stabilising this intermediate without using tedious trapping methods. Since the

C-loop is highly conserved in ABC transporters and the positioning of the glutamine is almost identical to the ATP bound dimeric HlyB-NBD in case of the dimeric NBDs MalK (Chen et al, 2003a) and MJ0796 (Smith et al, 2002) it is likely that such a nucleotide analogue, if it would be feasible for a single ABC system, it would apply for the majority of ABC systems.

1.3 The catalytic mode of the HlyB-NBD

How ATP hydrolysis occurs in ATPases is a fundamental question, because ATP hydrolysis is coupled to the functional mode of the protein, such as rotation of V-type ATPases or transport in case of ABC transporters. Any uncoupled and uncontrolled hydrolysis would be detrimental. In case of ABC transporters the NBDs have to dimerize during the ATP hydrolysis cycle. The cooperativity of HlyB-NBD in steady state ATPase measurements clearly underlines this fact. Structural work done with HlyB-NBD but also other biochemical investigations for related systems clearly show that the dimeric form in which the Walker A motif is adjacent the C-loop (Fetsch & Davidson, 2002; Loo et al, 2002; Zaitseva et al, 2005a) is the active species.

How is the ATP cleaved if an ATPase active form is generated? For the F_1F_0 -ATPase and SecA a general base mechanism was proposed (Abrahams et al, 1994; Sato et al, 1996; Zito et al, 2005). In these cases a conserved glutamate is thought to abstract a proton from the catalytically active water. For ABC transporters a glutamate adjacent the Walker B motif was proposed to constitute this catalytic base (Geourjon et al, 2001; Smith et al, 2002). This suggestion is supported by mutational analysis done for MJ0796, MJ1267 (Moody et al, 2002) and BmrA (Orelle et al, 2003). In HlyB the mutation of this glutamate into glutamine (E631Q) exhibits surprisingly 10 % ATPase activity of the wild type (Zaitseva et al, 2005b). Detectable ATP turnover was measured in human and mouse P-gp (Tomblin et al, 2004; Urbatsch et al, 2000) and the EQ mutant in case of *Sulfolobus solfataricus* GlcV exhibits even 20 % of the wild type activity (Verdon et al, 2003b) challenging the general base mechanism with the glutamate being the key residue.

Since the behaviour of the mutants is only a weak indication that a general base mechanism is not applying, the work presented here could clearly show that a general base mechanism is not present in HlyB. ATPase measurements are directly assessing the ATP cleavage since in

case of HlyB viscosity measurements could show that the turnover is independent of the viscosity pointing to the fact that a chemical reaction is the rate limiting step (Zaitseva et al, 2005a).

What are the reasons why a general base mechanism is not applying?

No decrease in ATPase activity was detectable if D₂O was added in increasing concentrations, $k_{\text{cat}}(\text{H}_2\text{O})/k_{\text{cat}}(\text{D}_2\text{O})$ remained essentially constant. For example, F₁F₀-ATPase (Amano et al, 1994) or phospholipase C (Martin & Hergenrother, 1999), which are assumed to follow general base catalysis, showed an increase in $k_{\text{cat}}(\text{H}_2\text{O})/k_{\text{cat}}(\text{D}_2\text{O})$ ratio of more than two (Dorgan & Schuster, 1981). On the other hand, the GTPase p21ras, which is presumed to use SAC, displayed only a slight decrease in $k_{\text{cat}}(\text{H}_2\text{O})/k_{\text{cat}}(\text{D}_2\text{O})$ in the presence of D₂O (Schweins et al, 1995; Schweins & Warshel, 1996). Extrapolation of the k_{cat} values to 100% D₂O resulted in a $k_{\text{cat}}(\text{H}_2\text{O})/k_{\text{cat}}(\text{D}_2\text{O})$ of 0.79 for HlyB-NBD, similar to the value of 0.71 reported for p21ras (Schweins & Warshel, 1996). The experiment in D₂O implied that proton abstraction might not be the rate-limiting step in this system.

Further support that the glutamate is not the catalytic base in HlyB stems from the pH profile of the ATPase (Zaitseva et al, 2005b). Here the pH-optimum is around pH 7 and the $V_{\text{max } 50\%}$ values were determined to be 6.1 and 8.2. At a pH lower than pH 6 ATP is still protonated whereas at a decrease at a pH higher than 8 might not be explained by an essential glutamate, rather by the deprotonation of a histidine. This histidine is either directly influencing the ATP or indirect by disturbing the dimer interface. The latter case seems unlikely since no histidine is involved in the dimer interface. Most likely the highly conserved histidine at the position 662 is causing that decrease also supported by ATPase measurement performed with NBD1 of the human TAP (Ernst et al, 2006).

Again this result does not exclude the possibility that a base mechanism may still operate upstream of the rate-limiting step in the catalytic cycle. Nevertheless, all these results are urging to consider alternative mechanisms. Thus, SAC (substrate assisted catalysis) might apply, where the substrate participating in catalysis might be either ATP itself, as it has been suggested for some GTPases (Schweins et al, 1995), or conceivably the cofactor, Mg²⁺.

Support for SAC stems from the modulation of ATPase activity by divalent metal ions. SAC depends on the substrate having the proper pK_a value, therefore a detectable difference should be measured if different divalent metals are catalysing the ATPase. In contrast to F₁F₀-

ATPase (Papageorgiou et al, 1998), turnover numbers for the HlyB-NBD ATPase activity decrease with $\text{Mg}^{2+} > \text{Mn}^{2+} > \text{Co}^{2+}$, as well as the catalytic efficiency ($k_{\text{eff}} = k_{\text{cat}}/K_{0.5}$). k_{cat} and k_{eff} correlate with the pK_a values of the metal ion-aqua complexes and their strength to act as a Lewis acid but not with their atomic radius. This modulation of activity, which is qualitatively identical to that of P-gp (Urbatsch et al, 1995), implies that a proton abstraction step is influenced by the presence of different metal ions.

Since SAC depends on the substrate having the proper pK_a value this could provide an explanation for the need for the signature motif to complete the ATPase hydrolysis pocket. Within a binding site, the microenvironment imposed by the protein will affect the pK_a value of ATP. Thus, one can easily envision that dimerization and the resulting interaction of amino acids of the C-loop motif with the γ -phosphate group will modify the intrinsic pK_a values of the bound ATP molecule. Calculation of the different pK_a values of the amino acids in the monomeric and dimeric state of HlyB-NBD clearly state that dimerization induces drastic changes in the individual pK_a values in the region of the Walker A motif and the region covering the Walker B/D-loop/H-loop (Hanekop et al, 2006).

The mutation of the proposed glutamate in HlyB-NBD does not abolish ATPase activity whereas the substitution of H-loop histidine into alanine clearly eliminates ATPase activity. In other systems the activity was also reduced to background level (*E. coli* HisP; H211R and H211D, Nikaido & Ames, 1999, *E. coli* MalK, H192R, Davidson & Sharma, 1997, *S. cerevisiae* Mdl1, H631A, Hofacker et al, 2007, human TAP1-NBD homodimer, Q701, Ernst et al, 2006 and MRP1, H1486L and H1486F, Yang & Chang, 2007). What is the role of the H-loop? The position of the histidine 662 in HlyB coincides with those residues of the proteins suggested to be essential for catalysis in other NTPases (Zaitseva et al, 2005a). All those residues are able to form hydrogen bonds, therefore the exchange of the histidine to an amino acid also able forming a hydrogen bond (with the γ -phosphate of ATP) would compensate to some extent the missing histidine. This is for example the case in MRP1 and TAP2. Still the histidine is highly favoured among ABC systems due to the feature that histidine can form two hydrogen bonds. This bidentate character of this residue renders it most likely indispensable. One interaction is formed to the γ -phosphate of ATP, the other interaction is consequently formed to the proposed catalytic glutamate (see Figure D3). The catalytic dyad formed by the histidine and glutamate would satisfactorily explain the effects caused by mutational analysis: If the carboxylate is missing the histidine would not be fixed in place, therefore flickering around and being largely unable to interact with the γ -phosphate.

In some cases such HlyB an interaction will occur causing a poor activity. On the other hand if the histidine is missing no direct interaction to the γ -phosphate can occur. If both residues are present the carboxyl moiety of the glutamate forms two interactions with the histidine, one with the backbone amide and one with the nitrogen of the imidazole ring. Histidine on the other hand polarizes the putative catalytic water molecule and interacts with the γ -phosphate group of ATP. This latter interaction likely serves to stabilise the transition state. In other words, the histidine represents the most important residue essential for hydrolysis holding all molecules needed for hydrolysis together (= the linchpin), while the glutamate adopts a platform-like function orienting the side chain of the histidine in a productive configuration.

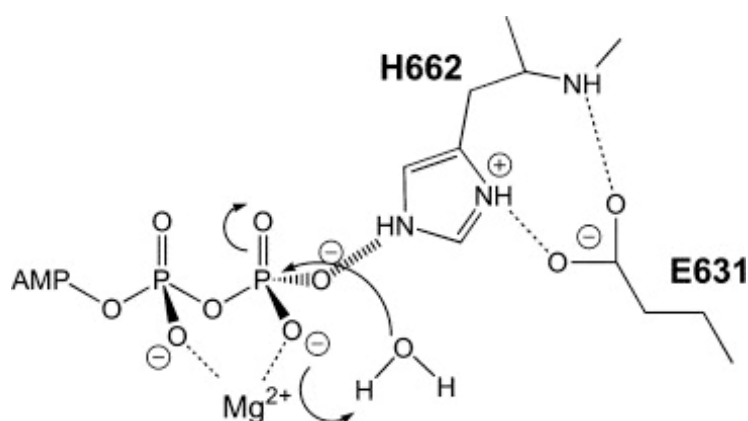


Figure D3: Schematic representation of the linchpin model.

This linchpin model is consistent with all data obtained so far for isolated NBDs but inconsistent with the DNA mismatch repair protein *E. coli* MutS and the multidrug transporter *S. cerevisiae* Pdr5p. In MutS a H728A mutant exhibits an even increased ATPase activity (Junop et al, 2001) whereas in Pdr5p the H1068A mutant had an altered substrate spectra with an uncoupled ATPase (Ernst et al, 2008). In the latter case the EQ (E1036Q) was inactive in transport and in ATPase activity pointing to a more pronounced role of this residue. Certainly, these results challenge the role of the histidine but further studies on full-length asymmetric ABC transporters need to be done in order to clarify the exact role of the histidine since it might also play an important role in the communication in between the substrate binding site and the ATP hydrolysis site (Ernst et al, 2008; Zaitseva et al, 2005a). The linchpin model with SAC might be the extreme case applying for a canonical ABC transporter. It is conceivable that modifications in the usually highly conserved residues

slightly chance this mechanism in order to modify the ATPase cycle to the specific needs of the transporter.

Full length ABC transporter often exhibit degenerated motifs (e.g. *S. cerevisiae* PDR5, human TAP1/2 or human CFTR) in which one ATP binding pocket is inactive due to a degenerated C-loop or a mutation in the H-loop. Obviously these transporters are also fully functional. Can active NBDs serve as model system since they contain two functional ATP binding pockets? In a mixture of wild type HlyB-NBD with the ATPase deficient mutant HlyB-NBD H662A also the mixed dimers contribute to the overall ATPase activity indicating that ATP hydrolysis takes places in one ATP-binding site independent of the other site of the NBD heterodimer. Such a scenario is reminiscent of the model of ATPase activity proposed for Mdl1p-NBD (Janas et al, 2003), which states that the hydrolysis of each ATP molecule in Mdl1p-NBD occurs in a sequential fashion. This conclusion is based on the assumption that an unrestricted random association of monomers upon mixing is happening. In HisP, mutations of the corresponding histidine (H211) to arginine or aspartate (Nikaido & Ames, 1999) gave different results with respect to ATPase activity of the heterodimers. While the H221R mutation displayed similar results to those described for HlyB-NBD H662A, heterodimers of HisP containing the H221D mutation were ATPase-deficient. On the basis of the recently determined crystal structure of the HlyB-NBD H662 in complex with ATP/Mg²⁺ (Zaitseva et al, 2005a), two possible explanations for the latter mutant arise. First, the electrostatic repulsion between the side chain of aspartate and the γ -phosphate of ATP might disrupt the formation of stable heterodimers. However, in this model, H662 of HlyB NBD forms vital interactions with the D-loop of the trans monomer in the sandwich dimer, which are necessary for monomer-monomer communications. Introduction of an aspartate would severely influence this cross-talk and perhaps prevent ATP-hydrolysis even in a single site. This points to the overall conclusion that one has now obtained important insights in how ATP is hydrolysed.

2. Cloning and expression of the inner membrane components of the haemolysin system

2.1 Cloning and overexpression

Membrane protein overexpression in a functional state is one of the first hurdles encountered in the analysis of membrane proteins. The biogenesis of integral membrane proteins involves many steps such as targeting of the nascent polypeptide chain to the membrane, insertion into and assembly in the membrane. Each of these steps requires distinct components (Xie & Dalbey, 2008). *E. coli* is the most commonly used expression host. Exceeding the capacity of the cell to process the nascent membrane protein correctly may result in the production of aggregated material (inclusion bodies). Since refolding of membrane proteins is at the moment possible only for a few proteins, functional overexpression of the desired membrane proteins in the cytoplasmic membrane is preferred.

The amount of well-folded protein produced in the membrane can often be increased by systematic optimization of several parameters such as the expression strain, induction temperature, growth medium, promoter strength and systematic addition to the C- and N-terminus of the protein (Lewinson et al, 2008; Mohanty & Wiener, 2004; Wang et al, 2003). Furthermore starting with several ORFs encoding for homologous proteins might increase the probability of finding a highly expressed and well-folded membrane protein with the same function. This approach has been done impressively by the group of Kaspar Locher, solving several X-ray structures of ABC transporters (Hollenstein et al, 2007a; Locher et al, 2002). However, we have chosen the approach of focussing on a single system, the *E. coli* haemolysin system, using several plasmids, with largely differing features. Almost the same approach has been also done for the yeast mitochondrial ABC transporter Mdl1 (Hofacker et al, 2007). This approach failed in overexpression in *E. coli* and *L. lactis*, whereas the haemolysin system was successfully expressed in *L. lactis*. *L. lactis* was previously reported to be a good alternative to *E. coli* as membrane protein overexpression host (Kunji et al, 2003), although this statement cannot be generalized (Surade et al, 2006). Certainly the huge variety of strains, plasmids and protocols are still missing in this organism, but new methods arise which expand the tool boxes available in *L. lactis* (Siren et al, 2008).

It is unclear why the overexpression in *E. coli* failed, although some overexpression is present since secretion is present (as shown by the secretion experiments). Since the haemolysin machinery is an *E. coli* protein complex and therefore, in this case, homologous overexpression takes place, it is important to look at the physiological regulation of the natural expression environment.

How is the expression of the haemolysin machinery regulated? The structural genes *hlyCABD* are organized on one transcriptional unit driven mainly by a single promoter but also additional components are present (Cross et al, 1990; Vogel et al, 1988). In the intergenic region of *hlyA* and *hlyB* a terminator region is present limiting the expression of the membrane complex and favouring the expression of the soluble proteins HlyA and HlyC (Koronakis et al, 1989a). In the *E. coli* plasmids encoding for HlyB and HlyD used in this work neither the region upstream of the promoter is present nor the intergenic region in between *hlyA* and *hlyB*. Thus, there should not be any regulation by these regions. A modulation that cannot be ruled out is the influence of proteins binding directly to *hlyB* and *hlyD*. Rather unknown is that even bacteria are able to influence the expression by histone like proteins. During this work it became evident that those proteins have an impact on the transcription level of *hlyB* and *hlyD* (Muller et al, 2006). A knock-out of *hns* resulted into an increased virulence and more strikingly in a higher transcription of the transporter genes *hlyB* and *hlyD* by the factor of 3 to 5. Hoping that the absence of this regulation might also increase the overexpression in this work, protein expression with the *E. coli* strains S2303 and S614 (both are *hns* knock-outs) was tested with pSJ030. Unfortunately no significant change in expression was observed.

However, not all *E. coli* membrane proteins are successfully overexpressed in *E. coli*. Impressive work by the group of Gunnar von Heijne show that HlyB and HlyD is not an exception. Also other membrane proteins are not overexpressed in *E. coli* although they are intrinsic *E. coli* proteins (Daley et al, 2005). In this report judging the overexpression by GFP fusions some proteins were neither overexpressed nor do the cells show any response to the induction, resembling the situation observed also for HlyB and HlyD. Unluckily HlyB and HlyD, non *E. coli* K-12 proteins, were not included in this work (G. von Heijne, personal communication).

In the *in vivo* background it might not be useful for the cell to overexpress the haemolysin system excessively for example due to interference with other TolC dependent systems. However, any regulation by differential codon usage (Saier, 1995) could also be ruled out by

supplying rare tRNAs. What might regulate the expression of the Hly system is still unclear but a regulation on the mRNA level might be conceivable.

The fact that overexpression worked well in *L. lactis* allowed successful purification. Nevertheless, the overexpression in *E. coli* is clearly preferable, for example due to *in vivo* assays possible only in the Gram-negative bacterium. This would allow rapid screening of mutants.

Pushing expression in *E. coli* might be possible either by fusions to highly expressed membrane proteins to the N-terminus of HlyB or HlyD or truncations where only the ABC core domain (TMD and NBD) is expressed lacking the C39 domain.

2.2 Solubilisation and purification

The successful solubilisation is a prerequisite for purification and the choice of the proper detergent not only dictates the solubilisation efficiency but also the stability of the protein since certain detergents may destroy the integrity of the protein. Out of 6 detergents tested the best detergent for extraction and purification proved to be the zwitterionic Fos-Choline 14 (FC-14) in line with a more comprehensive detergent screen performed for HlyB (Oswald, 2008). This detergent has to be handled with care, because several reports state that FC-14 tends to unfold proteins (Kiefer, 2003; Lewinson et al, 2008). Also the structure of the mechanosensitive channel MscS solved with FC-14 may not correspond to the closed, resting state present in the membrane (Akitake et al, 2007; Bass et al, 2002; Lewinson et al, 2008). Furthermore, it was only recently reported that FC-12, having a shorter chain length, might keep membrane proteins in a soluble but unfolded state (Geertsma et al, 2008).

Since also positive reports are present, in which an ABC transporter could be properly solubilised and purified (Hanekop, 2006), FC-14 was used for protein extraction and purification. However the proposed inner membrane complex was torn apart by the solubilisation and it remains to be clarified how stable the protein complex present in the inner membrane is, since for other HasA system the membrane fusion protein only interacts if the substrate is present (Letoffe et al, 1996). By employing a decahistidintag HlyB could be successfully purified by a single step, with additional gel filtration as polishing step. The protein preparation was 95 % pure and homogenous as judged by gel filtration and SDS-PAGE.

2.3 ATPase induction by addition of HlyACterm

Any uncertainty concerning the detergent can be ruled out if the activity of the protein can be proven. HlyACterm contains all the necessary information needed for secretion and clearly shows an induction of the ATPase activity of HlyB underlining that the transported substrate indeed interacts with the ABC transporter (Benabdelhak et al, 2003) and the chosen detergent can be used to purify ATPase active HlyB. The ATPase with an turnover of 1.0 ATP/min is low compared other ABC systems where higher ATP turnover rates have been reported (300 ATP/min for the stimulated TAP transporter (Gorbulev et al, 2001), 240 ATP/min for the multi drug transporter Pgp (Sharom et al, 1995) and CFTR with 60 ATP/min (Li et al, 1996)). The HlyB-NBD exhibited also a low ATPase activity of around 12 ATP/min. Other ABC transporters with a low ATPase include for example the osmoprotection system OpuA from *L. lactis* (van der Heide et al, 2001), its homologue from *B. subtilis* (Horn et al, 2003) and the *E. coli* Flippase MsbA (Doerrler & Raetz, 2002), having all, depending on the state, a turnover of around 1-3 ATP/min. It is important to stress that the turnover rates are difficult to judge as also in these cases background ATPases may influence the final numbers.

A modulation of the ATPase hydrolysis upon substrate addition has been reported for several ABC transporters connected to multidrug resistance, since the detergent as well as the present lipids might induce the basal ATPase hydrolysis, which is only up- or downregulated by adding other substrates (Ernst et al, 2008; Sharom, 1995). An induction of ATPase activity by the substrate has been seen for several reconstituted systems with binding protein dependent ABC transporters being the best examples (Davidson et al, 1992; Liu et al, 1997; Patzlaff et al, 2003). In these cases the ATPase is strictly coupled to the presence of the substrate and the substrate binding protein. In case of the Hly system, HlyA might take over the function of the substrate bound to the substrate binding protein. However these systems were are all reconstituted and HlyB activity can be already measured in detergent solution. Any induction in other systems is not seen in detergent solution (Davidson et al, 1996; Liu et al, 1997), reasoning that the signal given by the liganded substrate binding protein is not properly transmitted.

What will happen upon substrate binding? In the TAP transporter peptide binding induces a conformational change that triggers ATP hydrolysis in both subunits of the TAP complex (Chen et al, 2003b). This is also seen for the binding protein dependent maltose permease (Mannering et al, 2001) and ABC transporters binding and transporting hydrophobic

substances (Manciu et al, 2003; Sonveaux et al, 1999). In line with these reports one can imagine that the NBDs of HlyB only form ATPase active dimers if the substrate HlyA is present, in line with dimer formation upon binding of a liganded substrate binding protein to an importer. In case of HlyB the signal is not needed to be transmitted across the membrane. However, compared to an ABC importer a transport at this step is very unlikely since TolC needs to dock to the inner membrane complex (Balakrishnan et al, 2001). The infertile arrangement could be resolved by dissociation of HlyA with subsequent ATP hydrolysis resetting HlyB. This assumption is supported by the fact that the affinity of HlyA to HlyB-NBD is decreased upon addition of ATP (Benabdelhak et al, 2003).

Of course, the importance of HlyD is unclear, HlyD is far more than just an adaptor from the inner to the outer membrane (Pimenta et al, 2005) and an essential component of Type I secretion systems. Very likely the periplasmatic coiled-coil regions of HlyD might be released by the presence of the substrate sensed by HlyB and enables TolC recruitment and binding, as shown for the AcrA/TolC interaction (Lobedanz et al, 2007). It will be exciting to see how the events of recruitment and events of transport are coordinated by this molecular machine, since it is hard to imagine that HlyA is transport by a single ATP hydrolysis step.

3. Usage of fusions to an HlyA fragment for secretion

3.1 Creating a system that allows screening of fusion proteins

Protein fusions are frequently used to selectively add a feature to a protein. Widely used for example is the fusion of a polyhistidine sequence to the N- or C-terminus of a protein for fast purification (Hengen, 1995). Not only for chromatographic processes fusion proteins present a valuable tool. By adding a specific sequence folding can be improved (e.g. MalE fusions), detection is eased (e.g. GFP or FLAG-tag fusions (Terpe, 2003) or protein targeting can be varied (MalE or PhoA fusions for periplasmatic expression). Usually vectors encoding promising fusion proteins in frame of a multiple cloning site are available commercially spreading the use of certain fusion proteins. The secretion of proteins into the extracellular media by the Type I secretion system is theoretically a perfect tool for heterologous expression in *E.coli*: It represents the least level of proteolysis, simple purification and protein

folding can be improved due to the low local protein concentration. The protein might be diluted but current techniques like affinity chromatography or expanded-bed chromatography deal easily with such obstacles. Compared to other secretion systems Type I secretion is completely independent of the *sec* machinery, therefore does not impede with essential host processes like the integration of membrane proteins and it is composed of as little as three components needed for successful secretion in sharp contrast to the also *sec* independent Type III (Cornelis, 2006) or Type IV secretion systems (Cascales & Christie, 2003). Exploiting the Type I secretion system for heterologous secretion was up to now always a rather empirical method where different targets were chosen for their secretion ability (Blight et al, 1994; Blight & Holland, 1994; Chervaux et al, 1995; Fernandez et al, 2000; Fraile et al, 2004; Gentschev et al, 2002; Gentschev et al, 2000; Gentschev et al, 1996). The uncertainty, if a protein is secreted or not will sooner or later cause that other systems engineered to release proteins into the media will soon outpace the usage of the Type I secretion system. Other promising systems are Type V secretion (Henderson et al, 2004) where proteins upon display on the outer membrane can be cleaved off by OmpT (Maurer et al, 1997) or certainly protein secretion in Gram-positive bacteria like *Bacillus subtilis* and its Gram-positive relatives (Harwood & Cranenburgh, 2008).

One aim of this work was to create a simple vector pair encoding on one plasmid the inner membrane components and on the other plasmid a fragment of *hlyA* which could be fused by routine cloning methods to any ORF. For the expression of the inner membrane component the low-copy, kanamycin conferring vector pK184 with a p15A replicon was chosen, which is compatible to common expression plasmids and is not harming the cells due to high overexpression of the membrane proteins (Jobling & Holmes, 1990). To increase the potential number of inserts, LIC as method to avoid usage of restriction enzymes was used (Doyle, 2005). Therefore a DNA cassette coding for the LIC sequences was introduced into pBADHisB. Herein several ORFs could be cloned. The vector pair was successfully tested and HlyACterm could be successfully purified with a yield of around 100 mg/liter culture. The next step and the next aim was to challenge the transport machinery with several fusion proteins with biomedical and biotechnical impact (MalE, Interferon α 2, Interferon β , Interferon receptor fragments, lipases). These were successfully cloned by LIC. Several of those genes contained cysteines and possessed a high pI, both features rather untypical for Type I substrates (Delepelaire, 2004). Also some highly expressed proteins such as MalE were chosen.

All of them were successfully overexpressed under the control of the arabinose promoter, nevertheless none of them secreted to a significant amount. Reasoning that fast aggregation or folding impedes with the transport process, MalE-HlyA mutants with changed folding behaviour were designed.

3.2 Engineered fusion proteins which are able to secrete

The main question is how to overcome the lack of secretion competence of the fusion proteins. Several attempts can be envisioned to increase secretion efficiency. (I) By introducing mutations randomly the secretion apparatus can be redesigned. This has been done for the Hly system, however secretion capacity did not increase significantly and the resulting mutants exhibited predominantly a higher secretion at lower temperatures and not at standard growth conditions (Sugamata & Shiba, 2005). (II) The secretion signal can be altered to increase efficiencies. The exchange and modification has been done with success for the general secretion system of *E. coli* (Suciu & Inouye, 1996; Tanji et al, 1991). In these cases mutations or exchange of the secretion signal significantly increased the amount of the secreted protein. The versatility of Type I systems is illustrated by the remarkable collection of signal sequence variants that can be transported. However, choosing the best secretion signal for a certain Type I secretion system is much more complicated. In general every Type I system has only one substrate specifically secreted by a certain secretion signal. Some secretion signals can be interchanged (Akatsuka et al, 1997; Omori & Idei, 2003) mainly in between the single subgroups of the Type I systems (Jenewein et al, 2008), but an increase of secretion efficiency was not reported by this approach and it still remains a trial and error procedure without any rational. Ling and coworkers used a combinatorial approach for HlyA secretion to dissect the secretion signal, but the wildtype HlyA was the most efficiently secreted protein among some other mutants (Hui & Ling, 2002; Hui et al, 2000). Nevertheless, the bottleneck for secretion in these studies could also be the total expression of the toxin. A directed approach is almost impossible since it is not fully understood which features need to be incorporated in the secretion signal. (III) A comprehensive approach using metabolic engineering revealed that “slowly translated” HlyA molecules are more efficiently secreted as it was tested on haemolysis agar plates (Sugamata & Shiba, 2005). However an increase by the factor of 4 would not change the situation for heterologous fusion proteins significantly. (IV) The final possibility is to change the substrate, the chosen protein, itself.

What do the natural substrates possess and how can we modify potential targets so that they have similar secretion abilities like the natural substrates?

To answer this question, mutations in the MalE-HlyA fusion were designed. MalE itself also has no cysteines and a weak acidic pI. Therefore it is rather surprising just by looking at the physicochemical parameters that it is not secreted by fusion to C-terminus of HlyA. We consequently focussed on other features common to Type I substrates to answer the question why Type I substrates are so efficiently secreted. An important feature of most proteins is the presence of glycine repeats. These repeats enable the protein upon Ca^{2+} binding to adopt a functional fold. In the absence of Ca^{2+} , Type I substrates are not or only partially active i.e. folded. This is a remarkable difference to other secreted proteins which fold autonomously but are not substrates of the Type I secretion system.

The working hypothesis after the unsuccessful secretion trials therefore was clear: A stable folding withdraws the substrates from the secretion machinery. Support for this hypothesis came from experiments performed with *E. coli* dihydrofolate reductase (DHFR). The wild type fusion was also not secreted if fused to a HlyA fragment. Only C-terminal modification enabled transport of an active mutant protein (Nakano et al, 1992). The authors claim that a stable fold is not achieved if the C-terminus is modified. Studies published after this report revealed that the C-terminus is heavily involved in the folding mechanism of DHFR (Arai & Iwakura, 2005). Further support is derived from the rather atypical Type I substrate HasA from *S. marcescens*. If the HasA secretion machinery is reconstituted in *E. coli* the SecB protein is essential for HasA secretion as it slows down folding of HasA by the factor of 3200 shifts the relaxation time from 0.02 s to 77 s (Wolff et al, 2003). Strikingly mutants folding much slower do secrete independently of SecB. Thus folding kinetics dictates the secretion ability. HasA is unluckily an unsuitable model for a Type I substrate, since it does not contain any glycine repeats. This knowledge for homologous secretion was also never adapted to fusion proteins.

We therefore choose the well characterized MalE protein as example. *In vivo* MalE is translated as a preprotein, possessing an N-terminal secretion signal. After having left the ribosome the nascent polypeptide binds quickly to the SecB chaperone, which holds the preprotein in an unfolded conformation (Hardy & Randall, 1991; Weiss et al, 1988). The leader peptide retards folding enabling efficient SecB binding; MalE devoid of the leader will bind to SecB but is rapidly released due to the faster folding rate (Liu et al, 1989). SecB does not specifically bind the leader peptide but rather unspecific to the MalE core without any

secondary structure present in MalE (Bechtluft et al, 2007; Collier et al, 1988; Randall et al, 1990). This protein complex can engage SecA as its membrane receptor (Hartl et al, 1990). SecA is activated and threads the polypeptide through the SecYEG translocon, empowered by the hydrolysis of ATP and the proton gradient, across the membrane (de Keyzer et al, 2003; Driessen & Nouwen, 2008; Schiebel et al, 1991). Upon reaching the periplasm the signal sequence of MalE is removed by the leader peptidase, MalE finally folds and can finally act as maltose binding protein.

Mutations in the MalE core are additive to the effect of the signal peptide and can compensate the effect of a mutated signal peptide (Chun et al, 1993; Collier & Bassford, 1989). These MalE mutants slow down folding (V8G, A276G and Y283D), but are still able to bind maltose *in vivo* (Collier & Bassford, 1989). The mutations relevant for folding are all localized in domain I underlining the importance of this domain for folding (Figure D4).

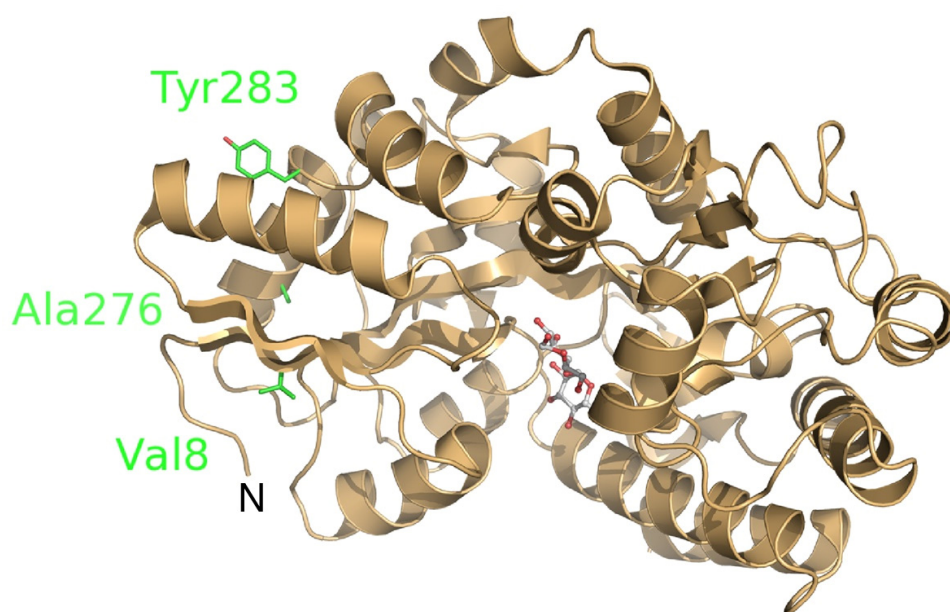


Figure D4: Structure of the MalE protein with bound maltose as substrate in the central cleft of the substrate binding protein (pdb code 3MBP). The positions of the amino acid mutations are highlighted in sticks. N: the amino terminus of the protein.

The amino acid exchange Y283D in the fusion protein MalE-HlyA enabled successful secretion to around 10 percent of the amount observed for HlyACterm. However for the mutant MalE-V276G-HlyA only marginal secretion was observed, despite the fact that this mutant refolds in presence of SecB with relaxation time of 750 s. This is ten times slower

than HasA in the presence of SecB (77 s, Wolff et al, 2003). Rationalising that HasA is a protein of only 188 amino acids, and it is likely that upon recruitment to the HasA transport system folding can no longer occur, whereas in case of a HlyA-MalE fusions the HlyA moiety is independently recruited to the inner membrane system and the MalE protein can further fold even if HlyA is recruited. Further speculating using the data that the folding of MalE is accelerated if HlyA is absent it is imaginable that the folding of the MalE core accelerates if HlyA is recruited to the transporter or even already integrated into the transport system. A clear answer for this discrepancy will certainly come from N-terminally truncated HlyA proteins fused to MalE. In this case the MalE-A276G-HlyA might more often lose the race between folding and translocation.

Since SecB is essential for the efficient transport of MalE by the *sec* system, one can argue that the experiments shown here are easily explained by the idea that SecB is elusively binding the MalE-Y283D-HlyA mutant rendering it transport competent, whereas the other mutants are not bound by SecB. SecB binds also to the species of the fusion proteins, which are not secreted, but is not blocking rather retarding this process. It is important to stress that all experiments were performed at physiological growth temperature of 30°C, in sharp contrast to reports where this blockage was reported where always at lower temperatures (5 °C/10°C/25°C; Hardy & Randall, 1991; Liu et al, 1989). Retardation rather than blockage of folding might also not be the function, since blocking folding would have tremendous effect on other proteins being detrimental to the cell (Ullers et al, 2004). We therefore argue with folding rates: The preMalE protein itself folds under the same conditions used in this work with a relaxation of 28 s. Comparing this value with the relaxation times measured for MalE-V8G-HlyA and MalE-A276G-HlyA (78 s and 240 s) SecB should certainly be able to handle these proteins, so that they would be efficiently secreted by *sec* system (just by looking at the folding rate and certainly not at the missing secretion signal) however these proteins are still not secreted by the Hly system. The binding of SecB to the fusion proteins with retardation of the folding rate is certainly not sufficient.

Using this data obtained for MalE mutants fused to a fragment of HlyA, we therefore suggest a kinetic partitioning model for Type I substrates: Unless the substrates are in an unfolded form, the substrates cannot pass the membrane although they might be recruited to the membrane complex. However, compared to the *sec* system the kinetic window for Type I substrates is largely shifted to slow folding, explaining that Type I substrates do not fold in the cell, rather folding is usually induced by addition of Ca²⁺.

One can also argue that the secreted fusion protein MalE-Y283D-HlyA is less stable and can be unfolded by the Hly system, but this event is unlikely since the unfolding kinetics measured in this work, directly correlated with the unfolding energy, is similar for all fusion proteins.

How can these data explain the data already obtained for other fusion proteins? Several other fusion proteins have been tested, so far mostly using the Hly system (Blight et al, 1994). It is important to stress that in some reports no secretion was observed initially while secretion was enabled by slight modification of the C-terminus (Kenny et al, 1991; Nakano et al, 1992). At least in case of the DHFR fusion to a HlyA fragment it is now clear that these truncations affect the folding kinetics (Arai & Iwakura, 2005).

Lorenzo and coworkers reported that the Hly system mediated secretion of immunoglobulin folds (Fernandez & de Lorenzo, 2001; Fernandez et al, 2000; Fraile et al, 2004). Secretion of antibody fragments by a Type I system would tremendously increase interest of this system. Looking at the folding behaviour of immunoglobulin folds, the above-proposed kinetic partitioning model for Type I substrate can explain this case. Immunoglobulin folds like for example IgG1 have been reported to fold very slowly (*in vitro* in the order of 50-500 s) (Isenman et al, 1979; Rowe, 1976). Therefore a fusion to the HlyA secretion signal could well mediate transport by a Type I system. The secretion of antibody fragments also answers the questions if cysteine-containing proteins can be transported with the Hly system. Still it remains questionable why RTX substrates usually contain no cysteines if the formation of disulphides after secretion is possible (Fernandez et al, 2000; Li et al, 2002). Disulphide bridges would increase the protein stability in the extracellular space. It can be speculated that free cysteines might bind metal ions in the cytosol, which can interfere with the secretion process. Another explanation might be that the channel of TolC is large enough so that adjacent cysteines can cross-bridge during transport and this might plug the machinery. Introduction of cysteines into the secreted MalE mutant will certainly help to answer this question.

3.3 A model for the “perfect” Type I substrate

Upon translation of the protein by the ribosome (Figure D5, I) the protein encounters several fates: The protein folds rather slow and it can be directly recruited to the transport machinery

(II). Alternatively the protein can rapidly fold into its native structure (III), therefore a secretion competent state is lost and the protein remains in the cytosol. It will bind to chaperones like SecB, acting as holdase, impeding with quick folding (II and III). The slower the folding rate, the more likely is the recruitment to the Type I system. On the other hand, if the microenvironment (pH, local concentration, missing contact partners such as chaperones) or required processing does not allow proper folding inclusion bodies will finally form (IV). Protein aggregates represent most likely a mirror image of the folding intermediate kinetically trapped and precipitated due to the exposure of hydrophobic patches (Georgiou et al, 1994; Przybycien et al, 1994). These inclusion bodies are not available for cellular processes like secretion; therefore only proteins with slow folding rates can tackle the Type I system. However, inclusion body formation will not compete with routes II and III. It will rather privilege route II since soluble proteins might impede with Type I secretion (Debarbieux & Wandersman, 2001).

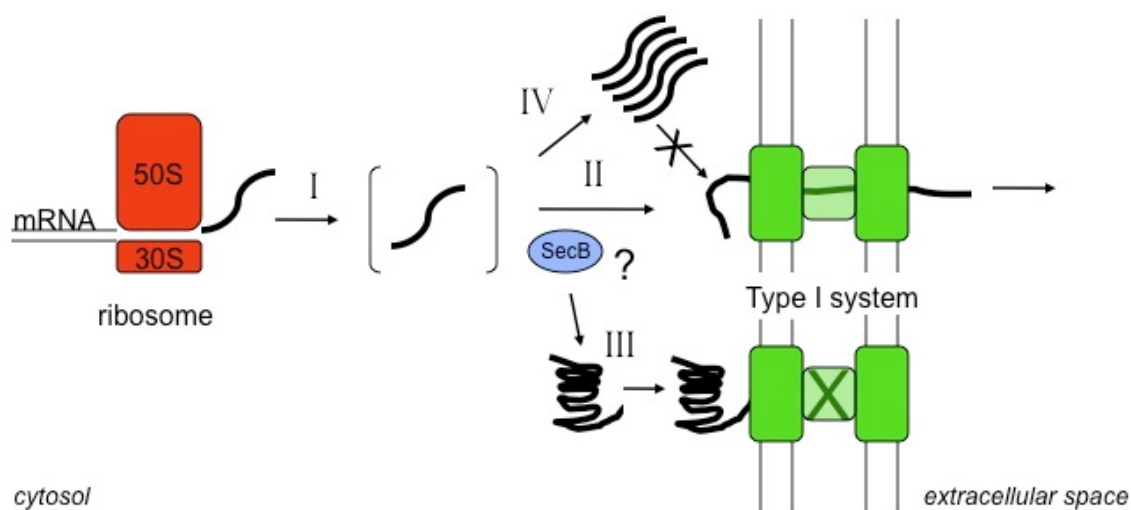


Figure D5: Proposed model for Type I secretion. The ribosome is depicted in red. The Type I secretion machinery is depicted in green. The chaperone SecB is shown in blue. Inner and outer membranes are shown as lines. I – IV used as pin-points explained in the text.

What substrates might be suited to explore the secretion space for Type I system. A good starting point will be small substrates such as the muscle acylphosphatase (AcP). The 27 mutants of the strictly two state folding AcP have been extensively characterized in terms of folding kinetics and folding energetics (Chiti et al, 1999). Another interesting substrate to test is the thiol-disulfide exchange protein thioredoxin which folds with a very slow relaxation time of 300-800 s *in vitro* due to proline isomerisation (Kelley & Richards, 1987). The

exchange of proline 76 to alanine increases the folding kinetics by more than a factor of 10. It will be interesting to see if these two species of the disulphide forming protein will be secreted by the Hly system. Additionally it might be interesting if proline insertions acting as molecular timer allow deceleration of folding and efficient secretion. A random insertion is possible using LIC and autoinducing media enabling high-throughput screening of randomly inserted prolines.

Any predictions how proteins can reside unfolded in the cytosol, without disturbing any host function, but become folded after secretion, comparable to the classic RTX proteins, is still far from possible. Nevertheless also non-RTX toxins possess a folding switch (Yao et al, 2006). Concerning this it will be interesting to see how the cell deals with all the unfolded peptides. Are they degraded? From what direction does this occur? Does chaperone overexpression help keeping substrates accessible for Type I secretion?

This is the first time, that a heterologous fusion protein was engineered to for secretion by a Type I system. With some patience and diligence, open questions can now be easily answered.

4. Outlook

Reaction mechanisms are always an extreme view of the reality. SAC as hydrolysis mechanism might apply for the Hly system, but for other ABC systems an additional modulation might happen, so that the hydrolysis event is not anymore the rate-limiting step. This however has not been shown and awaits further experiments. Intriguingly, the hydrolysis event has to be coupled to the transport process. How the transmission of the energy derived by the hydrolysis occurs within the NBD and further on towards the TMDs is still not clear.

The full-length ABC transporter HlyB is active in detergent upon addition of the substrate. Reconstitution back into lipids is the next logical step. Is the induction of the hydrolysis changed if the soluble HlyD fragment is added to the proteoliposomes? Or can HlyD reconstituted with HlyB forming a functional complex? Certainly help for characterisation of the Type I secretion would a TolC independent transport system, reminiscent of the MalE independent maltose permease. The selection of random mutants of HlyB/D, able to secrete an essential protein (like β -lactamase) into the periplasm, might be a possible experimental set-up. However, awesome progress had been made in membrane protein biochemistry, modern tools like membrane-scaffold proteins enable studying even complex two-membrane systems in a native-like but soluble environment.

The knowledge that constrains a Type I substrate will definitely allow the specific design of Type I substrates. Starting with N-terminal truncations of HlyAC_{term} might increase the efficiency of available fusion partners. Other fusions using proteins excessively studied in folding behaviour will proof and enlarge the presented concept. This is not only of interest for secretion in terms of biomedical and biotechnical applications but also selective reporters can be designed addressing for example the directionality of transport.

References

- Abrahams JP, Leslie AG, Lutter R, Walker JE (1994) Structure at 2.8 Å resolution of F₁-ATPase from bovine heart mitochondria. *Nature* **370**(6491): 621-628
- Abramson J, Iwata S, Kaback HR (2004) Lactose permease as a paradigm for membrane transport proteins. *Mol Membr Biol* **21**(4): 227-236
- Ahmadian MR, Stege P, Scheffzek K, Wittinghofer A (1997) Confirmation of the arginine-finger hypothesis for the GAP-stimulated GTP-hydrolysis reaction of Ras. *Nat Struct Biol* **4**(9): 686-689
- Akama H, Matsuura T, Kashiwagi S, Yoneyama H, Narita S, Tsukihara T, Nakagawa A, Nakae T (2004) Crystal structure of the membrane fusion protein, MexA, of the multidrug transporter in *Pseudomonas aeruginosa*. *J Biol Chem* **279**(25): 25939-25942
- Akatsuka H, Binet R, Kawai E, Wandersman C, Omori K (1997) Lipase secretion by bacterial hybrid ATP-binding cassette exporters: molecular recognition of the LipBCD, PrtDEF, and HasDEF exporters. *J Bacteriol* **179**(15): 4754-4760
- Akitake B, Anishkin A, Liu N, Sukharev S (2007) Straightening and sequential buckling of the pore-lining helices define the gating cycle of MscS. *Nat Struct Mol Biol* **14**(12): 1141-1149
- Al-Shawi MK, Parsonage D, Senior AE (1990) Adenosine triphosphatase and nucleotide binding activity of isolated beta-subunit preparations from *Escherichia coli* F₁F₀-ATP synthase. *J Biol Chem* **265**(10): 5595-5601
- Alder NN, Theg SM (2003) Energetics of protein transport across biological membranes. a study of the thylakoid DeltapH-dependent/cpTat pathway. *Cell* **112**(2): 231-242
- Aleksandrov L, Aleksandrov AA, Chang XB, Riordan JR (2002) The First Nucleotide Binding Domain of Cystic Fibrosis Transmembrane Conductance Regulator Is a Site of Stable Nucleotide Interaction, whereas the Second Is a Site of Rapid Turnover. *J Biol Chem* **277**(18): 15419-15425
- Amano T, Tozawa K, Yoshida M, Murakami H (1994) Spatial precision of a catalytic carboxylate of F₁-ATPase beta subunit probed by introducing different carboxylate-containing side chains. *FEBS Lett* **348**(1): 93-98
- Ambudkar SV, Kim IW, Xia D, Sauna ZE (2006) The A-loop, a novel conserved aromatic acid subdomain upstream of the Walker A motif in ABC transporters, is critical for ATP binding. *FEBS Lett* **580**(4): 1049-1055
- Andersen C, Koronakis E, Bokma E, Eswaran J, Humphreys D, Hughes C, Koronakis V (2002) Transition to the open state of the TolC periplasmic tunnel entrance. *Proc Natl Acad Sci U S A* **99**(17): 11103-11108
- Arai M, Iwakura M (2005) Probing the interactions between the folding elements early in the folding of *Escherichia coli* dihydrofolate reductase by systematic sequence perturbation analysis. *J Mol Biol* **347**(2): 337-353
- Arechaga I, Miroux B, Karrasch S, Huijbregts R, de Kruijff B, Runswick MJ, Walker JE (2000) Characterisation of new intracellular membranes in *Escherichia coli* accompanying large scale over-production of the b subunit of F(1)F(o) ATP synthase. *FEBS Lett* **482**(3): 215-219
- Aslanidis C, de Jong PJ (1990) Ligation-independent cloning of PCR products (LIC-PCR). *Nucleic Acids Res* **18**(20): 6069-6074

- Balakrishnan L, Hughes C, Koronakis V (2001) Substrate-triggered recruitment of the TolC channel-tunnel during type I export of hemolysin by *Escherichia coli*. *J Mol Biol* **313**(3): 501-510
- Basolo F, Pearson RG (1967) *Mechanisms of inorganic reactions; a study of metal complexes in solution*, 2d edn. New York,: Wiley.
- Bass RB, Strop P, Barclay M, Rees DC (2002) Crystal structure of *Escherichia coli* MscS, a voltage-modulated and mechanosensitive channel. *Science* **298**(5598): 1582-1587
- Baumann U, Wu S, Flaherty KM, McKay DB (1993) Three-dimensional structure of the alkaline protease of *Pseudomonas aeruginosa*: a two-domain protein with a calcium binding parallel beta roll motif. *Embo J* **12**(9): 3357-3364
- Bavro VN, Pietras Z, Furnham N, Perez-Cano L, Fernandez-Recio J, Pei XY, Misra R, Luisi B (2008) Assembly and channel opening in a bacterial drug efflux machine. *Mol Cell* **30**(1): 114-121
- Baneyx F, Mujacic M (2004) Recombinant protein folding and misfolding in *Escherichia coli*. *Nat Biotechnol* **22**(11): 1399-1408
- Baykov AA, Evtushenko OA, Avaeva SM (1988) A malachite green procedure for orthophosphate determination and its use in alkaline phosphatase-based enzyme immunoassay. *Anal Biochem* **171**(2): 266-270
- Bechtluft P, van Leeuwen RG, Tyreman M, Tomkiewicz D, Nouwen N, Tepper HL, Driessen AJ, Tans SJ (2007) Direct observation of chaperone-induced changes in a protein folding pathway. *Science* **318**(5855): 1458-1461
- Benabdelhak H, Kiontke S, Horn C, Ernst R, Blight MA, Holland IB, Schmitt L (2003) A specific interaction between the NBD of the ABC-transporter HlyB and a C-terminal fragment of its transport substrate haemolysin A. *J Mol Biol* **327**(5): 1169-1179
- Benabdelhak H, Schmitt L, Horn C, Jumel K, Blight MA, Holland IB (2005) Positive co-operative activity and dimerization of the isolated ABC ATPase domain of HlyB from *Escherichia coli*. *Biochem J* **386**(Pt 3): 489-495
- Bhakdi S, Trantum-Jensen J (1991) Alpha-toxin of *Staphylococcus aureus*. *Microbiol Rev* **55**(4): 733-751
- Bilwes AM, Quezada CM, Croal LR, Crane BR, Simon MI (2001) Nucleotide binding by the histidine kinase CheA. *Nat Struct Biol* **8**(4): 353-360
- Bishop L, Agbayani R, Jr., Ambudkar SV, Maloney PC, Ames GF (1989) Reconstitution of a bacterial periplasmic permease in proteoliposomes and demonstration of ATP hydrolysis concomitant with transport. *Proc Natl Acad Sci U S A* **86**(18): 6953-6957
- Blank K, Morfill J, Gump H, Gaub HE (2006) Functional expression of *Candida antarctica* lipase B in *Escherichia coli*. *J Biotechnol* **125**(4): 474-483
- Blight MA, Chervaux C, Holland IB (1994) Protein secretion pathway in *Escherichia coli*. *Curr Opin Biotechnol* **5**(5): 468-474
- Blight MA, Holland IB (1994) Heterologous protein secretion and the versatile *Escherichia coli* haemolysin translocator. *TIBTECH* **12**: 450-455
- Bloemendal M, Johnson WC, Jr. (1995) Structural information on proteins from circular dichroism spectroscopy possibilities and limitations. *Pharm Biotechnol* **7**: 65-100
- Bolhuis H, van Veen HW, Molenaar D, Poolman B, Driessen AJ, Konings WN (1996) Multidrug resistance in *Lactococcus lactis*: evidence for ATP-dependent drug extrusion from the inner leaflet of the cytoplasmic membrane. *Embo J* **15**(16): 4239-4245
- Bowie JU (2001) Stabilizing membrane proteins. *Curr Opin Struct Biol* **11**(4): 397-402

- Bowler MW, Montgomery MG, Leslie AG, Walker JE (2006) How azide inhibits ATP hydrolysis by the F-ATPases. *Proc Natl Acad Sci U S A* **103**(23): 8646-8649
- Boyer PD (1997) The ATP synthase--a splendid molecular machine. *Annu Rev Biochem* **66**: 717-749
- Bradford MM (1976) A rapid and sensitive method for the quantitation of microgram quantities of protein utilizing the principle of protein-dye binding. *Anal Biochem* **72**: 248-254
- Brooks HJ, O'Grady F, McSherry MA, Cattell WR (1980) Uropathogenic properties of Escherichia coli in recurrent urinary-tract infection. *J Med Microbiol* **13**(1): 57-68
- Busso D, Stierle M, Thierry JC, Moras D (2008) A comparison of inoculation methods to simplify recombinant protein expression screening in Escherichia coli. *Biotechniques* **44**(1): 101-106
- Casadaban MJ, Cohen SN (1980) Analysis of gene control signals by DNA fusion and cloning in Escherichia coli. *J Mol Biol* **138**(2): 179-207
- Carlier MF (1991) Nucleotide hydrolysis in cytoskeletal assembly. *Curr Opin Cell Biol* **3**(1): 12-17
- Cascales E, Christie PJ (2003) The versatile bacterial type IV secretion systems. *Nat Rev Microbiol* **1**(2): 137-149
- Chen J, Lu G, Lin J, Davidson AL, Quijcho FA (2003a) A tweezers-like motion of the ATP-binding cassette dimer in an ABC transport cycle. *Mol Cell* **12**(3): 651-661
- Chen J, Sharma S, Quijcho FA, Davidson AL (2001) Trapping the transition state of an ATP-binding cassette transporter: evidence for a concerted mechanism of maltose transport. *Proc Natl Acad Sci U S A* **98**(4): 1525-1530
- Chen M, Abele R, Tampe R (2003b) Peptides induce ATP hydrolysis at both subunits of the transporter associated with antigen processing. *J Biol Chem* **278**(32): 29686-29692
- Chervaux C, Holland IB (1996) Random and directed mutagenesis to elucidate the functional importance of helix II and F-989 in the C-terminal secretion signal of Escherichia coli hemolysin. *J Bacteriol* **178**(4): 1232-1236
- Chervaux C, Sauvonnnet N, Le Clainche A, Kenny B, Hung AL, Broome-Smith JK, Holland IB (1995) Secretion of active beta-lactamase to the medium mediated by the Escherichia coli haemolysin transport pathway. *Mol Gen Genet* **249**(2): 237-245
- Chiti F, Taddei N, White PM, Bucciantini M, Magherini F, Stefani M, Dobson CM (1999) Mutational analysis of acylphosphatase suggests the importance of topology and contact order in protein folding. *Nat Struct Biol* **6**(11): 1005-1009
- Chun SY, Strobel S, Bassford P, Jr., Randall LL (1993) Folding of maltose-binding protein. Evidence for the identity of the rate-determining step in vivo and in vitro. *J Biol Chem* **268**(28): 20855-20862
- Cole PA, Burn P, Takacs B, Walsh CT (1994) Evaluation of the catalytic mechanism of recombinant human Csk (C-terminal Src kinase) using nucleotide analogs and viscosity effects. *J Biol Chem* **269**(49): 30880-30887
- Collier DN, Bankaitis VA, Weiss JB, Bassford PJ, Jr. (1988) The antifolding activity of SecB promotes the export of the E. coli maltose-binding protein. *Cell* **53**(2): 273-283
- Collier DN, Bassford PJ, Jr. (1989) Mutations that improve export of maltose-binding protein in SecB- cells of Escherichia coli. *J Bacteriol* **171**(9): 4640-4647
- Cook KH, Schmid FX, Baldwin RL (1979) Role of proline isomerization in folding of ribonuclease A at low temperatures. *Proc Natl Acad Sci U S A* **76**(12): 6157-6161
- Cornelis GR (2006) The type III secretion injectisome. *Nat Rev Microbiol* **4**(11): 811-825

- Cross MA, Koronakis V, Stanley PL, Hughes C (1990) HlyB-dependent secretion of hemolysin by uropathogenic *Escherichia coli* requires conserved sequences flanking the chromosomal hly determinant. *J Bacteriol* **172**(3): 1217-1224
- Daley DO, Rapp M, Granseth E, Melen K, Drew D, von Heijne G (2005) Global topology analysis of the *Escherichia coli* inner membrane proteome. *Science* **308**(5726): 1321-1323
- Dall'Acqua W, Carter P (2000) Substrate-assisted catalysis: molecular basis and biological significance. *Protein Sci* **9**(1): 1-9
- Davidson AL, Laghaeian SS, Mannering DE (1996) The maltose transport system of *Escherichia coli* displays positive cooperativity in ATP hydrolysis. *J Biol Chem* **271**(9): 4858-4863
- Davidson AL, Sharma S (1997) Mutation of a single MalK subunit severely impairs maltose transport activity in *Escherichia coli*. *J Bacteriol* **179**(17): 5458-5464
- Davidson AL, Shuman HA, Hikaido H (1992) Mechanism of maltose transport in *E.coli*. Transmembrane signaling by periplasmic binding proteins. *Proc Natl Acad Sci U S A* **89**: 2360-2364
- Davidson AL, Dassa E, Orelle C, Chen J (2008) Structure, function, and evolution of bacterial ATP-binding cassette systems. *Microbiol Mol Biol Rev* **72**(2): 317-364
- Dawson RJ, Locher KP (2006) Structure of a bacterial multidrug ABC transporter. *Nature* **443**(7108): 180-185
- Dawson RJ, Locher KP (2007) Structure of the multidrug ABC transporter Sav1866 from *Staphylococcus aureus* in complex with AMP-PNP. *FEBS Lett* **581**(5): 935-938
- de Keyzer J, van der Does C, Driessen AJ (2003) The bacterial translocase: a dynamic protein channel complex. *Cell Mol Life Sci* **60**(10): 2034-2052
- Dean M, Rzhetsky A, Allikmets R (2001) The human ATP-binding cassette (ABC) transporter superfamily. *Genome Res* **11**(7): 1156-1166
- Debarbieux L, Wandersman C (2001) Folded HasA inhibits its own secretion through its ABC exporter. *Embo J* **20**(17): 4657-4663
- Dekker N, Cox RC, Kramer RA, Egmond MR (2001) Substrate specificity of the integral membrane protease OmpT determined by spatially addressed peptide libraries. *Biochemistry* **40**(6): 1694-1701
- Delepelaire P (1994) PrtD, the integral membrane ATP-binding cassette component of the *Erwinia chrysanthemi* metalloprotease secretion system, exhibits a secretion signal-regulated ATPase activity. *J Biol Chem* **269**(45): 27952-27957
- Delepelaire P (2004) Type I secretion in gram-negative bacteria. *Biochim Biophys Acta* **1694**(1-3): 149-161
- Delepelaire P, Wandersman C (1990) Protein secretion in gram-negative bacteria. The extracellular metalloprotease B from *Erwinia chrysanthemi* contains a C-terminal secretion signal analogous to that of *Escherichia coli* alpha-hemolysin. *J Biol Chem* **265**(28): 17118-17125
- Derynck R, Remaut E, Saman E, Stanssens P, De Clercq E, Content J, Fiers W (1980) Expression of human fibroblast interferon gene in *Escherichia coli*. *Nature* **287**(5779): 193-197
- Desvaux M, Parham NJ, Scott-Tucker A, Henderson IR (2004) The general secretory pathway: a general misnomer? *Trends Microbiol* **12**(7): 306-309
- Dinh T, Paulsen IT, Saier MH, Jr. (1994) A family of extracytoplasmic proteins that allow transport of large molecules across the outer membranes of gram-negative bacteria. *J Bacteriol* **176**(13): 3825-3831
- Doerrler WT, Raetz CR (2002) ATPase activity of the MsbA lipid flippase of *Escherichia coli*. *J Biol Chem* **277**(39): 36697-36705

- Dorgan LJ, Schuster SM (1981) The effect of nitration and D₂O on the kinetics of beef heart mitochondrial adenosine triphosphatase. *J Biol Chem* **256**(8): 3910-3916
- Doyle SA (2005) High-throughput cloning for proteomics research. *Methods Mol Biol* **310**: 107-113
- Drew D, Lerch M, Kunji E, Slotboom DJ, de Gier JW (2006) Optimization of membrane protein overexpression and purification using GFP fusions. *Nat Methods* **3**(4): 303-313
- Driessen AJ (2001) SecB, a molecular chaperone with two faces. *Trends Microbiol* **9**(5): 193-196
- Driessen AJ, Nouwen N (2008) Protein translocation across the bacterial cytoplasmic membrane. *Annu Rev Biochem* **77**: 643-667
- Dumon-Seignovert L, Cariot G, Vuillard L (2004) The toxicity of recombinant proteins in *Escherichia coli*: a comparison of overexpression in BL21(DE3), C41(DE3), and C43(DE3). *Protein Expr Purif* **37**(1): 203-206
- Durfee T, Nelson R, Baldwin S, Plunkett G, 3rd, Burland V, Mau B, Petrosino JF, Qin X, Muzny DM, Ayele M, Gibbs RA, Csorgo B, Posfai G, Weinstock GM, Blattner FR (2008) The complete genome sequence of *Escherichia coli* DH10B: insights into the biology of a laboratory workhorse. *J Bacteriol* **190**(7): 2597-2606
- Ernst R, Koch J, Horn C, Tampe R, Schmitt L (2006) Engineering ATPase activity in the isolated ABC cassette of human TAP1. *J Biol Chem* **281**(37): 27471-27480
- Ernst R, Kueppers P, Klein CM, Schwarzmuller T, Kuchler K, Schmitt L (2008) A mutation of the H-loop selectively affects rhodamine transport by the yeast multidrug ABC transporter Pdr5. *Proc Natl Acad Sci U S A* **105**(13): 5069-5074
- Eswaran J, Hughes C, Koronakis V (2003) Locking TolC entrance helices to prevent protein translocation by the bacterial type I export apparatus. *J Mol Biol* **327**(2): 309-315
- Faller LD (1989) Competitive binding of ATP and the fluorescent substrate analogue 2',3'-O-(2,4,6-trinitrophenyl)cyclohexadienylidene adenosine 5'-triphosphate to the gastric H⁺,K⁺-ATPase: evidence for two classes of nucleotide sites. *Biochemistry* **28**(16): 6771-6778
- Fath MJ, Skvirsky RC, Kolter R (1991) Functional complementation between bacterial MDR-like export systems: colicin V, alpha-hemolysin, and *Erwinia* protease. *J Bacteriol* **173**(23): 7549-7556
- Felmlee T, Pellett S, Welch RA (1985) Nucleotide sequence of an *Escherichia coli* chromosomal hemolysin. *J Bacteriol* **163**(1): 94-105
- Fernandez LA, de Lorenzo V (2001) Formation of disulphide bonds during secretion of proteins through the periplasmic-independent type I pathway. *Mol Microbiol* **40**(2): 332-346
- Fernandez LA, Sola I, Enjuanes L, de Lorenzo V (2000) Specific secretion of active single-chain Fv antibodies into the supernatants of *Escherichia coli* cultures by use of the hemolysin system. *Appl Environ Microbiol* **66**(11): 5024-5029
- Fersht A (1999) *Structure and mechanism in protein science*, 2 edn. New York: W.H. Freeman.
- Fetsch EE, Davidson AL (2002) Vanadate-catalyzed photocleavage of the signature motif of an ATP-binding cassette (ABC) transporter. *Proc Natl Acad Sci U S A* **99**(15): 9685-9690
- Fraile S, Munoz A, de Lorenzo V, Fernandez LA (2004) Secretion of proteins with dimerization capacity by the haemolysin type I transport system of *Escherichia coli*. *Mol Microbiol* **53**(4): 1109-1121
- Futai M (1974) Orientation of membrane vesicles from *Escherichia coli* prepared by different procedures. *J Membr Biol* **15**(1): 15-28
- Gadsby DC, Vergani P, Csanady L (2006) The ABC protein turned chloride channel whose failure causes cystic fibrosis. *Nature* **440**(7083): 477-483

- Gao M, Cui HR, Loe DW, Grant CE, Almquist KC, Cole SP, Deeley RG (2000) Comparison of the functional characteristics of the nucleotide binding domains of multidrug resistance protein 1. *J Biol Chem* **275**(17): 13098-13108
- Geertsma ER, Groeneveld M, Slotboom DJ, Poolman B (2008) Quality control of overexpressed membrane proteins. *Proc Natl Acad Sci U S A* **105**(15): 5722-5727
- Geertsma ER, Poolman B (2007) High-throughput cloning and expression in recalcitrant bacteria. *Nat Methods* **4**(9): 705-707
- Gentschev I, Dietrich G, Goebel W (2002) The E. coli alpha-hemolysin secretion system and its use in vaccine development. *Trends Microbiol* **10**(1): 39-45
- Gentschev I, Dietrich G, Spreng S, Kolb-Maurer A, Daniels J, Hess J, Kaufmann SH, Goebel W (2000) Delivery of protein antigens and DNA by virulence-attenuated strains of Salmonella typhimurium and Listeria monocytogenes. *J Biotechnol* **83**(1-2): 19-26
- Gentschev I, Mollenkopf H, Sokolovic Z, Hess J, Kaufmann SH, Goebel W (1996) Development of antigen-delivery systems, based on the Escherichia coli hemolysin secretion pathway. *Gene* **179**(1): 133-140
- Georgiou G, Valax P, Ostermeier M, Horowitz PM (1994) Folding and aggregation of TEM beta-lactamase: analogies with the formation of inclusion bodies in Escherichia coli. *Protein Sci* **3**(11): 1953-1960
- Geourjon C, Orelle C, Steinfels E, Blanchet C, Deleage G, Di Pietro A, Jault JM (2001) A common mechanism for ATP hydrolysis in ABC transporter and helicase superfamilies. *Trends Biochem Sci* **26**(9): 539-544
- Gerber S, Comellas-Bigler M, Goetz BA, Locher KP (2008) Structural basis of trans-inhibition in a molybdate/tungstate ABC transporter. *Science* **321**(5886): 246-250
- Gherardini FC, Hobbs MM, Stamm LV, Bassford PJ, Jr. (1990) Complementation of an Escherichia coli proC mutation by a gene cloned from Treponema pallidum. *J Bacteriol* **172**(6): 2996-3002
- Goody RS, Frech M, Wittinghofer A (1991) Affinity of guanine nucleotide binding proteins for their ligands: facts and artefacts. *Trends Biochem Sci* **16**(9): 327-328
- Goody RS, Hofmann W, Mannherz GH (1977) The binding constant of ATP to myosin S1 fragment. *Eur J Biochem* **78**(2): 317-324
- Gorbulev S, Abele R, Tampe R (2001) Allosteric crosstalk between peptide-binding, transport, and ATP hydrolysis of the ABC transporter TAP. *Proc Natl Acad Sci U S A* **98**(7): 3732-3737
- Gray L, Mackman N, Nicaud JM, Holland IB (1986) The carboxy-terminal region of haemolysin 2001 is required for secretion of the toxin from Escherichia coli. *Mol Gen Genet* **205**(1): 127-133
- Guzman LM, Belin D, Carson MJ, Beckwith J (1995) Tight regulation, modulation, and high-level expression by vectors containing the arabinose PBAD promoter. *J Bacteriol* **177**(14): 4121-4130
- Hanahan D (1983) Studies on transformation of Escherichia coli with plasmids. *J Mol Biol* **166**(4): 557-580
- Hanekop N (2006) Strukturbiologische Charakterisierung des ABC-Transporters LmrA aus L. lactis und des Substratbindepoteins EhuB aus S. meliloti. . Institute of Biochemistry, Johann Wolfgang Goethe-Universität, Frankfurt
- Hanekop N, Zaitseva J, Jenewein S, Holland IB, Schmitt L (2006) Molecular insights into the mechanism of ATP-hydrolysis by the NBD of the ABC-transporter HlyB. *FEBS Lett* **580**(4): 1036-1041
- Hanke C, Hess J, Schumacher G, Goebel W (1992) Processing by OmpT of fusion proteins carrying the HlyA transport signal during secretion by the Escherichia coli hemolysin transport system. *Mol Gen Genet* **233**(1-2): 42-48

- Hardy SJ, Randall LL (1991) A kinetic partitioning model of selective binding of nonnative proteins by the bacterial chaperone SecB. *Science* **251**(4992): 439-443
- Hartl FU, Lecker S, Schiebel E, Hendrick JP, Wickner W (1990) The binding cascade of SecB to SecA to SecY/E mediates preprotein targeting to the *E. coli* plasma membrane. *Cell* **63**: 269-279
- Harwood CR, Cranenburgh R (2008) Bacillus protein secretion: an unfolding story. *Trends Microbiol* **16**(2): 73-79
- Henderson IR, Navarro-Garcia F, Desvaux M, Fernandez RC, Ala'Aldeen D (2004) Type V protein secretion pathway: the autotransporter story. *Microbiol Mol Biol Rev* **68**(4): 692-744
- Hengen PN (1995) Purification of His-tag fusion proteins from *Escherichia coli*. *TIBS* **20**: 285-286
- Hertzberg EL, Hinkle PC (1974) Oxidative phosphorylation and proton translocation in membrane vesicles prepared from *Escherichia coli*. *Biochem Biophys Res Commun* **58**(1): 178-184
- Heveker N, Bonnaffé D, Ullmann A (1994) Chemical fatty acylation confers hemolytic and toxic activities to adenylate cyclase protoxin of *Bordetella pertussis*. *J Biol Chem* **269**(52): 32844-32847
- Higgins CF, Linton KJ (2004) The ATP switch model for ABC transporters. *Nat Struct Mol Biol* **11**(10): 918-926
- Higgins MK, Bokma E, Koronakis E, Hughes C, Koronakis V (2004) Structure of the periplasmic component of a bacterial drug efflux pump. *Proc Natl Acad Sci U S A* **101**(27): 9994-9999
- Hille B (1992) *Ionic channels of excitable membranes*, 2nd edn. Sunderland, Mass.: Sinauer Associates.
- Hinsa SM, Espinosa-Urgel M, Ramos JL, O'Toole GA (2003) Transition from reversible to irreversible attachment during biofilm formation by *Pseudomonas fluorescens* WCS365 requires an ABC transporter and a large secreted protein. *Mol Microbiol* **49**(4): 905-918
- Hiratsuka T (2003) Fluorescent and colored trinitrophenylated analogs of ATP and GTP. *Eur J Biochem* **270**(17): 3479-3485
- Hofacker M, Gompf S, Zutz A, Presenti C, Haase W, van der Does C, Model K, Tampe R (2007) Structural and functional fingerprint of the mitochondrial ATP-binding cassette transporter Mdl1 from *Saccharomyces cerevisiae*. *J Biol Chem* **282**(6): 3951-3961
- Holland IB, Cole SP, Kuchler K, Higgins C (2003) *ABC Proteins from bacteria to men*, London: Academic Press.
- Hollenstein K, Dawson RJ, Locher KP (2007a) Structure and mechanism of ABC transporter proteins. *Curr Opin Struct Biol* **17**(4): 412-418
- Hollenstein K, Frei DC, Locher KP (2007b) Structure of an ABC transporter in complex with its binding protein. *Nature* **446**(7132): 213-216
- Horn C, Bremer E, Schmitt L (2003) Nucleotide dependent monomer/dimer equilibrium of OpuAA, the nucleotide-binding protein of the osmotically regulated ABC transporter OpuA from *Bacillus subtilis*. *J Mol Biol* **334**(3): 403-419
- Horn C, Jenewein S, Tschapek B, Bouschen W, Metzger S, Bremer E, Schmitt L (2008) Monitoring conformational changes during the catalytic cycle of OpuAA, the ATPase subunit of the ABC transporter OpuA from *Bacillus subtilis*. *Biochem J* **412**(2): 233-244
- Hui D, Ling V (2002) A combinatorial approach toward analyzing functional elements of the *Escherichia coli* hemolysin signal sequence. *Biochemistry* **41**(17): 5333-5339
- Hui D, Morden C, Zhang F, Ling V (2000) Combinatorial analysis of the structural requirements of the *Escherichia coli* hemolysin signal sequence. *J Biol Chem* **275**(4): 2713-2720

- Hung LW, Wang IX, Nikaido K, Liu PQ, Ames GF, Kim SH (1998) Crystal structure of the ATP-binding subunit of an ABC transporter. *Nature* **396**(6712): 703-707
- Hvorup RN, Goetz BA, Niederer M, Hollenstein K, Perozo E, Locher KP (2007) Asymmetry in the structure of the ABC transporter-binding protein complex BtuCD-BtuF. *Science* **317**(5843): 1387-1390
- Isenman DE, Lancet D, Pecht I (1979) Folding pathways of immunoglobulin domains. The folding kinetics of the Cgamma3 domain of human IgG1. *Biochemistry* **18**(15): 3327-3336
- Janas E, Hofacker M, Chen M, Gompf S, van der Does C, Tampe R (2003) The ATP hydrolysis cycle of the nucleotide-binding domain of the mitochondrial ATP-binding cassette transporter Mdl1p. *J Biol Chem* **278**(29): 26862-26869
- Jarchau T, Chakraborty T, Garcia F, Goebel W (1994) Selection for transport competence of C-terminal polypeptides derived from Escherichia coli hemolysin: the shortest peptide capable of autonomous HlyB/HlyD-dependent secretion comprises the C-terminal 62 amino acids of HlyA. *Mol Gen Genet* **245**(1): 53-60
- Jenewein S, Schmitt L, Holland IB (2008) Type I Secretion. In *Bacterial protein secretion*, Woolridge K (ed). Horizon Press
- Jobling MG, Holmes RK (1990) Construction of vectors with the p15a replicon, kanamycin resistance, inducible lacZ alpha and pUC18 or pUC19 multiple cloning sites. *Nucleic Acids Res* **18**(17): 5315-5316
- Johnson JM, Church GM (1999) Alignment and structure prediction of divergent protein families: periplasmic and outer membrane proteins of bacterial efflux pumps. *J Mol Biol* **287**(3): 695-715
- Jones HE, Holland IB, Baker HL, Campbell AK (1999) Slow changes in cytosolic free Ca²⁺ in Escherichia coli highlight two putative influx mechanisms in response to changes in extracellular calcium. *Cell Calcium* **25**(3): 265-274
- Junop MS, Obmolova G, Rausch K, Hsieh P, Yang W (2001) Composite active site of an ABC ATPase: MutS uses ATP to verify mismatch recognition and authorize DNA repair. *Mol Cell* **7**(1): 1-12
- Juranka P, Zwang F, Kulpa J, Endicott J, Blight M, Holland IB, Ling V (1992) Characterization of the hemolysin transporter, HlyB, using an epitope insertion. *J Biol Chem* **267**: 3764,3770
- Kadaba NS, Kaiser JT, Johnson E, Lee A, Rees DC (2008) The high-affinity E. coli methionine ABC transporter: structure and allosteric regulation. *Science* **321**(5886): 250-253
- Karpowich N, Martsinkevich O, Millen L, Yuan YR, Dai PL, MacVey K, Thomas PJ, Hunt JF (2001) Crystal structures of the MJ1267 ATP binding cassette reveal an induced-fit effect at the ATPase active site of an ABC transporter. *Structure* **9**(7): 571-586
- Kelley RF, Richards FM (1987) Replacement of proline-76 with alanine eliminates the slowest kinetic phase in thioredoxin folding. *Biochemistry* **26**(21): 6765-6774
- Kenny B, Haigh R, Holland IB (1991) Analysis of the haemolysin transport process through the secretion from Escherichia coli of PCM, CAT or beta-galactosidase fused to the Hly C-terminal signal domain. *Mol Microbiol* **5**(10): 2557-2568
- Kenny B, Taylor S, Holland IB (1992) Identification of individual amino acids required for secretion within the haemolysin (HlyA) C-terminal targeting region. *Mol Microbiol* **6**(11): 1477-1489
- Kiefer H (2003) In vitro folding of alpha-helical membrane proteins. *Biochim Biophys Acta* **1610**(1): 57-62
- Kim IW, Peng XH, Sauna ZE, FitzGerald PC, Xia D, Muller M, Nandigama K, Ambudkar SV (2006) The conserved tyrosine residues 401 and 1044 in ATP sites of human P-glycoprotein are critical for ATP binding and hydrolysis: evidence for a conserved subdomain, the A-loop in the ATP-binding cassette. *Biochemistry* **45**(24): 7605-7616

- Kispal G, Sipos K, Lange H, Fekete Z, Bedekovics T, Janaky T, Bassler J, Aguilar Netz DJ, Balk J, Rotte C, Lill R (2005) Biogenesis of cytosolic ribosomes requires the essential iron-sulphur protein Rli1p and mitochondria. *Embo J* **24**(3): 589-598
- Koebmann BJ, Westerhoff HV, Snoep JL, Nilsson D, Jensen PR (2002) The glycolytic flux in *Escherichia coli* is controlled by the demand for ATP. *J Bacteriol* **184**(14): 3909-3916
- Kojima Y, Kobayashi M, Shimizu S (2003) A novel lipase from *Pseudomonas fluorescens* HU380: gene cloning, overproduction, renaturation-activation, two-step purification, and characterization. *J Biosci Bioeng* **96**(3): 242-249
- Kolling R, Hollenberg CP (1996) The hemolysin B protein, expressed in *Saccharomyces cerevisiae*, accumulates in binding-protein (BiP)-containing structures. *Eur J Biochem* **239**(2): 356-361
- Koronakis V, Cross M, Hughes C (1989a) Transcription antitermination in an *Escherichia coli* haemolysin operon is directed progressively by cis-acting DNA sequences upstream of the promoter region. *Mol Microbiol* **3**(10): 1397-1404
- Koronakis V, Hughes C, Koronakis E (1993) Atpase activity and atp/adp-induced conformational change in the soluble domain of the bacterial protein translocator hlyB. *Mol Microbiol* **8**(N6): 1163-1175
- Koronakis V, Koronakis E, Hughes C (1989b) Isolation and analysis of the C-terminal signal directing export of *Escherichia coli* hemolysin protein across both bacterial membranes. *Embo J* **8**(2): 595-605
- Koronakis V, Li J, Koronakis E, Stauffer K (1997) Structure of TolC, the outer membrane component of the bacterial type I efflux system, derived from two-dimensional crystals. *Mol Microbiol* **23**(3): 617-626
- Koronakis V, Sharff A, Koronakis E, Luisi B, Hughes C (2000) Crystal structure of the bacterial membrane protein TolC central to multidrug efflux and protein export. *Nature* **405**(6789): 914-919
- Kuhn A (1995) Major coat proteins of bacteriophage Pf3 and M13 as model systems for Sec-independent protein transport. *FEMS Microbiol Rev* **17**(1-2): 185-190
- Kuipers OP, Beerthuyzen MM, Siezen RJ, De Vos WM (1993) Characterization of the nisin gene cluster nisABTCIPR of *Lactococcus lactis*. Requirement of expression of the nisA and nisI genes for development of immunity. *Eur J Biochem* **216**(1): 281-291
- Kuipers OP, de Ruyter PG, Kleerebezem M, de Vos WM (1997) Controlled overproduction of proteins by lactic acid bacteria. *Trends Biotechnol* **15**(4): 135-140
- Kunji ER, Chan KW, Slotboom DJ, Floyd S, O'Connor R, Monne M (2005) Eukaryotic membrane protein overproduction in *Lactococcus lactis*. *Curr Opin Biotechnol* **16**(5): 546-551
- Kunji ER, Slotboom DJ, Poolman B (2003) *Lactococcus lactis* as host for overproduction of functional membrane proteins. *Biochim Biophys Acta* **1610**(1): 97-108
- Lakowicz JR (1999) *Principles of Fluorescence Spectroscopy*, 2 edn. New York: Kluwer Academic/Pleum Publishers.
- Lally ET, Kieba IR, Sato A, Green CL, Rosenbloom J, Korostoff J, Wang JF, Shenker BJ, Ortlepp S, Robinson MK, Billings PC (1997) RTX toxins recognize a beta2 integrin on the surface of human target cells. *J Biol Chem* **272**(48): 30463-30469
- Lamken P, Gavutis M, Peters I, Van der Heyden J, Uze G, Piehler J (2005) Functional cartography of the ectodomain of the type I interferon receptor subunit ifnar1. *J Mol Biol* **350**(3): 476-488
- Lamken P, Lata S, Gavutis M, Piehler J (2004) Ligand-induced assembling of the type I interferon receptor on supported lipid bilayers. *J Mol Biol* **341**(1): 303-318
- Lammens A, Schele A, Hopfner KP (2004) Structural biochemistry of ATP-driven dimerization and DNA-stimulated activation of SMC ATPases. *Curr Biol* **14**(19): 1778-1782

- Lanyi JK (2004) Bacteriorhodopsin. *Annu Rev Physiol* **66**: 665-688
- Lee PA, Tullman-Ereck D, Georgiou G (2006) The bacterial twin-arginine translocation pathway. *Annu Rev Microbiol* **60**: 373-395
- Letoffe S, Delepelaire P, Wandersman C (1996) Protein secretion in gram-negative bacteria: assembly of the three components of ABC protein-mediated exporters is ordered and promoted by substrate binding. *Embo J* **15**(21): 5804-5811
- Letoffe S, Ghigo JM, Wandersman C (1994) Secretion of the *Serratia marcescens* HasA protein by an ABC transporter. *J Bacteriol* **176**(17): 5372-5377
- Lewinson O, Lee AT, Rees DC (2008) The funnel approach to the precrystallization production of membrane proteins. *J Mol Biol* **377**(1): 62-73
- Li C, Ramjeesingh M, Wang W, Garami E, Hewryk M, Lee D, Rommens JM, Galley K, Bear CE (1996) ATPase activity of the cystic fibrosis transmembrane conductance regulator. *J Biol Chem* **271**(45): 28463-28468
- Li Y, Chen CX, von Specht BU, Hahn HP (2002) Cloning and hemolysin-mediated secretory expression of a codon-optimized synthetic human interleukin-6 gene in *Escherichia coli*. *Protein Expr Purif* **25**(3): 437-447
- Liang ST, Xu YC, Dennis P, Bremer H (2000) mRNA composition and control of bacterial gene expression. *J Bacteriol* **182**(11): 3037-3044
- Liu CE, Liu PQ, Ames GFL (1997) Characterization of the adenosine-triphosphatase activity of the periplasmic histidine permease, a traffic atpase (abc transporter). *J Biol Chem* **272**(35): 21883-21891
- Liu G, Topping TB, Randall LL (1989) Physiological role during export for the retardation of folding by the leader peptide of maltose-binding protein. *Proc Natl Acad Sci U S A* **86**(23): 9213-9217
- Lobedanz S, Bokma E, Symmons MF, Koronakis E, Hughes C, Koronakis V (2007) A periplasmic coiled-coil interface underlying TolC recruitment and the assembly of bacterial drug efflux pumps. *Proc Natl Acad Sci U S A* **104**(11): 4612-4617
- Locher KP, Lee AT, Rees DC (2002) The *E. coli* BtuCD structure: a framework for ABC transporter architecture and mechanism. *Science* **296**(5570): 1091-1098
- Loo TW, Bartlett MC, Clarke DM (2002) The "LSGGQ" motif in each nucleotide-binding domain of human P-glycoprotein is adjacent to the opposing walker A sequence. *J Biol Chem* **277**(44): 41303-41306
- Ludwig A, Jarchau T, Benz R, Goebel W (1988) The repeat domain of *Escherichia coli* haemolysin (HlyA) is responsible for its Ca²⁺-dependent binding to erythrocytes. *Mol Gen Genet* **214**(3): 553-561
- Luirink J, von Heijne G, Houben E, de Gier JW (2005) Biogenesis of inner membrane proteins in *Escherichia coli*. *Annu Rev Microbiol* **59**: 329-355
- Ma D, Cook DN, Alberti M, Pon NG, Nikaido H, Hearst JE (1995) Genes *acrA* and *acrB* encode a stress-induced efflux system of *Escherichia coli*. *Mol Microbiol* **16**(1): 45-55
- Mackman N, Baker K, Gray L, Haigh R, Nicaud JM, Holland IB (1987) Release of a chimeric protein into the medium from *Escherichia coli* using the C-terminal secretion signal of haemolysin. *Embo J* **6**(9): 2835-2841
- Mackman N, Holland IB (1984) Functional characterization of a cloned haemolysin determinant from *E. coli* of human origin, encoding information for the secretion of a 107K polypeptide. *Mol Gen Genet* **196**(1): 129-134
- Manciu L, Chang XB, Buyse F, Hou YX, Gustot A, Riordan JR, Ruyschaert JM (2003) Intermediate structural states involved in MRP1-mediated drug transport. Role of glutathione. *J Biol Chem* **278**(5): 3347-3356
- Mannerling DE, Sharma S, Davidson AL (2001) Demonstration of conformational changes associated with activation of the maltose transport complex. *J Biol Chem* **276**(15): 12362-12368

- Mao L, Wang Y, Liu Y, Hu X (2003) Multiple intermolecular interaction modes of positively charged residues with adenine in ATP-binding proteins. *J Am Chem Soc* **125**(47): 14216-14217
- Mao Q, Leslie EM, Deeley RG, Cole SP (1999) ATPase activity of purified and reconstituted multidrug resistance protein MRP1 from drug-selected H69AR cells. *Biochim Biophys Acta* **1461**(1): 69-82
- Martin C, Higgins CF, Callaghan R (2001) The vinblastine binding site adopts high- and low-affinity conformations during a transport cycle of P-glycoprotein. *Biochemistry* **40**(51): 15733-15742
- Martin SF, Hergenrother PJ (1999) Catalytic cycle of the phosphatidylcholine-preferring phospholipase C from *Bacillus cereus*. Solvent viscosity, deuterium isotope effects, and proton inventory studies. *Biochemistry* **38**(14): 4403-4408
- Maurer J, Jose J, Meyer TF (1997) Autodisplay: one-component system for efficient surface display and release of soluble recombinant proteins from *Escherichia coli*. *J Bacteriol* **179**(3): 794-804
- McCarter JD, Stephens D, Shoemaker K, Rosenberg S, Kirsch JF, Georgiou G (2004) Substrate specificity of the *Escherichia coli* outer membrane protease OmpT. *J Bacteriol* **186**(17): 5919-5925
- Midgett CR, Madden DR (2007) Breaking the bottleneck: eukaryotic membrane protein expression for high-resolution structural studies. *J Struct Biol* **160**(3): 265-274
- Miroux B, Walker JE (1996) Over-production of proteins in *Escherichia coli*: mutant hosts that allow synthesis of some membrane proteins and globular proteins at high levels. *J Mol Biol* **260**(3): 289-298
- Mohanty AK, Wiener MC (2004) Membrane protein expression and production: effects of polyhistidine tag length and position. *Protein Expr Purif* **33**(2): 311-325
- Monne M, Chan KW, Slotboom DJ, Kunji ER (2005) Functional expression of eukaryotic membrane proteins in *Lactococcus lactis*. *Protein Sci* **14**(12): 3048-3056
- Moody J, Millen L, Binns D, Hunt JF, Thomas PJ (2002) Cooperative, ATP-dependent dimerization of ATP-binding cassettes during the catalytic cycle of ABC transporters. *J Biol Chem* **277**: 21111-21114
- Morbach S, Tebbe S, Schneider E (1993) The ATP-binding cassette (ABC) transporter for maltose/maltodextrins of *Salmonella typhimurium*. *J Biol Chem* **268**: 18617-18621
- Morova J, Osicka R, Masin J, Sebo P (2008) RTX cytotoxins recognize β_2 integrin receptors through N-linked oligosaccharides. *Proc Natl Acad Sci U S A* **105**(14): 5355-5360
- Mou TC, Gille A, Suryanarayana S, Richter M, Seifert R, Sprang SR (2006) Broad specificity of mammalian adenylyl cyclase for interaction with 2',3'-substituted purine- and pyrimidine nucleotide inhibitors. *Mol Pharmacol* **70**(3): 878-886
- Mourino M, Munoa F, Balsalobre C, Diaz P, Madrid C, Juarez A (1994) Environmental regulation of alpha-haemolysin expression in *Escherichia coli*. *Microb Pathog* **16**(4): 249-259
- Muller CM, Dobrindt U, Nagy G, Emody L, Uhlin BE, Hacker J (2006) Role of histone-like proteins H-NS and StpA in expression of virulence determinants of uropathogenic *Escherichia coli*. *J Bacteriol* **188**(15): 5428-5438
- Nadanaciva S, Weber J, Wilke-Mounts S, Senior AE (1999) Importance of F1-ATPase residue alpha-Arg-376 for catalytic transition state stabilization. *Biochemistry* **38**(47): 15493-15499
- Nakano H, Kawakami Y, Nishimura H (1992) Secretion of genetically-engineered dihydrofolate reductase from *Escherichia coli* using an *E. coli* alpha-hemolysin membrane translocation system. *Appl Microbiol Biotechnol* **37**(6): 765-771
- Nicaud JM, Mackman N, Gray L, Holland IB (1986) The C-terminal, 23 kDa peptide of *E. coli* haemolysin 2001 contains all the information necessary for its secretion by the haemolysin (Hly) export machinery. *FEBS Lett* **204**(2): 331-335

- Nikaido K, Ames GF (1999) One intact ATP-binding subunit is sufficient to support ATP hydrolysis and translocation in an ABC transporter, the histidine permease. *J Biol Chem* **274**(38): 26727-26735
- Ogino H, Hiroshima S, Hirose S, Yasuda M, Ishimi K, Ishikawa H (2004) Cloning, expression and characterization of a lipase gene (lip3) from *Pseudomonas aeruginosa* LST-03. *Mol Genet Genomics* **271**(2): 189-196
- Oldham ML, Khare D, Quirocho FA, Davidson AL, Chen J (2007) Crystal structure of a catalytic intermediate of the maltose transporter. *Nature* **450**(7169): 515-521
- Omori K, Idei A (2003) Gram-negative bacterial ATP-binding cassette protein exporter family and diverse secretory proteins. *J Biosci Bioeng* **95**(1): 1-12
- Orelle C, Dalmas O, Gros P, Di Pietro A, Jault JM (2003) The conserved glutamate residue adjacent to the Walker-B motif is the catalytic base for ATP hydrolysis in the ATP-binding cassette transporter BmrA. *J Biol Chem* **278**(47): 47002-47008
- Oswald C (2008) Structure-function studies of ABC transporters HlyB from *Escherichia coli* and ChoX from *Sinorhizobium meliloti*. Inst. of Biochemistry, University of Düsseldorf,
- Oswald C, Holland IB, Schmitt L (2006) The motor domains of ABC-transporters. What can structures tell us? *Naunyn Schmiedebergs Arch Pharmacol* **372**(6): 385-399
- Oswald C, Jenewein S, Smits SH, Holland IB, Schmitt L (2008a) Water-mediated protein-fluorophore interactions modulate the affinity of an ABC-ATPase/TNP-ADP complex. *J Struct Biol* **162**(1): 85-93
- Oswald C, Smits SH, Bremer E, Schmitt L (2008b) Microseeding – A Powerful Tool for Crystallizing Proteins Complexed with Hydrolyzable Substrates. *Int J Mol Sci* **9**: 1131-1141
- Pace CN (1986) Determination and analysis of urea and guanidine hydrochloride denaturation curves. *Methods Enzymol* **131**: 266-280
- Papageorgiou S, Melandri AB, Solaini G (1998) Relevance of divalent cations to ATP-driven proton pumping in beef heart mitochondrial F₀F₁-ATPase. *J Bioenerg Biomembr* **30**(6): 533-541
- Park S, Liu G, Topping TB, Cover WH, Randall LL (1988) Modulation of folding pathways of exported proteins by the leader sequence. *Science* **239**(4843): 1033-1035
- Patzlaff JS, van der Heide T, Poolman B (2003) The ATP/substrate stoichiometry of the ATP-binding cassette (ABC) transporter OpuA. *J Biol Chem* **278**(32): 29546-29551
- Perez-Iratxeta C, Andrade-Navarro MA (2008) K2D2: estimation of protein secondary structure from circular dichroism spectra. *BMC Struct Biol* **8**: 25
- Piehler J, Schreiber G (1999) Biophysical analysis of the interaction of human ifnar2 expressed in *E. coli* with IFN α 2. *J Mol Biol* **289**(1): 57-67
- Pimenta AL, Racher K, Jamieson L, Blight MA, Holland IB (2005) Mutations in HlyD, part of the type 1 translocator for hemolysin secretion, affect the folding of the secreted toxin. *J Bacteriol* **187**(21): 7471-7480
- Prive GG (2007) Detergents for the stabilization and crystallization of membrane proteins. *Methods* **41**(4): 388-397
- Przybycien TM, Dunn JP, Valax P, Georgiou G (1994) Secondary structure characterization of beta-lactamase inclusion bodies. *Protein Eng* **7**(1): 131-136
- Pukatzki S, Ma AT, Sturtevant D, Krastins B, Sarracino D, Nelson WC, Heidelberg JF, Mekalanos JJ (2006) Identification of a conserved bacterial protein secretion system in *Vibrio cholerae* using the *Dictyostelium* host model system. *Proc Natl Acad Sci U S A* **103**(5): 1528-1533

- Raine A, Ullers R, Pavlov M, Lührink J, Wikberg JE, Ehrenberg M (2003) Targeting and insertion of heterologous membrane proteins in *E. coli*. *Biochimie* **85**(7): 659-668
- Ramaen O, Masscheleyn S, Duffieux F, Pamard O, Oberkamp M, Lallemand JY, Stoven V, Jacquet E (2003) Biochemical characterization and NMR studies of the nucleotide-binding domain 1 of multidrug-resistance-associated protein 1: evidence for interaction between ATP and Trp653. *Biochem J* **376**(Pt 3): 749-756
- Randall LL, Topping TB, Hardy SJ (1990) No specific recognition of leader peptide by SecB, a chaperone involved in protein export. *Science* **248**(4957): 860-863
- Rapoport TA (2007) Protein translocation across the eukaryotic endoplasmic reticulum and bacterial plasma membranes. *Nature* **450**(7170): 663-669
- Rapp M, Granseth E, Seppala S, von Heijne G (2006) Identification and evolution of dual-topology membrane proteins. *Nat Struct Mol Biol* **13**(2): 112-116
- Rensland H, John J, Linke R, Simon I, Schlichting I, Wittinghofer A, Goody RS (1995) Substrate and product structural requirements for binding of nucleotides to H-ras p21: the mechanism of discrimination between guanosine and adenosine nucleotides. *Biochemistry* **34**(2): 593-599
- Riggs P (2001) Expression and purification of maltose-binding protein fusions. *Curr Protoc Mol Biol* **Chapter 16**: Unit16 16
- Riordan JR, Rommens JM, Kerem B, Alon N, Rozmahel R, Grzelczak Z, Zielenski J, Lok S, Plavsic N, Chou JL, et al. (1989) Identification of the cystic fibrosis gene: cloning and characterization of complementary DNA. *Science* **245**(4922): 1066-1073
- Robson A, Collinson I (2006) The structure of the Sec complex and the problem of protein translocation. *Embo Rep* **7**(11): 1099-1103
- Roosild TP, Greenwald J, Vega M, Castronovo S, Riek R, Choe S (2005) NMR structure of Mistic, a membrane-integrating protein for membrane protein expression. *Science* **307**(5713): 1317-1321
- Rosenbaum DM, Cherezov V, Hanson MA, Rasmussen SG, Thian FS, Kobilka TS, Choi HJ, Yao XJ, Weis WI, Stevens RC, Kobilka BK (2007) GPCR engineering yields high-resolution structural insights into beta2-adrenergic receptor function. *Science* **318**(5854): 1266-1273
- Rowe ES (1976) Dissociation and denaturation equilibria and kinetics of a homogeneous human immunoglobulin Fab fragment. *Biochemistry* **15**(4): 905-916
- Royer CA (2006) Probing protein folding and conformational transitions with fluorescence. *Chem Rev* **106**(5): 1769-1784
- Saier MH, Jr. (1995) Differential codon usage: a safeguard against inappropriate expression of specialized genes? *FEBS Lett* **362**(1): 1-4
- Sato K, Mori H, Yoshida M, Mizushima S (1996) Characterization of a potential catalytic residue, Asp-133, in the high affinity ATP-binding site of *Escherichia coli* SecA, translocation ATPase. *J Biol Chem* **271**(29): 17439-17444
- Sauna ZE, Smith MM, Müller M, Kerr KM, Ambudkar SV (2001) The mechanism of action of multidrug-resistance-linked P-glycoprotein. *J Bioenerg Biomembr* **33**(6): 481-491
- Scheu AK, Economou A, Hong GF, Ghelani S, Johnston AW, Downie JA (1992) Secretion of the *Rhizobium leguminosarum* nodulation protein NodO by haemolysin-type systems. *Mol Microbiol* **6**(2): 231-238
- Schiebel E, Driessen AJ, Hartl FU, Wickner W (1991) Delta mu H⁺ and ATP function at different steps of the catalytic cycle of preprotein translocase. *Cell* **64**(5): 927-939

Schlor S, Schmidt A, Maier E, Benz R, Goebel W, Gentschev I (1997) In vivo and in vitro studies on interactions between the components of the hemolysin (HlyA) secretion machinery of Escherichia coli. *Mol Gen Genet* **256**(3): 306-319

Schmees G, Stein A, Hunke S, Landmesser H, Schneider E (1999) Functional consequences of mutations in the conserved 'signature sequence' of the ATP-binding-cassette protein MalK. *Eur J Biochem* **266**(2): 420-430

Schmitt L, Benabdelhak H, Blight MA, Holland IB, Stubbs MT (2003) Crystal Structure of the Nucleotide-binding Domain of the ABC-transporter Haemolysin B: Identification of a Variable Region Within ABC Helical Domains. *J Mol Biol* **330**(2): 333-342

Schmitt L, Tampe R (2002) Structure and mechanism of ABC transporters. *Curr Opin Struct Biol* **12**(6): 754-760

Schneider E, Wilken S, Schmid R (1994) Nucleotide-induced conformational-changes of malk, a bacterial atp binding cassette transporter protein. *J Biol Chem* **269**(N32): 20456-20461

Schowen KB, Schowen RL (1982) Solvent isotope effects of enzyme systems. *Methods Enzymol* **87**: 551-606

Schulein R, Gentschev I, Mollenkopf HJ, Goebel W (1992) A topological model for the haemolysin translocator protein HlyD. *Mol Gen Genet* **234**(1): 155-163

Schulein R, Gentschev I, Schlor S, Gross R, Goebel W (1994) Identification and characterization of two functional domains of the hemolysin translocator protein HlyD. *Mol Gen Genet* **245**(2): 203-211

Schweins T, Geyer M, Scheffzek K, Warshel A, Kalbitzer HR, Wittinghofer A (1995) Substrate-assisted catalysis as a mechanism for GTP hydrolysis of p21ras and other GTP-binding proteins. *Nat Struct Biol* **2**(1): 36-44

Schweins T, Warshel A (1996) Mechanistic analysis of the observed linear free energy relationships in p21ras and related systems. *Biochemistry* **35**(45): 14232-14243

Schweins T, Wittinghofer A (1994) GTP-binding proteins. Structures, interactions and relationships. *Curr Biol* **4**(6): 547-550

Senior AE, al-Shawi MK, Urbatsch IL (1995) The catalytic cycle of P-glycoprotein. *FEBS Lett* **377**(3): 285-289

Sharom FJ (1995) Characterization and functional reconstitution of the multidrug transporter. *J Bioenerg Biomem* **27**: 15-22

Sharom FJ, Yu X, Chu JW, Doige CA (1995) Characterization of the ATPase activity of P-glycoprotein from multidrug-resistant Chinese hamster ovary cells. *Biochem J* **308** (Pt 2): 381-390

Sheps JA, Cheung I, Ling V (1995) Hemolysin transport in Escherichia coli. Point mutants in HlyB compensate for a deletion in the predicted amphiphilic helix region of the HlyA signal. *J Biol Chem* **270**(24): 14829-14834

Shyamala V, Baichwal V, Beall E, Ames GF (1991) Structure-function analysis of the histidine permease and comparison with cystic fibrosis mutations. *J Biol Chem* **266**(28): 18714-18719

Singer SJ, Nicolson GL (1972) The fluid mosaic model of the structure of cell membranes. *Science* **175**: 720-731

Siren N, Salonen K, Leisola M, Nyssola A (2008) A new and efficient phosphate starvation inducible expression system for Lactococcus lactis. *Appl Microbiol Biotechnol* **79**(5): 803-810

Smith PC, Karpowich N, Millen L, Moody JE, Rosen J, Thomas PJ, Hunt JF (2002a) ATP binding to the motor domain from an ABC transporter drives formation of a nucleotide sandwich dimer. *Mol Cell* **10**(1): 139-149

Sonveaux N, Vigano C, Shapiro AB, Ling V, Ruysschaert JM (1999) Ligand-mediated tertiary structure changes of reconstituted P-glycoprotein. A tryptophan fluorescence quenching analysis. *J Biol Chem* **274**(25): 17649-17654

- Sorensen HP, Mortensen KK (2005) Advanced genetic strategies for recombinant protein expression in *Escherichia coli*. *J Biotechnol* **115**(2): 113-128
- Stanley P, Packman LC, Koronakis V, Hughes C (1994) Fatty acylation of two internal lysine residues required for the toxic activity of *Escherichia coli* hemolysin. *Science* **266**(5193): 1992-1996
- Stegmeier JF, Polleichtner G, Brandes N, Hotz C, Andersen C (2006) Importance of the adaptor (membrane fusion) protein hairpin domain for the functionality of multidrug efflux pumps. *Biochemistry* **45**(34): 10303-10312
- Storer AC, Cornish-Bowden A (1976) Concentration of MgATP²⁻ and other ions in solution. Calculation of the true concentrations of species present in mixtures of associating ions. *Biochem J* **159**(1): 1-5
- Story TM, Steitz TA (1992) Structure of the RecA-ADP Komplex. *Nature* **355**: 374-376
- Strathdee CA, Lo RY (1989) Cloning, nucleotide sequence, and characterization of genes encoding the secretion function of the *Pasteurella haemolytica* leukotoxin determinant. *J Bacteriol* **171**(2): 916-928
- Studier FW (2005) Protein production by auto-induction in high density shaking cultures. *Protein Expr Purif* **41**(1): 207-234
- Studier FW, Moffatt BA (1986) Use of bacteriophage T7 RNA polymerase to direct selective high-level expression of cloned genes. *J Mol Biol* **189**(1): 113-130
- Suciu D, Inouye M (1996) The 19-residue pro-peptide of staphylococcal nuclease has a profound secretion-enhancing ability in *Escherichia coli*. *Mol Microbiol* **21**(1): 181-195
- Sugamata Y, Shiba T (2005) Improved secretory production of recombinant proteins by random mutagenesis of hlyB, an alpha-hemolysin transporter from *Escherichia coli*. *Appl Environ Microbiol* **71**(2): 656-662
- Surade S, Klein M, Stolt-Bergner PC, Muenke C, Roy A, Michel H (2006) Comparative analysis and "expression space" coverage of the production of prokaryotic membrane proteins for structural genomics. *Protein Sci* **15**(9): 2178-2189
- Tanji Y, Gennity J, Pollitt S, Inouye M (1991) Effect of OmpA signal peptide mutations on OmpA secretion, synthesis, and assembly. *J Bacteriol* **173**(6): 1997-2005
- Terpe K (2003) Overview of tag protein fusions: from molecular and biochemical fundamentals to commercial systems. *Appl Microbiol Biotechnol* **60**(5): 523-533
- Thanabalu T, Koronakis E, Hughes C, Koronakis V (1998) Substrate-induced assembly of a contiguous channel for protein export from *E.coli*: reversible bridging of an inner-membrane translocase to an outer membrane exit pore. *Embo J* **17**(22): 6487-6496
- Tobias JW, Shrader TE, Rocap G, Varshavsky A (1991) The N-end rule in bacteria. *Science* **254**(5036): 1374-1377
- Tomblin G, Bartholomew LA, Urbatsch IL, Senior AE (2004) Combined mutation of catalytic glutamate residues in the two nucleotide binding domains of P-glycoprotein generates a conformation that binds ATP and ADP tightly. *J Biol Chem* **279**(30): 31212-31220
- Tomkiewicz D, Nouwen N, Driessen AJ (2008) Kinetics and energetics of the translocation of maltose binding protein folding mutants. *J Mol Biol* **377**(1): 83-90
- Topping TB, Woodbury RL, Diamond DL, Hardy SJ, Randall LL (2001) Direct demonstration that homotetrameric chaperone SecB undergoes a dynamic dimer-tetramer equilibrium. *J Biol Chem* **276**(10): 7437-7441
- Uchida K, Mori H, Mizushima S (1995) Stepwise movement of preproteins in the process of translocation across the cytoplasmic membrane of *Escherichia coli*. *J Biol Chem* **270**(52): 30862-30868

- Uebel S, Kraas W, Kienle S, Wiesmüller K-H, Jung G, Tampé R (1997) Recognition principle of the TAP-transporter disclosed by combinatorial peptide libraries. *Proc Natl Acad Sci USA* **94**: 8976-8981
- Uhlen P, Laestadius A, Jahnukainen T, Soderblom T, Backhed F, Celsi G, Brismar H, Normark S, Aperia A, Richter-Dahlfors A (2000) Alpha-haemolysin of uropathogenic E. coli induces Ca²⁺ oscillations in renal epithelial cells. *Nature* **405**(6787): 694-697
- Ullers RS, Luirink J, Harms N, Schwager F, Georgopoulos C, Genevaux P (2004) SecB is a bona fide generalized chaperone in Escherichia coli. *Proc Natl Acad Sci U S A* **101**(20): 7583-7588
- Urbatsch IL, Al-Shawei MK, Senior AE (1994) Characterization of the ATPase activity of purified chinese hamster P-glycoprotein. *Biochemistry* **33**: 7069-7076
- Urbatsch IL, Julien M, Carrier I, Rousseau ME, Cayrol R, Gros P (2000) Mutational analysis of conserved carboxylate residues in the nucleotide binding sites of P-glycoprotein. *Biochemistry* **39**(46): 14138-14149
- Urbatsch IL, Sankaran B, Weber J, Senior AE (1995) P-glycoprotein is stably inhibited by vanadate-induced trapping of nucleotide at a single catalytic site. *J Biol Chem* **270**(33): 19383-19390
- Vakharia H, German GJ, Misra R (2001) Isolation and characterization of Escherichia coli tolC mutants defective in secreting enzymatically active alpha-hemolysin. *J Bacteriol* **183**(23): 6908-6916
- Valeva A, Walev I, Kemmer H, Weis S, Siegel I, Boukhallouk F, Wassenaar TM, Chavakis T, Bhakdi S (2005) Binding of Escherichia coli hemolysin and activation of the target cells is not receptor-dependent. *J Biol Chem* **280**(44): 36657-36663
- van der Does C, de Keyzer J, van der Laan M, Driessen AJ (2003) Reconstitution of purified bacterial preprotein translocase in liposomes. *Methods Enzymol* **372**: 86-98
- van der Does C, den Blaauwen T, de Wit JG, Manting EH, Groot NA, Fekkes P, Driessen AJ (1996) SecA is an intrinsic subunit of the Escherichia coli preprotein translocase and exposes its carboxyl terminus to the periplasm. *Mol Microbiol* **22**(4): 619-629
- van der Does C, Tampe R (2004) How do ABC transporters drive transport? *Biol Chem* **385**(10): 927-933
- van der Heide T, Stuart MC, Poolman B (2001) On the osmotic signal and osmosensing mechanism of an ABC transport system for glycine betaine. *Embo J* **20**(24): 7022-7032
- van Nuland NA, Chiti F, Taddei N, Raugei G, Ramponi G, Dobson CM (1998) Slow folding of muscle acylphosphatase in the absence of intermediates. *J Mol Biol* **283**(4): 883-891
- Verdon G, Albers SV, Dijkstra BW, Driessen AJ, Thunnissen AM (2003a) Crystal structures of the ATPase subunit of the glucose ABC transporter from Sulfolobus solfataricus: nucleotide-free and nucleotide-bound conformations. *J Mol Biol* **330**(2): 343-358
- Verdon G, Albers SV, van Oosterwijk N, Dijkstra BW, Driessen AJ, Thunnissen AM (2003b) Formation of the productive ATP-Mg²⁺-bound dimer of GlcV, an ABC-ATPase from Sulfolobus solfataricus. *J Mol Biol* **334**(2): 255-267
- Vogel M, Hess J, Then I, Juarez A, Goebel W (1988) Characterization of a sequence (hlyR) which enhances synthesis and secretion of hemolysin in Escherichia coli. *Mol Gen Genet* **212**(1): 76-84
- Wagner S, Baars L, Ytterberg AJ, Klussmeier A, Wagner CS, Nord O, Nygren PA, van Wijk KJ, de Gier JW (2007) Consequences of membrane protein overexpression in Escherichia coli. *Mol Cell Proteomics* **6**(9): 1527-1550
- Wagner S, Bader ML, Drew D, de Gier JW (2006) Rationalizing membrane protein overexpression. *Trends Biotechnol* **24**(8): 364-371

- Walker JE, Saraste M, Runswick MJ, Gray NJ (1982) Distantly related sequences in the α - and β -subunits of ATP synthase, myosin, kinases and other ATP-requiring enzymes and a common nucleotide binding fold. *Embo J* **1**: 945-951
- Wallin E, von Heijne G (1998) Genome-wide analysis of integral membrane proteins from eubacterial, archaean, and eukaryotic organisms. *Protein Sci* **7**(4): 1029-1038
- Wandersman C, Deleplaire P (1990) TolC, an Escherichia coli outer membrane protein required for hemolysin secretion. *Proc Natl Acad Sci U S A* **87**(12): 4776-4780
- Wang DN, Safferling M, Lemieux MJ, Griffith H, Chen Y, Li XD (2003) Practical aspects of overexpressing bacterial secondary membrane transporters for structural studies. *Biochim Biophys Acta* **1610**(1): 23-36
- Wang RC, Seror SJ, Blight M, Pratt JM, Broome-Smith JK, Holland IB (1991) Analysis of the membrane organization of an Escherichia coli protein translocator, HlyB, a member of a large family of prokaryote and eukaryote surface transport proteins. *J Mol Biol* **217**(3): 441-454
- Ward A, Reyes CL, Yu J, Roth CB, Chang G (2007) Flexibility in the ABC transporter MsbA: Alternating access with a twist. *Proc Natl Acad Sci U S A* **104**(48): 19005-19010
- Watanabe R, Masui R, Mikawa T, Takamatsu S, Kato R, Kuramitsu S (1994) Interaction of Escherichia coli RecA protein with ATP and its analogues. *J Biochem* **116**(5): 960-966
- Weiss JB, Ray PH, Bassford PJ, Jr. (1988) Purified secB protein of Escherichia coli retards folding and promotes membrane translocation of the maltose-binding protein in vitro. *Proc Natl Acad Sci U S A* **85**(23): 8978-8982
- Welch RA, Dellinger EP, Minshew B, Falkow S (1981) Haemolysin contributes to virulence of extra-intestinal E. coli infections. *Nature* **294**(5842): 665-667
- Welch RA, Hull R, Falkow S (1983) Molecular cloning and physical characterization of a chromosomal hemolysin from Escherichia coli. *Infect Immun* **42**(1): 178-186
- Wells JM, Wilson PW, Le Page RW (1993) Improved cloning vectors and transformation procedure for Lactococcus lactis. *J Appl Bacteriol* **74**(6): 629-636
- White HD, Belknap B, Jiang W (1993) Kinetics of binding and hydrolysis of a series of nucleoside triphosphates by actomyosin-S1. Relationship between solution rate constants and properties of muscle fibers. *J Biol Chem* **268**(14): 10039-10045
- Wickner W, Schekman R (2005) Protein translocation across biological membranes. *Science* **310**(5753): 1452-1456
- Wilson JE, Chin A (1991) Chelation of divalent cations by ATP, studied by titration calorimetry. *Anal Biochem* **193**(1): 16-19
- Wolff N, Sapriel G, Bodenreider C, Chaffotte A, Deleplaire P (2003) Antifolding activity of the SecB chaperone is essential for secretion of HasA, a quickly folding ABC pathway substrate. *J Biol Chem* **278**(40): 38247-38253
- Wood WB (1966) Host specificity of DNA produced by Escherichia coli: bacterial mutations affecting the restriction and modification of DNA. *J Mol Biol* **16**(1): 118-133
- Wu KH, Tai PC (2004) Cys32 and His105 are the critical residues for the calcium-dependent cysteine proteolytic activity of CvaB, an ATP-binding cassette transporter. *J Biol Chem* **279**(2): 901-909
- Xie K, Dalbey RE (2008) Inserting proteins into the bacterial cytoplasmic membrane using the Sec and YidC translocases. *Nat Rev Microbiol* **6**(3): 234-244
- Yang R, Chang XB (2007) Hydrogen-bond formation of the residue in H-loop of the nucleotide binding domain 2 with the ATP in this site and/or other residues of multidrug resistance protein MRP1 plays a crucial role during ATP-dependent solute transport. *Biochim Biophys Acta* **1768**(2): 324-335

- Yao Y, Martinez-Yamout MA, Dickerson TJ, Brogan AP, Wright PE, Dyson HJ (2006) Structure of the Escherichia coli quorum sensing protein SdiA: activation of the folding switch by acyl homoserine lactones. *J Mol Biol* **355**(2): 262-273
- Young R, Bremer H (1976) Polypeptide-chain-elongation rate in Escherichia coli B/r as a function of growth rate. *Biochem J* **160**(2): 185-194
- Yuan YR, Blecker S, Martsinkevich O, Millen L, Thomas PJ, Hunt JF (2001) The crystal structure of the MJ0796 ATP-binding cassette. Implications for the structural consequences of ATP hydrolysis in the active site of an ABC transporter. *J Biol Chem* **276**(34): 32313-32321
- Zaitseva J, Holland IB, Schmitt L (2004) The role of CAPS buffer in expanding the crystallization space of the nucleotide-binding domain of the ABC transporter haemolysin B from Escherichia coli. *Acta Crystallogr D Biol Crystallogr* **60**(Pt 6): 1076-1084
- Zaitseva J, Jenewein S, Jumpertz T, Holland IB, Schmitt L (2005a) H662 is the linchpin of ATP hydrolysis in the nucleotide-binding domain of the ABC transporter HlyB. *Embo J* **24**(11): 1901-1910
- Zaitseva J, Jenewein S, Wiedenmann A, Benabdelhak H, Holland IB, Schmitt L (2005b) Functional characterization and ATP-induced dimerization of the isolated ABC-domain of the haemolysin B transporter. *Biochemistry* **44**(28): 9680-9690
- Zaitseva J, Oswald C, Jumpertz T, Jenewein S, Wiedenmann A, Holland IB, Schmitt L (2006) A structural analysis of asymmetry required for catalytic activity of an ABC-ATPase domain dimer. *Embo J* **25**(14): 3432-3443
- Zhang F, Sheps JA, Ling V (1993) Complementation of transport-deficient mutants of Escherichia coli alpha-hemolysin by second-site mutations in the transporter hemolysin B. *J Biol Chem* **268**(26): 19889-19895
- Zhong X, Tai PC (1998) When an ATPase is not an ATPase: at low temperatures the C-terminal domain of the ABC transporter CvaB is a GTPase. *J Bacteriol* **180**(6): 1347-1353
- Zito CR, Antony E, Hunt JF, Oliver DB, Hingorani MM (2005) Role of a conserved glutamate residue in the Escherichia coli SecA ATPase mechanism. *J Biol Chem* **280**(15): 14611-14619

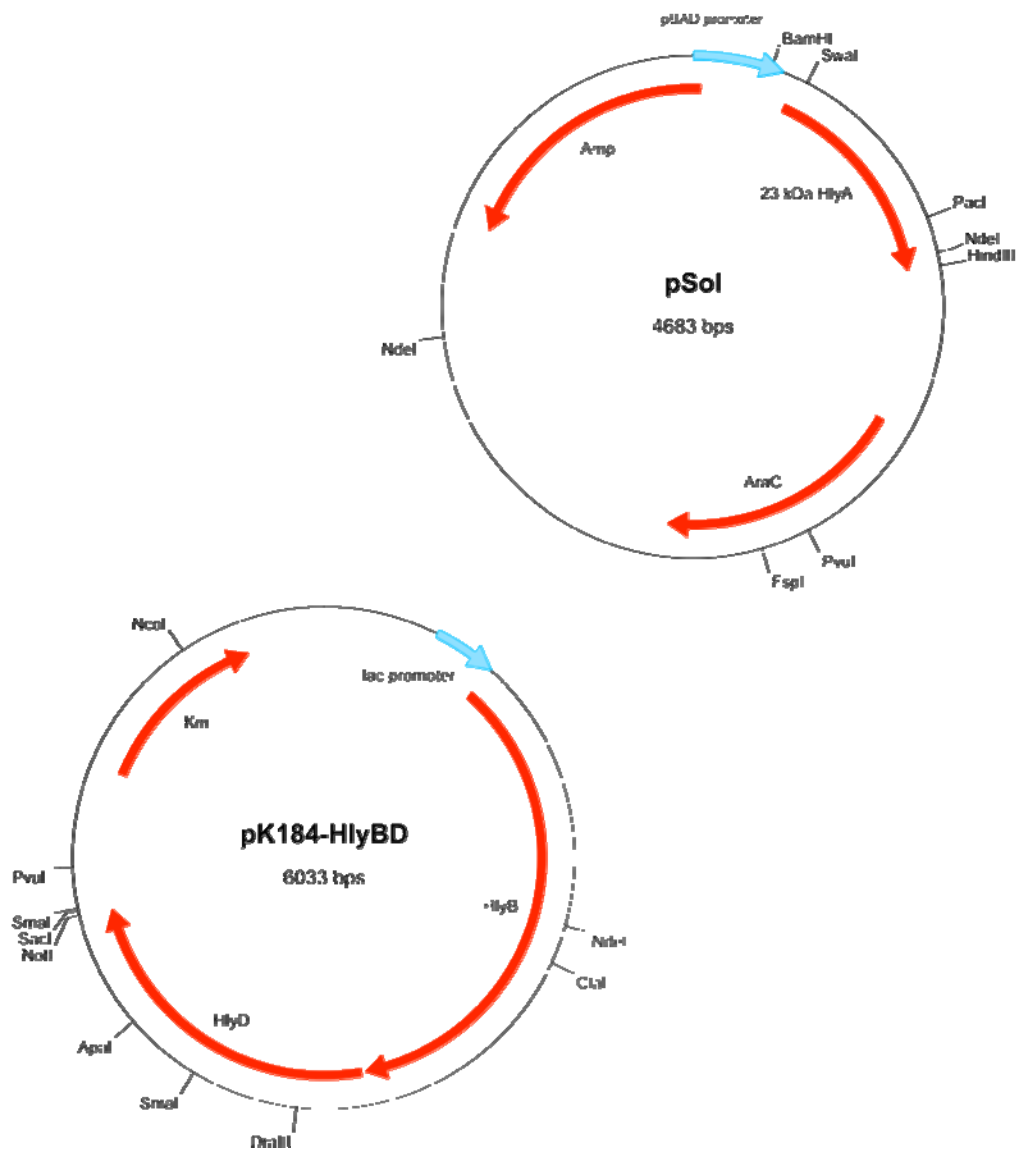
Abbreviations

ABC	ATP binding cassette
ADP	Adenosine-5'-diphosphate
AMP	Adenosin-5'-monophosphate
AMP-PNP	Adenosin-5'-[β , γ -imido]-triphosphate
APS	Ammonium persulfate
ATP	Adenosine-5'-triphosphate
Bp/bps	Base pair(s)
BSA	Bovine serum albumine
CAPS	Cyclohexylaminoethanesulfonic acid
CFTR	Cystic fibrosis transmembrane conductance regulator
CMC	Critical micelle concentration
CV	Column volume
DDM	Dodecyl- β -D-maltopyranoside
DNA	Desoxyribonucleic acid
DTT	Dithiothreitol
<i>E. coli</i>	<i>Escherichia coli</i>
EDTA	Ethylene diamine tetracetic acid
GTP	Guanosine-5'-triphosphate
HEPES	N-(2-hydroxyethyl)piperazine-N'-2-ethanesulfonic acid
Hly	Haemolysin
HlyACterm	C-terminal 23 kDa fragment of HlyA
Hly-NBD	Haemolysin B nucleotide-binding domain
IDA	Iminodiacetic acid
IMAC	Immobilised metal ion affinity chromatography
<i>L. lactis</i>	<i>Lactococcus lactis</i>
MDR	Multidrug resistance
MFP	Membrane fusion protein
Min	Minutes
<i>M. jannaschii</i>	<i>Methanococcus jannaschii</i>
MRP	Multidrug resistance-related protein
MWCO	Molecular weight cutoff
NBD	Nucleotide binding domain
NTA	Nitrilotriacetic acid
OD	Optical density
OMP	Outer membrane protein
PAGE	Polyacrylamide gel electrophoresis

PDB	Protein data bank
PVDF	Polyvinilidene difluoride
<i>S. cerevisiae</i>	<i>Saccharomyces cerevisiae</i>
<i>S. marcescens</i>	<i>Serratia marcescens</i>
SDR	Structurally diverse region
SDS	Sodium dodecylsulfate
SPR	Surface plasmon resonance
TAP	Transporter associated with antigen processing
TEMED	N, N, N', N'-Tetramethylethylenediamine
TM	Transmembrane
TNP-ATP	2'(or 3')-O-(2, 4, 6-trinitrophenyl)-adenosine-5'-monophosphate
TRIS	Trishydroxymethylaminomethane
WT	Wild type

Appendix

Amp	Ampicilin resistance marker
Km	Kanamycin resistance marker



Danksagung

Besonderer Dank gilt meinem Doktorvater Prof. Dr. Lutz Schmitt, der mich stets unterstütze und dem Geist seiner Leute stets freien Lauf gibt. Lutz, vielen Dank!

Many thanks to our cooperation partner Prof. Dr. I. Holland for being patient, excited and generous at once.

Vielen Dank an Prof. Dr. J. Jose für die Übernahme des Koreferats.

Dank an Prof. Dr. M. Grieshaber für seine Freude an der Wissenschaft nach selbst so vielen Jahren.

Der grösste Dank gilt den Leuten um mich, die Wissenschaft leben und die Freude daran haben. Sei es an der Methodik, an den Ergebnissen, am Erklären oder am doch so häufigen Knobeln und Rätseln. Ihr habt mich alle geprägt und motiviert.

,

Natürlich danke ich auch den Leuten außerhalb dieses Kreises, die mich unterstützt haben, sei es im Sport oder auch so. Andi, wir werden auch weiterhin klettern, halt nur nicht so oft.

Meiner Freundin Tina für Teilen von Freud und Leid! Meist Freud...

Natürlich meinen Eltern Margret und Siegfried, ohne deren Unterstützung die Arbeit sicherlich nicht möglich gewesen wäre.

Curriculum vitae

Personal information

Name	Stefan Jenewein
Date of birth	23 Feb 1978
Place of birth	Heilbronn/Neckargartach

University education

9/2005	Followed Prof. L. Schmitt to the University of Düsseldorf
11/2003	Start of the Ph.D. thesis in Biochemistry in the Institute of Biochemistry, Frankfurt (Supervisor: Prof. L. Schmitt) with the topic “The Escherichia coli haemolysin transporter – A paradigm for Type I secretion“.
8/2003	Degree Diplom-Biochemist, University Frankfurt with the emphasis in Biophysics and Biochemistry. Grade: 1.0 with honours
1/2003 - 7/2003	Diploma thesis with the topic „Biophysikalische Charakterisierung der nukleotidbindenden Domäne des ABC-Transporters OpuA aus <i>B. subtilis</i> “ under supervision of Dr. L. Schmitt und Prof. R. Tampé, Institute of Biochemistry, University Frankfurt
8/2000	Intermediate diploma in Biochemistry. Grade: 1.0
10/1998 - 8/2003	Studies in Biochemistry the Johann Wolfgang Goethe-University in Frankfurt/M.

Civilian service

8/1997-9/1998	Service as paramedic at the German Red Cross, Heilbronn
---------------	---

School education

8/1988 – 7/1997 Justinus-Kerner-Gymnasium in Weinsberg;

8/1984 – 6/1988 Primary school in Weinsberg

Prizes and scholarships

12/2003 Proctor & Gamble Prize (best Diploma thesis in Biochemistry)

since 12/2001 Scholarship of e-fellows.net

8/2001 – 10/2001 DAAD Scholarship (Scientific internship at the University of Michigan, USA)

7/1997 Prize for excellence at the final school exam (Abitur)

List of publications

Zaitseva J*, **Jenewein S***, Jumpertz T, Holland IB, Schmitt L (2005) H662 is the linchpin of ATP hydrolysis in the nucleotide-binding domain of the ABC transporter HlyB. *Embo J* **24**(11):1901-10

Zaitseva J, **Jenewein S**, Wiedenmann A, Benabdelhak H, Holland IB, Schmitt L (2005) Functional characterization and ATP-induced dimerization of the isolated ABC-domain of the haemolysin B transporter. *Biochemistry* **44**(28):9680-90.

Zaitseva J, **Jenewein S**, Oswald C, Jumpertz T, Holland IB, Schmitt L (2005) A molecular understanding of the catalytic cycle of the nucleotide-binding domain of the ABC transporter HlyB *Biochem Soc Trans* **33**(5):990-5

Hanekop N, Zaitseva J, **Jenewein S**, Holland IB, Schmitt L (2006) Molecular insights into the mechanism of ATP-hydrolysis by the NBD of the ABC-transporter HlyB *FEBS Lett* **580**(4):1036-41

Horn C, **Jenewein S**, Sohn-Bosser L, Bremer E, Schmitt L (2005) Biochemical and structural analysis of the *Bacillus subtilis* ABC transporter OpuA and its isolated subunits. *J Mol Microbiol Biotechnol* **10**(2-4):76-91

Zaitseva J, Oswald C, Jumpertz T, **Jenewein S**, Wiedenmann A, Holland IB, Schmitt L (2006) A structural analysis of asymmetry required for catalytic activity of an ABC-ATPase domain dimer. *Embo J* **25**(14):3432-43

Jenewein S, Schmitt L (2007) Eine molekulare Analyse der ATP-Hydrolyse *BIOspektrum* (1) 20-23

Oswald C*, **Jenewein S***, Smits, SH, Holland IB, Schmitt L. (2007) Water-mediated protein-fluorophore interactions modulate the affinity of an ABC-ATPase/TNP-ADP complex. *Journal of Structural Biology* **162**(1):85-93

Horn C*, **Jenewein S***, Tschapek B, Bremer E, Schmitt L. (2008) Monitoring conformational changes during the catalytic cycle of OpuAA, the ATPase subunit of the ABC-transporter OpuA from *B. subtilis*. *Biochem J* **412** 233-244.

Jenewein S, Holland IB, Schmitt L. "Bacterial Type I Secretion" in Bacterial protein secretion (ed K. Woolridge), Horizon Publishers book chapter *in press*

Jenewein S, Smits S, Holland IB, Schmitt L. Kinetic partitioning assigns substrates to Type I secretion *in preperation*

* equally contributed

Hiermit versichere ich, dass ich die vorgelegte Arbeit selbständig verfasst und keine anderen als die angegebenen Quellen und Hilfsmittel verwendet habe.

Zitate wurden kenntlich gemacht.

Stefan Jenewein

Düsseldorf, den 08.09.2008